
Herpesvirus Nuclear Egress and the Analysis of Involved Viral and Cellular Key Players

**Inauguraldissertation
zur
Erlangung des akademischen Grades eines
Doktors der Naturwissenschaften
(Dr. rer. nat.)
der
Mathematisch-Naturwissenschaftlichen Fakultät
der
Universität Greifswald**

Greifswald, June 2020

vorgelegt von:
Julia Elisabeth Hölper
geboren am 23.02.1992
in Lüdinghausen

Dekan: Prof. Dr. Gerald Kerth

1. Gutachter: Prof. Dr. Dr. h.c. Thomas C. Mettenleiter

2. Gutachter: Prof. Dr. Wolfram Antonin

Tag der Promotion: 17.09.2020

For my family.

Contents

List of abbreviations	6
1 Introduction	9
1.1 The Family of <i>Herpesviridae</i>	9
1.2 PrV and its Replication Cycle	11
1.3 The Nucleus - the Site of Viral Replication	14
1.3.1 The Nuclear Envelope	14
1.3.2 Nuclear Pore Complexes	16
1.3.3 The Nucleoskeleton	16
1.3.4 Nuclear Envelope-associated Proteins	17
1.3.5 NPC-independent Transport	23
1.3.6 The ESCRT Machinery at the NE	24
1.4 The Escape: How Herpesviruses Exit the Nucleus	26
1.4.1 The Nuclear Egress Complex	26
1.4.2 Envelopment at the INM	29
1.4.3 De-envelopment at the ONM	31
1.5 CRISPR Genome Editing	34
1.6 The Objectives	36
2 Publications	38
2.1 Paper I	39
2.2 Paper II	59
2.3 Paper III	81
3 Own Contribution to Publications	97
4 Results and Discussion	101
4.1 Analyzing the Role of Cellular Proteins in Nuclear Egress	101
4.2 How the NEC Facilitates the Initial Budding Step	107
4.2.1 Characterization of the Viral Nuclear Egress Complex	107
4.2.2 Analyzing the NEC-Capsid Interaction	111

Summary	116
Zusammenfassung	117

Appendix

A Bibliography	119
B Curriculum Vitae	148
C Publications	149
C.1 Publications that are part of this thesis	149
C.2 Publications that are not part of this thesis	149
D Scientific presentations	150
E Eigenständigkeitserklärung	153
Acknowledgments	154

List of Abbreviations

A	alanine	<i>et al.</i>	and others (from Latin <i>et alii</i>)
aa	amino acid		
AAA+	ATPases associated with diverse cellular activities	ER	endoplasmic reticulum
		ESCRT	endosomal sorting complex required for transport
approx.	approximately		
ATP	adenosine triphosphate	F	phenylalanine
ATPase	adenosine triphosphatase	Fig.	figure, figures
BAF	barrier-to-autointegration factor	FL	full length
		G	Golgi, guanosine <u>or</u> glycine
<i>C. elegans</i>	<i>Caenorhabditis elegans</i>		
C-terminus	carboxy-terminus	G418	geneticin
Cas9	CRISPR-associated protein 9	gRNA	guide RNA
CRISPR	clustered regularly interspaced short palindromic repeats	GTPase	guanosine triphosphatase
		h	hour
crRNA	CRISPR RNA	H10	alpha-helical region 10
CVSC	capsid vertex-specific component	HCMV	Human Cytomegalovirus
		HDR	homology directed repair
Cyt	cytoplasm	HHV	Human Herpesvirus
D	aspartic acid, aspartate	HSV	Herpes Simplex Virus
DKO	double knock-out	IE	immediate-early
DNA	deoxyribonucleic acid	InDel	insertions <u>or</u> deletions
ds	double-stranded	INM	inner nuclear membrane
DSB	double-strand break	<i>in vitro</i>	in the glass (from Latin)
E	glutamic acid/ glutamate <u>or</u> early	<i>in vivo</i>	within the living (from Latin)
EBV	Epstein-Barr Virus	K	lysine
e.g.	for example (from Latin <i>exempli gratia</i>)	kbp	kilobase pairs
eGFP	enhanced green fluorescent protein	KASH	Klarsicht/ANC-1/SYNE homology
		KO	knock-out
		KSHV	Kaposi's Sarcoma Herpesvirus

L	late	<i>p.i.</i>	post infection (from Latin <i>post infectionem</i>)
LAP1	lamina-associated polypeptide 1	PP	protein phosphatase
LEM	LAP2, Emerin, MAN1	pAb	polyclonal antibody
LD	luminal domain	PAM	protospacer adjacent motif
LINC	linker of nucleoskeleton and cytoskeleton	PKC	protein kinase C
LULL1	luminal domain-like LAP1	PNS	perinuclear space
mAbs	monoclonal antibodies	PrV	Pseudorabies Virus
M	mitochondria	Q	glutamine
MEF	mouse embryonic fibroblast	R	arginine
Mg ²⁺	magnesium cation	RER	rough ER
MT	microtubule	RK13	rabbit kidney cell line
N	asparagine	RNA	ribonucleic acid
N-terminus	amino-terminus	RNP	ribonucleoprotein
NE	nuclear envelope	S	serine
NEBD	nuclear envelope breakdown	SUN	Sad1p/UNC-84 homology
NEC	nuclear egress complex	T	threonine
NES	nuclear export signal	T=	triangulation number
NHEJ	non-homologous end joining	TEM	transmission electron microscopy
NLS	nuclear localization signal	TGN	trans-Golgi network
NP	nuclear pore	TMD	transmembrane domain
NPC	nuclear pore complex	Tor	Torsin
NR	nucleoplasmic reticulum	tracrRNA	trans-activating crRNA
NTR	nuclear transport receptors	U _L	unique long
Nuc	nucleus	U _S	unique short
Nup	nucleoporin	Vps4	vacuolar protein sorting-associated protein 4
nt	nucleotide(s)	VZV	Varicella-Zoster Virus
ONM	outer nuclear membrane	WT	wild type
<i>p</i>	probability	Y	tyrosine
PBD	protein data bank	α	alpha
		β	beta
		Δ	Delta
		γ	gamma

Introduction 1

As obligatory parasites, herpesviruses have co-evolved with their host for 1.5 billion years to efficiently hijack and manipulate cellular structures for their own advantage. Over decades, researchers have revealed unknown cellular mechanisms by close analysis of viruses. Thereby, a 'DNA-like-RNA' was detected in T2 phage-infected *E. coli*, not knowing that mRNA was discovered [Astrachan and Volkin, 1958]. Research on viruses also provided the first evidence that the genetic code was read in sets of three nucleotides by experiments using the T4 phage [Crick *et al.*, 1961]. Years later, the first nuclear localization signal (NLS) was discovered in the protein sequence of the Simian Virus 40 large T-antigen [Kalderon *et al.*, 1984] - to name only a few. Our understanding of cell regulation is far from complete and this thesis is intended to contribute in further understanding of herpesvirus infection mechanisms.

1.1 The Family of *Herpesviridae*

The order *Herpesvirales* consists of three families, the *Alloherpesviridae*, which includes the herpesviruses of fish and amphibians, the *Malacoherpesviridae* with herpesviruses from invertebrates and the *Herpesviridae*, which comprises over 100 species of viruses in mammals, birds and reptiles [Davison *et al.*, 2009; Davison, 2010].

A common characteristic of all herpesviruses is their nearly identical morphology of the mature virus particle (Figure 1). All herpesvirus particles consist of four structural components: the large double-stranded (ds) linear DNA genome, which is enclosed by an icosahedral capsid (T = 16) [Booy *et al.*, 1991]. This capsid in turn is surrounded by a proteinaceous layer, the tegument [Zhou *et al.*, 1999]. Finally, the tegument with the nucleocapsid is enveloped by a host-cell-derived lipid membrane, containing several virus-encoded (glyco)proteins [Granzow *et al.*, 1997; Mettenleiter *et al.*, 2009]. The non-segmented genome with a size of 120 to 300 kbp and coding for up to 200 proteins classify the *Herpesviridae* among the largest and most complex dsDNA viruses [Mettenleiter, 2002; Davison *et al.*, 2009; Davison, 2010].

1 Introduction

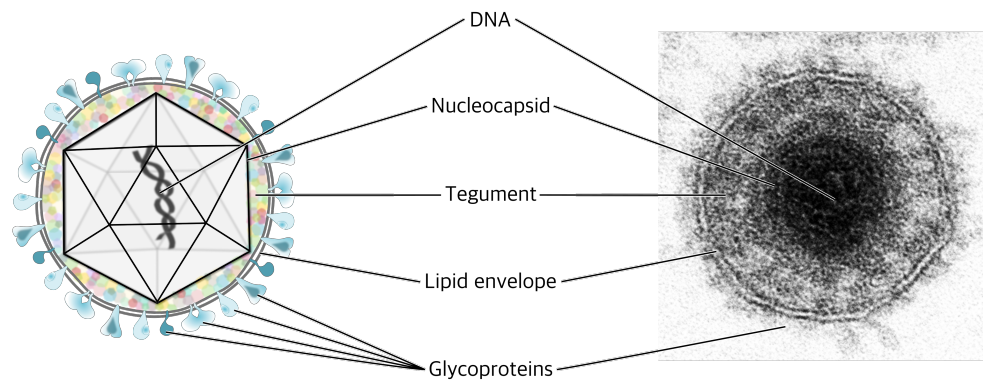


Figure 1: Morphology of a Herpesvirus Particle. Schematic representation of a Herpesvirus particle is shown left. The icosahedral nucleocapsid containing the viral dsDNA is embedded in the tegument layer, which is surrounded by the lipid envelope, spiked with viral glycoproteins. The transmission electron microscopic (TEM) image of the Pseudorabies Virus particle is kindly provided by FLI's laboratory for electron microscopy, Dr. Kati Franzke.

Several biological properties are shared between all members of the *Herpesviridae*: first, the replication of the viral DNA and the assembly of the capsids occur in the nucleus. Second, all further steps of maturation take place in the cytoplasm. Third, all herpesviruses code for a diversity of enzymes that play a role in nucleic acid metabolism, replication and protein processing. Finally, the hallmark of herpesviruses is their ability to establish a life-long latency in their hosts, which can result in virus reactivation, e.g. induced by local trauma or systemic stress [Croen, 1991; Davison, 2010; Grinde, 2013; Pellet and Roizman, 2013], leading to further spread to naïve hosts.

Based on biological characteristics and sequence homologies the family *Herpesviridae* is divided into the three subfamilies alpha- (α -), beta- (β -) and gamma- (γ -) *Herpesvirinae* [Davison, 2010]. Each subfamily shares unique genomic features and biological properties, while some properties involved in critical steps of the replication cycle are conserved throughout all subfamilies [McGeoch *et al.*, 2006; Fossum *et al.*, 2009].

Alphaherpesvirinae are characterized by a broad host spectrum, a short lytic replication cycle, a pronounced neurotropism and the establishment of latency in sensory ganglia of their hosts [Weir, 1998; Davison, 2010; Weidner-Glunde *et al.*, 2020]. The α -herpesviruses include the human pathogens Herpes Simplex Virus 1 and 2 (HSV-1 or -2, *HHV-1/-2*) and Varicella-Zoster Virus (VZV, *HHV-3*). The animal pathogens Pseudorabies Virus (PrV, *SuHV-1*) and Bovine herpesvirus 1 (*BoHV-1*) are well studied members of the α -herpesviruses leading to serious outbreaks of disease, resulting in high mortalities and great economic losses.

Betaherpesvirinae are more restricted in their host range, have a prolonged replication cycle and can establish latency in hematopoietic stem cells [Weidner-Glunde *et al.*, 2020]. Members of the β -herpesviruses are e.g. the human Cytomegalovirus (HCMV, *HHV-5*) and the human Herpesvirus 6 (*HHV-6*).

Gammaherpesvirinae comprise herpesviruses with a narrow host range and transforming potential, usually infecting immune cells with the establishment of latency in lymphoid tissues [Weidner-Glunde *et al.*, 2020]. Members of the γ -herpesviruses are e.g. Epstein-Barr Virus (EBV, *HHV-4*) and Kaposi's Sarcoma Herpesvirus (KSHV, *HHV-8*).

1.2 PrV and its Replication Cycle

In this thesis, the Pseudorabies Virus (PrV), also known as *Suid alphaherpesvirus 1*, was used to analyze the involvement of viral and cellular key players in the herpesviral replication cycle. PrV is phylogenetically classified into the genus *Varicellovirus* and is the causative agent of Aujeszky's disease.

PrV has a broad host spectrum, infecting a range of mammals including ruminants, carnivores and rodents [Pensaert and Kluge, 1989]. Members of the families *Hominidae* (e.g. higher primates and humans) as well as *Equidae* (e.g. horses or goats) can resist infection [Mettenleiter, 2000], yet there have been recent indications of few human infections [Zhao *et al.*, 2018; Wang *et al.*, 2019, 2020]. The only natural hosts of PrV are members of the family *Suidae*. While infection of piglets results in high mortalities, the infection of adult swine causes only mild or no clinical signs [Pomeranz *et al.*, 2005; Mettenleiter, 2008]. Infection of other susceptible hosts typically induce serious neurological disease characterized by extreme pruritus with self-mutilation, hypersalivation, uncoordinated movements and paralysis. The so-called 'mad itch' leads to a fatal outcome [Hanson, 1954; Mettenleiter, 2008; Pellet and Roizman, 2013]. Since the clinical signs are similar to those described for rabies, it was designated as pseudorabies [Pomeranz *et al.*, 2005]. Due to a successful vaccination strategy, domestic pig populations in Western Europe, North America and New Zealand are considered PrV-free. In wild boar populations PrV is still circulating, leading to infrequent infections of hunting dogs (reviewed in Freuling *et al.* [2017])

Its short replication cycle in a variety of animal and human cell lines and the absent or low pathogenicity to humans makes PrV a suitable model for analysis of α -herpesviral molecular processes [Webster and Granoff, 1994; Mettenleiter, 2000].

PrV, like other herpesviruses, has a complex replication cycle, as depicted in Figure 2. Infection is initiated by binding of the attachment glycoprotein (g)C to cellular heparan sulfate proteoglycans and subsequent binding of gD to the more specific receptors, like nectin-1 and -2 on the cellular surface [Granzow *et al.*, 2005; Eisenberg *et al.*, 2012]. PrV appears to be able to use multiple other receptors, which is suspected to be the reason for the broad host range [Mettenleiter, 2001]. The fusion of the viral envelope with the cell membrane is mediated by the viral fusion machinery, consisting of gH/gL and gB [Heldwein and Krummenacher, 2008; Eisenberg *et al.*, 2012] and results in release of the

1 Introduction

DNA-containing capsid and the tegument proteins into the cytoplasm. In addition to fusion at the plasma membrane, the viral glycoproteins can also initiate pH-independent fusion with the endosomal membrane after endocytosis [Kielian, 2014; Boulant *et al.*, 2015]. After fusion, some tegument proteins remain attached to the nucleocapsid mediating the microtubule-based capsid transport towards the nucleus by interaction with the cellular dynein/dynactin protein complex [Sodeik *et al.*, 1997; Luxton *et al.*, 2006], while others prime the cell for synthesis of viral components and initiate the host cell shut-off [Kwong and Frenkel, 1989; Mettenleiter, 2006].

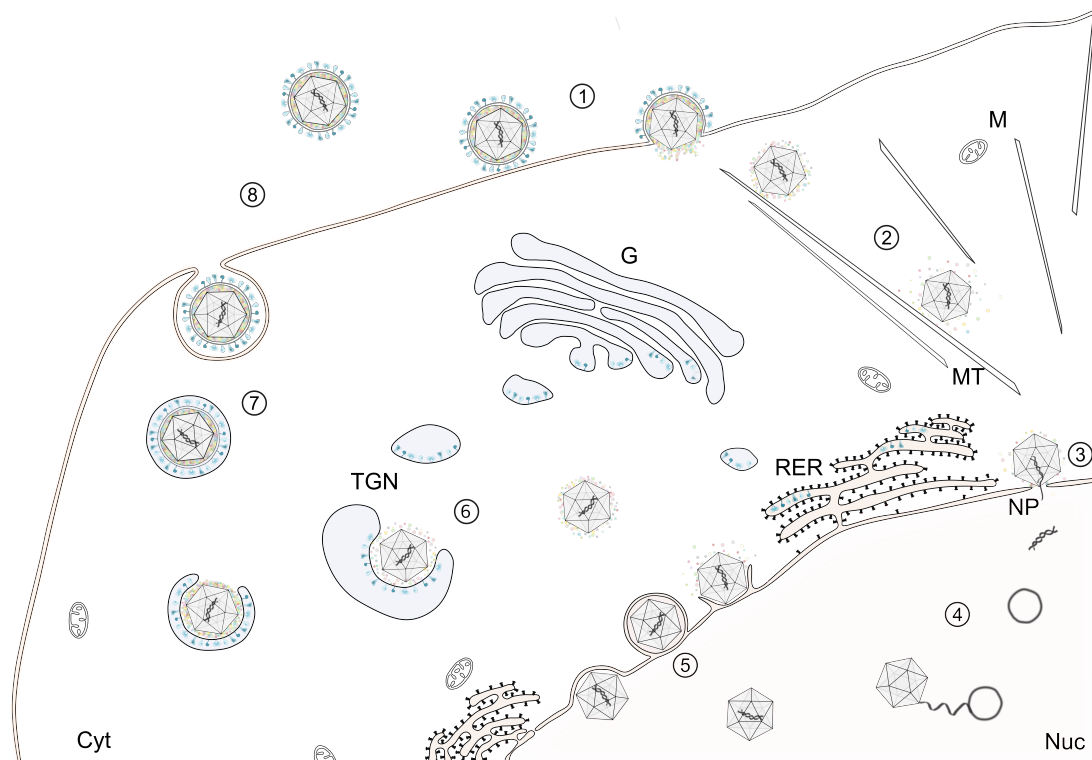


Figure 2: Schematic Overview on the Alphaherpesviral Replication Cycle. After attachment and penetration (1), the capsid is transported along microtubules (MT) to the nucleus (Nuc) by interaction of capsid-attached tegument proteins with motor proteins (2). After docking at the nuclear pore (NP) (3), the viral genome is released into the nucleus. Here, transcription of viral genes and genome replication occurs. The capsid assembles autocatalytically, the viral genome is encapsidated (4) and the mature capsid leaves the nucleus by budding through the nuclear membranes (5). Final maturation occurs in the cytoplasm (Cyt) by budding into vesicles of the trans-Golgi network (TGN) containing viral glycoproteins (6), resulting in an enveloped virion within a transport vesicle. After transport to the cell surface (7), the vesicle and plasma membrane fuse, releasing the mature, enveloped virion from the cell (8). G: Golgi apparatus; M: mitochondria; RER: rough endoplasmic reticulum

At the nuclear pore (NP), the genome is released into the nucleus [Newcomb *et al.*, 2001]. There the DNA circularizes and is available for transcription and replication which results in production and transport of new virion components to sites of assembly [Strang and Stow, 2005]. The genome of PrV is about 143 kbp long and codes for approx. 70 proteins [Klupp *et al.*, 2004]. The genome is divided into a unique long (U_L)

and a unique short (U_S) region with the U_S region being enclosed by an internal and a terminal repeat sequence [Ben-Porat *et al.*, 1983; Davison and Wilkie, 1983]. PrV's open reading frames were named according to the HSV-1 gene nomenclature, which is based on the localization of the genes, while the gene products are marked by a prefixed 'p' [Mettenleiter, 2000; Pomeranz *et al.*, 2005].

Genes are expressed in a coordinated cascade characterized by three kinetic classes: immediate-early (IE), early (E) and late (L) genes [Hones and Roizman, 1974, 1975]. Some tegument proteins are important for transactivation of IE gene expression [Kwong and Frenkel, 1989]. IE-proteins promote the expression of E-genes, with E-genes mainly coding for enzymes involved in DNA replication and the viral nucleic acid metabolism. Further, they induce the transcription of L-genes, which are mainly coding for structural proteins. Capsid proteins are translocated into the nucleus where spherical procapsids are formed autocatalytically [Heming *et al.*, 2017]. Genome insertion into the procapsid leads to structural rearrangements resulting in an icosahedral capsid [Cardone *et al.*, 2012]. In the infected host cell nucleus, three major capsid forms are detected, the empty A-capsids, the scaffold containing B-capsids and the DNA containing mature C-capsids. A- and B-capsids may represent assembly intermediates or abortive capsid forms resulting from unsuccessful packaging, while C-capsids are the major substrate for export [Tandon *et al.*, 2015].

During nuclear egress, the nuclear lamina is locally dissolved through phosphorylation, e.g. by protein kinase C (PKC). The mature nucleocapsid buds at the inner nuclear membrane into the perinuclear space (PNS), thereby forming a primary enveloped virion in the PNS. Subsequent fusion of the primary envelope with the outer nuclear membrane releases the viral capsid into the cytoplasm, where it gains its final tegument and envelope by budding into trans-Golgi derived vesicles (reviewed in Hellberg *et al.* [2016]). Since the major part of this thesis is focusing on the nuclear egress, a detailed description can be found in section 1.4.

Release of the mature virions occurs after fusion of the vesicle with the cellular plasma membrane. Herpesviruses can not only infect their host cell from the cell surface, but can also spread directly from cell-to-cell, enabling the virus to hide from extracellular immunity [Zsak *et al.*, 1992; Johnson and Huber, 2002; Pellet and Roizman, 2013; Roller *et al.*, 2014].

1.3 The Nucleus - the Site of Viral Replication

The nucleus is the major characteristic of eukaryotic cells, distinguishing them from prokaryotic bacteria and archaea. The boundary of the nucleus, and thus the separation of cytoplasm and nucleoplasm, is formed by the nuclear envelope (NE).

The nucleus harbors the majority of the genetic information in the form of DNA. Genomic DNA is tightly condensed to fit into this sub-cellular compartment. For this the DNA is organized in a structure called chromatin, a highly dynamic nucleoprotein complex, which can be modified to tightly packed, inactive regions named heterochromatin or the loosely packed, transcriptionally active euchromatin [Stralfors and Ekwall, 2011]. Chromatin is organized in large loops of DNA, some of which are attached to the NE [Zuleger *et al.*, 2011]. Chromatin plays important roles in maintaining DNA replication and repair, preventing damage and controlling of gene expression (reviewed in Felsenfeld and Groudine [2003]).

1.3.1 The Nuclear Envelope

Structurally, the NE is organized into two concentric phospholipid bilayers designated as the inner (INM) and outer (ONM) nuclear membrane. The INM and ONM are separated by the PNS, being contiguous with the lumen of the endoplasmic reticulum (ER).

Both membranes convey different functional properties and harbor different subsets of membrane proteins. The ONM is continuous with the membrane of the rough ER and studded with ribosomes [D'Angelo *et al.*, 2006], whereas the INM harbors a unique set of membrane proteins [Holmer and Worman, 2001; Schirmer *et al.*, 2003] of which approx. 100 different proteins have been described, but with only limited knowledge on their function.

Analysis of those proteins in the last decade gave an insight into their functional diversity with roles in structural maintenance, mitosis, nuclear anchoring and migration, mechano-sensory and gene expression functions [Worman and Courvalin, 2000; Schirmer and Foisner, 2007; Katta *et al.*, 2014]. These proteins provide interaction with the nucleo- or cytoskeleton. The structural characteristics of the NE, as well as some characteristic proteins are schematically shown in Figure 3.

Initially, the NE was viewed as a simple convex surface which was pierced by NP. Nowadays it is known that the NE is interrupted by intranuclear membranes and invaginations that reach deep into the nucleoplasm and could even cross the nucleus completely [Dupuy-Coin *et al.*, 1986; Fricker *et al.*, 1997; Malhas *et al.*, 2011]. This nucleoplasmic reticulum (NR) occurs in numerous cells and tissues, both under normal cellular conditions [Fricker *et al.*, 1997; Johnson *et al.*, 2003], as well as in pathological states such as cancer [Malhas and Vaux, 2014].

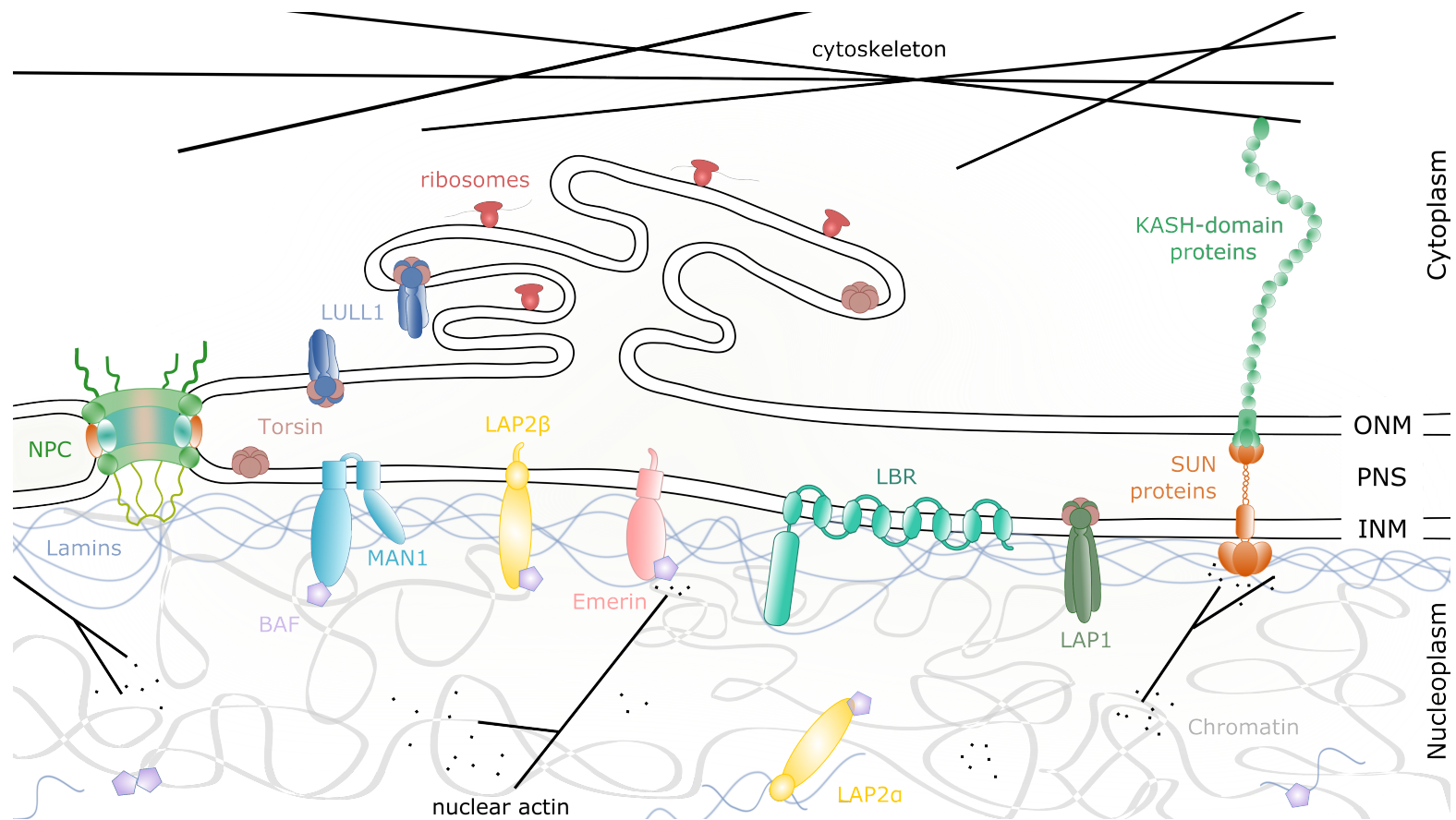


Figure 3: Schematic Overview on the Nuclear Envelope. The nuclear envelope (NE) consists of an inner (INM) and an outer nuclear membrane (ONM) separated by the perinuclear space (PNS). The ONM is contiguous with the rough endoplasmic reticulum membrane. Nuclear pore complexes (NPC) are inserted in the NE, allowing the transport of cargo through the NE. The nucleoskeleton is a complex network of lamins and nuclear actin and connected directly or indirectly to the peripheral chromatin. Several INM proteins like LBR, Emerin, LAP2, LAP1, LULL1, MAN1 or Torsins are embedded in the NE. Interaction with the nuclear lamina or chromatin is mediated by some of them, either directly or indirectly via the protein BAF. The LINC complex, consisting of INM SUN- and ONM KASH-domain containing proteins forms a direct connection between nucleoskeletal and cytoskeletal structures. Abbreviations of proteins are explained in the text.

1.3.2 Nuclear Pore Complexes

The separation of the genome-related from cytoplasmic processes by the NE requires a regulated transport between both compartments. This transport is facilitated by multi-protein assemblies named nuclear pore complex (NPC). The two lipid bilayers are fused at sites where NPCs are inserted. NPCs mediate both passive diffusion of small molecules like water, sugars and ions as well as active bidirectional nucleo-cytoplasmic transport of a wide range of cargo through the NE [Wente and Rout, 2010]. NPCs are formed by a complex assembly of conserved nucleoporins (Nups) [Alber *et al.*, 2007; Wente and Rout, 2010]. Multiple copies of approx. 30 Nups build a cylindrical structure containing three stacked rings. The inner ring spans the fused nuclear membranes building a central pore, while the outer rings sandwich the inner from the cytoplasmic and nucleoplasmic site (see Fig. 3) [von Appen and Beck, 2016]. Pore membrane proteins (POMs) form a luminal ring, directly interfacing with the inner ring, thereby anchoring the NPC to the NE [Cohen *et al.*, 2005].

In order to pass through the NPC, the cargo associates with nuclear transport receptors (NTRs) [Mackmull *et al.*, 2017]. Recognition of the cargo takes place via specific transport sequences like NLS or nuclear export signals (NES) [Kim *et al.*, 2017]. Beside the cargo and the NTR the small GTPase Ran is crucial for efficient nuclear transport by shuttling active (RanGTP) and inactive (RanGDP) forms between the nucleus and the cytoplasm [Lui and Huang, 2009]. For this, the associated cytoplasmic filaments and the nuclear basket are suggested to represent docking sites for transport complexes [Rout and Aitchison, 2001]. In addition, the nuclear basket was described to associate with chromatin and most likely with elements of the nucleoskeleton [Zuleger *et al.*, 2011; Sood and Brickner, 2014], thereby supporting structural integrity.

1.3.3 The Nucleoskeleton

The nucleoskeleton is an important structural feature of the nucleus. The peripheral nucleoskeleton is composed of the nuclear lamina, a complex network of nuclear lamins and their INM-associated proteins, mediating structural maintenance and regulation of gene expression.

The nuclear lamina is a proteinaceous meshwork of nuclear lamins. Lamins are type V intermediate filaments, interacting with each other to form an irregular filamentous meshwork. Most mammalian cells contain four different lamins, namely lamin A, B1, B2 and C. B-type lamins are ubiquitously expressed, while lamins of the A- or C-type are mostly expressed in differentiated cells [Stuurman *et al.*, 1998; Dechat *et al.*, 2008, 2010; Prokocimer *et al.*, 2009]. B-type lamins are directly associated to the INM through their farnesylated C-terminus [Adam, 2017]. In lesser amounts, lamins can also locate in

the nucleoplasm [Moir *et al.*, 2000]. The lamin meshwork has to dissociate during mitosis, which is mainly regulated through phosphorylation by PKC and cyclin-dependent kinase 1 [Guttinger *et al.*, 2009]. At the end of mitosis, assembly of lamins is induced by dephosphorylation through protein phosphatase 1 (PP1) and PP2A [Huguet *et al.*, 2019].

The internal nucleoskeleton consisting of nuclear actin possesses a variety of structural and functional roles in transcription, processing and export of messenger RNAs, as well as chromatin remodeling (reviewed in Hendzel [2014]) underlining its importance in the organization of the genome and regulation of gene expression [Shumaker *et al.*, 2003]. Most nuclear actin is found in form of short filaments or as monomeric actin [Kokai *et al.*, 2014]. Direct binding of nuclear actin to lamins [Simon *et al.*, 2010], as well as the growing information on INM or nuclear proteins that contain both, actin- and lamin-binding domains (see Fig. 3), illustrate the molecular crosstalk between these two types of nucleoskeleton and NE (reviewed in Shumaker *et al.* [2003]).

1.3.4 Nuclear Envelope-associated Proteins

1.3.4.1 Lamin B receptor

The lamin B receptor (LBR) is an integral INM protein containing eight transmembrane domains (TMD) [Worman *et al.*, 1988]. Through its nucleoplasmic N-terminus it interacts with B-type lamins and heterochromatin, thereby tethering chromatin to the nuclear periphery (see Fig. 3) [Olins *et al.*, 2010]. This in turn regulates the chromatin organization and might influence DNA replication, transcription or repair (reviewed in Prokocimer *et al.* [2009]; Dechat *et al.* [2009, 2010]).

1.3.4.2 LEM-Domain Containing Proteins

A prominent and well-characterized family of INM proteins are the LEM-domain proteins [Wagner and Krohne, 2007]. LEM-domain proteins all share an N-terminal LAP2-Emerin-MAN1 (LEM) domain (reviewed in Wilson and Foisner [2010]), a globular module of approx. 40 amino acids (aa) mediating interaction with the essential chromatin-associated protein barrier-to-autointegration factor (BAF) [Zheng *et al.*, 2000; Brachner and Foisner, 2011]. In addition, all LEM-proteins can bind A- and B-type lamins [Wilson and Foisner, 2010]. LEM-domain proteins are involved in a diversity of cellular processes including replication and cell cycle control, chromatin organization and nuclear assembly, as well as the regulation of gene expression and signaling pathways (reviewed in Wagner and Krohne [2007]).

LEM-domain proteins can be distinguished by their domain organization [Barton *et al.*, 2015]. Emerin and a diversity of Lamina-associated polypeptide 2 (LAP2) isoforms are transmembrane proteins of the INM (group I), containing a large nucleoplasmic domain including the LEM motif, a single TMD and a short luminal domain (LD) [Furukawa *et al.*, 1995]. Emerin was shown to bind directly to lamins and indirectly via the BAF to chromatin [Margalit *et al.*, 2007]. In addition, Emerin stimulates the polymerization of nuclear actin [Holaska *et al.*, 2004; Ho *et al.*, 2013], thereby modulating both the peripheral and the internal nucleoskeleton. All LAP2 isoforms harbor an additional LEM-like domain, mediating direct binding to DNA, rather than to the BAF [Cai *et al.*, 2001]. The second group of LEM proteins include the proteins MAN1 and LEM2 possessing two TMD [Lin *et al.*, 2000; Brachner *et al.*, 2005]. Despite its interaction with the BAF, MAN1 can also interact directly with Emerin via its N-terminal nucleoplasmic region [Mansharamani and Wilson, 2005]. Furthermore, among the LEM proteins some, such as LAP2 α and Ankle1 (Ankyrin repeat and LEM-domain-containing protein, LEM3), lack a TMD and localize in the nucleo- and/ or cytoplasm [Harris *et al.*, 1995; Brachner and Foisner, 2011; Brachner *et al.*, 2012].

1.3.4.3 The LINC Complex

The nucleus is anchored in the cell by proteins which link the nuclear lamina and chromatin in the nucleoplasm with the actin filaments, microtubules and intermediate filaments in the cytoplasm [Jahed and Mofrad, 2019]. This physical interaction across the NE is mediated by the linker of nucleoskeleton and cytoskeleton (LINC) complex [Crisp *et al.*, 2006; Starr and Fridolfsson, 2010]. The LINC complex is composed of KASH (Klar-sicht/ANC-1/SYNE homology) proteins interacting with SUN (Sad1p/UNC-84 homology) proteins, which are present in all plant, animal and fungal cells [Razafsky and Hodzic, 2009; Zhou *et al.*, 2012]. It mechanically connects the nucleus with the cytoskeleton, mediating several fundamental cellular processes including cell division, meiotic chromosome pairing and mechano-regulation of gene expression (reviewed in Meinke and Schirmer [2015]).

SUN-domain family members are embedded in the INM. They consist of a variable N-terminus, followed by a TMD connecting to a predicted luminal coiled-coil segment localized in the PNS. SUN-domain proteins reach into the PNS with their C-terminal part, containing the SUN-domain at the very end, leaving their N-terminus in the nucleoplasm [Starr, 2011]. In the nucleoplasm, SUN proteins interact directly with a variety of nuclear factors such as chromatin, nuclear lamins and INM proteins like Emerin [Crisp *et al.*, 2006; Haque *et al.*, 2006; Rothballer and Kutay, 2013]. There are different forms of SUN proteins described in the human genome: SUN1 and SUN2 are ubiquitously expressed in somatic cells, while SUN3, SUN4 and SUN5 are testis-specific [Starr and

Fridolfsson, 2010; Gob *et al.*, 2010; Meinke and Schirmer, 2015]. The length of the coiled-coil segment varies between the different SUN homologs. They are predicted to mediate the proper spacing of approx. 30 to 50 nm of the nuclear membranes [Sosa *et al.*, 2013; Rothballer *et al.*, 2013], but conflicting findings suggested this might be true for nuclei in cell culture, but not *in vivo* [Cain and Starr, 2015].

On the cytoplasmic side, this anchorage is mediated by KASH domain-containing proteins, which are tail-anchored, single-spanning transmembrane proteins with a short luminal C-terminus. The KASH proteins localize in the ONM inserting their KASH-domain into the PNS and their large variable N-terminal domain into the cytoplasm [Starr, 2011]. The N-terminal domain targets a great number of components of the cytoskeleton and signaling proteins to the ONM [Rothballer and Kutay, 2013; Luxton and Starr, 2014; Kim *et al.*, 2015]. To date, six KASH proteins are described in humans, which are called nesprin 1 to 4 (nuclear envelope spectrin-repeat proteins) [Rajgor and Shanahan, 2013], KASH-5 [Horn *et al.*, 2013] and LRMP (lymphoid-restricted membrane protein) [Lindeman and Pelegri, 2012].

In the PNS, three KASH domains are predicted to interact with a platform, most likely build by SUN homotrimers, thereby forming a stable complex [Crisp *et al.*, 2006; Starr and Fridolfsson, 2010; Sosa *et al.*, 2012; Tapley and Starr, 2013]. Interestingly, LINC complexes are able to form higher order complexes, to increase their mechanical stability. In fibroblasts, nuclei move away from a wound edge by using retrograde actin movement. For this, SUN/KASH bridges arrange linearly, thereby assembling into transmembrane actin-associated nuclear (TAN) lines [Luxton *et al.*, 2010, 2011; Borrego-Pinto *et al.*, 2012]. So far, the molecular mechanism of TAN line assembly remains poorly defined.

Although the LINC complex is involved in many essential cellular processes, it is still unknown how assembly, clustering or disassembly is achieved. The regulation of multi-protein complexes in cells is often accomplished by AAA+ ATPases [Hanson and Whiteheart, 2005]. They are widely distributed in cells and participate in many important functions, including in vesicle transport, budding and fission of vesicles, organelle assembly, membrane dynamics and protein unfolding (reviewed in Erzberger and Berger [2006]; White and Lauring [2007]). Recent evidence proposed a role for Torsin AAA+ ATPases, especially TorA, to be required for assembly of functional LINC complexes [Nery *et al.*, 2008; Vander Heyden *et al.*, 2009; Saunders, 2017; Dominguez Gonzalez *et al.*, 2018; Gill *et al.*, 2019; Chalfant *et al.*, 2019].

1.3.4.4 Torsins and their Cofactors LULL1 and LAP1

The Torsin family belongs to the superfamily of AAA+ ATPases. AAA+ ATPases operate as ring-shaped oligomeric structures which utilize energy derived from ATP-hydrolysis to structurally remodel their target molecules [Stinson *et al.*, 2013]. Most active AAA+

1 Introduction

ATPases oligomerize into hexameric ring structures, while those with two AAA+ domains have a stacked or double-ring appearance [White and Lauring, 2007]. Oligomerization is critical for ATP hydrolysis, since the ATP molecules are positioned between two subunits within the ring. A conserved arginine from either subunit interacts with the active-site pocket of the neighboring subunit, thereby stimulating hydrolysis [Glynn *et al.*, 2009, 2012; Stinson *et al.*, 2013]. This results in conformational changes within the ring structure [Stinson *et al.*, 2013]. The hydrophobic stretches in the central pore can bind and physically pull on substrates, thereby inducing remodeling [White and Lauring, 2007; Martin *et al.*, 2008; Glynn *et al.*, 2009].

The human genome encodes for at least five Torsins: TorA (*TOR1A*), TorB (*TOR1B*), Tor2 (*TOR2A*), Tor3 (*TOR3A*) and Tor4 (*TOR4A*) with various expression levels in different tissues.

Torsins are characterized as atypical members of the AAA+ superfamily:

They are the only AAA+ ATPases known to associate with membranes and subsequently reside within the shared lumen of ER and NE of mammalian cells [Kustedjo *et al.*, 2000; Breakefield *et al.*, 2001; Vander Heyden *et al.*, 2009; Jungwirth *et al.*, 2010].

They contain a non-canonical Walker A motif [Nagy *et al.*, 2009], where GxxxxGKN (x represents any aa) is used instead of GxxxxGK[T/S] as in canonical AAA+ ATPases.

They lack the conserved arginine finger, which is needed for ATP hydrolysis [Zhao *et al.*, 2013; Sosa *et al.*, 2014; Brown *et al.*, 2014]. Therefore, cofactors are required.

While TorA and B have been the subject of numerous studies, the research on Tor2, Tor3 and especially Tor4 is still at its beginning. In the following, the focus is laid on TorA and TorB due to their ubiquitous expression. Furthermore, TorA is expressed highly in neuronal tissue, which is interesting with regard to the neurotropism of α -herpesviruses [Jungwirth *et al.*, 2010; Rose *et al.*, 2015]. TorA and B have 85% similarity in their aa sequence and a number of publications described a functional redundancy of TorA and TorB [Kim *et al.*, 2010; Turner *et al.*, 2015].

TorA and B (see Fig. 4) are composed of an N-terminal signal peptide, followed by a hydrophobic stretch, that has been shown to function in ER retention, possibly through membrane association [Vander Heyden *et al.*, 2009, 2011]. The Walker A and B motifs, which convey ATP binding and hydrolysis, are located downstream [Breakefield *et al.*, 2001]. The Walker A motif (GxxxxGKN), especially the lysine (K) is critical for ATP binding, since it directly contacts the phosphates of the ATP molecule [Saraste *et al.*, 1990]. The consensus sequence of the Walker B motif however is hhhhDE, where h represents a hydrophobic aa. While the aspartate (D) residue coordinates and stabilizes the Mg^{2+} ion, required for ATP hydrolysis, the glutamate (E) in this motif is thought to activate water for the hydrolysis reaction [Iyer *et al.*, 2004]. Mutation of the glutamate residue to glutamine (Q) or alanine (A) impedes the ATPase activity, while binding

of the nucleotide is still possible [Hanson and Whiteheart, 2005]. Additionally, there are two sensor motifs (sensor I and II) that mediate the nucleotide binding [Zhu *et al.*, 2010; Wendler *et al.*, 2012; Demircioglu *et al.*, 2016]. The sensor I motif is composed of a polar residue that helps coordinating and attracting the water for the hydrolysis reaction, while the sensor II motif with the consensus sequence GCK plays a role in ATP turnover. Sensor II is additionally described to regulate cofactor binding [Zhu *et al.*, 2008, 2010].

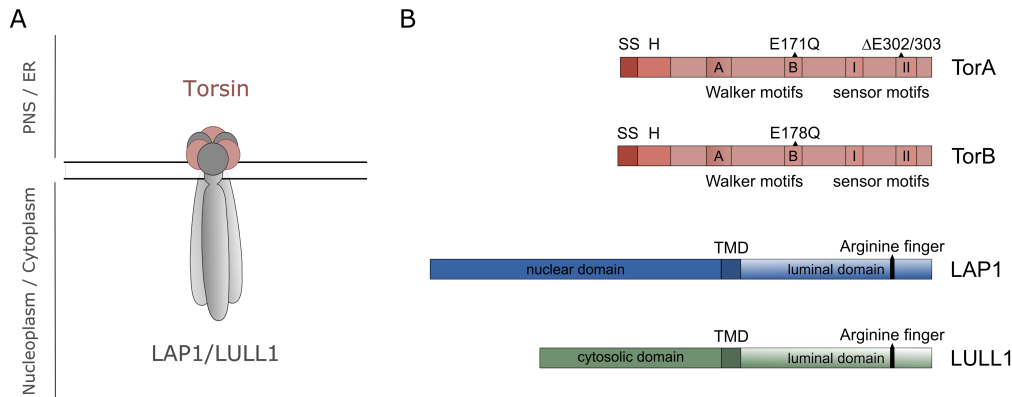


Figure 4: Schematic Models of Torsins and their Cofactors. Shown is the proposed hexameric assembly for Torsin and its cofactor LAP1 or LULL1 (A). Torsins may form a mixed alternating ring with either cofactor, but Torsin assembly seems to be highly dynamic and may also result in heterodimers or homohexamers (not shown in the scheme). Further, the domain organization of the TorA, TorB, LAP1 and LULL1 proteins is depicted in (B). SS: signal sequence; H: hydrophobic stretch; $\Delta E302/303$: in-frame deletion in TorA that leads to DYT1 dystonia; EQ: aa exchange in TorA/TorB that leads to an ATP hydrolysis-deficient mutant; TMD: transmembrane domain.

In active AAA+ proteins the ATPase activity is typically stimulated by a highly conserved arginine residue [Glynn *et al.*, 2009, 2012; Stinson *et al.*, 2013]. Due to lack of this residue, Torsins are not able to hydrolyze ATP *in vitro* [Zhao *et al.*, 2013; Sosa *et al.*, 2014; Brown *et al.*, 2014] and therefore need to be activated by specific cofactors [Brown *et al.*, 2014]. The known regulatory cofactors of TorA and TorB are LAP1 (lamina-associated polypeptide 1, encoded by *TOR1AIP1*) and LULL1 (luminal domain-like LAP1, encoded by *TOR1AIP2*).

Besides the predicted heterohexameric ring structure (Torsin:cofactor, 3:3) [Zhao *et al.*, 2013; Sosa *et al.*, 2014; Brown *et al.*, 2014], Torsin-cofactor heterodimers [Demircioglu *et al.*, 2016], as well as Torsin homohexamers [Vander Heyden *et al.*, 2009; Jungwirth *et al.*, 2010] were described in the past. Recently, the interaction of Torsins with their cofactors was shown to be more dynamic than previously thought [Chase *et al.*, 2017]. The resulting model describes Torsins to assemble in homohexamers in dependence of ATP. Upon binding, the LAP1 cofactors disassemble the Torsin hexameric ring with simultaneous ATP hydrolysis and loss of a TorA subunits from the ring. This argues against a stable, mixed Torsin-cofactor ring. Although this model still needs further validation,

1 Introduction

it might describe a yet unknown mode of Torsin or AAA+ATPase regulation in the cell [Chase *et al.*, 2017].

Both cofactors are type II transmembrane proteins comprising an N-terminal hydrophilic nucleo- or cytoplasmic domain, a TMD and a C-terminal LD (see Fig. 4) [Zhao *et al.*, 2013; Martin *et al.*, 1995]. In addition to its Torsin activating function, LAP1 was described to bind with its N-terminal domain to lamins [Maison *et al.*, 1997] and to interact with Emerin [Shin *et al.*, 2013]. The LD of LAP1 and LULL1 both extending to the PNS/ER are approx. 60 % identical [Goodchild and Dauer, 2005]. Further, they are sufficient for interaction and activation of the ATPase activity of TorA [Zhao *et al.*, 2013]. Structural analyses revealed an AAA+ like fold of the cofactors, although they lack the ability to bind ATP [Sosa *et al.*, 2014; Demircioglu *et al.*, 2016]. The conserved arginine finger, stimulating the ATPase activity by an active-site complementation mechanism, is also located in the LD [Zhao *et al.*, 2013; Brown *et al.*, 2014; Sosa *et al.*, 2014; Demircioglu *et al.*, 2016]. LULL1 and LAP1 have a different localization in the cell pointing to specific, non-redundant functions. While LAP1 localizes to the INM, LULL1 is specifically targeted to the peripheral ER and does not enter the INM [Zhao *et al.*, 2013].

Minor changes in the aa sequence of the TorA protein impair the functional interaction with either the cofactors or the nucleotide as discovered in an autosomal-dominant movement disorder in humans, called early onset torsion dystonia 1 (DYT1/TOR1A dystonia) [Ozelius *et al.*, 1997]. The most frequent disease-linked form TorA Δ E302/303 lacks a single glutamic acid residue in the C-terminus of the protein (see position in Fig. 4) [Goodchild and Dauer, 2004; Naismith *et al.*, 2004; Gonzalez-Alegre, 2019] resulting in a weakened binding to LAP1/LULL1 [Ozelius *et al.*, 1997]. None of the other Torsins are yet linked to any human diseases. Nonetheless, EQ mutations in the Walker B domain of TorA or TorB lead to expression of ATP hydrolysis-deficient Torsin molecules (see position in Fig. 4) [Naismith *et al.*, 2004; Hanson and Whiteheart, 2005]. These mutations function as substrate traps, where the mutants can bind, but no longer hydrolyze ATP, exerting dominant-negative effects on the endogenous wild type (WT) proteins when overexpressed in the cell [Whiteheart *et al.*, 1994; Hewett *et al.*, 2000; Hanson and Whiteheart, 2005; Vander Heyden *et al.*, 2009; Rose *et al.*, 2014].

At the cellular level, Torsins play a role in many cellular processes (reviewed in Rose *et al.* [2015]), most of them critically important at the NE.

TorA is involved in NE architecture. It was shown that a TorA knock-out (TorA_{KO}) in mice, as well as expression of TorA Δ E302/303, resulted in severe defects in NE architecture leading to vesicle- or bubble-like structures [Naismith *et al.*, 2004; Goodchild *et al.*, 2005; Kim *et al.*, 2010]. Further, TorA is associated with the KASH domains of the proteins nesprin-1, -2 and -3 [Nery *et al.*, 2008]. The significance of this interaction was not addressed so far but one might speculate that this interaction contributes to nuclear morphology. Furthermore, a knock-down of TorA disrupted the localization of KASH

proteins [Saunders and Luxton, 2016], whereas overexpression of the LULL1 cofactor results in concentration of TorA to the NE, thereby displacing LINC complexes [Vander Heyden *et al.*, 2009]. Besides the LINC complex, TorA might also have an influence on the spacing of the nuclear membranes. Expression of the TorA_{EQ} mutant resulted in reduced spacing between the INM and ONM compared to the WT condition [Naismith *et al.*, 2004]. In accordance, recent publications attribute to Torsins a role in LINC assembly, disassembly or regulation: TorA was shown to interact with SUN1 and SUN2 in a heterologous yeast system [Chalfant *et al.*, 2019], while its localization to the NE was found to be SUN1-dependent [Jungwirth *et al.*, 2011].

However, future studies need to analyze the potential role of Torsins in LINC regulation in order to identify the underlying mechanism.

1.3.5 NPC-independent Transport of Large RNPs and Herpesviral Capsids

Traffic into and out of the nucleus was thought to occur exclusively through NPCs (reviewed in Adam [2001]; Kohler and Hurt [2007]), but the nuclear egress of herpesvirus capsids is an exception (for detailed information see section 1.4). With approx. 125 nm diameter, their size by far exceeds the 40 nm threshold for passing through intact NP [Pante and Kann, 2002]. There is no evidence that infection impairs or alters the function of NPC, even at later stages of infection, pointing to a continued integrity of the NE [Hofemeister and O'Hare, 2008; Nagel *et al.*, 2008].

Beside this, a cellular vesicle-mediated mechanism transporting large ribonucleoproteins (RNP) was discovered in *Drosophila* differentiation at neuromuscular junctions [Hatch and Hetzer, 2012; Speese *et al.*, 2012]. Nuclear import of fragments of the DFz2 (DFz2) receptor results in colocalization of the proteolytic DFz2C fragment in characteristic foci at the NE. These foci colocalize with large RNP complexes, as well as with A-type lamins (LamC). The formation of these DFz2C complexes requires LamC and the cellular PKC. So far, it was assumed that all RNAs and RNP complexes, which are synthesized and assembled in the nucleus, enter the cytoplasm by transit through the NPC [Kohler and Hurt, 2007]. These DFz2C-RNP complexes contain mRNAs encoding for postsynaptic proteins, have an average size of 192 nm and are far too large to pass through unaltered NPC [Pante and Kann, 2002]. Therefore, these large RNP complexes are suggested to leave the nucleus by budding through the nuclear membranes, resembling the herpesviral nuclear egress. After budding, the vesicles probably translocate to sites of synapse formation. In addition to *Drosophila* larval muscle cells, the authors identified similar structures in salivary gland, Schneider-2 (S2) and midgut cells [Speese *et al.*, 2012]. Furthermore, granules in the PNS were described earlier for mice, pointing to an alternate nucleo-cytoplasmic export, without any experimental validation yet [Szollosi and Szollosi, 1988].

Recent evidence revealed Torsins to be involved in remodeling of the NE and important for the translocation of RNP particles from the nucleus into the cytoplasm. A down-regulation of Torsins or the expression of a mutated version resulted in abnormal attachment of the large RNPs to the INM, raising the possibility that Torsins might be involved in INM scission after primary envelopment [Jokhi *et al.*, 2013]. Further, it has been suggested that this Torsin-dependent budding process could be involved in protein quality control [Rose and Schlieker, 2012]. A mutation in the OOC-5 gene (TorA orthologue in *C. elegans*) was shown to result in mislocalized NPC components and impaired nuclear import [VanGompel *et al.*, 2015], also pointing to a contribution of Torsins in NE transport processes. Beside RNP exit, Torsins were described to be involved in herpesvirus nuclear egress (further described in section 1.4.2).

The awareness on the existence of both mechanisms - herpesviral nuclear egress and large RNP budding - as well as the parallels in the molecular mechanism point to a common cellular mechanism. Speese *et al.* [2012] suggest that herpesviruses may make use of a cellular mechanism already used for RNP transport. How much this herpesviral and cellular egress mechanisms have in common has not been clarified yet.

1.3.6 The ESCRT Machinery - A Damage Control Machinery at the NE

First discovered as regulators of cargo sorting in the endocytic pathway [Frankel and Audhya, 2018], the multi-subunit endosomal sorting complex required for transport (ESCRT) pathway was later shown to fulfill essential roles in evolutionarily conserved membrane remodeling processes at the nuclear membrane (reviewed in Hurley [2015]; Olmos *et al.* [2015]; Vietri *et al.* [2015]; Olmos and Carlton [2016]; Vietri *et al.* [2016]; Ventimiglia *et al.* [2018]; Gatta and Carlton [2019]).

The core ESCRT machinery is build from multiple complexes functioning in a highly regulated cascade consisting of ESCRT-I, -II, -III, all composed of a diversity of subunits and the Vps4 (vacuolar protein sorting-associated protein 4) complex. Site-specific adaptor proteins recruit additional factors to assemble the core machinery at different cellular membrane systems, where they initiate membrane bending, vesicle formation and scission from membranes, while the AAA+ ATPase Vps4 subsequently disassembles the ESCRT complexes [Schoneberg *et al.*, 2017; McCullough *et al.*, 2018].

Recent findings suggest an involvement of ESCRT-III in reformation and sealing of the NE after mitosis, NPC insertion and quality control [Olmos *et al.*, 2015; Vietri *et al.*, 2015; Ventimiglia *et al.*, 2018; Gatta and Carlton, 2019]. Moreover, ESCRTs are also required for efficient repair of NE ruptures arising during migration [Denais *et al.*, 2016; Raab *et al.*, 2016] or mechanical stress by cytoskeletal forces [Hatch and Hetzer, 2016]. So far, little is known about the regulation of ESCRT function at the NE. First results point to a role of the INM protein LEM2 contributing to the ESCRT-III activation at the NE [Olmos *et al.*, 2015; Thaller *et al.*, 2019]. LEM2 recruits CHMP7 (charged multivesicular body protein

7), which was shown to be essential for localization of the ESCRT-III components to the NE [Olmos and Carlton, 2016; Denais *et al.*, 2016; Gu *et al.*, 2017].

In addition, the ESCRT pathway was described to assume a prominent role in NPC biogenesis. In growing interphase nuclei, NPCs are suggested to be inserted in the NE by fusion of the inner and ONM (reviewed in D'Angelo *et al.* [2006]; Dultz and Ellenberg [2010]; Otsuka and Ellenberg [2018]). Although the molecular mechanisms underlying this fusion event remain not resolved, ESCRT-III, Vps4 as well as several other cellular proteins like Nups and POMs are described to be involved in this process (reviewed in Fichtman *et al.* [2010]; Otsuka and Ellenberg [2018]). Furthermore, ESCRT-III also serves as a surveillance system for defective NPC assembly intermediates [Webster *et al.*, 2014]. There are speculations that proteins of the LEM-domain family, specifically Heh2 (yeast orthologue of MAN1), recruit the ESCRT-III subunit Snf7 and Vps4 to destabilize malformed NPC assemblies [Webster *et al.*, 2016].

The ESCRT pathway is working at the NE - but to understand how ESCRT-III activation and recruitment function at the molecular level requires more extensive research, focusing on the NE-specific arm of the ESCRT pathway.

1.4 The Escape: How Herpesviruses Exit the Nucleus

Herpesviruses use two different sub-cellular compartments for their assembly. Whereas capsid formation and genome packaging take place in the nucleus, final virus maturation proceeds in the cytoplasm, which requires an efficient translocation through the NE.

A vesicular transport process based on an envelopment and de-envelopment strategy is used at the NE to overcome the barrier [Skepper *et al.*, 2001]. Since PrV belongs to the family of α -herpesviruses this part mainly focuses on the α -herpesvirus nuclear egress. The nuclear egress of mature capsids (Figure 5A) can be divided into three steps (reviewed by Mettenleiter *et al.* [2009]; Johnson and Baines [2011]; Mettenleiter *et al.* [2013]; Banfield [2019]):

- (I) Assembly of the nuclear egress complex (NEC), modulation of the nuclear lamina and recruitment of the nucleocapsid (section 1.4.1).
- (II) Budding of the nucleocapsid at the INM resulting in a primary enveloped virion located in the PNS (section 1.4.2).
- (III) Fusion of the primary envelope with the ONM, releasing the capsid into the cytoplasm (section 1.4.3).

1.4.1 The Nuclear Egress Complex

The NEC, composed of two viral proteins designated as pUL31 and pUL34 in the α -herpesviruses PrV and HSV, is required for efficient translocation of herpesvirus nucleocapsids from the nucleus into the PNS [Reynolds *et al.*, 2001; Fuchs *et al.*, 2002]. pUL31 and pUL34 are well conserved throughout the *Herpesviridae*, having orthologues in HCMV (pUL50 and pUL53), in EBV (BFLF1 and BFLF2) and KSHV (ORF67 and ORF69) [Gonnella *et al.*, 2005; Farina *et al.*, 2005; Milbradt *et al.*, 2007; Camozzi *et al.*, 2008; Santarelli *et al.*, 2008]. Both proteins are essential for efficient nuclear egress of herpesvirus capsids [Johnson and Baines, 2011; Mettenleiter *et al.*, 2013].

pUL34 is a tail-anchored type-II membrane protein, which has a conserved N-terminal region, whereas the C-terminus is variable (Fig. 6A) [Haugo *et al.*, 2011]. It is efficiently anchored in the NE, even in the absence of other viral proteins [Meyer and Radsak, 2000; Schuster *et al.*, 2012; Passvogel *et al.*, 2013]. Large parts of the C-terminal domain can be replaced by domains from orthologue herpesvirus proteins or cellular proteins like Emerin, Lap2 β or LBR [Ott *et al.*, 2011; Schuster *et al.*, 2012].

pUL31 is a soluble nuclear protein containing a variable N-terminus and a more conserved C-terminus. Sequence comparison of pUL31 among the family of *Herpesviridae* revealed four conserved regions (CR1 to 4), in which the interaction domain for NEC

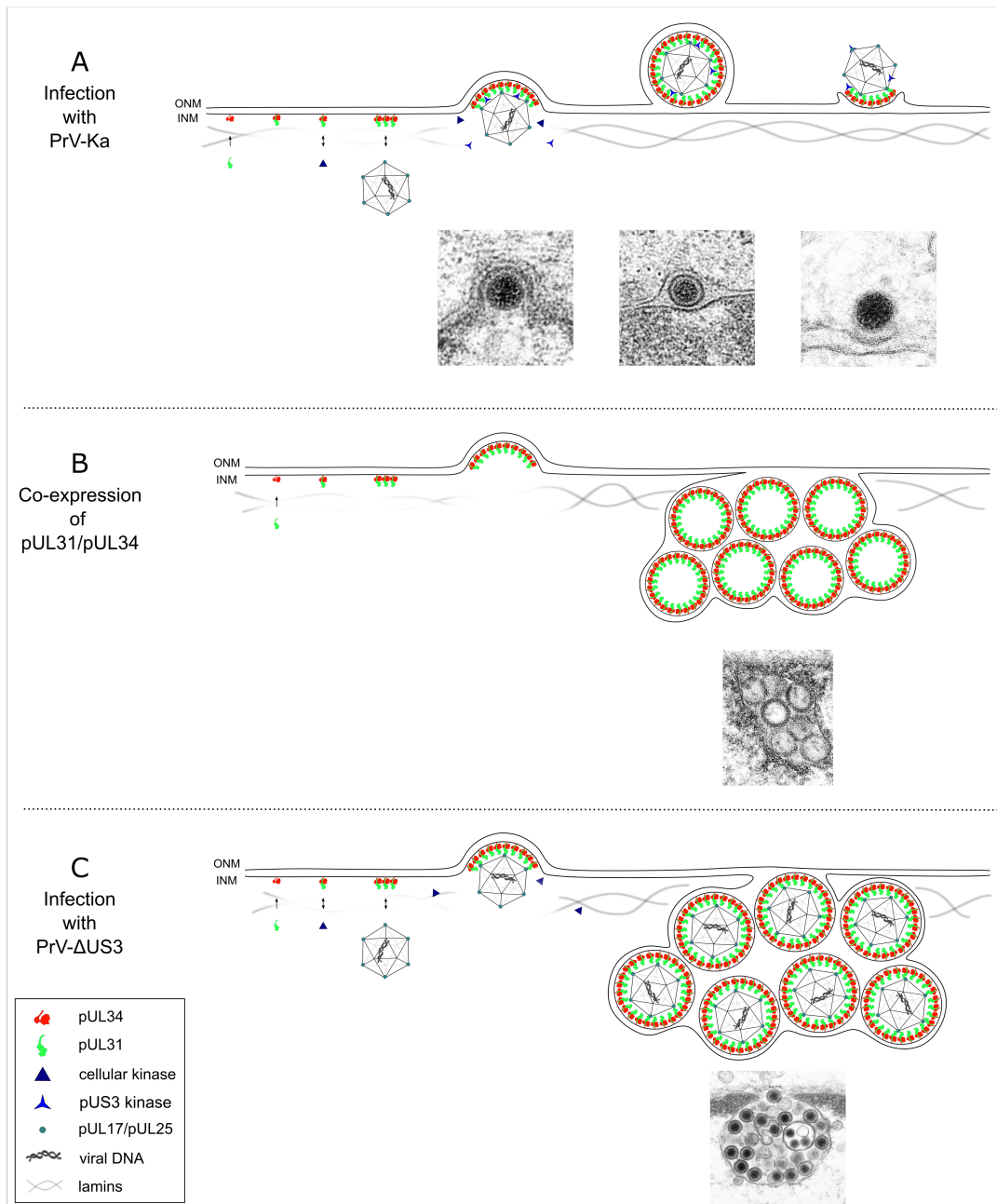


Figure 5: Schematic Model of Nuclear Egress of the Alphaherpesvirus PrV. Membrane remodeling, budding and scission at the INM are mediated by the NEC, build by pUL34 (red), a tail-anchored viral nuclear membrane protein binding the soluble viral pUL31 (green). During infection, the NEC recruits viral and cellular protein kinases, resulting in partial dissolution of the nuclear lamina. Nucleocapsids bud through the INM into the PNS by oligomerization of the NEC. After budding and scission, a primary enveloped virion is located in the PNS. This primary envelope then fuses with the ONM thereby releasing the nucleocapsid into the cytoplasm (A). Co-expression of both proteins in mammalian cells is sufficient for vesicle formation from the INM (B). Infection with a PrV mutant lacking the α -herpesvirus-specific protein kinase pUS3 leads to accumulations of primary enveloped virions in invaginations of the INM (C). The TEM images illustrate the different stages and are kindly provided by FLI's laboratory for electron microscopy, Dr. Kati Franzke.

1 Introduction

formation was mapped to CR1 (Fig. 6A) [Schnee *et al.*, 2006]. pUL31 is transported into the nucleus by a classical bipartite NLS via an importin-mediated translocation [Passvogel *et al.*, 2015; Funk *et al.*, 2015]. Several possible phosphorylation sites were detected in pUL31, e.g. for the PKC [Fuchs *et al.*, 2002] or the viral kinase pUS3 [Mou *et al.*, 2009] thought to regulate UL31 activity. A conserved zinc finger motif consisting of three cysteines contributed by CR1 and a histidine by CR3 takes part in stabilization of the pUL31- and NEC-structure [Zeev-Ben-Mordehai *et al.*, 2015; Bigalke and Heldwein, 2015b; Hagen *et al.*, 2015; Bigalke and Heldwein, 2017]. Mutating the zinc finger motif in PrV pUL31 impairs heterodimer formation [Zeev-Ben-Mordehai *et al.*, 2015]. Both proteins possess a globular core, but pUL31 forms in addition an N-terminal hook reaching around the core and fitting into a groove of pUL34 (see Fig. 6B).

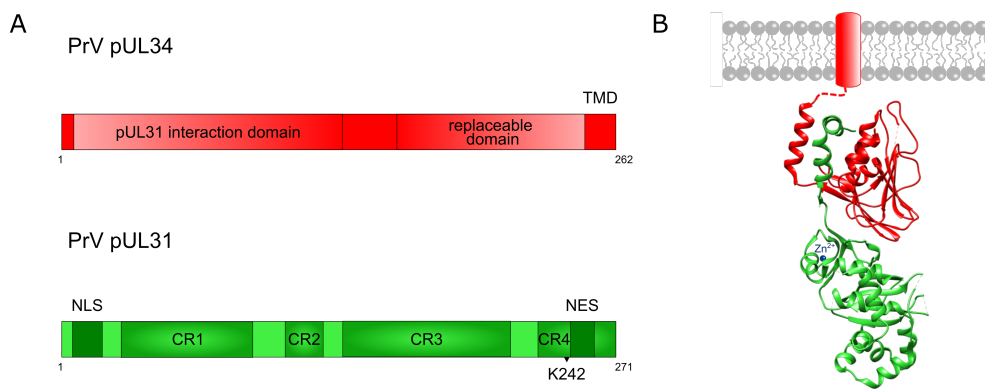


Figure 6: The Nuclear Egress Complex. The schematic domain organization of pUL34 and pUL31 proteins is depicted in (A). In pUL34 the N-terminal region is important for interaction with pUL31, the C-terminal part can be replaced by foreign sequences while the TMD mediates integration in the INM. In pUL31 the conserved regions (CR) 1 to 4, as well as the NLS and the NES are labeled. The K242 position was shown to be important for efficient budding of mature capsids. (B) shows the crystal structure of the PrV NEC (PBD: 5E8C, resolution: 2.9 Å, Zeev-Ben-Mordehai *et al.* [2015]), in which pUL34 is shown in red and pUL31 is depicted in green. Bacterially expressed truncated proteins were used (pUL31: 26-271 aa, pUL34: 1-179 aa) for crystallization. Unresolved regions are specified by dashed lines and the pUL31 bound Zn²⁺ ion is indicated in blue. The INM and the TMD of pUL34 are depicted schematically.

The NEC can partially dissolve the nuclear lamina [Bjerke and Roller, 2006; Reynolds *et al.*, 2004; Simpson-Holley *et al.*, 2004]. This is mediated by recruitment of cellular and viral factors, namely cellular PKC [Park and Baines, 2006; Leach and Roller, 2010] and the viral kinases pUS3 [Mou *et al.*, 2007; Reynolds *et al.*, 2001; Purves *et al.*, 1991] or pUL13 [Cano-Monreal *et al.*, 2009]. Apart from B-type lamins, PKC can also phosphorylate INM proteins like Emerin during HSV-1 infection [Leach *et al.*, 2007; Leach and Roller, 2010], which reduces the association of Emerin to the lamina, thereby potentially contributing to the reorganization of chromatin during infection and to the weakening of the lamina. Furthermore, the NEC can bind directly to A/C-type lamins and thereby disturbs the lamin meshwork resulting in a weakened lamina [Reynolds *et al.*, 2004; Mou *et al.*, 2008]. In contrast to the disintegration of the nuclear lamina during

mitosis, complete dissolution of the lamina would be counterproductive, as the nucleus would lose its stability. Therefore, the lamina network is only partially dissolved during herpesvirus infection [Park and Baines, 2006].

Partial disintegration of the nuclear lamina and reorganization of chromatin [Bjerke and Roller, 2006; Park and Baines, 2006; Mettenleiter *et al.*, 2013] pave the way for the capsid to reach the INM, but how exactly is not yet resolved.

It is possible that by reorganization of the chromatin during infection, the capsids can freely diffuse in the nucleus thereby attaching to the NE by chance [Bosse *et al.*, 2015; Myllys *et al.*, 2016; Aho *et al.*, 2017]. Moreover, it is possible that there is an active transport of the nucleocapsids to the NE via nuclear actin [Forest *et al.*, 2005], although this is discussed controversially [Bosse *et al.*, 2014; Bosse and Enquist, 2016; Myllys *et al.*, 2016]. A third possibility is that the nucleocapsids are recruited from the replication site to NE by pUL31. This could be mediated by conformational changes in the N-terminal domain of pUL31 which subsequently target the bound capsids to the INM [Leelawong *et al.*, 2011; Funk *et al.*, 2015]. Further research is needed to determine the molecular details of this process more precisely.

1.4.2 Envelopment at the INM

During envelopment the newly generated nucleocapsids bud at the INM by oligomerization of the NEC. In the absence of one or both complex partners the nucleocapsids are trapped in the nucleus, while in presence of both, pUL31 is recruited to the INM to form the NEC by direct interaction with the INM-bound pUL34 [Roller *et al.*, 2000; Reynolds *et al.*, 2001; Fuchs *et al.*, 2002]. Interestingly, co-expression of the NEC components is sufficient to mediate membrane bending and budding from the INM of eukaryotic cells and from synthetic lipid membranes [Klupp *et al.*, 2007; Desai *et al.*, 2012; Bigalke *et al.*, 2014; Lorenz *et al.*, 2015]. Generation of empty vesicles in the PNS indicates that no other viral proteins are required for the initial budding step. A schematic model of how vesicle budding occurs in presence of the NEC proteins is presented in Figure 5B.

The process of nuclear egress appears to be of high specificity. Formation of empty vesicles, as seen in co-expression experiments, is rarely observed in WT virus infection [Johnson and Baines, 2011; Mettenleiter *et al.*, 2013], whereas the majority of budding capsids are mature DNA-filled C-capsids [Klupp *et al.*, 2011; Newcomb *et al.*, 2017]. This indicates that oligomerization of the NEC might be blocked until mature nucleocapsids trigger the budding reaction [Klupp *et al.*, 2011; Newcomb *et al.*, 2017]. The capsid vertex-specific component (CVSC), mainly consisting of pUL17 and pUL25, is enriched on mature C-capsids and is likely to be the trigger for this maturation-dependent primary envelopment and might act as an exit permit [Klupp *et al.*, 2006; Trus *et al.*, 2007; Toropova *et al.*, 2011; Newcomb *et al.*, 2017]. Data indicated direct contacts between the CVSC and the NEC using cryo-electron tomography of primary enveloped particles

1 Introduction

[Newcomb *et al.*, 2017]. A direct interaction between pUL31 and a capsid protein was not yet shown for PrV [Leelawong *et al.*, 2011], while for HSV-1 a direct interaction with the CVSC was confirmed [Yang and Baines, 2011; Yang *et al.*, 2014; Takeshima *et al.*, 2019]. For PrV, however, interaction of the capsid and pUL31 was reported also in the absence of pUL25 [Leelawong *et al.*, 2011], allowing docking of capsids to the INM in the absence of pUL25, while budding did not ensue [Klupp *et al.*, 2006]. This points to more than one putative NEC binding partner(s) on the capsid.

Until now, it is also unknown when the NEC dimer is formed and how it interacts with the capsid. Recent analyses suggested the membrane-distal part of pUL31 as the interaction domain to the nucleocapsid [Bigalke *et al.*, 2014; Hagen *et al.*, 2015; Zeev-Ben-Mordehai *et al.*, 2015]. A lysine in the alpha-helical region H10 of PrV pUL31 is crucial for efficient incorporation of the nucleocapsid into budding vesicles (position marked in Fig. 6A) [Rönfeldt *et al.*, 2017]. Replacing the lysine by alanine resulted in accumulation of empty vesicles in the PNS, while mature nucleocapsids were trapped in the nucleus.

Further, it is unclear how higher oligomer formation is triggered and how the complex mediates membrane bending. The recently elucidated crystal structures of the NEC from different *Herpesviridae* revealed high structural similarity with only moderate conservation at aa level [Bigalke and Heldwein, 2015b; Lye *et al.*, 2015; Walzer *et al.*, 2015; Zeev-Ben-Mordehai *et al.*, 2015]. These structural analyses together with data from multi-modal cryo imaging presented a current functional model of capsid envelopment: first a planar NEC layer is formed until nucleocapsids dock to the INM. This docking might change the structural conformation of the oligomerized NEC patch which drives formation of a spherical NEC coat engulfing the budding capsid [Hagen *et al.*, 2015].

Although the budding of vesicles can take place in presence of the NEC, it is not clear whether a cellular protein or mechanism is involved in efficient scission of the vesicles during the infection.

In the cytoplasm, a variety of cellular vesicle formation mechanisms occur, some of which catalyzed by the coordinated action of the ESCRT pathway. The formation of vesicles is induced by the ESCRT-III complex, while the AAA+ ATPase Vps4 dissociates the complex after successful scission [Otsuka and Ellenberg, 2018]. As described in section 1.3.6, the complex is also active at the NE and recent work on HSV-1 suggests a role for ESCRT-III and Vps4 in efficient nuclear egress [Arii *et al.*, 2018], while conflicting findings have been reported [Crump *et al.*, 2007; Kharkwal *et al.*, 2014].

Since budding of large RNPs at the INM was described to resemble herpesvirus nuclear egress and TorA is thought to play a role in the scission these vesicles (see section 1.3.5), a similar mechanism could be assumed for herpesviruses. Recent analyses revealed that a KO of TorA, as well as of TorA and TorB in combination, only had minor effects on HSV-1 replication showing no defect in nuclear egress [Turner *et al.*, 2015]. Another

study showed that TorA, as well as TorB overexpression resulted in virus-like vesicles which were identified as primary virions in cytoplasmic structures, most likely in the ER [Maric *et al.*, 2011]. Interestingly, those vesicles were shown to contain TorA and pUL34, pointing to efficient budding at the INM and an impairment of the de-envelopment process of primary enveloped virions which promotes their escape into the ER.

Members of the vesicle-associated membrane protein (VAMP) family, which are involved in cellular vesicle-associated transport processes, were described to accumulate in the nuclear fraction after HSV-1 infection [Saiz-Ros *et al.*, 2019]. While VAMP7 was not characterized in detail, the vesicle-associated protein (VAP) B was shown to colocalize with pUL34. A knock-down of the VAPB protein reduced viral progeny titers with accumulation of viral particles in the nucleus, pointing to a role in efficient vesicle budding at the INM.

The LINC complex was described to have an important role in nuclear spacing (see section 1.3.4.3). Since budding of the nucleocapsids of about 125 nm requires more space than the regular spacing of the NE (approx. 30 to 50 nm) [Cain and Starr, 2015], a structural reorganization of the LINC complex is assumed. At the same time, the spacing between the primary envelope and both nuclear membranes remains similar during infection [Klupp *et al.*, 2017]. It was recently demonstrated that the expression of SUN2_{LD}, which was described to disturb endogenous protein function in a dominant-negative manner [Crisp *et al.*, 2006], resulted in a severe dilation of the PNS and ER, as well as an escape of primary enveloped virions from the PNS into the ER during PrV infection [Klupp *et al.*, 2017]. This was accompanied by a 10-fold titer decrease. Accordingly, the structural reorganization seems important, while the maintenance of the LINC complex integrity is required for efficient nuclear egress of PrV.

1.4.3 De-envelopment at the ONM

During de-envelopment, the nucleocapsid is released into the cytoplasm by fusion of its primary envelope with the ONM. The underlying mechanism is unknown.

The proteins gD, gH and gB are part of the viral fusion machinery mediating entry of the virus [Eisenberg *et al.*, 2012] and were reasonable candidates for mediating fusion step leading to de-envelopment at the ONM. In HSV-1-infected cells all three were found to localize at the NE using immuno-gold labeling in TEM analyses [Stannard *et al.*, 1996; Skepper *et al.*, 2001]. Although primary enveloped virions are heavily coated with gold particles specifically binding gD [Skepper *et al.*, 2001], further analyses revealed that gD is not involved in nuclear egress. Its deletion did not alter the exit from the nucleus [Farnsworth *et al.*, 2007]. However, the combined deletion of gB and gH [Farnsworth *et al.*, 2007], as well as mutations in the fusion loops of gB in concurrent absence of gH [Wright *et al.*, 2009], resulted in an accumulation of primary enveloped virions in the

1 Introduction

PNS. A single deletion or mutation showed only minor or no defects in nuclear egress [Farnsworth *et al.*, 2007]. However, nuclear egress was not blocked completely, since intracytoplasmic nucleocapsids as well as mature virions on the cell surface were observed.

As for HSV-1 infection, the single deletion of either gD, gH or gB did not affect nuclear egress in PrV infection. Interestingly, and in contrast to HSV-1, the simultaneous deletion of gB and gH did not impede nuclear egress of PrV [Klupp *et al.*, 2008]. Additionally, none of the tested viral glycoproteins were found either at the nuclear membrane or in primary virions during PrV infection [Klupp *et al.*, 2008]. These results indicate that the fusion mechanisms utilized for entry and egress are distinct and that a different fusion mechanism has to exist which mediates the efficient exit from the nucleus.

Another viral protein which seems to play a role in the secondary egress step and which is incorporated into the primary enveloped virions is the viral serine/threonine kinase pUS3, only found in the α -herpesvirus subfamily [Granzow *et al.*, 2004]. pUS3 is required for efficient de-envelopment of primary enveloped virions [Klupp *et al.*, 2001; Reynolds *et al.*, 2002]. In the absence of pUS3 (Δ US3) [Purves *et al.*, 1987; Wagenaar *et al.*, 1995; Klupp *et al.*, 2001; Reynolds *et al.*, 2002] or after impairment of its kinase function (US3 Δ kin) [Kato *et al.*, 2011; Sehl *et al.*, 2020], primary enveloped virions accumulate in invaginations of the INM pointing to a regulatory role in efficient nucleocapsid release. However, pUS3 is not essential for viral egress, since viral progeny titers are only approx. 10-fold reduced in most α -herpesviruses and cell lines tested [Purves *et al.*, 1987; Wagenaar *et al.*, 1995; Klupp *et al.*, 2001; Reynolds *et al.*, 2002; Kato *et al.*, 2011; Sehl *et al.*, 2020].

The pUS3-phosphorylation of pUL31, rather than pUL34, was shown to possess a regulatory role on the NEC [Purves *et al.*, 1991, 1992; Ryckman and Roller, 2004; Mou *et al.*, 2009]. After budding into the PNS, this phosphorylation might weaken the inter-complex interactions thereby changing the binding affinity between capsid and NEC enabling the capsid release [Bigalke and Heldwein, 2016; Newcomb *et al.*, 2017]. For PrV, pUS3 is not essential for the phosphorylation of pUL34, but it promotes its efficient localization to the NE [Klupp *et al.*, 2001]. A schematic model of how virus budding in absence of the viral kinase pUS3 occurs is presented in Figure 5C.

HSV-1 mutants lacking the viral proteins pUL20 [Baines *et al.*, 1991], pUL48 [Mossmann *et al.*, 2000] or pUL51 [Nozawa *et al.*, 2005] showed accumulations of enveloped virions in the PNS and were suggested to have defects in the final de-envelopment step. However, the knowledge on the function of these proteins in nuclear egress is limited. For PrV, no effects were detected deleting these genes.

Since no other viral proteins were found to be critically involved in herpesvirus nuclear egress, a cellular pathway is most likely. Although some candidates have already been examined in this context, little is known about the molecular mechanism.

1.4 *The Escape: How Herpesviruses Exit the Nucleus*

Cellular factors including p32, CD98hc (heavy chain) and β 1 integrin were described to be recruited to the NE upon HSV-1 infection [Hirohata *et al.*, 2015; Liu *et al.*, 2015]. Changes in the expression of those proteins resulted in accumulation of primary enveloped virions in the PNS, pointing to an involvement in de-envelopment.

Considering the results regarding the LINC complex and that TorA is a promising candidate for LINC complex regulation, the investigation the role of Torsins in the nuclear egress with a focus on the de-envelopment form an exciting starting point.

1.5 CRISPR Genome Editing, a Tool for Identification of Cellular Key Players

In 2013, the CRISPR/Cas9 technology emerged as a powerful tool for precise genome editing in eukaryotic cells [Jinek *et al.*, 2012; Cong *et al.*, 2013; Mali *et al.*, 2013]. We used this innovative tool to investigate the role of cellular proteins in the PrV replication cycle by generation of KO cell lines.

Originally the system was discovered as the adaptive immune system of prokaryotes (reviewed in Garneau *et al.* [2010]). Bacteria and archaea can respond to infections by incorporation of small DNA fragments of bacteriophages that have previously infected the cell [Jansen *et al.*, 2002]. The foreign fragments are integrated into the genome as spacers within the 'clustered regularly interspaced short palindromic repeat' (CRISPR) locus. Several spacer regions are stored and later transcribed as guide RNA (gRNA) consisting of a CRISPR RNA (crRNA) and the trans-activating crRNA (tracrRNA). They allow the precise degradation of the foreign DNA by binding of effector proteins, namely CRISPR-associated (Cas) ribonucleoproteins.

In detail, after specific recognition of the foreign DNA by binding of the gRNA, the Cas protein is guided to the binding site and induces a double-strand break (DSB) (reviewed in Rath *et al.* [2015]). CRISPRs are found in approx. 50% of all sequenced bacterial genomes and in 90% of the archaea [Grissa *et al.*, 2007; Hille *et al.*, 2018]. CRISPR systems are organized in two classes: while class I CRISPR systems need combinations of multiple Cas proteins, the class II system is based on only one large Cas protein [Makarova *et al.*, 2011].

The Cas enzyme together with CRISPR sequences form the basis of the gene editing technology known as CRISPR/Cas9. In this thesis, a modified class II CRISPR system of *Streptococcus (S.) pyogenes* was used to investigate the role of cellular proteins in the PrV replication cycle. For this, the pX330-NeoR vector was used, which is a modified version of pX330-U6-Chimeric_BB-CBh-hSpCas9 (*Addgene*, #42230) carrying an additional expression cassette for G418 resistance [Hübner *et al.*, 2018]. This allows the selection of transfected mammalian cells. The vector contains a variable spacer region (synthetic crRNA), which is important for recognition of the desired target sequence (protospacer) after transfection. The tracrRNA following the crRNA provides the stem-loop-structure important for the binding and the catalytic activity of the Cas9 nuclease. In contrast to the bacterial system, the normally individual parts crRNA and tracrRNA are combined by a -GAAA- linker to make a single chimeric gRNA. Usage of this chimeric gRNA results in 5-fold increased efficiency [Jinek *et al.*, 2012; Briner *et al.*, 2014; Cong *et al.*, 2013].

The synthetic crRNA part of the gRNA has to be properly chosen to target the genome region of interest and to avoid off-target effects [Zhang *et al.*, 2015]. Additionally, the vec-

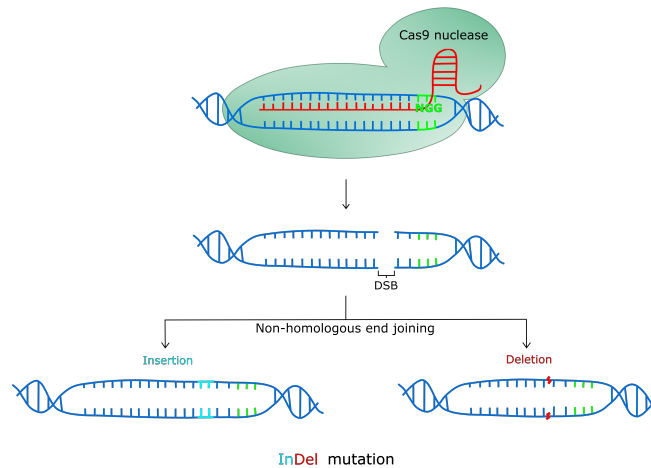


Figure 7: Schematic Model on how a Double Strand Break is Induced by Cas9 and Repaired by NHEJ during CRISPR/Cas9 Mutagenesis.

tor contains an improved version of *S. pyogenes* Cas9 which is human codon-optimized and also contains two NLS added to each terminus [Cong *et al.*, 2013]. In the nucleus, Cas9 binds to the region of interest dependent on the single gRNA and the protospacer adjacent motif (PAM) site. This PAM site follows immediately 3' of the protospacer, the complementary sequence of the gRNA. Different Cas9 proteins need different PAM sequences. Cas9 from *S. pyogenes* is dependent on the sequence 5'-NGG-3', where N can be any nt [Hsu *et al.*, 2013]. Upon binding of the gRNA to the protospacer, Cas9 induces a DSB two to three base pairs upstream of the PAM sequence [Doudna and Sontheimer, 2014] (see Fig. 7).

In this thesis, the CRISPR/Cas9 system was used to target the exons encoding the N-terminal part of proteins. Introduction of DSBs activate the error-prone cellular repair mechanism called non-homologous end joining (NHEJ) [Lieber, 2008], resulting in small insertions or deletions (InDel). This in turn can cause frame-shift mutations and lead to premature stop codons, thereby targeting the corresponding transcript either for degradation by nonsense-mediated mRNA decay or result in translation of a truncated protein [Reber *et al.*, 2018]. The generation of gene KOs in diploid cells requires mutations on both alleles.

Beside the described application of CRISPR/Cas9, the method can also be used for complete gene deletions, gene insertions by using homology-directed repair mechanisms, RNA targeting, base editing, gene regulation like CRISPR interference or CRISPR activation, gene therapy using viral vectors and high-throughput loss or gain of function screens with the help of genome-wide CRISPR libraries (reviewed in Pickar-Oliver and Gersbach [2019]).

1.6 The Objectives

Herpesvirus assembly and maturation take place in two different sub-cellular compartments: Newly assembled nucleocapsids have to overcome the NE barrier for their final maturation in the cytoplasm. To exit the nucleus, herpesviruses use a vesicle-mediated transport process. The main goal of this project was to provide a better understanding of how herpesviruses exit the nucleus focusing on the involved cellular and viral key players.

To date, the molecular mechanisms of de-envelopment during nuclear egress have not been elucidated and the question how the primary envelope is fused with the ONM remains unanswered. Neither the analysis of viral nor cellular proteins has revealed the molecular mechanism underlying this fusion event. Previous publications on the role of Torsin proteins in NE maintenance and modulation [Naismith *et al.*, 2004; Goodchild and Dauer, 2005; Jungwirth *et al.*, 2010; Kim *et al.*, 2010], vesicle transport through the NE [Jokhi *et al.*, 2013; Rose and Schlieker, 2012] as well as their already described role in herpesvirus infection [Maric *et al.*, 2011; Turner *et al.*, 2015] make them interesting candidates. In this thesis, the role of Torsins in the fusion of the primary envelope with the ONM was investigated in the context of PrV infection. In detail, I aimed at addressing the function of TorA and TorB in PrV infection either by generation of stable cell lines over-expressing GFP-tagged TorA or TorB constructs or by generation of KO cell lines by CRISPR/Cas9. Subsequently, these cell lines have been analyzed for their ability to replicate PrV to WT-like titers and ultrastructurally to visualize potential effects during nuclear egress. Elucidating the key components of the viral vesicular transport might also reveal further information on a putative underlying cellular pathway.

The NEC is the key viral player mediating the translocation of newly formed capsids from the nucleus into the PNS. The primary envelopment process and the NEC have been extensively investigated in the last decades without revealing all its details. In the second part, I focused on the budding process and planned to generate monoclonal antibodies (mAbs) against the NEC and its single components. The generation of NEC-specific mAbs should allow the analysis of the localization, expression kinetics and potential cofactors without visualizing a background of monomeric proteins. In addition, TEM analyses of immuno-gold labeled infected cells could help to answer where in the cell the NEC is formed and disassembled.

Finally, the interaction interface of the NEC with the nucleocapsid should be further analyzed. This is based on the finding that a lysine (K) at position 242 in the most membrane-distal part of the pUL31 component of the NEC is crucial for efficient incorporation of the nucleocapsid into budding vesicles. Replacing that lysine by alanine (A) resulted in an accumulation of empty vesicles in the PNS, while the mature nucleocapsids remained in the nucleus [Rönfeldt *et al.*, 2017]. To test whether the uptake

of the capsid into nascent vesicles is due to electrostatic interactions, this position was substituted by alanine and by other aa using site-directed mutagenesis thereby changing charge and size of the side chains. The resulting mutant proteins were used for complementation experiments. Furthermore, we generated and investigated revertants resulting from passaging of a PrV-Ka-UL31-K242A virus mutant.

Publications 2

Paper I:
**Function of Torsin AAA+ ATPases in Pseudorabies
Virus Nuclear Egress**




Julia E. Hölper, Barbara G. Klupp, G. W. Gant Luxton, Kati Franzke and
Thomas C. Mettenleiter

Cells
Volume 9, Article 738
Special Issue: Vesicular Trafficking Meets Nuclear Transport
DOI: 10.3390/cells9030738

March 2020

Article

Function of Torsin AAA+ ATPases in Pseudorabies Virus Nuclear Egress

Julia E. Hölper ¹ , Barbara G. Klupp ¹, G. W. Gant Luxton ² , Kati Franzke ³ and Thomas C. Mettenleiter ^{1,*} 

¹ Institute of Molecular Virology and Cell Biology, Friedrich-Loeffler-Institut, 17493 Greifswald-Insel Riems, Germany; julia.hoelper@fli.de (J.E.H.); barbara.klupp@fli.de (B.G.K.)

² Department of Genetics, Cell Biology and Development, University of Minnesota, Minneapolis, MN 55455, USA; gwgl@umn.edu

³ Institute of Infectology, Friedrich-Loeffler-Institut, 17493 Greifswald-Insel Riems, Germany; kati.franzke@fli.de

* Correspondence: thomas.mettenleiter@fli.de; Tel.: +49-38351-71250; Fax: +49-38351-71151

Received: 1 February 2020; Accepted: 15 March 2020; Published: 17 March 2020



Abstract: Newly assembled herpesvirus nucleocapsids traverse the intact nuclear envelope by a vesicle-mediated nucleo-cytoplasmic transport for final virion maturation in the cytoplasm. For this, they bud at the inner nuclear membrane resulting in primary enveloped particles in the perinuclear space (PNS) followed by fusion of the primary envelope with the outer nuclear membrane (ONM). While the conserved viral nuclear egress complex orchestrates the first steps, effectors of fusion of the primary virion envelope with the ONM are still mostly enigmatic but might include cellular proteins like SUN2 or ESCRT-III components. Here, we analyzed the influence of the only known AAA+ ATPases located in the endoplasmic reticulum and the PNS, the Torsins (Tor), on nuclear egress of the alphaherpesvirus pseudorabies virus. For this overexpression of wild type and mutant proteins as well as CRISPR/Cas9 genome editing was applied. Neither single overexpression nor gene knockout (KO) of TorA or TorB had a significant impact. However, TorA/B double KO cells showed decreased viral titers at early time points of infection and an accumulation of primary virions in the PNS pointing to a delay in capsid release during nuclear egress.

Keywords: herpesvirus; pseudorabies virus; nuclear egress; AAA+ ATPase; Torsin; CRISPR/Cas9

1. Introduction

Herpesviruses are double-stranded DNA viruses, which use the host cell nucleus and the cytoplasm for replication and morphogenesis. While transcription, DNA replication, assembly of viral capsids as well as viral genome encapsidation take place in the nucleus, the nucleocapsid has to be transferred to the cytoplasm for final virion maturation. With a diameter of approximately 125 nm, its size far exceeds the 40 nm threshold for passage through intact nuclear pores [1]. However, no evidence for a significant impairment or alteration of barrier and gating functions of nuclear pores was found even at late time points after infection [2] demonstrating continued integrity of the nuclear envelope.

In eukaryotic cells, the nuclear envelope (NE) separates the nuclear contents from the cytoplasm. It consists of two concentric lipid bilayers designated as the inner (INM) and outer nuclear membrane (ONM) which are separated by the perinuclear space (PNS). The PNS is contiguous with the lumen of the endoplasmic reticulum (ER) as is the ONM with the ER membrane. In contrast, the INM harbors a unique set of membrane proteins distinct from that of the ONM and ER. INM and ONM are fused at sites where nuclear pore complexes (NPCs) are inserted, which also allow the import of the herpesviral

genome at early stages of infection. Traffic into and out of the nucleus is thought to occur exclusively through NPCs (reviewed in Adam [3], Knockenhauer and Schwartz [4]). Interestingly, herpesvirus nucleocapsids are translocated through the nuclear envelope (NE) by a vesicle-mediated process designated as nuclear egress (reviewed in [5–7]).

Budding of herpesvirus nucleocapsids at the INM is driven by the nuclear egress complex (NEC) composed of two conserved herpesviral proteins designated as pUL31 and pUL34 in the alphaherpesviruses pseudorabies virus (PrV) and herpes simplex viruses (HSV-1, -2) [5–7]. The NEC is not only required for efficient nuclear egress, thereby generating primary enveloped virions in the PNS, but also sufficient for vesicle formation and scission from artificial lipid membranes and the INM, [8–11]. In a subsequent step, this primary envelope fuses with the ONM to release the nucleocapsids into the cytoplasm (reviewed in [12]).

Budding of nucleocapsids at the INM is quite well understood at the molecular level, while the fusion process of the primary envelope with the ONM remains mostly enigmatic. In contrast to reports for HSV-1 [13], the viral fusion machinery which is active during entry of herpesviruses is not involved in nuclear egress of PrV [14]. In addition, a variety of different PrV gene deletion mutants studied so far showed no detectable effect on nuclear egress arguing against a virus-encoded fusion machinery active at the NE. Only mutants lacking the alphaherpesvirus specific protein kinase pUS3 showed an impairment of nuclear translocation. In the absence of pUS3 [15–17] or by impairment of its kinase function [18–20] primary enveloped virions accumulate in herniations of the INM. However, pUS3 is not essential for viral replication and viral titers are only approx. 10-fold reduced. Based on these data, we speculated that herpesviruses might use a cellular machinery either already present in or recruited to the NE.

Although vesicle-mediated transport processes between cytoplasmic organelles and the plasma membrane are well studied, knowledge on vesicular transport and fusion events at the NE is poor. An example of such a cellular mechanism would be the fusion of the INM with the ONM that occurs during NPC insertion in a growing interphase nucleus (reviewed in Otsuka and Ellenberg [21]). This process is thought to involve an inside-out extrusion of the INM into and across the PNS followed by its subsequent fusion with the ONM [22,23]. Although the molecular mechanism underlying INM-ONM fusion remains incompletely understood, several cellular proteins have been implicated in this process including the multi-subunit endosomal sorting complex required for transport III (ESCRT-III) and the ATPase-associated with various cellular activities (AAA+) protein Vps4 (reviewed in Otsuka and Ellenberg [21]). Recent work suggests that ESCRT-III and Vps4 are also important for herpesvirus nuclear egress [24–26], but conflicting findings have been reported [27,28].

Two other potential cellular mediators of INM-ONM fusion during interphase NPC insertion are Torsin A (TorA) and TorB. As similar to Vps4, Torsins belong to the AAA+ ATPase superfamily. They function as molecular chaperones, which use energy derived from ATP-hydrolysis to remodel their target molecules and are involved in numerous processes including budding and fission of vesicles, and assembly as well as disassembly of protein complexes [29–35]. Torsins are composed of a N-terminal signal peptide, followed by a hydrophobic stretch (TorA and TorB) upstream of the Walker A and B motifs, which mediate ATP binding and hydrolysis [32]. TorA (*TOR1A*) and TorB (*TOR1B*) are atypical AAA+ proteins for the following three reasons. First, they contain a non-canonical Walker A motif [36]. Second, they and the related Tor2 (*TOR2A*), Tor3 (*TOR3A*), and Tor4 (*TOR4A*) proteins are the only AAA+ proteins known to reside within the contiguous ER lumen and PNS of the nuclear envelope [32,37–39]. Third, they lack the conserved ATP-hydrolysis-promoting arginine finger [35,40]. Consistent with the lack of an arginine finger, purified Tor proteins are unable to hydrolyze ATP in vitro [41]. Instead, they need to be activated by the direct interaction with the luminal domain of one of two known regulatory protein cofactors: the INM lamina-associated polypeptide 1 (LAP1) or the ER/ONM protein luminal domain-like LAP1 (LULL1). Mutations in TorA lead to an autosomal dominant disease in humans, called early-onset torsion dystonia 1 (DYT1/TOR1A dystonia) [42]. The most frequent disease linked form TorA Δ E302/303 lacks a single glutamic acid residue

at position Glu₃₀₂ or Glu₃₀₃ in the C-terminus of the protein [43–45]. None of the other Torsins are implicated in human disease. Nonetheless, EQ mutations in the Walker B domain of TorA or TorB lead to expression of ATP hydrolysis-deficient Torsin molecules [33,45] which exert dominant-negative effects [38,46,47]. While the substrates of TorA and TorB remain unknown, they and the related proteins Tor2 and Tor3 appear to function in a partially redundant manner [48–50]. Furthermore, in previous studies, TorA has been shown to play a role in NE maintenance. Specifically, severe defects in NE architecture with “blebbing” of the INM in neuronal tissue are observed in knockout (KO) mice or mice lacking proper Torsin function, by expression of the dystonia-related allele TorA Δ E302/303 [37,45,50–53]. This phenotype is reminiscent of the INM herniations, which were observed in cells overexpressing the NEC components [8] or in cells infected with US3-deletion mutants [15–17].

Consistent with a potential role during herpesvirus nuclear egress, overexpression of TorA or TorB resulted in slightly reduced HSV-1 titers in neuron-like and epithelial cells, as well as in the appearance of primary enveloped virions in cytoplasmic vesicles [54]. Moreover, HSV-1 replication was reduced in HeLa cells lacking both TorA and TorB [55]. To date, the molecular mechanism underlying the contribution of TorA and TorB to herpesvirus nuclear egress as well as interphase NPC biogenesis remains poorly defined. Nevertheless, a growing body of evidence supports the hypothesis that TorA is required for the assembly of functional linker of nucleoskeleton and cytoskeleton (LINC) complexes [39,48,56–59]. This conserved NE-spanning molecular bridge is present in all nucleated cells [60,61] and mechanically integrates the nucleus with the cytoskeleton mediating several fundamental cellular processes including cell division, DNA damage repair, meiotic chromosome pairing, mechano-regulation of gene expression, and nuclear positioning (reviewed in Meinke and Schirmer [62]).

LINC complexes are composed of ONM Klarsicht/ANC-1/SYNE homology (KASH)-domain and INM Sad1/UNC-84 homology (SUN)-domain containing proteins [63,64]. Although the LINC complex is involved in many essential cellular processes, it is still unknown how assembly and disassembly is achieved. TorA is reported to have affinity for the KASH domains of nesprin-1, -2, and -3 [56]. In addition, TorA was shown to interact with SUN1 and SUN2 in a heterologous system [48], while its localization to the NE was found to be SUN1-dependent [65]. Furthermore, a knockdown of TorA disrupted the localization of KASH proteins [66]. Interestingly, recent evidence proposed a role for Torsins in the translocation of large ribonucleoprotein (RNP) particles from the nucleus into the cytoplasm in neuromuscular junctions in *Drosophila* [67] through a pathway which mechanistically resembles nuclear egress of herpesvirus [68].

For PrV, we recently demonstrated that expression of the luminal SUN2 domain, which was described to disturb normal function in a dominant-negative (dn) manner [64], resulted in lower virus titers, a severe dilation of the PNS and the ER, and an escape of primary enveloped virions from the PNS into the ER [69]. Since this was similar to the effect reported for TorA overexpression on HSV-1 [54], we were interested to study the function of TorA and B in PrV infection. Here, we overexpressed GFP-tagged wild type or mutant proteins and used the CRISPR/Cas9 genome editing system for generation of cell lines lacking TorA, TorB and TorA/B to examine how modulation of their expression affects PrV replication with special focus on nuclear egress.

2. Material and Methods

2.1. Cells and Virus

Rabbit kidney cells (RK13, CCLV-Rie 109) were cultivated in Dulbecco’s modified Eagle’s minimum essential medium supplemented with 10% fetal calf serum, provided by the Friedrich-Loeffler-Institute bio bank (Greifswald, Insel Riems, Germany). PrV strain Kaplan (PrV-Ka) [70] was propagated on RK13 cells. RK13 cells were used throughout this study since (I) they propagate PrV to high titers; (II) are easy to transfect; (III) tolerate a wide panel of foreign protein expression; and (IV) are intensively studied in our laboratory for many years.

2.2. DNA Constructs

SS-EGFP-TorA_{WT}, SS-EGFP-TorA_{ΔE302/303}, SS-EGFP-TorB_{WT}, and SS-EGFP-TorB_{E178Q} constructs used in this work had been described [37,44,52,57]. Plasmid pDsRed2-ER was purchased from Takara Bio Europe, Inc. Constructs used to perform CRISPR/Cas9-mediated genome editing were generated as follows. Guide RNAs (gRNAs) were designed by targeting the first exon of TorA (*TOR1A*) or TorB (*TOR1B*) as predicted in the rabbit genome OryCun2.0 (*Oryctolagus cuniculus*, ensemble.org [71]) with the help of the online tool (<http://crispr.mit.edu/>). Four gRNAs with the highest score and the lowest probability for off-target effects were selected for each gene (Table 1). gRNAs were ordered as unmodified DNA oligonucleotides (MWG Eurofins, Ebersberg, Germany) with BbsI restriction overhang, hybridized and inserted into the BbsI-digested vector pX330-NeoR (kindly provided by Dr. W. Fuchs), which is a modified version of pX330-U6-Chimeric_BB-CBh-hSpCas9 (Addgene, Watertown, MA, USA, #42230) carrying an additional expression cassette for a G418 resistance for selection (previously described in Hübner, et al. [72]). The correct cloning of gRNAs was verified by Sanger sequencing at the Friedrich-Loeffler-Institut with HU6-F primer (5'-ATAATTTCTTGGGTAGTTTGCAG-3').

Table 1. Oligonucleotide sequences. Compatible 5' overhangs for restriction enzyme BbsI used for cloning are underlined.

Name	Sequence (5'–3')
TorA_gRNA#1_Fwd	<u>CACCCTGGCGGTAGCGCCGTCGG</u>
TorA_gRNA#1_Rev	<u>AAACCCGACCGCGCTACCGCCAG</u>
TorA_gRNA#2_Fwd	<u>CACCTGTCTGGCGGTAGCGCCGGT</u>
TorA_gRNA#2_Rev	<u>AAACACCGGCGCTACCGCCAGACA</u>
TorA_gRNA#3_Fwd	<u>CACCCGCGGTCGGTGGTCAGCGC</u>
TorA_gRNA#3_Rev	<u>AAACCGCTGACCACCGACCGCGG</u>
TorA_gRNA#4_Fwd	<u>CACCGTTCCTGCGCTGACCACCGA</u>
TorA_gRNA#4_Rev	<u>AAACGTCGGTGGTCAGCGCAGGAA</u>
TorB_gRNA #1_Fwd	<u>CACCGTGATTCTGAAGGCGCTGAC</u>
TorB_gRNA #1_Rev	<u>AAACGTCAGCGCCTCAGAATCAC</u>
TorB_gRNA #2_Fwd	<u>CACCCGCCTCAGAATCACTCCG</u>
TorB_gRNA #2_Rev	<u>AAACCGGAAGTGATTCTGAAGGCG</u>
TorB_gRNA #3_Fwd	<u>CACCTTTTGGTTTTTGGTAACGA</u>
TorB_gRNA #3_Rev	<u>AAACTCGTTACCAAAAACCAAAAA</u>
TorB_gRNA #4_Fwd	<u>CACCGAAGCTGTTCCGACAGCATC</u>
TorB_gRNA #4_Rev	<u>AAACGATGCTGTCCGAACAGCTTC</u>

2.3. Transfection of Cells for Co-Localization Studies

RK13 cells were seeded on coverslips in a 24-well dish and transiently co-transfected by calcium phosphate-precipitation [73] with an ER marker protein plasmid (pDsRed2-ER, Takara Bio Europe Saint-Germain-en-Laye, France) and plasmids expressing the GFP-tagged constructs. We used the calcium phosphate-coprecipitation method, although it is not very efficient, because it is milder to the cells and therefore allows to capture qualitative images later on.

2.4. Immunoblotting

Cells were transfected with 1 µg of plasmid DNA using polyethylenimine (PEI) [74], and harvested 24 h post transfection by scraping into the medium, pelleted, washed twice with phosphate-buffered saline (PBS) and lysed in SDS-containing sample buffer (0.13 M Tris-HCl, pH 6.8; 4% SDS; 20% glycerin; 0.01% bromophenol blue; 10% 2-mercaptoethanol). Here we used PEI transfection, instead of calcium phosphate-precipitation method, because PEI transfection is more efficient. Proteins were separated in SDS 10% polyacrylamide gels and after transfer to nitrocellulose membranes, blots were probed with a rabbit anti-GFP serum (kindly provided by Dr. G. M. Keil, FLI, Insel Riems, Germany) and a monoclonal antibody specific for alpha-tubulin (Sigma-Aldrich, Munich Germany, T5168) as loading

control. After incubation with secondary peroxidase-labelled antibodies and substrate (Clarity ECL western Blot substrate, Bio-Rad, Feldkirchen, Germany), chemiluminescence was recorded in a Bio-Rad Versa Doc imager.

2.5. Generation of Stably Expressing RK13 Cell Lines

For generation of cells stably overexpressing wild type or mutant forms of Torsins A and B, cells in a 6-well dish were transfected by calcium phosphate-coprecipitation [73] using 1.5 µg of plasmid DNA expressing protein constructs schematically depicted in Figure 1. Two days after transfection, cells were transferred to 10 cm plates (Corning, Kaiserslautern, Germany) and selected in medium containing 500 µg/mL G418 (Invitrogen, Schwerte, Germany). Ten to 14 days after transfection GFP-positive cell colonies were picked by aspiration and further analyzed. Cell clones were seeded on cover slips in a 24-well plate for analysis of protein localization.

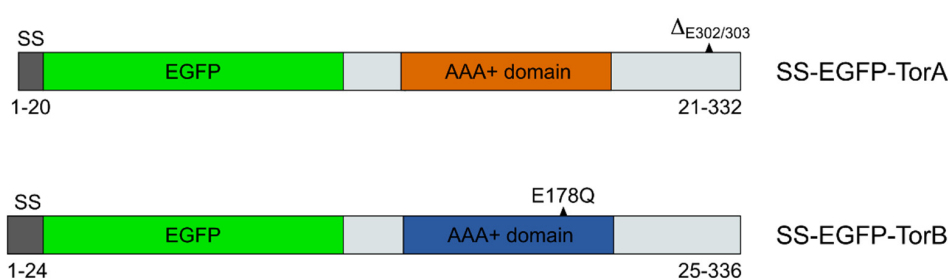


Figure 1. Schematic depiction of expression constructs used in this study. All constructs carried EGFP at the N-terminus. Mutations resulting in loss-of-function in TorA and B are indicated. Numbers given below represent the corresponding amino acid residues of the Torsins in the constructs used. SS: signal sequence.

2.6. Generation of Stable RK13 Knockout Cell Lines

Stable KO cell lines were generated by co-transfection of all four gRNA-containing pX330-NeoR constructs (1.5 µg per plasmid) using calcium phosphate-co-precipitation [73]. For DKO, all eight plasmids were co-transfected simultaneously. Two days after transfection in 6 well dishes, cells were transferred to 10 cm plates (Corning) and selected in medium containing 500 µg/mL G418 (Invitrogen). Ten to 14 days after transfection cell colonies were picked by aspiration and tested for KO by sequencing of the targeted gene sequence.

2.7. Test for Bi-Allelic Gene Knockout

DNA of the potential KO cell clones was isolated using Bradley Lysis Buffer (10 mM Tris, 10 mM EDTA, 0.5% SDS, 10 mM NaCl) with Pronase (1 mg/mL) and following ethanol precipitation. The targeted gene region was amplified with Phusion® High-Fidelity DNA Polymerase (NEB, Frankfurt am Main, Germany) and primers given in Table 2. The gel purified phosphorylated PCR products were then blunt-end cloned into EcoRV-digested and dephosphorylated pBluescript II SK (+) (Stratagene, Darmstadt, Germany). Ten white colonies each were randomly picked [75], plasmid DNA was isolated and sequenced using the vector specific T7 primer by Sanger sequencing. In cases where all ten sequenced plasmids carried identical inserts, plasmids of five additional bacterial clones were isolated and sequenced. Mutations induced by Cas9 nuclease were identified by nucleotide sequence alignments with the rabbit genome (OryCun2.0) using Geneious 11.1.5 (<https://www.geneious.com>).

Table 2. Primers used for amplification of targeted gene.

Name	Sequence (5'–3')
TorA_seq_Fwd	CACCGGAGACAGCTATAGCC
TorA_seq_Rev	GACCTTCTTGGCCAGATGCT
TorB_seq_Fwd	CCGCGCGAATGTGAAGTGCGCCCCGTGGAAC
TorB_seq_Rev	GTCTTGTGCTCATGCGGGAAGTGCAGTGTG

2.8. PrestoBlue Assay

Cell viability of modified and knockout cells was determined using Presto Blue™ Reagent (Thermo Scientific, Dreieich, Germany), a resazurin-based metabolic assay. RK13 wild type cells were used as control. 1×10^4 cells in 90 μ L volume were seeded in a black 96-well plate with a flat and clear bottom (Corning). At 24, 48 and 72 h after seeding 10 μ L Presto Blue Reagent was added to the cells and resuspended. The samples were incubated for 30 min at 37 °C. For each time point, cells were measured in triplicates and eight medium containing wells were included for background estimation. Before bottom-read measuring of fluorescence in a Tecan Reader at Ex560/Em590, the plate was shaken for 5 sec. Multiple reads per well (3×3) were performed using the i-control™ microtiter reader software. Blank-reduced raw data (fluorescence intensities) are given in the corresponding figures. For standardization, we used the following formula: (measured value – mean)/standard deviation. Statistics was applied on the standardized values.

2.9. In Vitro Replication Studies

To test the efficiency of PrV propagation in the generated cell lines, cells were infected with PrV-Ka at a multiplicity of infection (MOI) of 5. Cells and supernatants were harvested at different time points after infection (0, 4, 8, 12, 24 and 30 h p.i.). To determine the infectious virus titer, samples were thawed, cell debris was removed by centrifugation (2 min, 15,000 rpm), the supernatant was serially diluted (10^{-1} to 10^{-6}) and used to infect RK13 cells in 24 well culture plates. After incubation for 1 h, the inoculum was replaced by a semi solid medium allowing only direct cell-to cell spread of the virus. Cells were fixed after 2 days with formaldehyde and stained with crystal violet. Virus plaques, which were detectable as holes in the blue-stained cell monolayer, were counted in at least two different wells and mean values were calculated as plaque forming units per milliliter (pfu/mL).

Shown are mean values of three (EGFP-TorA, -B overexpressing cells) or six (knockout cells) independent experiments with corresponding standard deviations. To exclude clonal and putative second site effects at least three different cell clones were tested initially for each mutated cell line.

2.10. Statistics

For each assay at least three independent experiments were performed. The statistical significance of the data presented in Figures 5, 6, 7 and 8 was determined by a two-way ANOVA followed by Dunnett's multiple comparison test. All statistical tests were performed using GraphPad Prism version 8.1.0 (GraphPad Software, La Jolla, CA, USA). We compared the mean of each time point with the mean of the corresponding parental RK13 cells. A p -value ≤ 0.05 was considered significant and is presented in Figures 6 and 8 by the presence of asterisks (*, $p \leq 0.05$, **, $p \leq 0.01$, ***, $p \leq 0.0001$).

2.11. Laser Scanning Confocal Microscopy

For confocal microscopy, we used stably expressing RK13 cells and RK13 cells transiently co-expressing the GFP-tagged plasmids and an ER-marker plasmid [73]. In addition, RK13 and Torsin knockout cells were infected with 250 pfu of PrV-Ka. Cells in 24 well dishes were fixed with 4% paraformaldehyde for 15 min one day after seeding for the stable expressing cells or two days after transient transfection. Infected cells were analyzed 18 h p.i. Fixed cells were washed three times and then incubated for 30 min with 50 mM NH_4Cl in 1X PBS to quench the free aldehyde groups after

PFA fixation. The GFP-tagged proteins and the DsRed-ER marker proteins were directly visualized via their autofluorescence. After permeabilization with 0.1% Triton X-100 in 1x PBS and subsequent blocking for 20 min with 0.25% skimmed milk the viral antigen was stained with a polyclonal rabbit serum specific for pUL34 (1:500, [76]). Alexa-Fluor 568-conjugated goat anti-rabbit IgG (dilution 1:1000, Invitrogen) was used to detect bound antibody. The nuclei were counterstained with 300 mM DAPI for 5 min and cells were mounted in a drop of Kaiser's glycerol gelatin (Merck, Darmstadt, Germany). Samples were analyzed using with a confocal laser scanning microscope (Leica DMI 6000 TCS SP5, 63× oil-immersion objective, NA = 1.4; Leica, Wetzlar, Germany). Representative images were processed using the Fiji software [77,78]. Scale bars indicate 10 μ m.

2.12. Ultrastructural Analyses

RK13 and KO cell lines were infected with PrV-Ka at an MOI of 1 for 14 h and processed for transmission electron microscopy as described previously [76]. Numbers of primary virions present in the PNS in infected RK13 and RK13-TorA/B_{DKO} were counted in 10 different sections each.

3. Results

3.1. Influence of Torsin Overexpression on PrV Replication

To test whether overexpression of either the GFP-tagged wild type or mutated forms of (human) Torsins A and B has an effect on PrV replication, the different expression constructs (Figure 1) were transfected into RK13 cells for transient expression and generation of stably expressing cell lines. Torsins are well conserved in metazoans [34] and functional expression of the same constructs in murine cells was reported [66].

As expected, each of these constructs was targeted to the ER/NE when transiently expressed in RK13 cells (Figure 2) showing a clear colocalization with the DsRed2-tagged ER marker (DsRed2-ER) [38,46,47]. Consistent with previous reports, the expression of SS-EGFP-TorB_{E178Q} resulted in the appearance of dense protein accumulations within the ER [46]. Furthermore, each of the proteins was expressed in RK13 cells at the predicted molecular mass evaluated in western blot analysis (Figure 3). The SS-EGFP-tagged TorA and TorB constructs were ~65–70 kDa, with expression levels of TorB slightly higher than for TorA. Taken together, these results demonstrate that the GFP-Torsin constructs are expressed properly in RK13 cells.

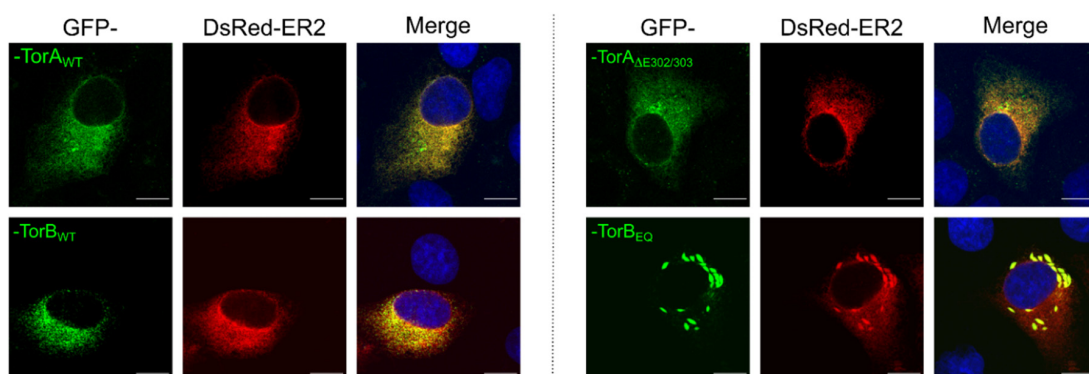


Figure 2. Localization of GFP-tagged constructs in RK13 cells. Representative images of RK13 cells transiently expressing the GFP-tagged constructs. Cells were co-transfected with plasmids expressing the DsRed2-ER marker and the GFP-tagged Torsins. Nuclei were counterstained with DAPI and autofluorescence was detected with a confocal laser scanning microscope. Scale bars indicate 10 μ m.

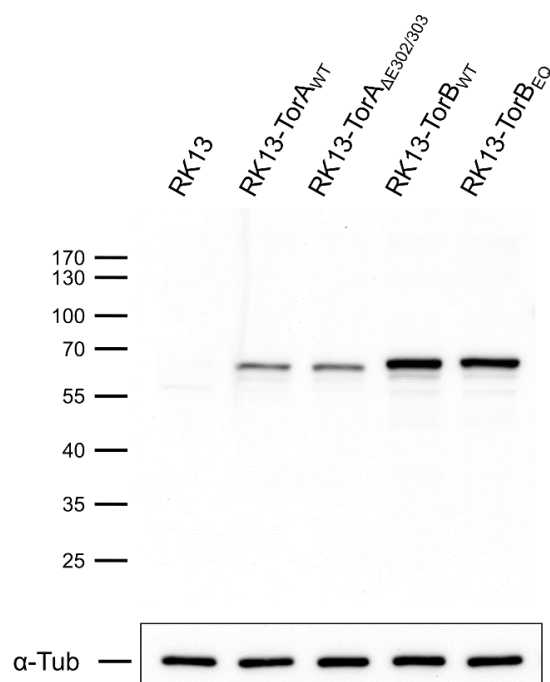


Figure 3. Expression of GFP-tagged Torsins in RK13 cells. Lysates of transfected cells were harvested, and proteins were separated in SDS 10%-polyacrylamide gels. Blots were probed with a GFP-specific rabbit antiserum and a monoclonal antibody against α -tubulin as loading control. Molecular masses of marker proteins (in kDa) are indicated on the left.

Stably expressing cell lines were selected for homogeneous GFP expression. The subcellular localization of each protein in these cell lines was indistinguishable from what was observed in transient expression (Figure 4). Ultrastructurally, cells overexpressing TorB showed a significant expansion of the rough ER with either diffuse matter (TorB_{WT}) or filled with protein filaments (TorB_{E178Q}) (data not shown) but no sinusoidal ER structures as reported for HeLa cells [46]. No deleterious effects on cellular metabolic activity were observed from overexpression of the GFP-tagged cellular genes (Figure 5). To test whether overexpression of these constructs influences virus replication, stably expressing cells as well as parental RK13 cells were infected with PrV strain Kaplan (PrV-Ka) [70] at an MOI of 5 and harvested at different time points after infection. As shown in Figure 6 small but significant 3- to 5-fold titer reduction was found after infection of RK13-TorA_{WT} at all time points later than 8 h after infection, while cells expressing the mutant form TorA _{Δ E302/303} supported PrV replication to similar titers as non-transgenic RK13 cells. For RK13-TorB_{WT} cells there were no significant changes in viral titers compared to parental RK13 cells, while infection of TorB_{E178Q} expressing cells resulted in 4 to 7-fold titer decrease at all time points after infection.

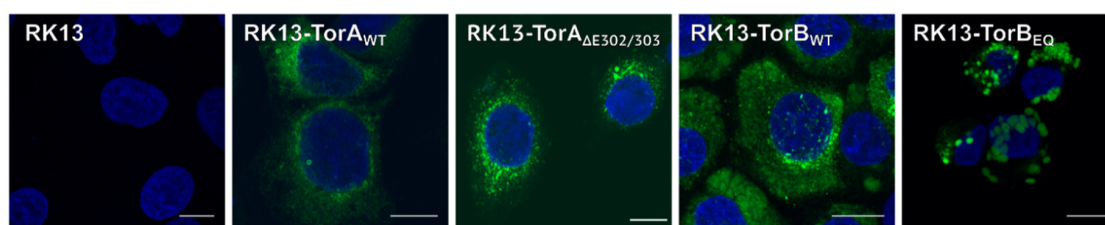


Figure 4. Localization of stably expressed RK13-GFP-TorA and -TorB. Representative merged images show the intracellular localization of RK13 cells stably expressing the GFP-tagged mutant and wild type proteins. Nuclei were stained with DAPI, and GFP autofluorescence was detected with a confocal laser scanning microscope. Scale bars indicate 10 μ m.

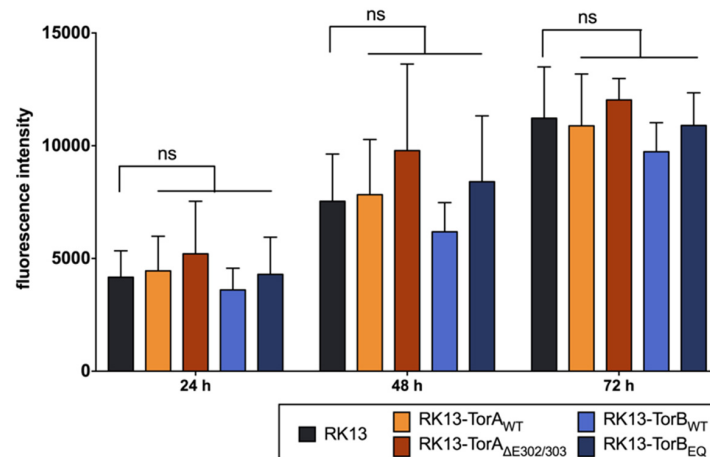


Figure 5. Cell viability of the modified cell lines. RK13 control and stably expressing RK13-GFP-TorA and -TorB cells were seeded with 1×10^4 cells per well and at 24, 48, and 72 h post seeding the mitochondrial activity was measured (in fluorescence intensities) via the Presto Blue Assay. Shown is the mean of three independent experiments, ns = statistically not significant.

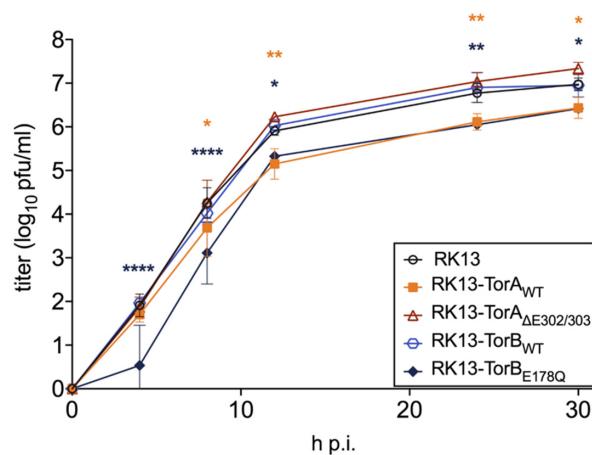


Figure 6. Effects of overexpression of Torsins on PrV replication. Stably expressing cell lines and parental RK13 cells were infected with PrV-Ka (MOI of 5) and harvested at different time points. Progeny virus titers were determined on RK13 cells. Given are mean values of three independent experiments with corresponding standard deviations. Statistically significant differences compared to the parental RK13 were determined by GraphPad Prism software and are indicated by asterisks in the same color as the corresponding graphs (*, $p \leq 0.05$, **, $p \leq 0.01$, ****, $p \leq 0.0001$).

3.2. Torsin A and Torsin B Are Required for Efficient PrV Replication in RK13 Cells

Torsin A and B are suggested to be functionally redundant [52]. Surprisingly, overexpression of the wild type TorA and the mutant TorB_{E178Q} slightly impaired PrV replication while the other two forms had no significant impact pointing to different mechanisms. We were interested to analyze whether this effect might be more pronounced when both proteins are targeted simultaneously. Since equivalent simultaneous expression of both proteins in cell lines is difficult to achieve and maintain, we decided to use the CRISPR/Cas9 genome editing system to generate single and double KO cell lines for TorA and TorB. Four guide RNAs per gene were designed (Table 1), cloned into vector pX330-NeoR [72], and transfected simultaneously into RK13 cells. Genomic DNA of several cell clones was isolated, and the target region was amplified by PCR using primers given in Table 2. The PCR products were cloned into pBluescript SK+ and plasmid DNA from at least ten bacterial colonies each was isolated and sequenced. Wild type sequences in comparison to the mutations found in the different

plasmids are summarized in Table 3. All cloned PCR products derived from RK13-TorB_{KO} and RK13-TorA/B_{DKO} exhibited only a single type of mutation indicating that both alleles carry the same deletion. Two different allelic variants were present in RK13-TorA_{KO} cells. In-frame deletions were found in the TorB allele of RK13-TorA/B_{DKO} cells ($\Delta 30$ bp, both alleles). Unfortunately, the tested antisera, which are specific for human Torsins, did not detect the corresponding homologs in RK13 cells (data not shown). As similar to the stably expressing cells described above, no deleterious effects on metabolic activity were observed in the KO cell lines (Figure 7).

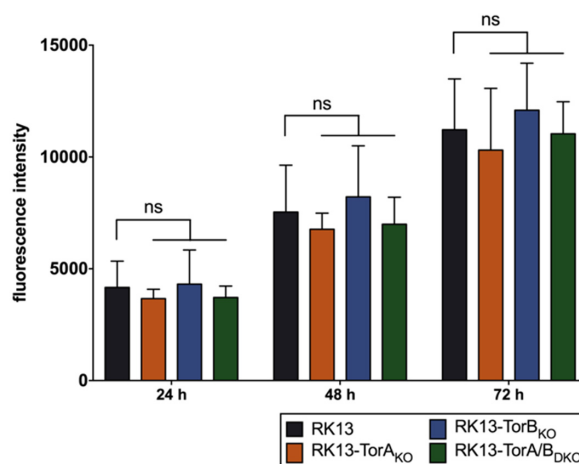


Figure 7. Cell viability of generated modified cell lines. RK13 control together with Torsin_{KO} cell lines were seeded with 1×10^4 cells per well and at 24, 48, and 72 h post seeding the mitochondrial activity was measured (in fluorescence intensities) with the Presto Blue Assay. Shown is the mean of three independent experiments, ns = statistically not significant.

The generated KO and DKO cell lines were tested for virus propagation by infection with PrV-Ka at an MOI of 5 and harvested at different times after infection. As shown in Figure 8, no significant differences in viral progeny titers were found for RK13-TorA_{KO} and RK13-TorB_{KO} cells. In TorA/B_{DKO} cells a significant drop in virus titer compared to the parental RK13 cells was observed at 4, 8 and 12 h after infection which disappeared at later time points.

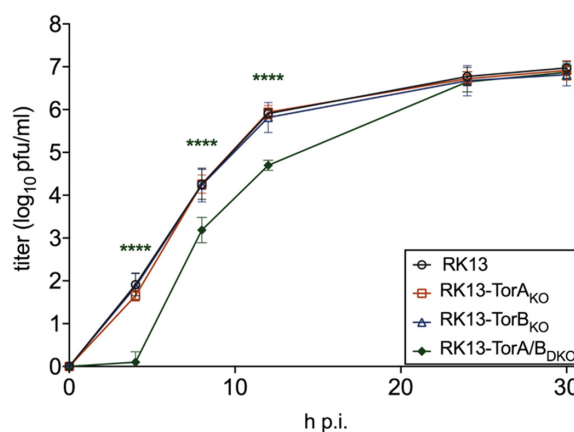


Figure 8. Effect of gene knockout on PrV replication. RK13 and Torsin_{KO} cell lines were infected with PrV-Ka (MOI of 5) and harvested at different time points after infection. Progeny virus titers were determined on RK13 cells. Shown are mean values of six independent experiments. Statistics were done with GraphPad Prism software and asterisks indicate statistically significant differences compared to the parental RK13 in the same color as the corresponding graph (****, $p \leq 0.0001$).

To test whether the absence of Torsin A and/or B influences nuclear envelope localization of the viral NEC component pUL34, parental RK13 and Torsin knockout cells were infected with PrV-Ka under plaque assay conditions. Cells were fixed after 18 h and stained with the monospecific anti-pUL34 rabbit serum [76]. As shown in Figure 9, no difference in nuclear rim staining for pUL34 was obvious independent of presence or absence of Torsins A, B or both proteins.

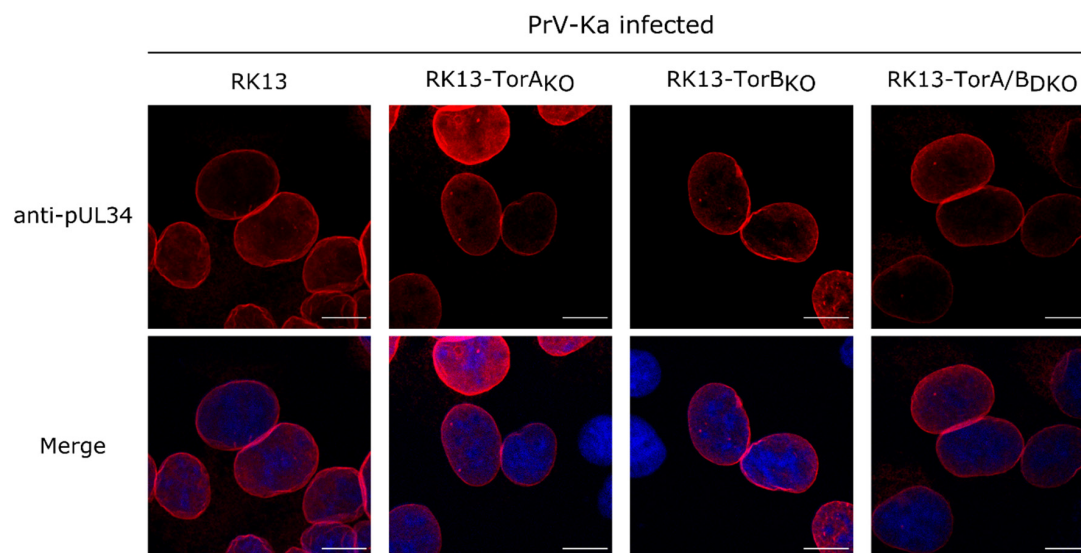


Figure 9. Localization of the NEC component pUL34 in PrV-Ka infected RK13 and Torsin_{KO} cells. Representative images showing undisturbed localization of the NEC component pUL34 (red) in infected RK13-Torsin_{KO} cells. Nuclei were counterstained with DAPI (blue) and the fluorescence was imaged with a confocal laser scanning microscope. Scale bars indicate 10 μ m.

Although no drastic effect on viral titers was observed, we analyzed nuclear egress at the ultrastructural level. All KO cell lines were infected with PrV-Ka at an MOI of 1 and processed for electron microscopy. We did not observe any impairment in nuclear egress or virion morphogenesis in infected RK13-TorA_{KO} and RK13-TorB_{KO} (data not shown). In contrast to previous studies [45,51–53], nuclear envelope blebbing in the Torsin KO cells was not obvious. However, in PrV infected RK13-TorA/B_{DKO} cells primary enveloped virions accumulated in the PNS which is in contrast to PrV infected parental RK13 cells, exhibiting only rare single virions in the PNS (Figure 10E; marked by an asterisk). We counted the number of primary enveloped virions in 10 sections each of PrV-Ka infected RK13 and RK13-TorA/B_{DKO} cells. While in RK13 cells 5 primary enveloped virions could be detected in 30 nuclei, infected RK13-TorA/B_{DKO} cells contained 593 primary virions in 52 nuclei. Compared to the accumulations observed in mutants lacking the pUS3 protein kinase [15], primary virions did not preferentially accumulate in herniations of the INM but were mainly found lined up in the PNS (Figure 10). Fission from the INM seemed to be less efficient in the absence of TorA/B since primary virions were frequently found still attached to the INM by a small neck (Figure 10, arrows).

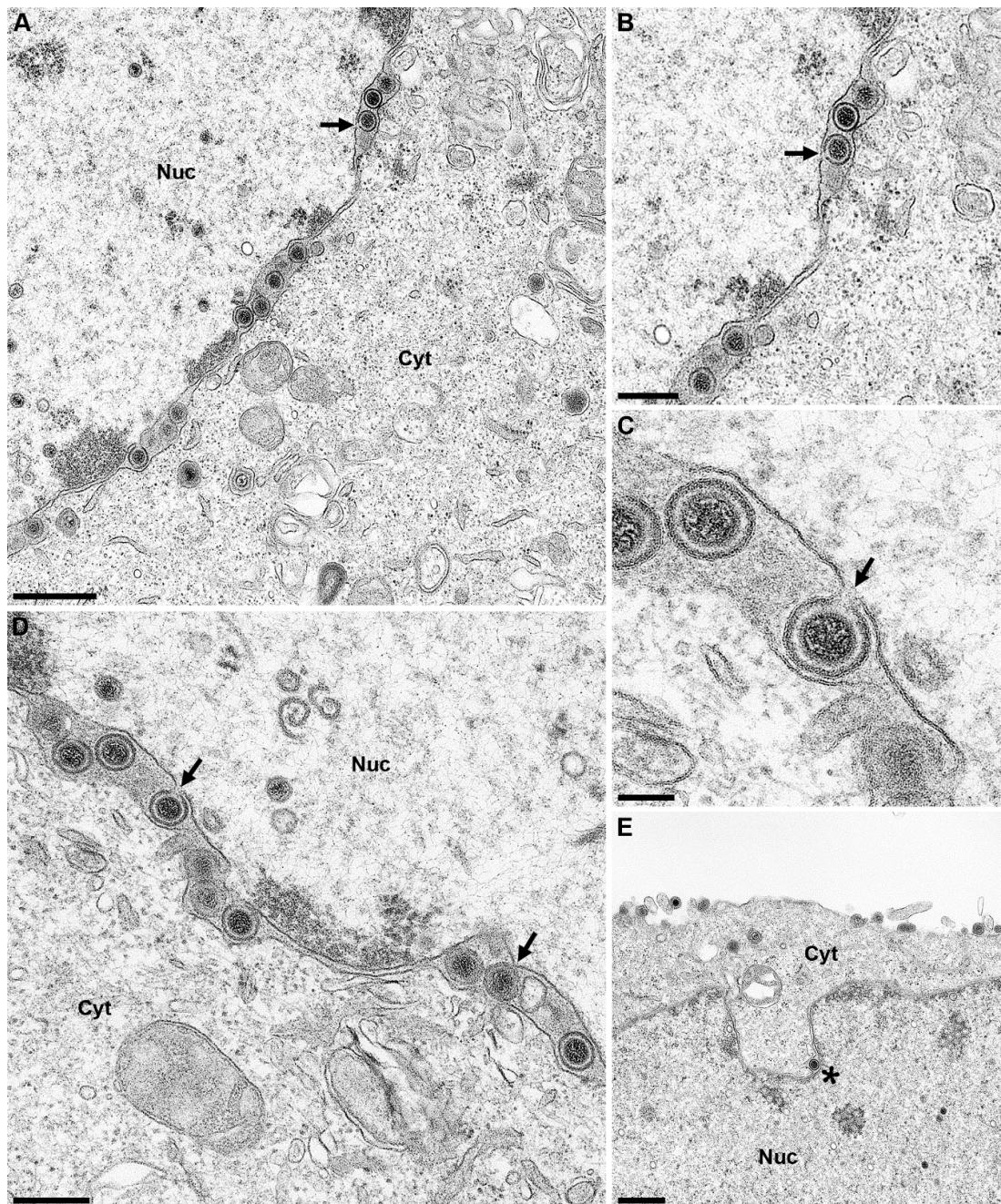


Figure 10. TorA/B DKO results in accumulation of primary enveloped virions in the PNS. RK13, RK13-TorA_{KO}, RK13-TorB_{KO} and RK13-TorA/B_{DKO} cells were infected with PrV-Ka (MOI of 1) and processed for electron microscopic imaging 14 h p.i. No obvious effect was found for the single KO cells (data not shown), while the TorA/B_{DKO} showed accumulations of primary virions within the PNS, many of them still connected to the INM by a short neck (indicated by arrows) (A–D). Panel (B) shows a higher magnification of the infected cell in panel (A), while panel (C) shows a higher magnification of panel (D). Panel (E) shows a rare case of a primary virion in the PNS in parental RK13 cells (marked by asterisk). Scale bars indicate 600 nm in panel (A,E), 300 nm in panel (B,C) and 100 nm in panel (D). Nuc: nucleus, Cyt: cytoplasm.

Table 3. Summary of mutations detected in the KO cell lines.

Mutant	Genotype	Sequence	Mutations
TorA _{KO}	wild type	GAACCGGAAGAGCGTGTCTGGCGGTAGCGCCG . .GTCGGTGGTCAGCGCAGGAAGGCGCGGGGAGGCG	
	knockout	GAACCGGAAGAGCGTGTCTGGCGGTAGCGCGGTGGT--GGTCAGCGCAGGAAGGCGCGGGGAGGCG (3) GAACCGGAAGAGCGTGTCTGGCGGTAGCGCCG . .GT--GGTCAGCGCAGGAAGGCGCGGGGAGGCG (7)	1 nt Ex, 2 bp In, 4 bp Del Del4 bp Del
TorB _{KO}	wild type	CTTGAGAGAAGCTGTTCCGGACAGCATCTGGCCACGGAAGTGATTCTGAAGGCGCTGACCGGCTTCAAGA	
	knockout	CTTGAGAGAAGCTGTTCCGGACAGC-----CTGACCGGCTTCAAGA (15)	29 bp Del
TorA/B _{DKO}	TorA wild type	GAACCGGAAGAGCGTGTCTGGCGGTAGCGCCGGTCGGTGGTCAGCGCAGGAAGGCGCGGGGAGGCGCG	
	knockout	GAACCGGAAGAGCGTGTCTGGCGGTAGCGCCCG----TCAGCGCAGGAAGGCGCGGGGAGGCGCG (15)	1 nt Ex, 7 bp Del
TorA/B _{DKO}	TorB wild type	CTTGAGAGAAGCTGTTCCGGACAGCATCTGGCCACGGAAGTGATTCTGAAGGCGCTGACCGGCTTCAAGA	
	knockout	CTTGAGAGAAGCTGTTCCGGACA-----GCTGACCGGCTTCAAGA (15)	30 bp Del

The sequence for each targeted gene region was compared to the sequence of the parental RK13 sequence. Numbers in brackets indicate the frequency of InDel (Insertion or Deletion) mutations found in the clones sequenced. Deletion (Del) of a base pairs (bp) is shown as hyphen, insertion (In) of a bp is marked by a dot in the parental sequence and nucleotide (nt) exchanges (Ex) are shown in bold characters.

4. Discussion

Herpesvirus nucleocapsids rely on a vesicular pathway engaging the NE for nuclear egress. While the viral NEC orchestrates budding at and scission from the INM, no viral protein essential for de-envelopment at the ONM could be identified yet, while the pUS3 protein kinase exhibits a regulatory role (reviewed in Mettenleiter, Klupp and Granzow [5], Mettenleiter, Muller, Granzow and Klupp [7], and Johnson and Baines [6]).

Here, we analyzed a possible converging role for Torsin in herpesvirus nuclear egress by overexpressing them singly, and by generation of single and double KO cells using CRISPR/Cas9 based mutagenesis in the rabbit kidney cell line RK13. Torsins A and B seem to be ubiquitously expressed and are at least partially functionally redundant, complicating interpretation of experimental data generated by targeting only one form. Overexpression of TorA_{WT} or TorB_{E178Q}, which carries a mutation rendering the protein unable to hydrolyze ATP [46], resulted in a small but significant drop in virus titers compared to the non-transgenic RK13 control. A similar drop in virus titer was also observed for HSV-1 after infection of a neuronal cell line expressing TorA_{WT} [54]. Primary enveloped virions escaped into the lumen of the ER as it was shown after overexpression of a dominant-negative SUN2 [69]. These data support the notion that Torsins regulate the SUN/nesprin interaction and that an intact LINC complex/Torsin relationship is necessary to restrict primary virions in the PNS [54]. However, neither TorA_{WT} nor TorB_{E178Q} expression resulted in an obvious increase of the number of primary virions in cytoplasmic structures, alteration of the nuclear envelope or the spacing between the INM and ONM (data not shown). Due to the lack of antibodies detecting SUN proteins in RK13 cells, an influence of Tor expression on the LINC could not be tested.

We also generated single and double knockout cells by CRISPR/Cas9 mutagenesis, which was verified by sequencing of the corresponding gene regions. No obvious differences in growth or metabolic activity were observed between the modified cell lines stably expressing the respective Torsin constructs or in Torsin KO cell lines, compared to parental RK13 cells. In addition, we did not detect any morphological defects, indicating that the targeted proteins are non-essential for cellular proliferation under our cell culture conditions. Since we could not exclude second site effects, we always included different cell clones for each KO in the preliminary screens. In none of the KO cell lines wild-type sequences could be identified. Unfortunately, the available antisera against the corresponding proteins of human origin did not react with the rabbit homologs in the RK13 cell lysates. The used gRNAs were designed to target exons that are shared by all transcript variants of the gene of interest to minimize the chance that shorter but still functional protein isoforms might be expressed. Although the RK13-TorA/B_{DKO} cell line carries an in-frame deletion (aa 76–85) upstream of the Walker A motif (aa 105–112) in both alleles of the TorB gene and we cannot exclude expression of a truncated protein, the observed effects indicate a significant loss of function.

In contrast to the overexpression experiments, in which a slight but significant drop in progeny virus titers was found after infection of RK13-TorA_{WT} and RK13-TorB_{EQ} cells, none of the single KO cells showed a significant effect on infectious virus production or on localization of the NEC component pUL34. In ultrastructural analyses, we could not detect perturbations of the NE in cells lacking TorA or B, and primary virions were only rarely detected in the PNS or in cytoplasmic vesicles arguing against an impairment of nuclear egress. However, after infection of RK13-TorA/B_{DKO} cells a drop in virus titer occurred at early time points after infection. High-resolution imaging revealed striking accumulations of primary enveloped virions lined-up in the PNS, while accumulations in herniations of the ONM were only rarely detected. Many of the primary envelopes seemed to be connected to the INM indicating that in the absence of Torsin A and B scission might be impaired (Figure 10). In line with this, in a HeLa cell line where all four known Torsins had been eliminated simultaneously, NE blebs still connected to the INM had been described [50]. Unfortunately, these cell lines were not tested for effects on herpesvirus nuclear egress. It is tempting to speculate that not only Torsin A and B, but also other Torsins might be involved in this process. Incomplete scission of primary HSV-1 virions from the INM was also reported after depletion of ESCRT-III proteins [24]. It might be speculated that

recruitment of an AAA+ ATPase (Torsin/Vps4) might alleviate the scission process mediated by the NEC proteins.

It should be noted that we did not observe clear blebs of the INM into the PNS of our TorA/B_{DKO} cells, which contrasts previous reports from fibroblasts [52], HeLa cells [50], or neurons [53].

Torsins are supposed to function as regulators of the LINC complex [56] and an intact LINC complex may be required for efficient nuclear egress by restricting primary virions to the PNS in close proximity to the NE for efficient fusion of the primary envelope with the ONM [69]. In our TorA/B_{DKO} cells no impact on spacing between INM and ONM was apparent indicating no impairment of LINC.

In summary, we demonstrate that Torsins A and B, which might be involved in proper functioning of the LINC complex, play a role during nuclear egress of herpesvirus capsids. These results together with our previous findings on SUN2 impairment highlight the importance of this complex for vesicle-mediated herpesvirus capsid transport through the nuclear envelope.

Author Contributions: Conceptualization, T.C.M., B.G.K. and J.E.H.; methodology, J.E.H. and K.F.; software, J.E.H.; validation, T.C.M., B.G.K. and J.E.H.; formal analysis, J.E.H.; investigation, J.E.H.; resources, G.W.G.L.; data curation, T.C.M., B.G.K. and J.E.H.; writing—original draft preparation, J.E.H. and B.G.K.; writing—review and editing, T.C.M., B.G.K. and G.W.G.L.; visualization, J.E.H. and K.F.; supervision, T.C.M. and B.G.K.; project administration, T.C.M. and B.G.K.; funding acquisition, T.C.M. and B.G.K. All authors have read and agreed to the published version of the manuscript.

Funding: This study was supported by the Deutsche Forschungsgemeinschaft (DFG ME 854/12-2 to TCM) and the National Institutes of Health (GM129374 to GWGL).

Acknowledgments: We thank Karla Günther, Cindy Krüper, and Petra Meyer for technical support, Mandy Jörn for help with electron microscopic images and Susanne Amler for help with statistics. The pX330-NeoR vector was kindly provided by Walter Fuchs, the anti-EGFP serum by Günther M. Keil, the pDsRed2-ER marker plasmid by Birke A. Tews and the PrestoBlue Reagent by Anja Bauer. Further, we thank the Friedrich-Loeffler-Institut Collection of Cell Lines for their assistance in supplying cell lines and media.

Conflicts of Interest: The authors declare no conflict of interest.

References

1. Pante, N.; Kann, M. Nuclear pore complex is able to transport macromolecules with diameters of about 39 nm. *Mol. Biol. Cell* **2002**, *13*, 425–434. [[CrossRef](#)] [[PubMed](#)]
2. Hofemeister, H.; O'Hare, P. Nuclear pore composition and gating in herpes simplex virus-infected cells. *J. Virol.* **2008**, *82*, 8392–8399. [[CrossRef](#)] [[PubMed](#)]
3. Adam, S.A. The nuclear pore complex. *Genome Biol.* **2001**, *2*. [[CrossRef](#)] [[PubMed](#)]
4. Knochenhauer, K.E.; Schwartz, T.U. The Nuclear Pore Complex as a Flexible and Dynamic Gate. *Cell* **2016**, *164*, 1162–1171. [[CrossRef](#)]
5. Mettenleiter, T.C.; Klupp, B.G.; Granzow, H. Herpesvirus assembly: An update. *Virus Res.* **2009**, *143*, 222–234. [[CrossRef](#)]
6. Johnson, D.C.; Baines, J.D. Herpesviruses remodel host membranes for virus egress. *Nat. Rev. Microbiol.* **2011**, *9*, 382–394. [[CrossRef](#)]
7. Mettenleiter, T.C.; Müller, F.; Granzow, H.; Klupp, B.G. The way out: What we know and do not know about herpesvirus nuclear egress. *Cell. Microbiol.* **2013**, *15*, 170–178. [[CrossRef](#)]
8. Klupp, B.G.; Granzow, H.; Fuchs, W.; Keil, G.M.; Finke, S.; Mettenleiter, T.C. Vesicle formation from the nuclear membrane is induced by coexpression of two conserved herpesvirus proteins. *Proc. Natl. Acad. Sci. USA* **2007**, *104*, 7241–7246. [[CrossRef](#)]
9. Bigalke, J.M.; Heuser, T.; Nicastro, D.; Heldwein, E.E. Membrane deformation and scission by the HSV-1 nuclear egress complex. *Nat. Commun.* **2014**, *5*, 4131. [[CrossRef](#)]
10. Desai, P.J.; Pryce, E.N.; Henson, B.W.; Luitweiler, E.M.; Cothran, J. Reconstitution of the Kaposi's sarcoma-associated herpesvirus nuclear egress complex and formation of nuclear membrane vesicles by coexpression of ORF67 and ORF69 gene products. *J. Virol.* **2012**, *86*, 594–598. [[CrossRef](#)]
11. Lorenz, M.; Vollmer, B.; Unsay, J.D.; Klupp, B.G.; Garcia-Saez, A.J.; Mettenleiter, T.C.; Antonin, W. A single herpesvirus protein can mediate vesicle formation in the nuclear envelope. *J. Biol. Chem.* **2015**, *290*, 6962–6974. [[CrossRef](#)] [[PubMed](#)]

12. Mettenleiter, T.C. Herpesvirus assembly and egress. *J. Virol.* **2002**, *76*, 1537–1547. [[CrossRef](#)] [[PubMed](#)]
13. Farnsworth, A.; Wisner, T.W.; Webb, M.; Roller, R.; Cohen, G.; Eisenberg, R.; Johnson, D.C. Herpes simplex virus glycoproteins gB and gH function in fusion between the virion envelope and the outer nuclear membrane. *Proc. Natl. Acad. Sci. USA* **2007**, *104*, 10187–10192. [[CrossRef](#)] [[PubMed](#)]
14. Klupp, B.; Altenschmidt, J.; Granzow, H.; Fuchs, W.; Mettenleiter, T.C. Glycoproteins required for entry are not necessary for egress of pseudorabies virus. *J. Virol.* **2008**, *82*, 6299–6309. [[CrossRef](#)] [[PubMed](#)]
15. Klupp, B.G.; Granzow, H.; Mettenleiter, T.C. Effect of the pseudorabies virus US3 protein on nuclear membrane localization of the UL34 protein and virus egress from the nucleus. *J. Gen. Virol.* **2001**, *82*, 2363–2371. [[CrossRef](#)]
16. Wagenaar, F.; Pol, J.M.; Peeters, B.; Gielkens, A.L.; de Wind, N.; Kimman, T.G. The US3-encoded protein kinase from pseudorabies virus affects egress of virions from the nucleus. *J. Gen. Virol.* **1995**, *76 Pt 7*, 1851–1859. [[CrossRef](#)]
17. Reynolds, A.E.; Wills, E.G.; Roller, R.J.; Ryckman, B.J.; Baines, J.D. Ultrastructural localization of the herpes simplex virus type 1 UL31, UL34, and US3 proteins suggests specific roles in primary envelopment and egress of nucleocapsids. *J. Virol.* **2002**, *76*, 8939–8952. [[CrossRef](#)]
18. Schumacher, D.; McKinney, C.; Kaufer, B.B.; Osterrieder, N. Enzymatically inactive U(S)3 protein kinase of Marek's disease virus (MDV) is capable of depolymerizing F-actin but results in accumulation of virions in perinuclear invaginations and reduced virus growth. *Virology* **2008**, *375*, 37–47. [[CrossRef](#)]
19. Kato, A.; Liu, Z.; Minowa, A.; Imai, T.; Tanaka, M.; Sugimoto, K.; Nishiyama, Y.; Arii, J.; Kawaguchi, Y. Herpes simplex virus 1 protein kinase Us3 and major tegument protein UL47 reciprocally regulate their subcellular localization in infected cells. *J. Virol.* **2011**, *85*, 9599–9613. [[CrossRef](#)]
20. Sehl, J.; Portner, S.; Klupp, B.G.; Granzow, H.; Franzke, K.; Teifke, J.P.; Mettenleiter, T.C. Roles of the different isoforms of the pseudorabies virus protein kinase pUS3 in nuclear egress. *J. Virol.* **2020**. [[CrossRef](#)]
21. Otsuka, S.; Ellenberg, J. Mechanisms of nuclear pore complex assembly—Two different ways of building one molecular machine. *FEBS Lett.* **2018**, *592*, 475–488. [[CrossRef](#)] [[PubMed](#)]
22. D'Angelo, M.A.; Anderson, D.J.; Richard, E.; Hetzer, M.W. Nuclear pores form de novo from both sides of the nuclear envelope. *Science* **2006**, *312*, 440–443. [[CrossRef](#)] [[PubMed](#)]
23. Dultz, E.; Ellenberg, J. Live imaging of single nuclear pores reveals unique assembly kinetics and mechanism in interphase. *J. Cell Biol.* **2010**, *191*, 15–22. [[CrossRef](#)] [[PubMed](#)]
24. Arii, J.; Watanabe, M.; Maeda, F.; Tokai-Nishizumi, N.; Chihara, T.; Miura, M.; Maruzuru, Y.; Koyanagi, N.; Kato, A.; Kawaguchi, Y. ESCRT-III mediates budding across the inner nuclear membrane and regulates its integrity. *Nat. Commun.* **2018**, *9*, 3379. [[CrossRef](#)] [[PubMed](#)]
25. Lee, C.P.; Liu, G.T.; Kung, H.N.; Liu, P.T.; Liao, Y.T.; Chow, L.P.; Chang, L.S.; Chang, Y.H.; Chang, C.W.; Shu, W.C.; et al. The Ubiquitin Ligase Itch and Ubiquitination Regulate BFRF1-Mediated Nuclear Envelope Modification for Epstein-Barr Virus Maturation. *J. Virol.* **2016**, *90*, 8994–9007. [[CrossRef](#)] [[PubMed](#)]
26. Lee, C.P.; Liu, P.T.; Kung, H.N.; Su, M.T.; Chua, H.H.; Chang, Y.H.; Chang, C.W.; Tsai, C.H.; Liu, F.T.; Chen, M.R. The ESCRT machinery is recruited by the viral BFRF1 protein to the nucleus-associated membrane for the maturation of Epstein-Barr Virus. *PLoS Pathog.* **2012**, *8*, e1002904. [[CrossRef](#)]
27. Crump, C.M.; Yates, C.; Minson, T. Herpes simplex virus type 1 cytoplasmic envelopment requires functional Vps4. *J. Virol.* **2007**, *81*, 7380–7387. [[CrossRef](#)]
28. Kharkwal, H.; Smith, C.G.; Wilson, D.W. Blocking ESCRT-mediated envelopment inhibits microtubule-dependent trafficking of alphaherpesviruses in vitro. *J. Virol.* **2014**, *88*, 14467–14478. [[CrossRef](#)]
29. Neuwald, A.F.; Aravind, L.; Spouge, J.L.; Koonin, E.V. AAA+: A class of chaperone-like ATPases associated with the assembly, operation, and disassembly of protein complexes. *Genome Res.* **1999**, *9*, 27–43.
30. Erzberger, J.P.; Berger, J.M. Evolutionary relationships and structural mechanisms of AAA+ proteins. *Annu. Rev. Biophys. Biomol. Struct.* **2006**, *35*, 93–114. [[CrossRef](#)]
31. Laudermilch, E.; Schlieker, C. Torsin ATPases: Structural insights and functional perspectives. *Curr. Opin. Cell Biol.* **2016**, *40*, 1–7. [[CrossRef](#)] [[PubMed](#)]
32. Breakefield, X.O.; Kamm, C.; Hanson, P.I. TorsinA: Movement at many levels. *Neuron* **2001**, *31*, 9–12. [[CrossRef](#)]
33. Hanson, P.I.; Whiteheart, S.W. AAA+ proteins: Have engine, will work. *Nat. Rev. Mol. Cell Biol.* **2005**, *6*, 519–529. [[CrossRef](#)] [[PubMed](#)]

34. Rose, A.E.; Brown, R.S.; Schlieker, C. Torsins: Not your typical AAA+ ATPases. *Crit. Rev. Biochem. Mol. Biol.* **2015**, *50*, 532–549. [[CrossRef](#)]
35. Sosa, B.A.; Demircioglu, F.E.; Chen, J.Z.; Ingram, J.; Ploegh, H.L.; Schwartz, T.U. How lamina-associated polypeptide 1 (LAP1) activates Torsin. *eLife* **2014**, *3*, e03239. [[CrossRef](#)]
36. Nagy, M.; Wu, H.C.; Liu, Z.; Kedzierska-Mieszkowska, S.; Zolkiewski, M. Walker-A threonine couples nucleotide occupancy with the chaperone activity of the AAA+ ATPase ClpB. *Protein Sci.* **2009**, *18*, 287–293. [[CrossRef](#)]
37. Jungwirth, M.; Dear, M.L.; Brown, P.; Holbrook, K.; Goodchild, R. Relative tissue expression of homologous torsinB correlates with the neuronal specific importance of DYT1 dystonia-associated torsinA. *Hum. Mol. Genet.* **2010**, *19*, 888–900. [[CrossRef](#)]
38. Kustedjo, K.; Bracey, M.H.; Cravatt, B.F. Torsin A and its torsion dystonia-associated mutant forms are luminal glycoproteins that exhibit distinct subcellular localizations. *J. Biol. Chem.* **2000**, *275*, 27933–27939. [[CrossRef](#)]
39. Vander Heyden, A.B.; Naismith, T.V.; Snapp, E.L.; Hodzic, D.; Hanson, P.I. LULL1 retargets TorsinA to the nuclear envelope revealing an activity that is impaired by the DYT1 dystonia mutation. *Mol. Biol. Cell* **2009**, *20*, 2661–2672. [[CrossRef](#)]
40. Brown, R.S.; Zhao, C.; Chase, A.R.; Wang, J.; Schlieker, C. The mechanism of Torsin ATPase activation. *Proc. Natl. Acad. Sci. USA* **2014**, *111*, E4822–E4831. [[CrossRef](#)]
41. Zhao, C.; Brown, R.S.; Chase, A.R.; Eisele, M.R.; Schlieker, C. Regulation of Torsin ATPases by LAP1 and LULL1. *Proc. Natl. Acad. Sci. USA* **2013**, *110*, E1545–E1554. [[CrossRef](#)] [[PubMed](#)]
42. Ozelius, L.J.; Hewett, J.W.; Page, C.E.; Bressman, S.B.; Kramer, P.L.; Shalish, C.; de Leon, D.; Brin, M.F.; Raymond, D.; Corey, D.P.; et al. The early-onset torsion dystonia gene (DYT1) encodes an ATP-binding protein. *Nat. Genet.* **1997**, *17*, 40–48. [[CrossRef](#)]
43. Gonzalez-Alegre, P. Advances in molecular and cell biology of dystonia: Focus on torsinA. *Neurobiol. Dis.* **2019**, *127*, 233–241. [[CrossRef](#)] [[PubMed](#)]
44. Goodchild, R.E.; Dauer, W.T. Mislocalization to the nuclear envelope: An effect of the dystonia-causing torsinA mutation. *Proc. Natl. Acad. Sci. USA* **2004**, *101*, 847–852. [[CrossRef](#)] [[PubMed](#)]
45. Naismith, T.V.; Heuser, J.E.; Breakefield, X.O.; Hanson, P.I. TorsinA in the nuclear envelope. *Proc. Natl. Acad. Sci. USA* **2004**, *101*, 7612–7617. [[CrossRef](#)] [[PubMed](#)]
46. Rose, A.E.; Zhao, C.; Turner, E.M.; Steyer, A.M.; Schlieker, C. Arresting a Torsin ATPase reshapes the endoplasmic reticulum. *J. Biol. Chem.* **2014**, *289*, 552–564. [[CrossRef](#)]
47. Hewett, J.; Gonzalez-Agosti, C.; Slater, D.; Ziefer, P.; Li, S.; Bergeron, D.; Jacoby, D.J.; Ozelius, L.J.; Ramesh, V.; Breakefield, X.O. Mutant torsinA, responsible for early-onset torsion dystonia, forms membrane inclusions in cultured neural cells. *Hum. Mol. Genet.* **2000**, *9*, 1403–1413. [[CrossRef](#)]
48. Chalfant, M.; Barber, K.W.; Borah, S.; Thaller, D.; Lusk, C.P. Expression of TorsinA in a heterologous yeast system reveals interactions with luminal domains of LINC and nuclear pore complex components. *Mol. Biol. Cell* **2019**, *30*, 530–541. [[CrossRef](#)]
49. Pappas, S.S.; Liang, C.C.; Kim, S.; Rivera, C.O.; Dauer, W.T. TorsinA dysfunction causes persistent neuronal nuclear pore defects. *Hum. Mol. Genet.* **2018**, *27*, 407–420. [[CrossRef](#)]
50. Laudermilch, E.; Tsai, P.L.; Graham, M.; Turner, E.; Zhao, C.; Schlieker, C. Dissecting Torsin/cofactor function at the nuclear envelope: A genetic study. *Mol. Biol. Cell* **2016**, *27*, 3964–3971. [[CrossRef](#)]
51. Goodchild, R.E.; Kim, C.E.; Dauer, W.T. Loss of the dystonia-associated protein torsinA selectively disrupts the neuronal nuclear envelope. *Neuron* **2005**, *48*, 923–932. [[CrossRef](#)] [[PubMed](#)]
52. Kim, C.E.; Perez, A.; Perkins, G.; Ellisman, M.H.; Dauer, W.T. A molecular mechanism underlying the neural-specific defect in torsinA mutant mice. *Proc. Natl. Acad. Sci. USA* **2010**, *107*, 9861–9866. [[CrossRef](#)] [[PubMed](#)]
53. Tanabe, L.M.; Liang, C.C.; Dauer, W.T. Neuronal Nuclear Membrane Budding Occurs during a Developmental Window Modulated by Torsin Paralogs. *Cell Rep.* **2016**, *16*, 3322–3333. [[CrossRef](#)] [[PubMed](#)]
54. Maric, M.; Shao, J.; Ryan, R.J.; Wong, C.S.; Gonzalez-Alegre, P.; Roller, R.J. A functional role for TorsinA in herpes simplex virus 1 nuclear egress. *J. Virol.* **2011**, *85*, 9667–9679. [[CrossRef](#)]
55. Turner, E.M.; Brown, R.S.; Laudermilch, E.; Tsai, P.L.; Schlieker, C. The Torsin Activator LULL1 Is Required for Efficient Growth of Herpes Simplex Virus 1. *J. Virol.* **2015**, *89*, 8444–8452. [[CrossRef](#)]

56. Nery, F.C.; Zeng, J.; Niland, B.P.; Hewett, J.; Farley, J.; Irimia, D.; Li, Y.; Wiche, G.; Sonnenberg, A.; Breakefield, X.O. TorsinA binds the KASH domain of nesprins and participates in linkage between nuclear envelope and cytoskeleton. *J. Cell Sci.* **2008**, *121*, 3476–3486. [[CrossRef](#)]
57. Saunders, C.A.; Harris, N.J.; Willey, P.T.; Woolums, B.M.; Wang, Y.; McQuown, A.J.; Schoenhofen, A.; Worman, H.J.; Dauer, W.T.; Gundersen, G.G.; et al. TorsinA controls TAN line assembly and the retrograde flow of dorsal perinuclear actin cables during rearward nuclear movement. *J. Cell Biol.* **2017**, *216*, 657–674. [[CrossRef](#)]
58. Gill, N.K.; Ly, C.; Kim, P.H.; Saunders, C.A.; Fong, L.G.; Young, S.G.; Luxton, G.W.G.; Rowat, A.C. DYT1 Dystonia Patient-Derived Fibroblasts Have Increased Deformability and Susceptibility to Damage by Mechanical Forces. *Front. Cell. Dev. Biol.* **2019**, *7*, 103. [[CrossRef](#)]
59. Dominguez Gonzalez, B.; Billion, K.; Rous, S.; Pavie, B.; Lange, C.; Goodchild, R. Excess LINC complexes impair brain morphogenesis in a mouse model of recessive TOR1A disease. *Hum. Mol. Genet.* **2018**, *27*, 2154–2170. [[CrossRef](#)]
60. Zhou, X.; Graumann, K.; Evans, D.E.; Meier, I. Novel plant SUN-KASH bridges are involved in RanGAP anchoring and nuclear shape determination. *J. Cell Biol.* **2012**, *196*, 203–211. [[CrossRef](#)]
61. Razafsky, D.; Hodzic, D. Bringing KASH under the SUN: The many faces of nucleo-cytoskeletal connections. *J. Cell Biol.* **2009**, *186*, 461–472. [[CrossRef](#)] [[PubMed](#)]
62. Meinke, P.; Schirmer, E.C. LINC'ing form and function at the nuclear envelope. *FEBS Lett.* **2015**, *589*, 2514–2521. [[CrossRef](#)] [[PubMed](#)]
63. Starr, D.A.; Fridolfsson, H.N. Interactions between nuclei and the cytoskeleton are mediated by SUN-KASH nuclear-envelope bridges. *Annu. Rev. Cell Dev. Biol.* **2010**, *26*, 421–444. [[CrossRef](#)] [[PubMed](#)]
64. Crisp, M.; Liu, Q.; Roux, K.; Rattner, J.B.; Shanahan, C.; Burke, B.; Stahl, P.D.; Hodzic, D. Coupling of the nucleus and cytoplasm: Role of the LINC complex. *J. Cell Biol.* **2006**, *172*, 41–53. [[CrossRef](#)]
65. Jungwirth, M.T.; Kumar, D.; Jeong, D.Y.; Goodchild, R.E. The nuclear envelope localization of DYT1 dystonia torsinA-DeltaE requires the SUN1 LINC complex component. *BMC Cell Biol.* **2011**, *12*, 24. [[CrossRef](#)]
66. Saunders, C.A.; Luxton, G.W. LINCing defective nuclear-cytoskeletal coupling and DYT1 dystonia. *Cell. Mol. Bioeng.* **2016**, *9*, 207–216. [[CrossRef](#)]
67. Jokhi, V.; Ashley, J.; Nunnari, J.; Noma, A.; Ito, N.; Wakabayashi-Ito, N.; Moore, M.J.; Budnik, V. Torsin mediates primary envelopment of large ribonucleoprotein granules at the nuclear envelope. *Cell Rep.* **2013**, *3*, 988–995. [[CrossRef](#)]
68. Speese, S.D.; Ashley, J.; Jokhi, V.; Nunnari, J.; Barria, R.; Li, Y.; Ataman, B.; Koon, A.; Chang, Y.T.; Li, Q.; et al. Nuclear envelope budding enables large ribonucleoprotein particle export during synaptic Wnt signaling. *Cell* **2012**, *149*, 832–846. [[CrossRef](#)]
69. Klupp, B.G.; Hellberg, T.; Granzow, H.; Franzke, K.; Dominguez Gonzalez, B.; Goodchild, R.E.; Mettenleiter, T.C. Integrity of the Linker of Nucleoskeleton and Cytoskeleton Is Required for Efficient Herpesvirus Nuclear Egress. *J. Virol.* **2017**, *91*. [[CrossRef](#)]
70. Kaplan, A.S.; Vatter, A.E. A comparison of herpes simplex and pseudorabies viruses. *Virology* **1959**, *7*, 394–407. [[CrossRef](#)]
71. Zerbino, D.R.; Achuthan, P.; Akanni, W.; Amode, M.R.; Barrell, D.; Bhai, J.; Billis, K.; Cummins, C.; Gall, A.; Giron, C.G.; et al. Ensembl 2018. *Nucleic Acids Res.* **2018**, *46*, D754–D761. [[CrossRef](#)] [[PubMed](#)]
72. Hübner, A.; Petersen, B.; Keil, G.M.; Niemann, H.; Mettenleiter, T.C.; Fuchs, W. Efficient inhibition of African swine fever virus replication by CRISPR/Cas9 targeting of the viral p30 gene (CP204L). *Sci. Rep.* **2018**, *8*, 1449. [[CrossRef](#)] [[PubMed](#)]
73. Graham, F.L.; van der Eb, A.J. A new technique for the assay of infectivity of human adenovirus 5 DNA. *Virology* **1973**, *52*, 456–467. [[CrossRef](#)]
74. Boussif, O.; Lezoualc'h, F.; Zanta, M.A.; Mergny, M.D.; Scherman, D.; Demeneix, B.; Behr, J.P. A versatile vector for gene and oligonucleotide transfer into cells in culture and in vivo: Polyethylenimine. *Proc. Natl. Acad. Sci. USA* **1995**, *92*, 7297–7301. [[CrossRef](#)] [[PubMed](#)]
75. Ni, W.; Qiao, J.; Hu, S.; Zhao, X.; Regouski, M.; Yang, M.; Polejaeva, I.A.; Chen, C. Efficient gene knockout in goats using CRISPR/Cas9 system. *PLoS ONE* **2014**, *9*, e106718. [[CrossRef](#)]
76. Klupp, B.G.; Granzow, H.; Mettenleiter, T.C. Primary envelopment of pseudorabies virus at the nuclear membrane requires the UL34 gene product. *J. Virol.* **2000**, *74*, 10063–10073. [[CrossRef](#)] [[PubMed](#)]

77. Schneider, C.A.; Rasband, W.S.; Eliceiri, K.W. NIH Image to ImageJ: 25 years of image analysis. *Nat. Methods* **2012**, *9*, 671–675. [[CrossRef](#)]
78. Schindelin, J.; Arganda-Carreras, I.; Frise, E.; Kaynig, V.; Longair, M.; Pietzsch, T.; Preibisch, S.; Rueden, C.; Saalfeld, S.; Schmid, B.; et al. Fiji: An open-source platform for biological-image analysis. *Nat. Methods* **2012**, *9*, 676–682. [[CrossRef](#)]



© 2020 by the authors. Licensee MDPI, Basel, Switzerland. This article is an open access article distributed under the terms and conditions of the Creative Commons Attribution (CC BY) license (<http://creativecommons.org/licenses/by/4.0/>).

Paper II:
**Generation and Characterization of Monoclonal
Antibodies Specific for the Pseudorabies Virus
Nuclear Egress Complex**

Julia E. Hölper, Sven Reiche, Kati Franzke, Thomas C. Mettenleiter and
Barbara G. Klupp

Virus Research

submitted
05.06.2020

1
2
3 **Generation and characterization of monoclonal antibodies specific**
4 **for the Pseudorabies Virus nuclear egress complex**
5
6
7
8

9 Julia E. Hölper¹, Sven Reiche², Kati Franzke³, Thomas C. Mettenleiter¹, and Barbara G.
10 Klupp^{1*}
11

12
13 Institute of Molecular Virology and Cell Biology¹, Department of Experimental Animal Facilities
14 and Biorisk Management², and Institute of Infectology³, Friedrich-Loeffler-Institut, Greifswald-
15 Insel Riems, Germany
16
17
18

19
20
21 Short title: PrV NEC specific mAbs

22 Key words: herpesvirus, pseudorabies virus, nuclear egress complex, monoclonal antibodies,
23 immunoelectron microscopy
24
25
26
27

28 Manuscript information:

29 Figures: 7

30 Tables: 1

31 Abstract: 334 words

32 Text: 6083

33
34
35 * Corresponding author
36
37

38 Friedrich-Loeffler-Institut

39 Institute of Molecular Virology and Cell Biology

40 Südufer 10

41 17493 Greifswald-Insel Riems

42 Germany

43 Phone: +49-38351-71528

44 E-mail: barbara.klupp@fli.de
45
46
47
48
49
50
51
52
53
54
55
56
57
58
59

60
61
62 **Abstract**
63

64 During herpesvirus replication, newly synthesized nucleocapsids exit the nucleus by a vesicle-
65 mediated transport which requires the nuclear egress complex (NEC), composed of the
66 conserved viral proteins designated as pUL31 and pUL34 in the alphaherpesviruses
67 pseudorabies virus (PrV) and herpes simplex viruses. Oligomerization of the heterodimeric
68 NEC at the inner nuclear membrane (INM) results in membrane bending and budding of virus
69 particles into the perinuclear space. The INM-derived primary envelope then fuses with the
70 outer nuclear membrane to release nucleocapsids into the cytoplasm. The two NEC
71 components are necessary and sufficient for induction of vesicle budding and scission as
72 shown after co-expression in eukaryotic cells or in synthetic membranes. However, where and
73 when the NEC is formed, how membrane curvature is mediated and how it is regulated,
74 remains unclear.
75
76
77
78
79
80

81 While monospecific antisera raised against the different components of the PrV NEC aided in
82 the characterization and intracellular localization of the individual proteins, no NEC specific
83 tools have been described yet for any herpesvirus. To gain more insight into vesicle budding
84 and scission, we aimed at generating NEC specific monoclonal antibodies (mAbs). To this end,
85 mice were immunized with bacterially expressed soluble PrV NEC, which was previously used
86 for structure determination. Besides pUL31- and pUL34-specific mAbs, we also identified
87 mAbs, which reacted only in the presence of both proteins indicating specificity for the complex.
88 Confocal microscopy with those NEC-specific mAbs revealed small puncta along the nuclear
89 rim in PrV wild type infected cells. In contrast, huge speckles were detectable in cells infected
90 with a PrV mutant lacking the viral protein kinase pUS3, which is known to accumulate primary
91 enveloped virions in the PNS within large invaginations of the INM, or in cells co-expressing
92 pUL31 and pUL34. Kinetic experiments showed that while the individual proteins were
93 detectable already between 2 to 4 hours after infection, the NEC-specific mAbs produced
94 significant staining only after 4 to 6 hours in accordance with timing of nuclear egress. Taken
95 together, the data indicate that these mAbs specifically label the PrV NEC.
96
97
98
99
100
101
102
103

104 **Highlights**
105

- 106 • Generation of monoclonal antibodies (mAbs) specific for the PrV NEC
- 107 • First herpesvirus NEC specific mAbs
- 108 • Visualization of the NEC in infected and transfected cells
- 109 • NEC formation is detectable between 4 to 6 h post infection with no obvious “hot spots”
110 for nuclear egress
111
112
113
114
115
116
117
118

1. Introduction

Efficient translocation of newly assembled intranuclear nucleocapsids to the cytoplasm through the nuclear envelope requires the herpesvirus nuclear egress complex (NEC), an exceptional membrane budding and scission machinery acting at the inner nuclear membrane (INM). The NEC is composed of two conserved viral proteins designated as pUL31 and pUL34 in the alphaherpesviruses pseudorabies virus (PrV) and herpes simplex viruses 1 and 2 (HSV-1, -2). Expression of the NEC results in vesicle budding and scission from synthetic membranes as well as in vesiculation from the INM in eukaryotic cells (Fig. 1) (Bigalke, Heuser, Nicastro, & Heldwein, 2014; Desai, Pryce, Henson, Luitweiler, & Cothran, 2012; Klupp et al., 2007; Lorenz et al., 2015).

The crystal structures of the NECs from different herpesviruses showed a high similarity despite only moderate conservation at the amino acid level (Bigalke & Heldwein, 2015; Lye et al., 2015; Walzer et al., 2015; Zeev-Ben-Mordehai et al., 2015). Both proteins possess a globular core and only the pUL31 N-terminal domain forms a hook-like extension reaching around and inserting into a groove of pUL34. The transmembrane domain located at the C-terminus of pUL34 (Klupp, Granzow, & Mettenleiter, 2000; Shiba et al., 2000) anchors the complex in the nuclear envelope forming a platform for pUL31 at the INM. However, when and where the NEC dimer is assembled, how oligomerization is triggered, and how the NEC mediates membrane bending resulting in nucleocapsid uptake and scission of a membranous vesicle is still unclear. Data from a multimodal imaging approach indicated that first a flat NEC patch is formed at sites where nucleocapsids dock at the INM, which then transforms into a curved spherical coat finally engulfing the nucleocapsid (Hagen et al., 2015).

During nuclear egress, mature DNA-containing capsids are the predominant cargo for translocation while immature capsid forms or empty vesicles are only rarely observed in the PNS (Granzow, Klupp, & Mettenleiter, 2004; Newcomb et al., 2017) indicating that NEC formation and/or oligomerization is blocked until nucleocapsids trigger the budding reaction. The capsid vertex-specific component (CVSC) mainly consisting of pUL17 and pUL25, which is enriched on nucleocapsids (Newcomb et al., 2017; Toropova, Huffman, Homa, & Conway, 2011; Trus et al., 2007) seems to act as exit permit. A few direct contacts between the NEC and the CVSC could be visualized using cryo-electron tomography of primary enveloped particles (Newcomb et al., 2017) and an interaction between pUL31 and the CVSC was demonstrated for HSV-1 (Takeshima et al., 2019; Yang & Baines, 2011; Yang, Wills, Lim, Zhou, & Baines, 2014). In addition, a recent manuscript suggested a rearrangement of the hexameric HSV-1 NEC coat formed on synthetic membranes into pentameric structures in the presence of a truncated pUL25 indicating that the NEC coat is anchored at the capsids via pUL25 pentamers at the vertices (Draganova, Zhang, Zhou, & Heldwein, 2020).

178
179
180
181
182
183
184
185
186
187
188
189
190
191
192
193
194
195
196
197
198
199
200
201
202
203
204
205
206
207
208
209
210
211
212
213
214
215
216
217
218
219
220
221
222
223
224
225
226
227
228
229
230
231
232
233
234
235
236

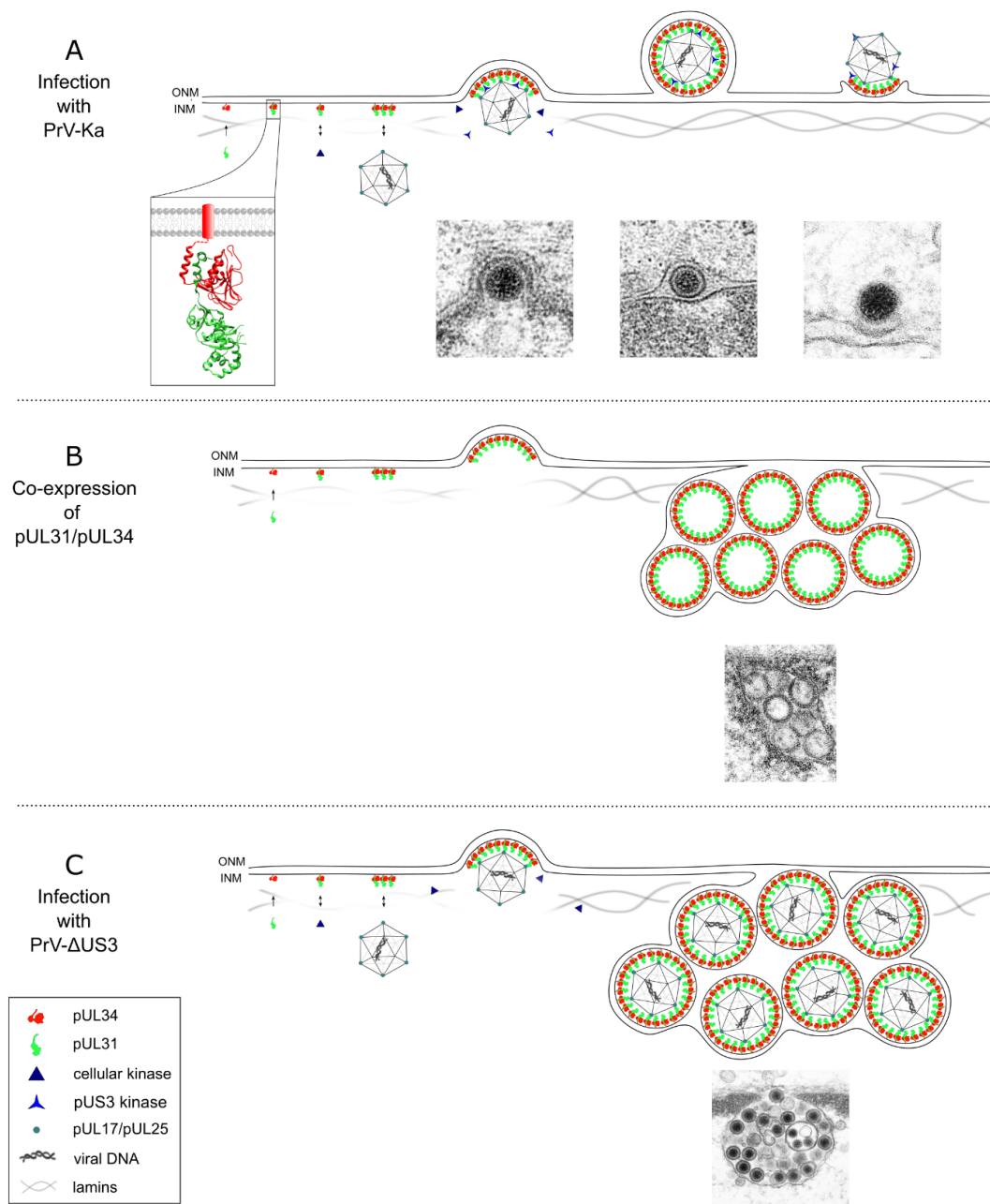


Fig. 1 Herpesvirus nuclear egress and vesicle formation at the INM. (A) In infected cells the viral tail-anchored nuclear membrane protein pUL34 recruits pUL31 to the inner nuclear membrane (INM) forming the nuclear egress complex (NEC). The PrV NEC structure (Zeev-Ben-Mordehai et al., 2015) is shown enlarged in the inset. The NEC recruits viral and cellular protein kinases, resulting in phosphorylation and partial dissolution of the nuclear lamina. The nucleocapsid attaches to the INM and buds into the perinuclear space (PNS) by oligomerization of the NEC. Budding and scission results in a primary enveloped virion in the PNS. The primary virion envelope subsequently fuses with the outer nuclear membrane (ONM) thereby releasing the nucleocapsid into the cytoplasm. (B) Co-expression of PrV pUL31 and pUL34 is sufficient for membrane budding, vesicle formation and scission from the INM, while fusion with the ONM seems to be inefficient resulting in an accumulation of membranous vesicles in the PNS. (C) Infection with a virus mutant lacking the protein kinase pUS3 leads to an accumulation of primary enveloped virions in large invaginations of the INM. Electron microscopic images illustrate the different stages.

237
238
239 pUL31 is assumed to bind to nucleocapsids already in the nucleoplasm governing transport to
240 the INM budding sites (Funk et al., 2015). For PrV, however, interaction of pUL31 with the
241 capsid was reported also in the absence of pUL25 (Leelawong, Guo, & Smith, 2011), and
242 capsids lacking pUL25 were able to reach the INM but budding did not ensue (Klupp, Granzow,
243 Keil, & Mettenleiter, 2006) pointing to several and probably promiscuous NEC binding
244 partner(s) on the capsid.
245
246
247

248
249 In the absence of enzymatically active alphaherpesvirus-specific protein kinase pUS3, primary
250 enveloped virions accumulate in huge invaginations of the INM (Klupp, Granzow, &
251 Mettenleiter, 2001; Reynolds, Wills, Roller, Ryckman, & Baines, 2002; Sehl et al., 2020;
252 Wagenaar et al., 1995) pointing to a modulatory role in the release of nucleocapsids from the
253 perinuclear space (PNS) (Fig. 1C). However, with the enrichment of primary virions in the PNS,
254 which are only rarely detected in wild type infected cells, these mutants serve as an invaluable
255 tool to study primary envelopment and composition of these particles (Granzow et al., 2004;
256 Newcomb et al., 2017).
257
258
259
260

261 For an in-depth characterization of NEC formation and the structural rearrangements resulting
262 in translocation of nucleocapsids from the nucleus into the cytoplasm, we generated
263 monoclonal antibodies (mAbs) against bacterially expressed soluble PrV pUL31/pUL34, which
264 was successfully used for elucidation of the NEC crystal structure (Zeev-Ben-Mordehai et al.,
265 2015). This approach resulted in the isolation of mAbs specific for either pUL31 or pUL34, but
266 also in mAbs reacting only in the presence of both complex partners, indicating that they
267 specifically detect the NEC.
268
269
270
271
272
273
274
275
276
277
278
279
280
281
282
283
284
285
286
287
288
289
290
291
292
293
294
295

296
297
298
299
300
301
302
303
304
305
306
307
308
309
310
311
312
313
314
315
316
317
318
319
320
321
322
323
324
325
326
327
328
329
330
331
332
333
334
335
336
337
338
339
340
341
342
343
344
345
346
347
348
349
350
351
352
353
354

2. Material and Methods

2.1 Viruses and cells. Rabbit kidney cells (RK13) were cultivated in Dulbecco's modified Eagle's minimum essential medium supplemented with 10 % fetal calf serum. The wild type PrV strain Kaplan (PrV-Ka) (Kaplan & Vatter, 1959) and the gene deletion mutants PrV- Δ UL31 (Fuchs, Klupp, Granzow, Osterrieder, & Mettenleiter, 2002), PrV- Δ UL34 (Klupp et al., 2000), as well as PrV- Δ US3 (Klupp et al., 2001) were used for infection. PrV-Ka and PrV- Δ US3 were propagated in RK13 cells, while PrV- Δ UL31 was grown in RK13-UL31 (Fuchs et al., 2002) and PrV- Δ UL34 in RK13-UL34 (Klupp et al., 2000) cells.

2.2 Expression and purification of the nuclear egress complex. Open reading frames encoding N-terminally truncated PrV pUL31 (aa 26-271) and pUL34 (aa 1-179) lacking the C-terminal transmembrane domain were cloned into pETDuet and expressed in *E. coli* strain LEMO21 (DE3) at 25°C. Purification was done as described (Zeev-Ben-Mordehai et al., 2015).

2.3 Immunization of BALB/c mice and cell fusion. Three female BALB/c mice were immunized four times intraperitoneally with 50 μ g of bacterially expressed pUL31/pUL34, mixed with an equal amount of GERBU Adjuvant MM (GERBU Biotechnik) in 4-week intervals. A final boost was set four days before mice were euthanized. Spleen cells were fused with SP2/0 myeloma cells in a ratio of 1:4 in the presence of polyethylene glycol 1500 (PEG, Sigma-Aldrich). Hybridoma cells were selected as described previously (Bussmann, Reiche, Jacob, Braun, & Jassoy, 2006; Fischer et al., 2018). Immunizations were performed in compliance with the national and European legislation, with approval by the competent authority of the Federal State of Mecklenburg-Western Pomerania, Germany.

2.4 Screening for pUL31-, pUL34-, and NEC-specific monoclonal antibodies. Supernatants of hybridoma cells were first screened by indirect immunofluorescence on RK13 cells infected with PrV-Ka at a low multiplicity of infection (MOI) in 96-well plates. Hybridomas, which produced positively reacting supernatants, were subcloned twice and further characterized.

2.5 Immunoblotting. Cells were infected with PrV-Ka, PrV- Δ UL31, PrV- Δ UL34, or PrV- Δ US3 at an MOI of 5 and harvested 24 h post infection (p.i.) by scraping into the medium. Cells were pelleted, washed twice with phosphate-buffered saline (PBS) and lysed in SDS-containing sample buffer (0.13 M Tris-HCl, pH 6.8; 4 % SDS; 20 % glycerin; 0.01 % bromophenol blue; 10 % 2-mercaptoethanol). Proteins were separated in SDS 10 % polyacrylamide gels and after transfer to nitrocellulose membranes, parallel blots were probed with the monospecific polyclonal rabbit sera (pUL31 pAb, pUL34 pAb, both 1:50,000) or with the hybridoma supernatants (1:10 dilutions). After incubation with secondary peroxidase-labelled antibodies

355
356
357 and substrate (Clarity ECL Western Blot Substrate, Bio-Rad), chemiluminescence was
358 recorded in a Bio-Rad Versa Doc imager.
359

360
361 **2.6 Indirect immunofluorescence on transfected and infected cells.** RK13 cells were
362 seeded on coverslips in a 24-well dish and transfected by calcium phosphate-coprecipitation
363 (Graham & van der Eb, 1973) with 1 µg of pcDNA-UL31 (Fuchs et al., 2002) and/or pcDNA-
364 UL34 (Klupp et al., 2000), or infected with PrV-Ka, PrV-ΔUL31, PrV-ΔUL34 or PrV-ΔUS3 with
365 approx. 250 plaque forming units (pfu)/well. Cells were fixed 2 d post transfection or 18 to 24h
366 p.i. with 4 % paraformaldehyde for 15 min. Fixed cells were washed three times and incubated
367 with 50 mM NH₄Cl in 1x PBS for 30 min. For expression kinetics, cells were infected with PrV-
368 Ka or PrV-ΔUS3 at an MOI of 5 and fixed after 2 h, 4 h, and 6 h p.i. Fixed samples were
369 permeabilized with 0.1 % Triton X-100 in 1x PBS. Samples were stained with the hybridoma
370 supernatants and/or with the polyclonal rabbit sera specific for pUL31 (pAb, 1:500, (Fuchs et
371 al., 2002)) and pUL34 (pAb, 1:500, (Klupp et al., 2000)). Alexa Fluor 488-conjugated goat anti-
372 rabbit or -mouse IgG and Alexa 568-conjugated goat anti-rabbit or anti-mouse IgG (dilution
373 1:1000, Invitrogen) were used to detect bound antibody. Nuclei were stained with 300 mM 4',6-
374 Diamidin-2-phenylindol (DAPI, Sigma-Aldrich) for 5 min, cells were mounted in a drop of
375 Kaiser's glycerol gelatin (Merck) and imaged with a confocal laser scanning microscope (Leica
376 DMI 6000 TCS SP5, 63x oil-immersion objective, NA = 1.4). Cells for determination of infection
377 kinetics were processed in parallel and all images were acquired with identical parameters
378 (laser excitation, detector settings, and zoom factor). Representative single images and Z-
379 stacks were processed using Fiji software version 1.52 (Schindelin et al., 2012; Schneider,
380 Rasband, & Eliceiri, 2012) and Icy software version 2.0 (de Chaumont et al., 2012).
381
382
383
384
385
386
387
388
389
390

391 **2.7 Ultrastructural analyses.** RK13 cell lines were infected with PrV-Ka and PrV-ΔUS3 at an
392 MOI of 1 for 14 h and processed for transmission electron microscopy. They were fixed in 0.5
393 % glutaraldehyde buffered in 0.1 M PBS (pH 7.2) for 2 h at 4 °C. The fixed samples were
394 embedded in 1.8 % low-melting agarose, cut in small pieces (1 mm³) and postfixed in 0.5%
395 glutaraldehyde buffered in 1x PBS (pH 7.2) for 30 min (Serva). After that, samples were
396 blocked in 0.1 M NH₄Cl in 1 x PBS for 60 min, washed in 1x PBS and stained in 0.5 % aqueous
397 uranyl acetate overnight. During stepwise dehydration in ethanol, temperature was progressive
398 lowered until -20 °C with the help of the Leica EM ASF2. The samples were infiltrated with
399 Lowicryl resin K4M (Polyscience), filled in gelatin capsules and polymerized under UV light for
400 3 days. Ultrathin sections were prepared with an ultramicrotome (UC7; Leica), transferred to
401 formvar coated nickel grids (300 mesh, Athene; Plano), and stored until immunostaining.
402
403
404
405
406
407

408 For a better immunostaining of nuclear proteins, DNase I digestion was performed. DNase I
409 (NEB) was diluted 1:10 in its reaction buffer and grids were incubated 30 min at room
410
411
412
413

2 Publications

414
415
416 temperature. After washing with PBS the sections were blocked with 1 % cold-water fish
417 gelatin, 0.02 M glycine and 1 % bovine serum albumin (BSA) in 1 x PBS (Merck).
418
419 For staining with the monoclonal antibodies undiluted supernatants, as well as 1:10 and 1:50
420 dilutions in 1 % BSA in 1 x PBS were tested and incubated at 4 °C overnight. For staining with
421 the polyclonal monospecific antisera a 1:1000 dilution in 1 % BSA in 1 x PBS was prepared
422 and incubated at room temperature for 3 h. Bound antibodies were detected with immunogold
423 conjugate against mouse monoclonal antibodies (GMHL10; BBI solutions) and rabbit
424 polyclonal antisera (GAR10; BBI solutions), respectively. The conjugates were used in 1:50
425 dilutions and incubated for 1 h at room temperature.
426
427 After washing and drying the grids were counterstained with uranyl acetate and lead citrate
428 and finally examined with a Tecnai Spirit transmission electron microscope (FEI, NED) at an
429 accelerating voltage of 80 kV.
430
431
432
433
434
435
436
437
438
439
440
441
442
443
444
445
446
447
448
449
450
451
452
453
454
455
456
457
458
459
460
461
462
463
464
465
466
467
468
469
470
471
472

3. Results and Discussion

3.1 Screening of hybridoma cell clone supernatants.

Initial screening of the hybridoma supernatants was performed by indirect immunofluorescence of RK13 cells infected with PrV-Ka under plaque assay conditions. Non-infected cells in the same wells served as control and allowed exclusion of antibodies reacting with cellular antigens. Hybridoma cells, whose supernatant showed a virus-positive reactivity, were subcloned twice and screened on pUL31 and pUL34 individually or co-expressing cells. For further characterization, RK13 cells were infected with PrV- Δ UL31, PrV- Δ UL34 and PrV- Δ US3, and tested by indirect immunofluorescence. Six hybridoma supernatants reacted specifically with pUL31, while eight showed reactivity for pUL34 as was evident by comparison with cells infected with the deletion mutants or expressing individual proteins. Four hybridoma supernatants showed positive staining only in the presence of both proteins in transfected as well as in infected cells pointing to complex-specific reactivity (Table 1).

Table 1: Overview on the reactivity of the monoclonal antibodies (mAbs).

	mAb	clone	Immunofluorescence							WB	Immune EM
			Infection				Transfection				
			PrV-Ka	Δ US3	Δ UL31	Δ UL34	pUL31	pUL34	pUL31/pUL34		
anti-pUL31	1	1A1 B3	+	+	-	+	+	-	+	+	-
	2	1A4 B3	+	+	-	+	+	-	+	+	n.t.
	5	3A12 C4	+	+	-	+	+	-	+	+	+
	9	2E12 C3	+	+	-	+	+	-	+	+	-
	11	2F6 D1	+	+	-	+	+	-	+	+	n.t.
	12	3G5 B3	+	+	-	+	+	-	+	+	n.t.
anti-pUL34	7	6C2 B2	+	+	+	-	-	+	+	-	-
	8	1D7 A1	+	+	+	-	-	+	+	-	n.t.
	A	4B1 C1	+	+	+	-	-	+	+	-	-

2 Publications

532
533
534
535
536
537
538
539
540
541
542
543
544
545
546
547
548
549
550
551
552
553
554
555
556
557
558
559
560
561
562
563
564
565
566
567
568
569
570
571
572
573
574
575
576
577
578
579
580
581
582
583
584
585
586
587
588
589
590

	B	7G7 A3	+	+	+	-	-	+	+	-	-
	D	7E11 A2	+	+	+	-	-	+	+	-	n.t.
	F	3H2 A3	+	+	+	-	-	+	+	-	-
	G	4G12 A3	+	+	+	-	-	+	+	-	n.t.
	H	7G6 A3	+	+	+	-	-	+	+	-	n.t.

anti-NEC	4	2A7 B2	+	+	-	-	-	-	+	-	-
	6	2B5 A2	+	+	-	-	-	-	+	-	-
	13	2H3 A1	+	+	-	-	-	-	+	-	-
	14	2H11 B1	+	+	-	-	-	-	+	-	-

mAbs were characterized by indirect immunofluorescence of infected and transfected cells, by western blotting (WB) with lysates of infected cells and immunoelectron microscopy (EM) on infected cells.

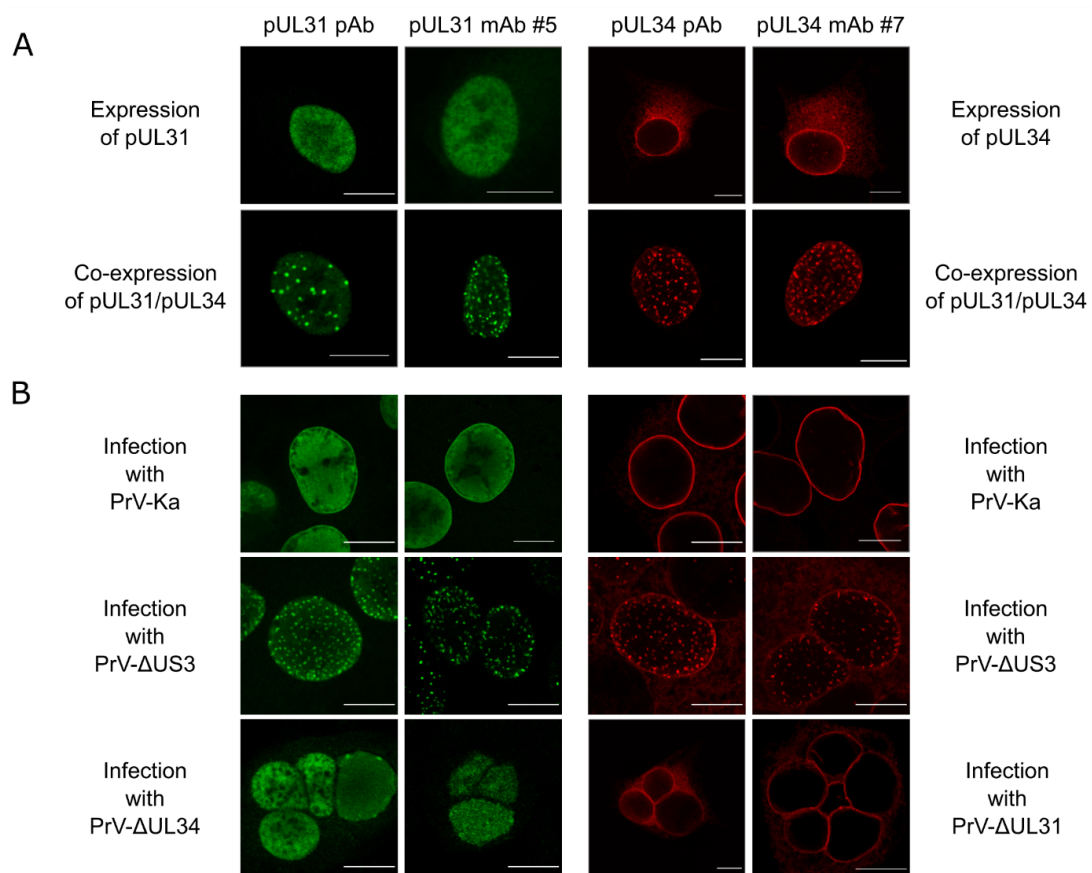
+, positive signal; -, no signal; n.t., not tested;

All hybridoma supernatants were further tested by immunoblotting of lysates of infected or transfected cells under denaturing conditions. Here, only the pUL31-specific hybridoma supernatants showed a positive reaction (Table 1), while the pUL34- and NEC-specific mAbs were negative, which suggests that these antibodies detect conformational epitopes.

3.2 Comparison of reaction pattern of the pUL31- and pUL34-specific monoclonal antibodies with the polyclonal monospecific sera.

To compare the reaction patterns of the pUL31- and pUL34-specific monoclonal antibodies present in the selected hybridoma supernatants with our well-characterized monospecific rabbit sera, transfected (Fig. 2A) or infected (Fig. 2B) RK13 cells were fixed, stained with the different antibodies and antisera, and processed for confocal laser scanning microscopy. In transfected cells, pUL31 localizes diffusely in the nucleus, while pUL34 is detectable predominantly at the nuclear rim but also in cytoplasmic structures, most likely the endoplasmic reticulum. Co-expression of both proteins resulted in the typical nuclear speckled pattern after staining with pUL31- and pUL34-specific antibodies (Fig. 2A) (Klupp et al., 2007).

591
592
593 In PrV-Ka infected and transfected cells pUL31 is found diffusely distributed in the nucleus but
594 also partly at the nuclear rim. Labelling of PrV-Ka infected cells with anti-pUL34 showed only
595 a smooth nuclear rim staining. In PrV- Δ US3 infected cells immunostaining revealed the typical
596 huge nuclear speckles after incubation with the anti-pUL31 as well as with the anti-pUL34
597 antibodies as described (Klupp et al., 2007). For anti-pUL34 antibodies, in addition to the
598 speckles, a nuclear rim staining was still evident. However, nuclear localization was less
599 prominent and more cytoplasmic fluorescence was detectable in the absence of pUS3 as
600 reported earlier (Klupp et al., 2001). After infection with PrV- Δ UL34, recruitment of pUL31 to
601 the nuclear rim was not detectable and in the absence of pUL31, staining for pUL34 was less
602 concentrated in the nuclear rim (Fig. 2B).



637
638
639
640
641
642
643
644
645
646
647
648
649

Fig. 2. Comparison of pUL31- and pUL34-specific polyclonal and monoclonal antibody labelling patterns. Staining patterns for the pUL31- and pUL34-specific pAbs and mAbs were compared using confocal laser scanning microscopy after transfection of the corresponding expression plasmids either individually or in combination (A) or after infection with PrV-Ka, PrV- Δ US3, PrV- Δ UL34, or PrV- Δ UL31 (B). Scale bars indicate 10 μ m.

In the transfected and infected cells, the pUL31- and pUL34-specific mAbs showed comparable staining as the polyclonal rabbit sera. In addition, no difference in the reaction pattern was evident for the different pUL31- and pUL34-specific mAbs (Table 1).

3.3 Characterization of the NEC-specific monoclonal antibodies.

2 Publications

Supernatants from four different hybridoma clones did not label singly transfected cells or cells infected with the UL31- or UL34-deletion mutants, but showed a robust reactivity with cells co-expressing pUL31/pUL34 as well as with cells infected with PrV-Ka or PrV- Δ US3 (Fig. 3, Table 1) suggesting that these antibodies specifically recognize the NEC. Previous structural analyses suggested that binding of pUL31 results in conformational changes in pUL34 (Bigalke & Heldwein, 2015; Zeev-Ben-Mordehai et al., 2015). Further, the N-terminal hook of pUL31 is most likely folded differently in the absence of pUL34 (Bigalke & Heldwein, 2017; Funk et al., 2015). Co-expression of pUL31 and pUL34 resulting in NEC formation, membrane deformation and vesicle scission probably results in generation of epitopes which are either not accessible or not present on the individual proteins. In fact, an extensive interface between pUL31 and pUL34 is formed in the heterodimeric NEC but also in the oligomeric NEC coat (Hagen et al., 2015; Zeev-Ben-Mordehai et al., 2015), which could harbor those antibody-binding sites.

To compare the staining of the NEC-specific mAbs with the localization of the individual complex components, singly and co-transfected cells were stained simultaneously with the mAbs and pAbs in different combinations. As expected, the singly transfected cells showed no specific staining with the NEC-specific mAb, while after co-transfection staining of the speckles showed a significant overlap between the NEC-specific mAb and the pUL31- or pUL34-specific pAbs (Fig. 3A).

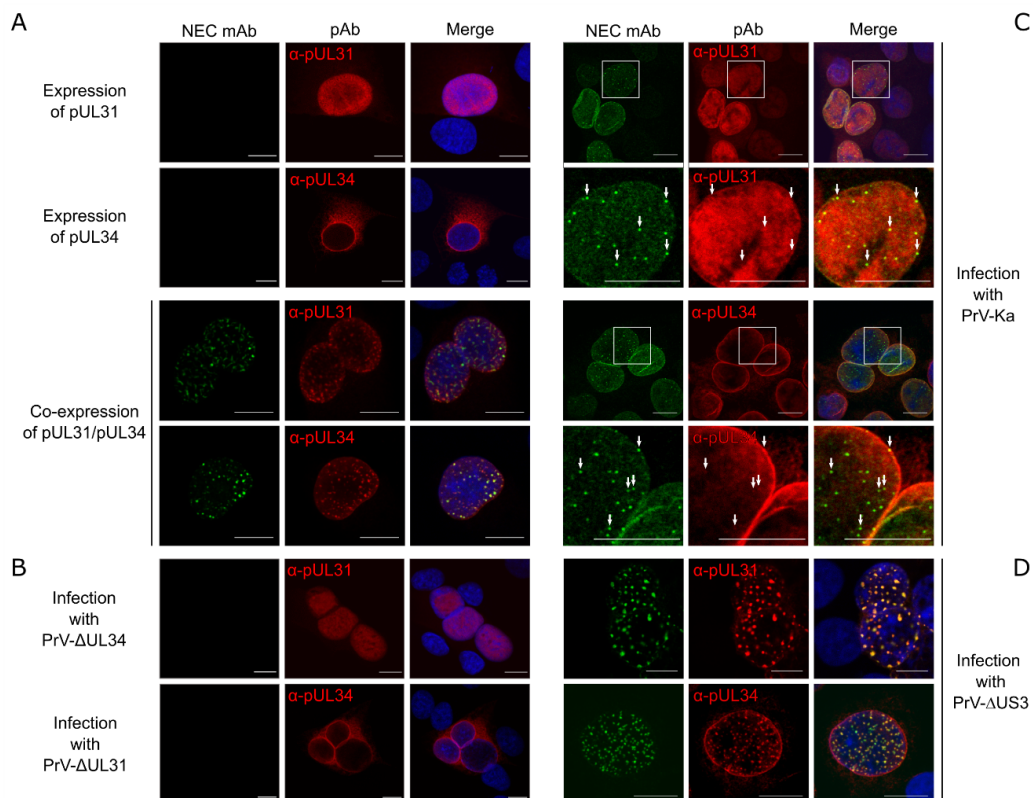


Fig. 3. Characterization of NEC-specific monoclonal antibodies. The reaction pattern for the hybridoma cell supernatants, which labelled only in presence of both NEC components, was compared with the staining pattern of the polyclonal anti-pUL31 and anti-pUL34 sera (pAb). (A) RK13 cells were transfected with pUL31 and pUL34 expression plasmids individually or in combination, or infected with the single gene deletion mutants (B), PrV-Ka (C), or PrV- Δ US3 (D) and labelled with a NEC-specific mAb and either the anti-pUL31 or the anti-pUL34 pAb. For a better visualization of co-localization, areas boxed in C are shown in higher magnification and arrows mark some brighter spots. Nuclei were stained with DAPI and scale bars indicate 10 μ m.

The NEC-specific mAbs showed no reactivity with cells infected with the UL31- or UL34-deletion mutants (Fig. 3B). Staining of PrV-Ka infected cells with these mAbs, however, revealed a small dotted and a faint diffuse nuclear staining (Fig. 3C). Co-staining with the polyclonal anti-pUL31 and anti-pUL34 sera showed an overlap at least in the puncta (Fig. 3C, some prominent dots marked by arrows). In contrast, a very strong and clear colocalization between the NEC-specific mAbs and the pUL31 or pUL34-specific pAb label was evident in PrV- Δ US3 infected cells (Fig. 3D). We speculate that the small dots in PrV-Ka infected cells or the large speckles in PrV- Δ US3 infected cells represent budding sites and/or primary enveloped virions. Comparison of the four different NEC-specific mAbs revealed similar staining patterns after co-transfection as well as infection with PrV-Ka and PrV- Δ US3 (Fig. 4).

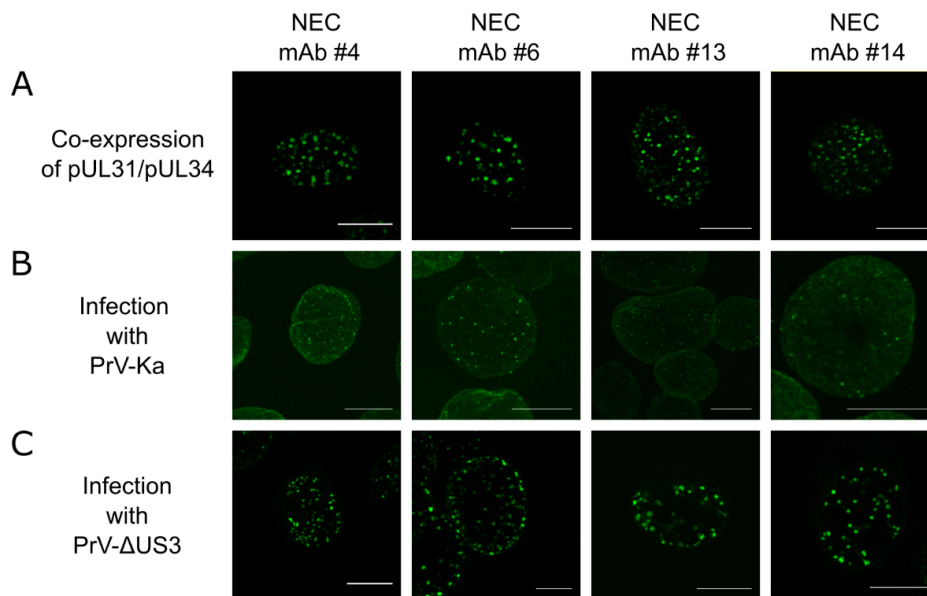
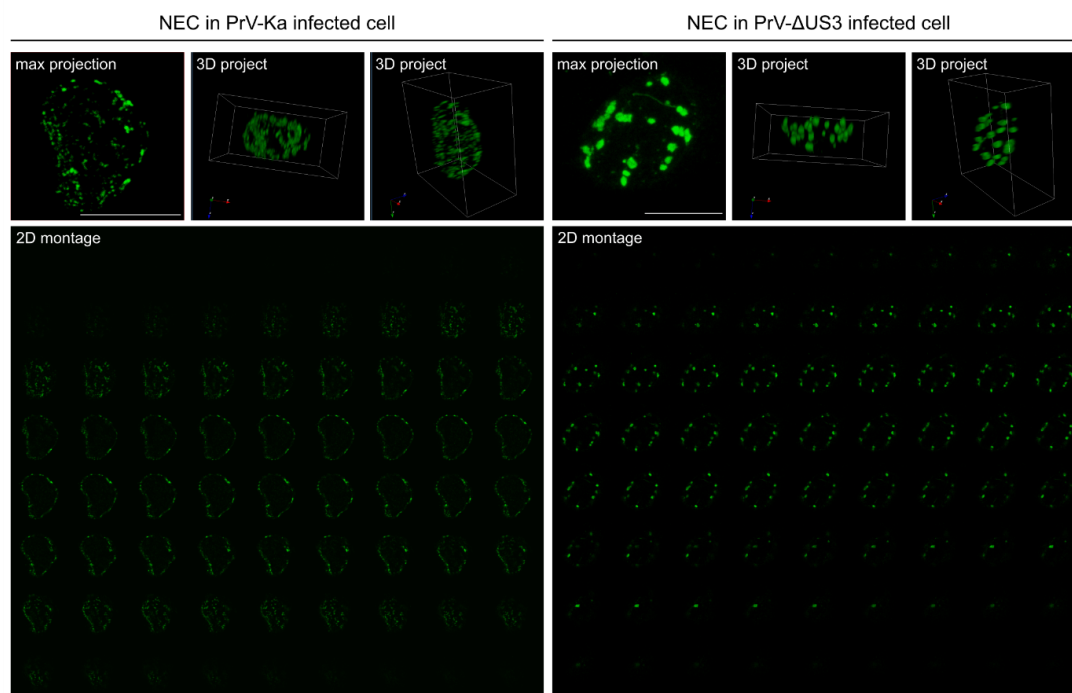


Fig. 4. Comparison of the staining pattern of the different NEC-specific mAbs. Reactivity of the four different NEC-specific mAbs in RK13 cells was compared by confocal laser scanning microscopy after co-transfection with the pUL31 and pUL34 expression plasmids (A), after infection with PrV-Ka (B) or after infection with PrV- Δ US3 (C). Scale bars indicate 10 μ m.

3.4 The NEC-specific signal is localized at the nuclear rim.

Despite using a confocal laser scanning microscope, the small and large speckles in infected and transfected cells appeared to be distributed throughout the whole nucleus. To investigate this in more detail, Z-stacks were generated from PrV-Ka and PrV- Δ US3 infected cells

768
769
770 incubated with the NEC-specific mAb #13 (Fig. 5). 3D projection showed that the dots are all
771 located along the nuclear rim indicating that they are derived from the INM. The distribution of
772 the small puncta detectable in the PrV-Ka infected cells as well as the huge speckles present
773 after infection with PrV- Δ US3 indicated budding along the nuclear envelope with no obvious
774 preferential locations or 'hot spots' (Fig. 5 and Suppl. Video 1 + 2). In contrast, nuclear egress
775 was suggested to occur predominantly adjacent to the assembly compartments in human
776 cytomegalovirus infected cells (Buchkovich et al., 2008).
777
778
779
780



805 **Fig. 5. Localization of NEC-specific staining at the nuclear envelope.** Three-dimensional
806 reconstruction of a PrV-Ka (left) and a PrV- Δ US3 infected cell (right) stained with the NEC-specific mAb
807 #13. Z-stacks were obtained with a step size of 0.13 μ m. Shown are stacks of approx. 70 optical sections
808 from each cell. The maximum projection shows the merged signals. For 3D reconstruction, the Ivy
809 software was used. The 2D projection (Fiji software) shows all sections individually. Scale bars indicate
810 10 μ m.

811 3.5 NEC expression kinetics.

812
813
814 Expression kinetics for the NEC components were analyzed in RK13 cells infected with a MOI
815 of 5 of PrV-Ka or PrV- Δ US3 (Fig. 6). Infected cells were fixed 2 h, 4 h, and 6 h after infection,
816 and imaged with constant settings using a confocal laser scanning microscope. As expected,
817 the specific signals increased over time. In PrV-Ka and PrV- Δ US3 infected cells expression of
818 pUL31 and pUL34 was first detected approx. 4 h p.i. Recruitment of pUL31 to the nuclear
819 envelope was not observed until 6 h after infection. In PrV- Δ US3 infected cells expression of
820 both proteins seemed to be slightly delayed but was comparable at 6 h p.i when small puncta
821 were already observed (Fig. 6). Small nuclear dots were also detectable 6 h p.i. in PrV-Ka and
822
823
824
825
826

PrV- Δ US3 infected cells after incubation with the NEC-specific mAbs, paralleling the appearance of nuclear rim staining for pUL31 and supporting the assumption that these dots represent either budding sites or primary enveloped virions. Imaging at later time points was not possible since the cells already showed cytopathic effect and detached from the cover slips.

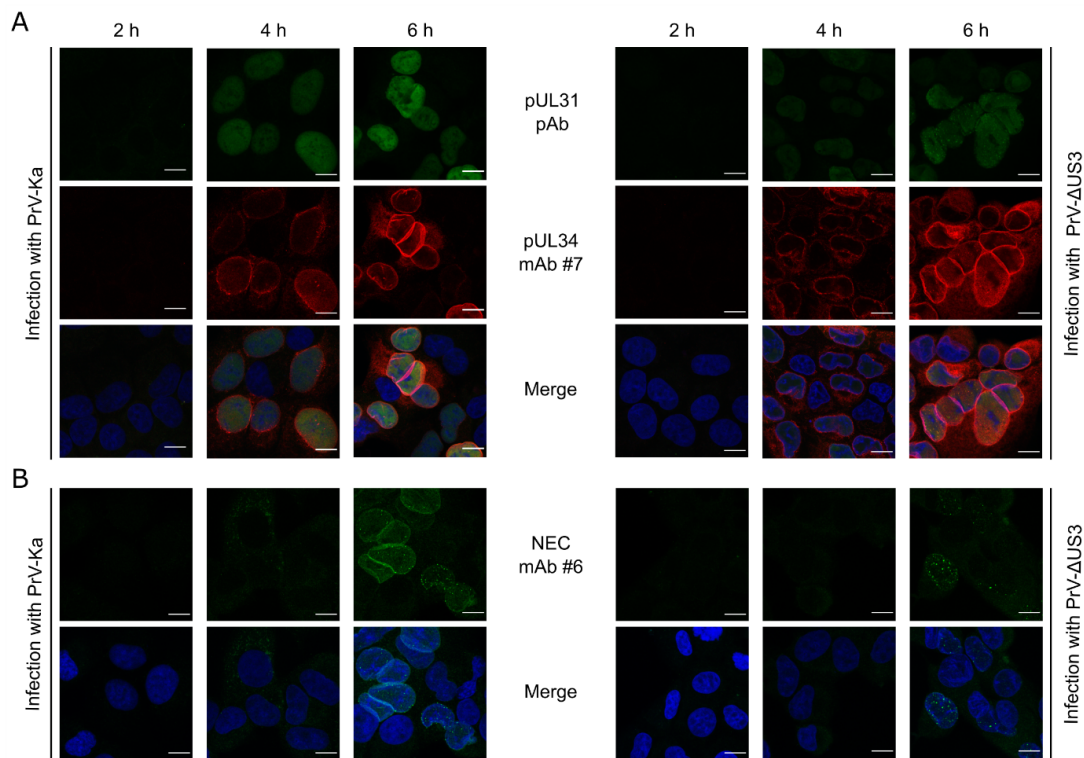


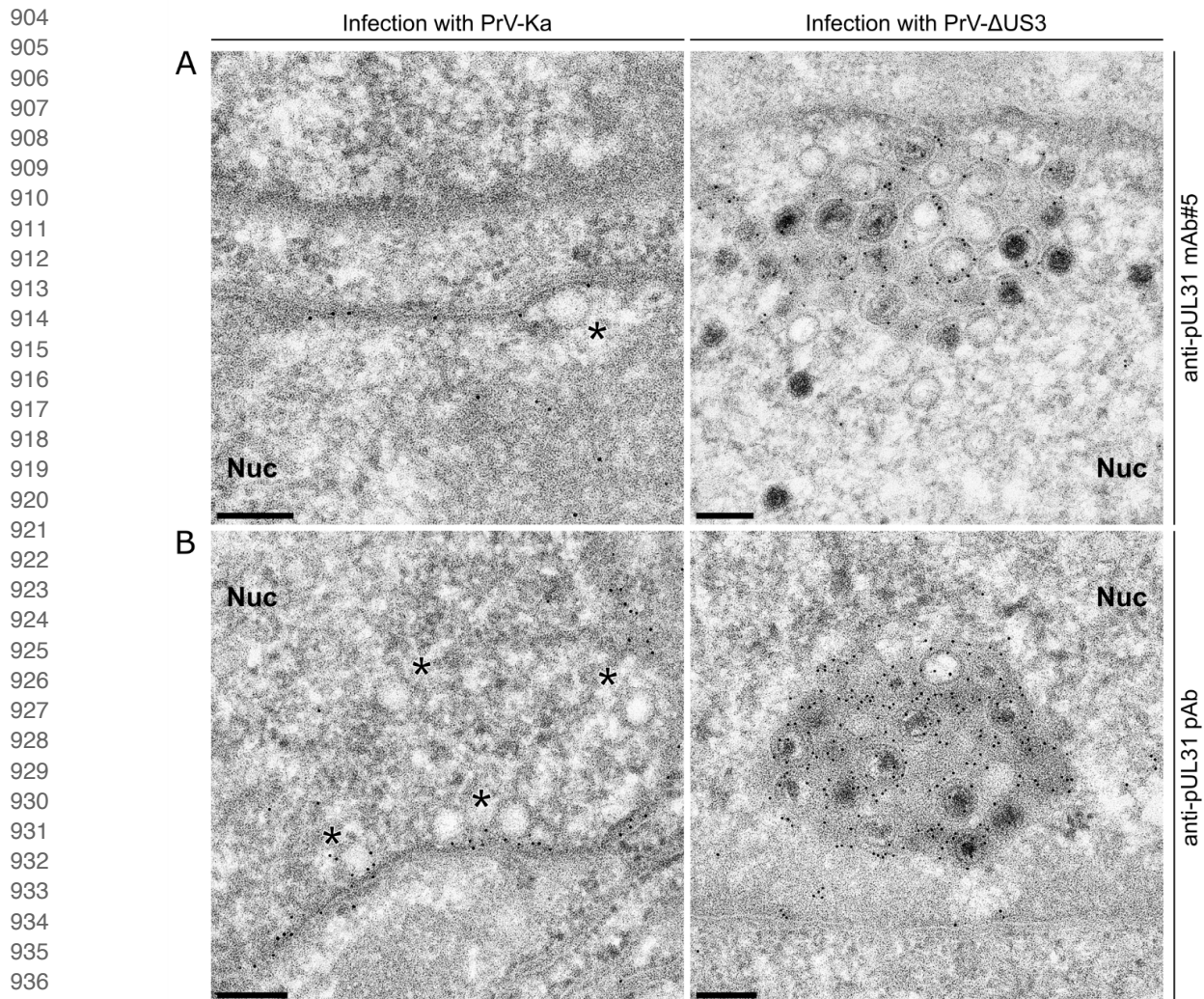
Fig. 6. NEC expression kinetics. Expression of the NEC components was investigated 2 h, 4 h, and 6 h after high MOI infection with PrV-Ka (left panels) or PrV- Δ US3 (right panels) by confocal laser scanning microscopy. The NEC components were visualized by staining with the anti-pUL31 pAb and anti-pUL34 mAb #7 (A), while for panel (B) the NEC-specific mAb #6 was used. Nuclei were stained with DAPI. Scale bars indicate 10 μ m.

3.6 Immunoelectron microscopic analyses.

A subset of pUL31- and pUL34-specific mAbs and all four NEC-specific mAbs were tested by immunoelectron microscopy on PrV-Ka- and PrV- Δ US3 infected cells (Table 1). Unfortunately, the anti-pUL34 and anti-NEC mAbs did not react under these conditions. In contrast, the pUL31 specific mAb #5 produced a clear labeling of the nuclear envelope in PrV-Ka infected cells with only few gold particles present in the nucleoplasm or on intranuclear capsids (Fig. 7A). In PrV- Δ US3 infected cells the gold particles were mainly associated with primary virions in INM herniations. Immune labeling with the monospecific anti-pUL31 serum revealed a comparable pattern (Fig. 7B).

886
887
888
889 Until now, it is not clear how mature nucleocapsids reach the INM for budding. One of the
890 hypotheses for HSV-1 suggests that capsids are escorted by pUL31 to the sites of nuclear
891 egress (Funk et al., 2015). In our studies, however, using either the potent pUL31-specific pAb
892 or the newly generated mAbs binding of pUL31 to the nucleocapsids was only rarely detected.
893

894
895 Despite the prominent staining achieved with the pUL34- and NEC-specific mAbs in indirect
896 immunofluorescence assays, unfortunately no label was found on the ultrathin sections. We
897 assume that the antigen density in these sections might be too small for a positive signal.
898 We assume that the antigen density in these sections might be too small for a positive signal.
899 Alternatively, the fixation method might change the native structure of the complex, thereby
900 masking or destroying the epitopes. Better results might be obtained on cryo sections, which
901 however, are not yet established in our facility.
902
903



938 **Fig. 7. Immunoelectron microscopy.** RK13 cells infected with PrV-Ka or PrV-ΔUS3 (MOI=1) were
939 processed for immunoelectron microscopy. pUL31 was detected with mAb #5 (A) or the pAb (B) and
940 gold-labeled secondary antibodies. Due to pretreatment with DNase I capsids often appear empty
941 (indicated by asterisks). Bars indicate 200 nm. Nuc: nucleus
942
943
944

945
946
947 **Author Contributions**
948 Conceptualization, T.C.M., B.G.K., and J.E.H.; data curation, T.C.M., B.G.K. and J.E.H.; formal
949 analysis, J.E.H.; funding acquisition, T.C.M. and B.G.K.; investigation, B.G.K., K.F. and J.E.H.;
950 methodology, B.G.K., J.E.H., K.F. and S.R.; project administration, T.C.M. and B.G.K.;
951 resources, K.F. and S.R.; software, J.E.H.; supervision, T.C.M., B.G.K.; validation, T.C.M.,
952 B.G.K. and J.E.H.; visualization, J.E.H.; supervision, T.C.M. and B.G.K.; roles/writing-original
953 draft, J.E.H. and B.G.K.; writing-review & editing, T.C.M., S.R., K.F. and B.G.K.;

954
955
956 **Acknowledgements**
957
958
959 This study was supported by the Deutsche Forschungsgemeinschaft (DFG ME 854/12-2). We
960 thank Karla Günther, Cindy Krüper, Petra Meyer, Mandy Jörn and Sven Sander for technical
961 support and Dr. Stefan Finke as well as Luca Zaack for help with confocal microscopy. We
962 thank Tzviya Zeev-Ben-Mordehai and Cathy Whittle for providing the bacterially expressed
963 proteins. Further, we thank the Friedrich-Loeffler-Institut Collection of Cell Lines for their
964 assistance in supplying cell lines and media.
965
966
967
968
969
970
971
972
973
974
975
976
977
978
979
980
981
982
983
984
985
986
987
988
989
990
991
992
993
994
995
996
997
998
999
1000
1001
1002
1003

1004
1005
1006
1007
1008
1009
1010
1011
1012
1013
1014
1015
1016
1017
1018
1019
1020
1021
1022
1023
1024
1025
1026
1027
1028
1029
1030
1031
1032
1033
1034
1035
1036
1037
1038
1039
1040
1041
1042
1043
1044
1045
1046
1047
1048
1049
1050
1051
1052
1053
1054
1055
1056
1057
1058
1059
1060
1061
1062

References

- Bigalke, J. M., & Heldwein, E. E. (2015). Structural basis of membrane budding by the nuclear egress complex of herpesviruses. *EMBO J*, *34*(23), 2921-2936. doi:10.15252/embj.201592359
- Bigalke, J. M., & Heldwein, E. E. (2017). Chapter Three - Have NEC Coat, Will Travel: Structural Basis of Membrane Budding During Nuclear Egress in Herpesviruses. In M. Kielian, T. C. Mettenleiter, & M. J. Roossinck (Eds.), *Adv Virus Res* (Vol. 97, pp. 107-141): Academic Press.
- Bigalke, J. M., Heuser, T., Nicastro, D., & Heldwein, E. E. (2014). Membrane deformation and scission by the HSV-1 nuclear egress complex. *Nat Commun*, *5*, 4131. doi:10.1038/ncomms5131
- Buchkovich, N. J., Maguire, T. G., Yu, Y., Paton, A. W., Paton, J. C., & Alwine, J. C. (2008). Human cytomegalovirus specifically controls the levels of the endoplasmic reticulum chaperone BiP/GRP78, which is required for virion assembly. *J Virol*, *82*(1), 31-39. doi:10.1128/JVI.01881-07
- Bussmann, B. M., Reiche, S., Jacob, L. H., Braun, J. M., & Jassoy, C. (2006). Antigenic and cellular localisation analysis of the severe acute respiratory syndrome coronavirus nucleocapsid protein using monoclonal antibodies. *Virus Res*, *122*(1-2), 119-126. doi:10.1016/j.virusres.2006.07.005
- de Chaumont, F., Dallongeville, S., Chenouard, N., Herve, N., Pop, S., Provoost, T., . . . Olivo-Marin, J. C. (2012). Icy: an open bioimage informatics platform for extended reproducible research. *Nat Methods*, *9*(7), 690-696. doi:10.1038/nmeth.2075
- Desai, P. J., Pryce, E. N., Henson, B. W., Luitweiler, E. M., & Cothran, J. (2012). Reconstitution of the Kaposi's sarcoma-associated herpesvirus nuclear egress complex and formation of nuclear membrane vesicles by coexpression of ORF67 and ORF69 gene products. *J Virol*, *86*(1), 594-598. doi:10.1128/JVI.05988-11
- Draganova, E. B., Zhang, J., Zhou, Z. H., & Heldwein, E. E. (2020). Structural basis for capsid recruitment and coat formation during HSV-1 nuclear egress. *bioRxiv*, 2020.2003.2011.988170. doi:10.1101/2020.03.11.988170
- Fischer, K., Diederich, S., Smith, G., Reiche, S., Pinho Dos Reis, V., Stroh, E., . . . Balkema-Buschmann, A. (2018). Indirect ELISA based on Hendra and Nipah virus proteins for the detection of henipavirus specific antibodies in pigs. *PLoS One*, *13*(4), e0194385. doi:10.1371/journal.pone.0194385
- Fuchs, W., Klupp, B. G., Granzow, H., Osterrieder, N., & Mettenleiter, T. C. (2002). The interacting UL31 and UL34 gene products of pseudorabies virus are involved in egress from the host-cell nucleus and represent components of primary enveloped but not mature virions. *J Virol*, *76*(1), 364-378.
- Funk, C., Ott, M., Raschbichler, V., Nagel, C. H., Binz, A., Sodeik, B., . . . Bailer, S. M. (2015). The Herpes Simplex Virus Protein pUL31 Escorts Nucleocapsids to Sites of Nuclear Egress, a Process Coordinated by Its N-Terminal Domain. *PLoS Pathog*, *11*(6), e1004957. doi:10.1371/journal.ppat.1004957
- Graham, F. L., & van der Eb, A. J. (1973). A new technique for the assay of infectivity of human adenovirus 5 DNA. *Virology*, *52*(2), 456-467.
- Granzow, H., Klupp, B. G., & Mettenleiter, T. C. (2004). The pseudorabies virus US3 protein is a component of primary and of mature virions. *J Virol*, *78*(3), 1314-1323. doi:10.1128/jvi.78.3.1314-1323.2004
- Hagen, C., Dent, K. C., Zeev-Ben-Mordehai, T., Grange, M., Bosse, J. B., Whittle, C., . . . Grunewald, K. (2015). Structural Basis of Vesicle Formation at the Inner Nuclear Membrane. *Cell*, *163*(7), 1692-1701. doi:10.1016/j.cell.2015.11.029
- Kaplan, A. S., & Vatter, A. E. (1959). A comparison of herpes simplex and pseudorabies viruses. *Virology*, *7*(4), 394-407.
- Klupp, B. G., Granzow, H., Fuchs, W., Keil, G. M., Finke, S., & Mettenleiter, T. C. (2007). Vesicle formation from the nuclear membrane is induced by coexpression of two conserved

1063
1064
1065
1066
1067
1068
1069
1070
1071
1072
1073
1074
1075
1076
1077
1078
1079
1080
1081
1082
1083
1084
1085
1086
1087
1088
1089
1090
1091
1092
1093
1094
1095
1096
1097
1098
1099
1100
1101
1102
1103
1104
1105
1106
1107
1108
1109
1110
1111
1112
1113
1114
1115
1116
1117
1118
1119
1120
1121

- herpesvirus proteins. *Proc Natl Acad Sci U S A*, 104(17), 7241-7246.
doi:10.1073/pnas.0701757104
- Klupp, B. G., Granzow, H., Keil, G. M., & Mettenleiter, T. C. (2006). The capsid-associated UL25 protein of the alphaherpesvirus pseudorabies virus is nonessential for cleavage and encapsidation of genomic DNA but is required for nuclear egress of capsids. *J Virol*, 80(13), 6235-6246. doi:10.1128/JVI.02662-05
- Klupp, B. G., Granzow, H., & Mettenleiter, T. C. (2000). Primary envelopment of pseudorabies virus at the nuclear membrane requires the UL34 gene product. *J Virol*, 74(21), 10063-10073.
- Klupp, B. G., Granzow, H., & Mettenleiter, T. C. (2001). Effect of the pseudorabies virus US3 protein on nuclear membrane localization of the UL34 protein and virus egress from the nucleus. *J Gen Virol*, 82(Pt 10), 2363-2371. doi:10.1099/0022-1317-82-10-2363
- Leelawong, M., Guo, D., & Smith, G. A. (2011). A physical link between the pseudorabies virus capsid and the nuclear egress complex. *J Virol*, 85(22), 11675-11684. doi:10.1128/JVI.05614-11
- Lorenz, M., Vollmer, B., Unsay, J. D., Klupp, B. G., Garcia-Saez, A. J., Mettenleiter, T. C., & Antonin, W. (2015). A single herpesvirus protein can mediate vesicle formation in the nuclear envelope. *J Biol Chem*, 290(11), 6962-6974. doi:10.1074/jbc.M114.627521
- Lye, M. F., Sharma, M., El Omari, K., Filman, D. J., Schuermann, J. P., Hogle, J. M., & Coen, D. M. (2015). Unexpected features and mechanism of heterodimer formation of a herpesvirus nuclear egress complex. *EMBO J*, 34(23), 2937-2952. doi:10.15252/embj.201592651
- Newcomb, W. W., Fontana, J., Winkler, D. C., Cheng, N., Heymann, J. B., & Steven, A. C. (2017). The Primary Enveloped Virion of Herpes Simplex Virus 1: Its Role in Nuclear Egress. *mBio*, 8(3), e00825-00817. doi:10.1128/mBio.00825-17
- Reynolds, A. E., Wills, E. G., Roller, R. J., Ryckman, B. J., & Baines, J. D. (2002). Ultrastructural localization of the herpes simplex virus type 1 UL31, UL34, and US3 proteins suggests specific roles in primary envelopment and egress of nucleocapsids. *J Virol*, 76(17), 8939-8952.
- Schindelin, J., Arganda-Carreras, I., Frise, E., Kaynig, V., Longair, M., Pietzsch, T., . . . Cardona, A. (2012). Fiji: an open-source platform for biological-image analysis. *Nat Methods*, 9(7), 676-682. doi:10.1038/nmeth.2019
- Schneider, C. A., Rasband, W. S., & Eliceiri, K. W. (2012). NIH Image to ImageJ: 25 years of image analysis. *Nat Methods*, 9(7), 671-675.
- Sehl, J., Portner, S., Klupp, B. G., Granzow, H., Franzke, K., Teifke, J. P., & Mettenleiter, T. C. (2020). Roles of the different isoforms of the pseudorabies virus protein kinase pUS3 in nuclear egress. *J Virol*, JVI.02029-02019. doi:10.1128/JVI.02029-19
- Shiba, C., Daikoku, T., Goshima, F., Takakuwa, H., Yamauchi, Y., Koiwai, O., & Nishiyama, Y. (2000). The UL34 gene product of herpes simplex virus type 2 is a tail-anchored type II membrane protein that is significant for virus envelopment. *J Gen Virol*, 81(Pt 10), 2397-2405. doi:10.1099/0022-1317-81-10-2397
- Takeshima, K., Arai, J., Maruzuru, Y., Koyanagi, N., Kato, A., & Kawaguchi, Y. (2019). Identification of the Capsid Binding Site in the Herpes Simplex Virus 1 Nuclear Egress Complex and Its Role in Viral Primary Envelopment and Replication. *J Virol*, JVI.01290-01219. doi:10.1128/JVI.01290-19
- Toropova, K., Huffman, J. B., Homa, F. L., & Conway, J. F. (2011). The herpes simplex virus 1 UL17 protein is the second constituent of the capsid vertex-specific component required for DNA packaging and retention. *J Virol*, 85(15), 7513-7522. doi:10.1128/JVI.00837-11
- Trus, B. L., Newcomb, W. W., Cheng, N., Cardone, G., Marekov, L., Homa, F. L., . . . Steven, A. C. (2007). Allosteric signaling and a nuclear exit strategy: binding of UL25/UL17 heterodimers to DNA-Filled HSV-1 capsids. *Mol Cell*, 26(4), 479-489. doi:10.1016/j.molcel.2007.04.010
- Wagenaar, F., Pol, J. M., Peeters, B., Gielkens, A. L., de Wind, N., & Kimman, T. G. (1995). The US3-encoded protein kinase from pseudorabies virus affects egress of virions from the nucleus. *J Gen Virol*, 76 (Pt 7), 1851-1859. doi:10.1099/0022-1317-76-7-1851
- Walzer, S. A., Egerer-Sieber, C., Sticht, H., Sevana, M., Hohl, K., Milbradt, J., . . . Marschall, M. (2015). Crystal Structure of the Human Cytomegalovirus pUL50-pUL53 Core Nuclear Egress Complex

2 Publications

1122
1123
1124
1125
1126
1127
1128
1129
1130
1131
1132
1133
1134
1135
1136
1137
1138
1139
1140
1141
1142
1143
1144
1145
1146
1147
1148
1149
1150
1151
1152
1153
1154
1155
1156
1157
1158
1159
1160
1161
1162
1163
1164
1165
1166
1167
1168
1169
1170
1171
1172
1173
1174
1175
1176
1177
1178
1179
1180

- Provides Insight into a Unique Assembly Scaffold for Virus-Host Protein Interactions. *J Biol Chem*, 290(46), 27452-27458. doi:10.1074/jbc.C115.686527
- Yang, K., & Baines, J. D. (2011). Selection of HSV capsids for envelopment involves interaction between capsid surface components pUL31, pUL17, and pUL25. *Proc Natl Acad Sci U S A*, 108(34), 14276-14281. doi:10.1073/pnas.1108564108
- Yang, K., Wills, E., Lim, H. Y., Zhou, Z. H., & Baines, J. D. (2014). Association of herpes simplex virus pUL31 with capsid vertices and components of the capsid vertex-specific complex. *J Virol*, 88(7), 3815-3825. doi:10.1128/JVI.03175-13
- Zeev-Ben-Mordehai, T., Weberruss, M., Lorenz, M., Cheleski, J., Hellberg, T., Whittle, C., . . . Grunewald, K. (2015). Crystal Structure of the Herpesvirus Nuclear Egress Complex Provides Insights into Inner Nuclear Membrane Remodeling. *Cell Rep*, 13(12), 2645-2652. doi:10.1016/j.celrep.2015.11.008

Paper III:
**Mutational Functional Analysis of the Pseudorabies
Virus Nuclear Egress Complex-Nucleocapsid
Interaction**

Sebastian Rönfeldt, Kati Franzke, Julia E. Hölper, Barbara G. Klupp and
Thomas C. Mettenleiter

Journal of Virology
Volume 94, Issue 8
DOI: 10.1128/JVI.01910-19

February 2020



Mutational Functional Analysis of the Pseudorabies Virus Nuclear Egress Complex-Nucleocapsid Interaction

Sebastian Rönfeldt,^a Kati Franzke,^b Julia E. Hölper,^a Barbara G. Klupp,^a Thomas C. Mettenleiter^a

^aInstitute of Molecular Virology and Cell Biology, Greifswald-Insel Riems, Germany

^bInstitute of Infectology, Friedrich-Loeffler-Institut, Greifswald-Insel Riems, Germany

ABSTRACT Herpesvirus nucleocapsids leave the nucleus by a vesicle-mediated translocation mediated by the viral nuclear egress complex (NEC). The NEC is composed of two conserved viral proteins, designated pUL34 and pUL31 in the alpha-herpesvirus pseudorabies virus (PrV). It is required for efficient nuclear egress and is sufficient for vesicle formation and scission from the inner nuclear membrane (INM). Structure-based mutagenesis identified a lysine at position 242 (K242) in pUL31, located in the most membrane distal part of the NEC, to be crucial for efficient nucleocapsid incorporation into budding vesicles. Replacing the lysine by alanine (K242A) resulted in accumulations of empty vesicles in the perinuclear space, despite the presence of excess nucleocapsids in the nucleus. However, it remained unclear whether the defect in capsid incorporation was due to interference with a direct, electrostatic interaction between the capsid and the NEC or structural restrictions. To test this, we replaced K242 with several amino acids, thereby modifying the charge, size, and side chain orientation. In addition, virus recombinants expressing pUL31-K242A were passaged and screened for second-site mutations. Compensatory mutations at different locations in pUL31 or pUL34 were identified, pointing to an inherent flexibility of the NEC. In summary, our data suggest that the amino acid at position 242 does not directly interact with the nucleocapsid but that rearrangements in the NEC coat are required for efficient nucleocapsid envelopment at the INM.

IMPORTANCE Herpesviruses encode an exceptional vesicle formation and scission machinery, which operates at the inner nuclear membrane, translocating the viral nucleocapsid from the nucleus into the perinuclear space. The conserved herpesviral nuclear egress complex (NEC) orchestrates this process. High-resolution imaging approaches as well as the recently solved crystal structures of the NEC provided deep insight into the molecular details of vesicle formation and scission. Nevertheless, the molecular mechanism of nucleocapsid incorporation remained unclear. In accordance with structure-based predictions, a basic amino acid could be pinpointed in the most membrane-distal domain of the NEC (pUL31-K242), indicating that capsid incorporation might depend on a direct electrostatic interaction. Our follow-up study, described here, however, shows that the positive charge is not relevant but that the overall structure matters.

KEYWORDS herpesvirus, nuclear egress complex, nuclear envelope, pUL31, pUL34, pseudorabies virus

Herpesviruses are large enveloped DNA viruses which replicate in two different cellular compartments. While viral DNA replication, capsid assembly, and genome packaging occur in the nucleus, final virus maturation proceeds in the cytoplasm. To transfer newly assembled nucleocapsids to the cytoplasm, herpesviruses use a unique vesicle-mediated pathway by budding through the inner nuclear membrane (INM) into

Citation Rönfeldt S, Franzke K, Hölper JE, Klupp BG, Mettenleiter TC. 2020. Mutational functional analysis of the pseudorabies virus nuclear egress complex-nucleocapsid interaction. *J Virol* 94:e01910-19. <https://doi.org/10.1128/JVI.01910-19>.

Editor Richard M. Longnecker, Northwestern University

Copyright © 2020 American Society for Microbiology. All Rights Reserved.

Address correspondence to Thomas C. Mettenleiter, thomas.mettenleiter@fli.de.

Received 9 November 2019

Accepted 4 February 2020

Accepted manuscript posted online 12 February 2020

Published 31 March 2020

the perinuclear space (PNS). This is subsequently followed by fusion of the INM-derived primary virion envelope with the outer nuclear membrane (ONM), releasing the nucleocapsids into the cytoplasm (reviewed in references 1 to 4).

Budding at and scission from the INM are coordinated by the viral nuclear egress complex (NEC), which is conserved throughout the *Herpesviridae*. The NEC consists of two viral proteins, designated pUL34 and pUL31 in the alphaherpesviruses pseudorabies virus (PrV) and herpes simplex virus (HSV). pUL34 is a tail-anchored membrane protein which is autonomously targeted to the nuclear envelope. pUL31 is diffusely distributed in the nucleus in the absence of pUL34 but is recruited to the INM by interaction with membrane-bound pUL34, forming the NEC (reviewed in references 1 to 4). NEC oligomerization at the INM most likely mediates membrane bending and vesicle scission. The ectopic expression of pUL31 and pUL34 is sufficient for vesicle formation and scission from the INM in eukaryotic cells but also from synthetic lipid bilayers, such as giant unilamellar vesicles, indicating that no other viral or cellular protein(s) is needed for vesiculation (5–7). Despite the simultaneous presence of the NEC components in the nucleus, in infected cells empty vesicles are only rarely observed, while nucleocapsids are apparently selected for translocation (8, 9). How nucleocapsids trigger this process and how they are incorporated into the nascent vesicles remained unclear.

Previous data suggested that pUL31 binds to capsids already in the nucleoplasm and mediates their transport to INM-located pUL34, initiating complex formation and oligomerization (10). The HSV-1 capsid vertex-specific component (CVSC), which is composed of pUL17 and pUL25 and which is enriched on mature capsids (9, 11), was shown to interact with pUL31 (12, 13). In addition, direct contacts between the NEC coat and the CVSC were visualized using cryo-electron tomography on primary enveloped particles (9). Recently, a direct interaction between pUL25 and the NEC was suggested by glutathione *S*-transferase-pulldown assays (14). In contrast, binding of PrV pUL31 also occurred independently of the pUL25 CVSC component (15), pointing to multiple binding partners or binding sites on the capsids. Due to the transient nature of the nucleocapsid-NEC interaction, which must be formed during envelopment at the INM but which needs to disengage during deenvelopment at the ONM, identification of interaction partners by classical biochemical approaches is difficult. In addition, the observation that preferentially mature nucleocapsids are enveloped at the INM indicates a complex structure-based interaction influenced by subsequent subtle structural changes, ranging from genome packaging and scaffold expulsion to addition of the CVSC.

To analyze this process, we modified potential capsid interaction interfaces on the NEC by site-directed mutagenesis (16) based on the crystal structures of the NECs from PrV, HSV-1 (17, 18), and human cytomegalovirus (19, 20), as well as high-resolution imaging of the PrV NEC (21). The NEC is an elongated rod-like structure, with the two, mostly globular components sitting on top of each other (Fig. 1A). Oligomerization of the NEC results in a tightly packed and curved hexameric, honeycomb-like structure (Fig. 1B). Based on these data, only the membrane-distal end of the NEC, formed by pUL31, appears to be accessible for interaction with the nucleocapsid, presumably involving electrostatic interactions (17, 18). To test this hypothesis, we isolated several PrV pUL31 mutants where predicted surface-exposed and charged amino acids were altered to alanine (16). These data resulted in the identification of the relevance of the most membrane-distal alpha-helical (H10) region (17) and especially a conserved lysine at position 242 (K242) as the key residue. Mutation of this lysine or the simultaneous exchange of the triad C241/K242/M243 for alanine (C241-243A) resulted in accumulations of empty membrane vesicles in the PNS, despite the intranuclear presence of numerous nucleocapsids, indicating that this region of pUL31 is crucial for nucleocapsid incorporation (16).

To further explore the role of H10 and K242 in this process, we generated additional mutants by replacing lysine 242 with acidic aspartic acid or glutamic acid with serine, glutamine, or tyrosine, which have smaller or larger side chains than glutamic acid, or

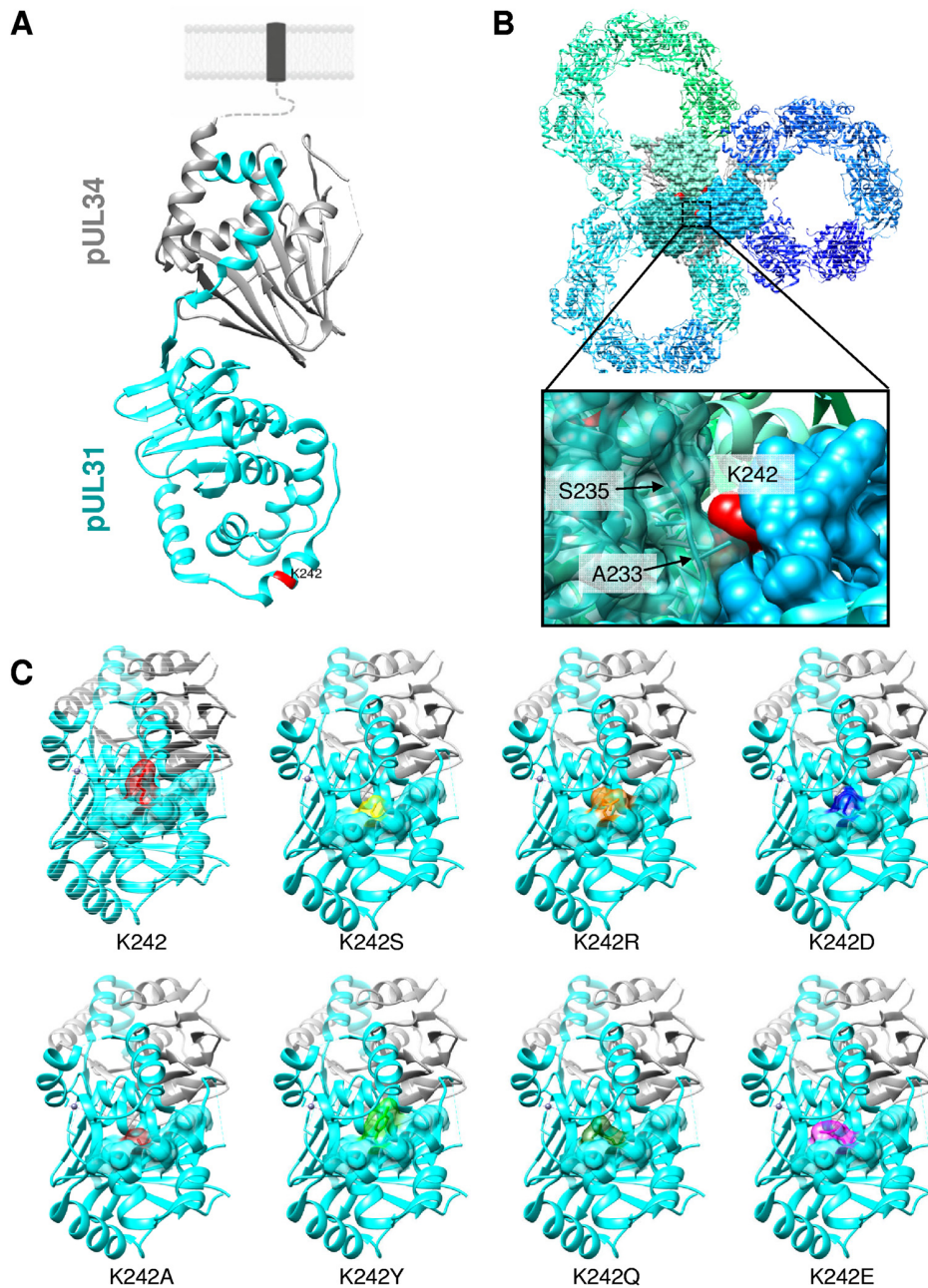


FIG 1 Structural prediction of the PrV NEC. (A) pUL34 is shown in gray and pUL31 is shown in cyan in the PrV NEC structure (17). The orientation toward and anchorage in the INM are indicated by the dotted line, and the transmembrane domain in a lipid bilayer is represented by a dark gray box. The location of the amino acid (K242) targeted in this study is indicated in red. (B) Bottom view of the membrane-distal end in the honeycomb array (17), with interacting interhexameric molecules being shown by surface representation with amino acid K242 in red. The zoomed image of the boxed region shows the interaction interface of different NEC heterodimers with one pUL31 in a semitransparent surface presentation, while the neighboring pUL34 is shown with its full surface. Amino acids in close proximity to K242 are indicated by arrows and given with the corresponding position. (C) A bottom view of the membrane-distal end of pUL31 with a partial surface presentation of alpha helix H10 is shown with amino acid K242 in red. Amino acid substitutions at position 242 are modeled into the NEC dimer structure (PDB accession number 5E8C). Molecular graphics and analysis were performed with the UCSF Chimera package (34).

with arginine, thereby maintaining the basic character. In addition, virus mutants carrying either the single K242A substitution or the triple C241-243A substitution were passaged in cell culture to select for second-site mutations compensating for the capsid incorporation defect.

TABLE 1 Primers used for site-directed mutagenesis

Primer name	Sequence (5' to 3') ^a
UL31 K242S	GAC ATT TAT TGC <u>AGC</u> ATG CGG GAC ATC AGC
UL31 K242Q	GAC ATT TAT TGC <u>CAG</u> ATG CGG GAC ATC AGC
UL31 K242Y	GC GAC ATT TAT TGC <u>TAC</u> ATG CGG GAC ATC AGC
UL31 K242R	G AGC GAC ATT TAT TGC <u>AGG</u> ATG CGG GAC ATC AGC
UL31 K242E	G AGC GAC ATT TAT TGC <u>GAG</u> ATG CGG GAC ATC AGC
UL31 K242D	GCG AGC GAC ATT TAT TGC <u>GAT</u> ATG CGG GAC ATC AGC
UL31 A242K	GC GAC ATT TAT TGC AAG ATG CGG GAC ATC AG

^aMismatches are underlined and in bold. Only the forward primer is shown; the reverse complementary primers are not depicted.

The data presented here indicate that capsid incorporation into primary vesicles is not dependent on a specific charge interaction with K242 but may require conformational flexibility within the NEC coat.

RESULTS

Structural predictions of the pUL31-K242 location in the NEC coat. A lysine residue at position 242 in the PrV pUL31 component of the NEC was found to be crucial for incorporation of nucleocapsids into INM-derived vesicles (16). While in the NEC heterodimer K242 seemed to be freely accessible at the surface (Fig. 1A), modeling of this residue into the hexagonal array showed that this position might indeed be more deeply buried and constrained by residues A233 and S235 in pUL31 of a neighboring hexamer, impairing or even prohibiting direct interaction with the nucleocapsid (Fig. 1B). To further analyze the role of K242 in nucleocapsid incorporation, we replaced this residue by the basic but larger arginine (R), the negatively charged but smaller glutamic acid (E) or aspartic acid (D), the small neutral serine (S), the large aromatic tyrosine (Y), or the medium-sized glutamine (Q). The influence of the amino acid exchanges was calculated and modeled into the heterodimeric NEC structure by using the intrinsic functions of the UCSF Chimera package (Fig. 1C). Mutants were generated by site-specific mutagenesis using the primers shown in Table 1 with pcDNA-UL31 as the template. Correct mutagenesis was verified by sequencing.

Intracellular localization of pUL31 mutants and colocalization with pUL34. The mutated pUL31 proteins were tested for correct nuclear targeting and interaction with the complex partner pUL34 by either transfection of the corresponding expression plasmids or cotransfection with pcDNA-UL34 (22) into rabbit kidney (RK13) cells and processed for confocal microscopy 2 days later. pUL31 was detected using a monoclonal anti-pUL31 antibody, while pUL34 was visualized by a monospecific rabbit antiserum (Fig. 2) (22). All pUL31 mutants showed the same diffuse distribution in the nucleus as native pUL31 (Fig. 2, top row), indicating stable expression and correct targeting. A punctate pUL31/pUL34-positive staining pattern comparable to that achieved with wild-type pUL31/pUL34 coexpression (Fig. 2, bottom three rows) indicated that complex formation and membrane deformation were not affected by the introduced changes. Only cotransfections of pcDNA-UL31-K242D and pcDNA-UL34 showed the presence of a higher level of pUL34 in the nuclear rim and in cytoplasmic structures.

Functional complementation of PrV-ΔUL31 by the pUL31-K242 substitutions. To investigate the ability of the generated mutants to complement the defect of PrV-ΔUL31, cell lines stably expressing the respective pUL31 mutants in *trans* were generated. Cell clones were isolated and tested by indirect immunofluorescence and immunoblotting, using monospecific anti-pUL31 rabbit serum (23). In contrast to the parental RK13 cells, expression of pUL31 could be detected in all transgenic cell lines. Anti-α-tubulin was included as a loading control (Fig. 3).

To test for functional complementation, RK13 and the pUL31-expressing RK13 cell lines (RK13-UL31 cells) were infected with PrV wild-type strain Kaplan (PrV-Ka) or PrV-ΔUL31 (23) at a multiplicity of infection (MOI) of 5. At 24 h postinfection (p.i.), the supernatant and cells were harvested and progeny virus titers were determined on

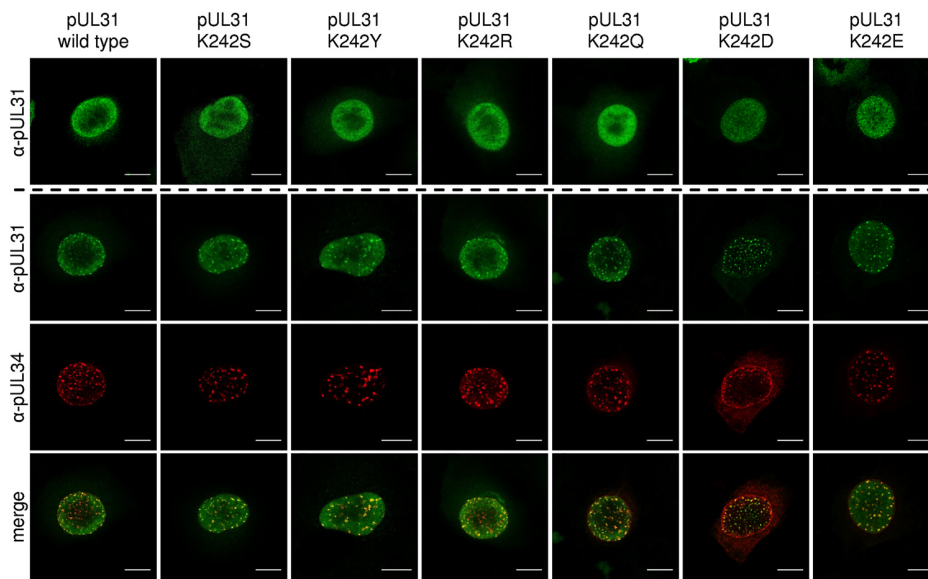


FIG 2 Intracellular localization of pUL31 mutants and colocalization with pUL34. Localization was tested after transfection of RK13 cells with the corresponding pUL31 expression plasmids (top row). Colocalization was analyzed after cotransfection with pcDNA-UL34. pUL31 was stained with a pUL31-specific monoclonal antibody (green, second row), while for pUL34, polyclonal anti-pUL34 serum (red, third row) was used. Merged channels are shown in the bottom row. Fluorescence was imaged with a confocal laser-scanning microscope (63 \times oil immersion objective, single slice; SP5; Leica Germany). Bars, 10 μ m.

RK13-UL31 cells (Fig. 4). Infection with PrV-Ka resulted in progeny titers of approximately 10^6 PFU/ml in all cell lines, similar to the findings for parental RK13 cells, indicating that none of the pUL31 mutants exerted a dominant negative effect. The titers of PrV- Δ UL31 derived from RK13-UL31-K242S and RK13-UL31-K242Y cells were only slightly reduced compared to those of PrV-Ka derived from the corresponding cells (6- and 10-fold lower, respectively), indicating functional complementation. The titers from RK13-UL31-K242Q cells were approximately 20-fold lower, while the titers resulting from infection of RK13-UL31-K242R cells were reduced 70-fold. No or only very low levels of complementation of PrV- Δ UL31 (reduced more than 100-fold) were found on RK13-UL31-K242E and RK13-UL31-K242D cells, which were in the range of those found

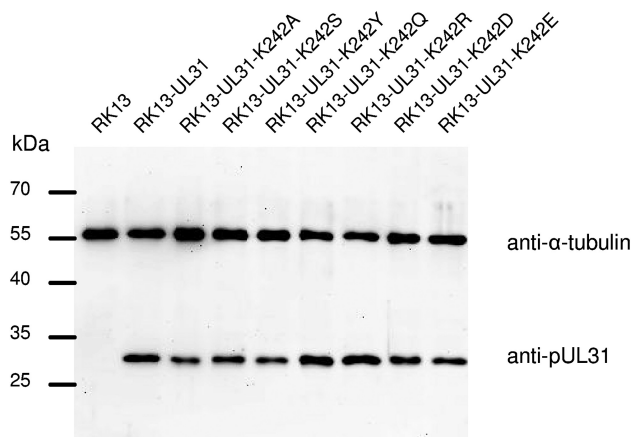


FIG 3 pUL31 expression in RK13 cells. Lysates of cell lines stably expressing native or mutated pUL31 as well as nontransgenic RK13 cells were separated in an SDS-10% polyacrylamide gel. Proteins were detected after transfer to nitrocellulose with the monospecific anti-pUL31 rabbit serum. As loading control, anti- α -tubulin was used. The molecular masses of the marker proteins (in kilodaltons) are indicated on the left.

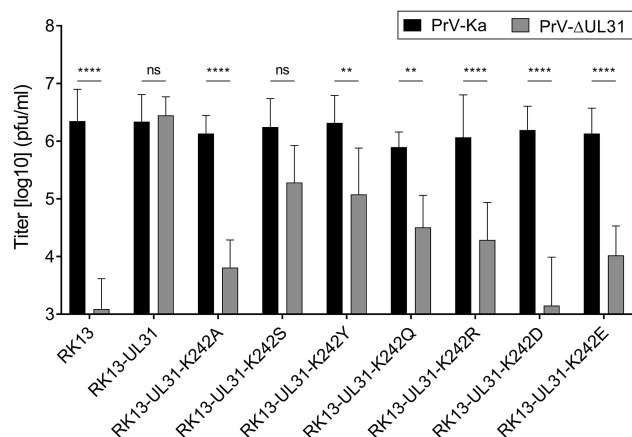


FIG 4 *trans*-Complementation assays. Functional complementation by the generated pUL31 mutants was tested after infection of the stably expressing cell lines with PrV-Ka and PrV-ΔUL31 at an MOI of 5. Cells and supernatant were harvested at 24 h p.i., and titers were determined on RK13-UL31 cells. Shown are the mean values from four independent experiments with the corresponding standard deviations. Statistically significant differences are indicated (**, $P \leq 0.01$; ****, $P \leq 0.0001$; ns, not significant).

on cells expressing pUL31-K242A or for nontransgenic RK13 cells (Fig. 4) (16), indicating that these pUL31 mutants are nonfunctional.

To characterize the effect of the substitutions on nuclear egress, cell lines were infected with PrV-ΔUL31 at an MOI of 1 and processed for electron microscopy. Surprisingly, none of the pUL31 mutant cell lines showed accumulations of empty vesicles within the PNS similar to those observed after infection of RK13-UL31-K242A cells (16) (Fig. 5A). In contrast, PrV-ΔUL31-infected RK13-UL31-K242S cells (Fig. 5B) and RK13-UL31-K242Y cells (Fig. 5C) showed all stages of virion morphogenesis, including nucleocapsids in the cytoplasm and virions at the plasma membrane, paralleling their complementation phenotype (Fig. 4). In PrV-ΔUL31-infected RK13 cells expressing pUL31-K242Q (Fig. 5D) or pUL31-K242R (Fig. 5E), intranuclear nucleocapsids were often detected in close apposition to the inner nuclear membrane, but membrane bending and/or budding was observed only infrequently. Only a few vesicle-like structures in the PNS were present in RK13-UL31-K242E cells (Fig. 5G), while nucleocapsids accumulated in the nucleus in RK13-UL31-K242D cells (Fig. 5F), paralleling the observed lack of complementation (Fig. 4).

Serial passaging of virus recombinants. The results obtained with the various constructs with amino acid substitutions at position K242 were unexpected, arguing against a direct electrostatic interaction between the K242 region within pUL31 alpha helix H10 and nucleocapsids. To analyze the NEC-nucleocapsid interaction further, virus recombinants expressing noncomplementing pUL31-K242A or pUL31-C241-243A were generated by homologous recombination. PrV-UL31-K242A and PrV-UL31-C241-243A exhibited strongly reduced growth properties comparable to those of PrV-ΔUL31 on the corresponding stably expressing cell lines (16), with only low progeny virus titers and striking accumulations of empty vesicles in the PNS. However, the production of a small amount of infectious virus progeny was observed and used for reversion analysis.

To select for compensating second-site mutations, PrV-UL31-K242A and PrV-UL31-C241-243A were passaged in RK13 and Vero cells. Within only a few cell passages, the titers of the supernatants reached up to 10^6 PFU/ml. Single plaques from several independent assays were isolated and tested. Genomic DNA of revertants which replicated to titers of at least 10^6 PFU/ml was isolated, and the UL31- and UL34-coding regions were amplified by PCR and sequenced. The mutations identified in pUL31 and pUL34 are summarized in Table 2. In this study, we subsequently focused on the pUL31 mutations.

Characterization of second-site mutations. To test whether the additional mutations in pUL31 are sufficient to compensate for the replication defect in pUL31-K242A

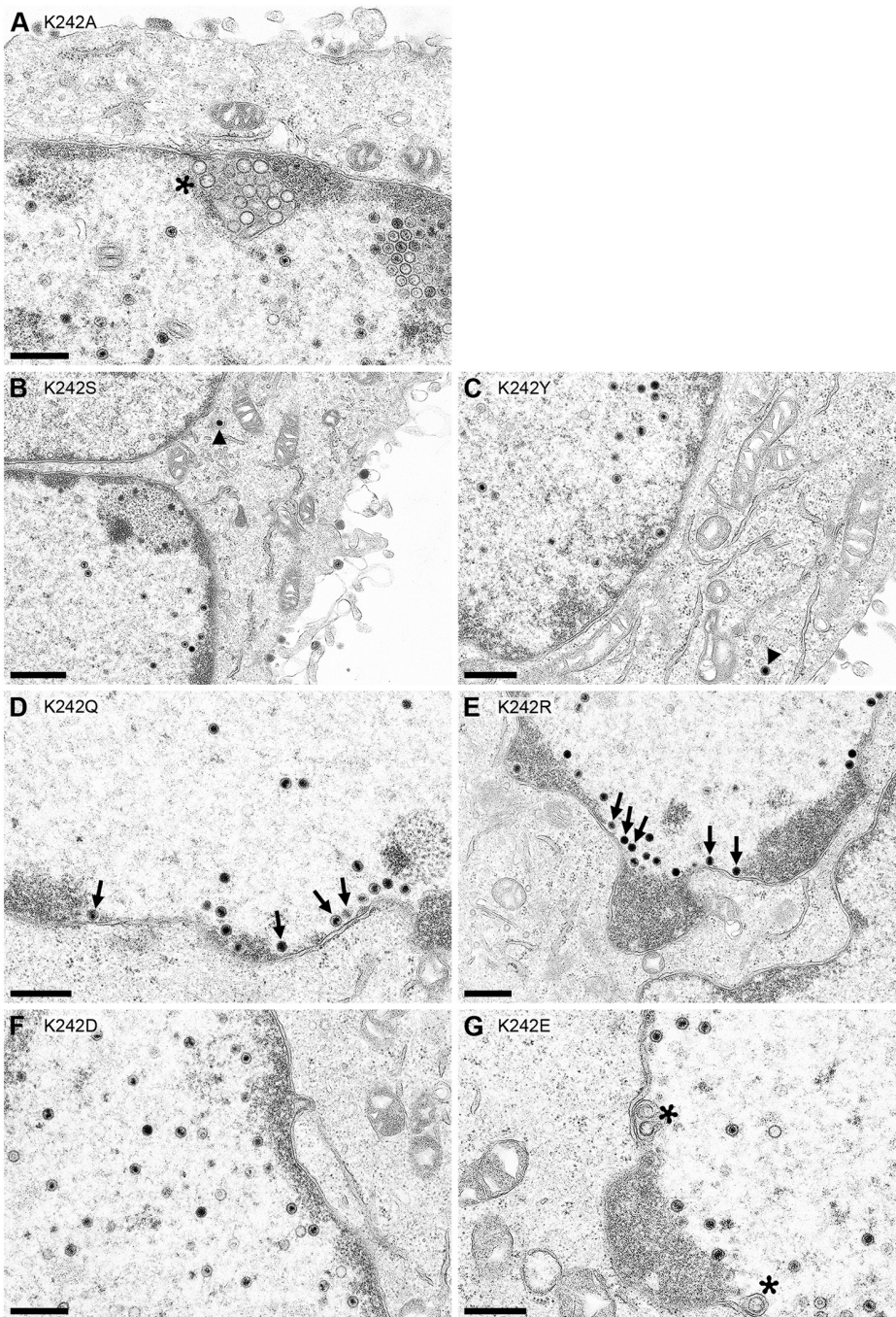


FIG 5 Ultrastructural analyses of cells expressing pUL31 mutants infected with PrV- Δ UL31. RK13-UL31-K242A (A), RK13-UL31-K242S (B), RK13-UL31-K242Y (C), RK13-UL31-K242Q (D), RK13-UL31-K242R (E), RK13-UL31-K242D (F), and RK13-UL31 K242E (G) cells were infected with PrV- Δ UL31 at an MOI of 1 and processed for electron microscopy at 14 h p.i. Representative images are shown. Asterisks mark empty vesicles in the PNS, arrows point to nucleocapsids close to the INM, and arrowheads indicate nucleocapsids or virions in the cytoplasm. Bars, 500 nm (A, C to G) and 800 nm (B).

and pUL31-C241-243A (16), the UL31 genes were cloned into pcDNA3. The localization and colocalization with pUL34 after transfection into RK13 cells were comparable to those of the wild-type proteins (data not shown), pointing to correct nuclear targeting and interaction with pUL34.

Stably expressing cell lines were isolated, tested for correct pUL31 expression (Fig. 6A), and infected with PrV- Δ UL31 and PrV-Ka as described above. The titers of

TABLE 2 Second-site mutations detected in reversion analyses

Mutant used for passaging	Cell line used for passaging	Second-site mutation in:	
		UL31	UL34
PrV-UL31-K242A	Vero	S40	— ^a
PrV-UL31-K242A	RK13	M79I	—
PrV-UL31-K242A	RK13	L115R	—
PrV-UL31-K242A	RK13	A137T	—
PrV-UL31-K242A	Vero	K242T	—
PrV-UL31-C241-243A	Vero	Y121H	—
PrV-UL31-C241-243A	RK13 + Vero	A126T	—
PrV-UL31-C241-243A	RK13 + Vero	G250R	—
PrV-UL31-K242A	Vero	—	G15W
PrV-UL31-K242A	Vero	—	T25M
PrV-UL31-K242A	Vero	—	A26V
PrV-UL31-K242A	RK13 + Vero	—	T98A
PrV-UL31-K242A	Vero	—	A99V

^a—, no mutation.

PrV-Ka reached at least 10^6 PFU/ml on all cell lines, demonstrating the absence of a dominant negative effect of the second-site mutations (Fig. 7). Only RK13-UL31-M79I/K242A replicated PrV-Ka to slightly lower titers. Nevertheless, complementation of PrV- Δ UL31 with, at the most, 10-fold reduced titers was observed for pUL31-M79I/K242A-, pUL31-A137T/K242A-, pUL31-K242T-, and pUL31-Y121H/C241-243A-expressing cells. RK13-UL31-S40A/K242A, RK13-UL31-L115R/K242A, RK13-UL31-A126T/C241-243A, and RK13-UL31-C241-243A/G250R cells showed a more pronounced deficiency for complementation with 10- to 30-fold lower titers, but these were still significantly above those derived from RK13-UL31-K242A or RK13-UL31-C241-243A cells (Fig. 7), pointing to at least partial compensation of the K242A/C241-243A defect.

To test whether the second-site mutations affect virus replication in the absence of the K242A or C241-243A substitutions, the latter were reverted by site-directed mutagenesis, resulting in pcDNA-UL31-S40A, pcDNA-UL31-M79I, pcDNA-UL31-L115R, pcDNA-UL31-Y121H, pcDNA-UL31-A126T, pcDNA-UL31-A137T, and pcDNA-UL31-G250R. Since the localization of the mutated pUL31 and colocalization with pUL34 were comparable to those of wild-type pUL31 (data not shown), stably expressing RK13 cells were generated and tested for pUL31 expression (Fig. 6B) and for functional complementation of PrV- Δ UL31 (Fig. 8). While pUL31-S40A, pUL31-M79I, pUL31-A126T, and pUL31-Y121H complementation of PrV- Δ UL31 produced wild-type-like titers with no detectable effect, expression of pUL31-L115R and pUL31-G250R resulted in progeny titers only in the range of those derived from nontransgenic RK13 cells, indicating that these mutations significantly impaired the pUL31 function in the absence of the K242A/C241-243A substitutions (Fig. 8).

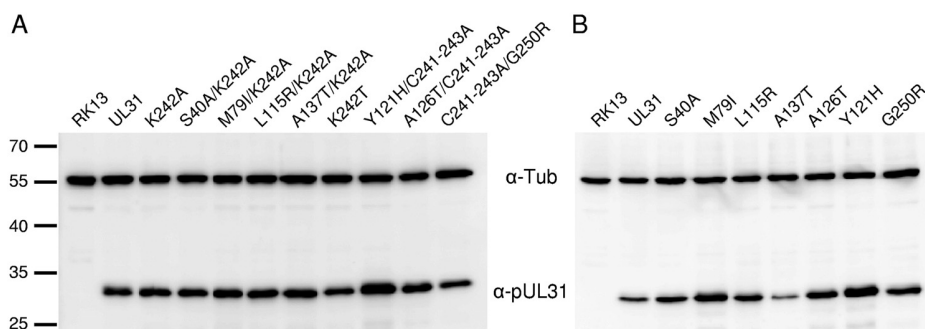


FIG 6 Immunoblot analysis of RK13 cells expressing pUL31 with second-site mutations. RK13 cells expressing UL31-K242A with the second-site mutations (A) or pUL31 carrying only these mutations (B) were harvested and tested for pUL31 expression with the monospecific anti-pUL31 serum. Anti- α -tubulin (α -Tub) was used as a loading control.

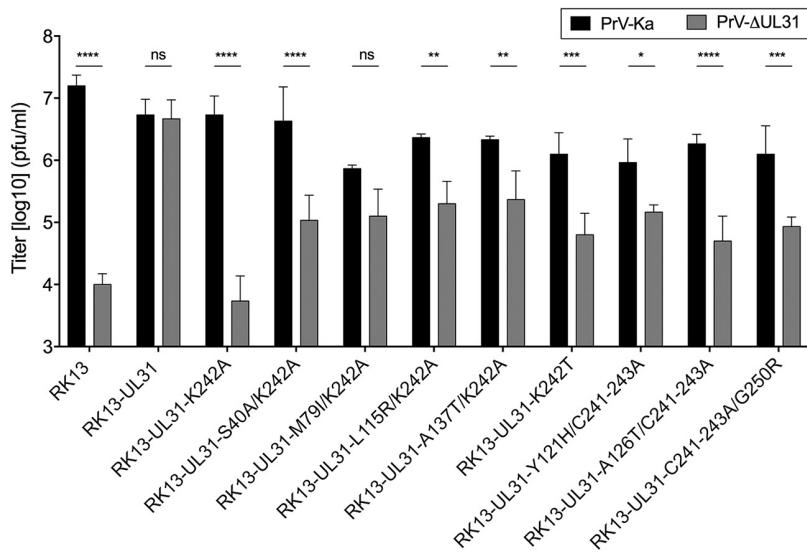


FIG 7 Complementation of PrV-ΔUL31 by second-site-mutated pUL31-K242A and pUL31-C241-243A. Complementation by pUL31-K242A and pUL31-C241-243A carrying second-site mutations was tested after infection of the stably expressing cell lines with PrV-Ka and PrV-ΔUL31 at an MOI of 5. Cells and supernatant were harvested at 24 h p.i., and titers were determined on RK13-UL31 cells. Shown are the mean values from three independent experiments with the corresponding standard deviations. Statistically significant differences were evaluated using GraphPad Prism software and are indicated (*, $P \leq 0.05$; **, $P \leq 0.01$; ***, $P \leq 0.001$; ****, $P \leq 0.0001$; ns, not significant).

In ultrastructural analyses, all stages of nuclear egress and virion formation could be observed in cells expressing pUL31 with substitutions in H10 in the presence of the second-site mutations, as shown for PrV-ΔUL31-infected RK13-UL31-K242T, RK13-UL31-S40A/K242A, RK13-UL31-L115R/K242A, and RK13-UL31-C241-243A/G250R cells (Fig. 9C to F). These data point to an at least partial reversion of the nucleocapsid incorporation defect observed in PrV-ΔUL31-infected RK13-UL31-K242A and RK13-UL31-C241-243A cells (16) or RK13 cells infected with PrV-UL31-K242A and PrV-UL31-C241-243A (Fig. 9A and B). Nevertheless, single empty vesicles in the PNS were still evident, indicating that capsid uptake into the nascent primary virion envelope may not be as efficient as that

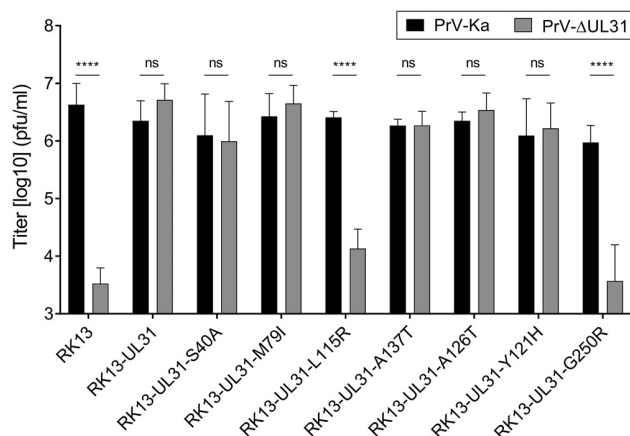


FIG 8 Effect of second-site mutations in the absence of the K242A mutation or the C241-243A mutations. The K242A and C241-243A mutations in plasmids expressing the pUL31 genes derived from the passaged mutants were repaired to the wild type by site-directed mutagenesis. Stably expressing cells were infected with PrV-Ka and PrV-ΔUL31 as described in the Fig. 7 legend. Shown are mean values from three independent experiments with the corresponding standard deviations (****, $P \leq 0.0001$; ns, not significant).

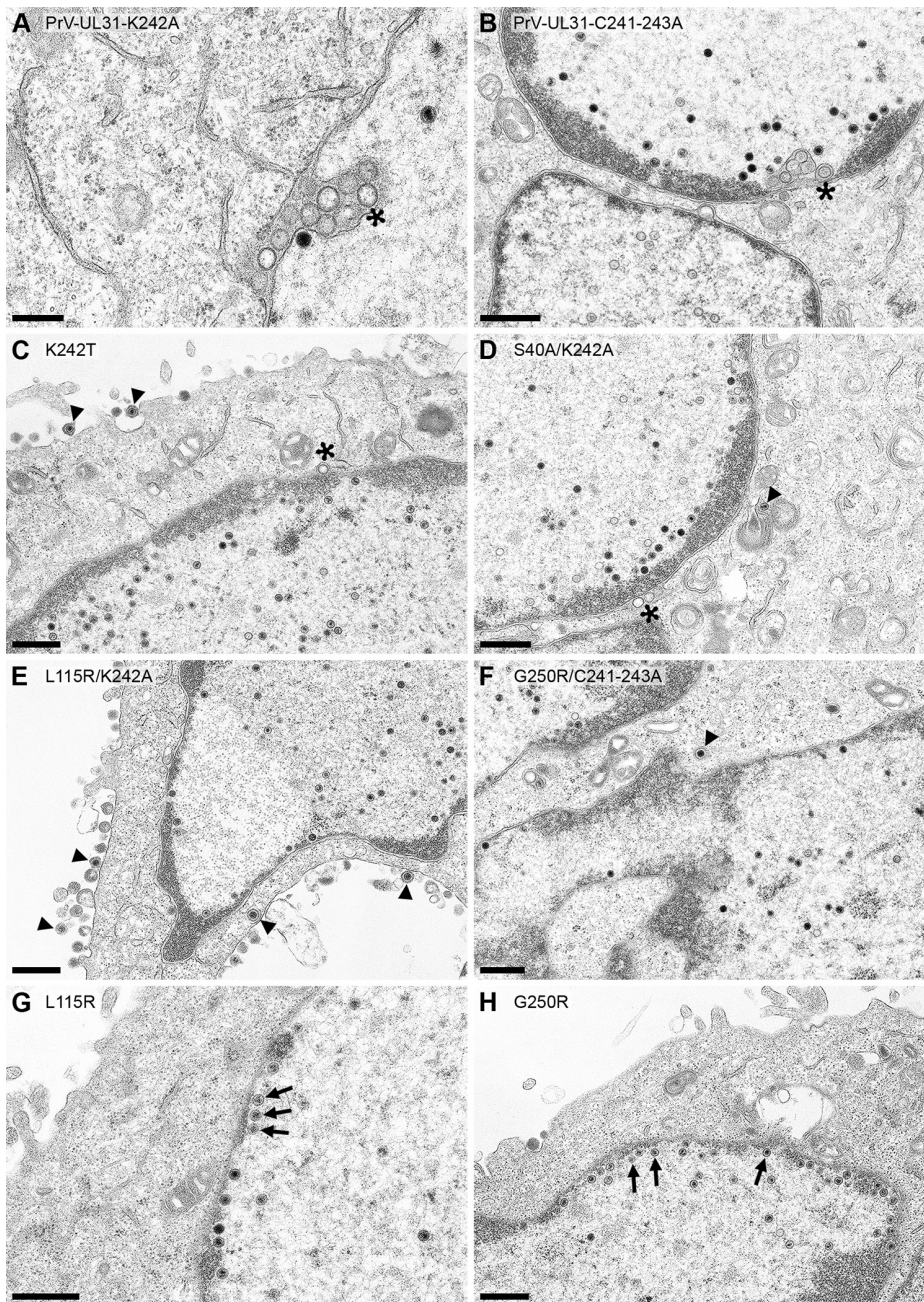


FIG 9 Ultrastructural analysis. RK13 cells were infected with PrV-UL31-K242A (A) or PrV-UL31-C241-243A (B). (C to H) RK13 cells expressing pUL31-K242T (C), pUL31-S40A/K242A (D), pUL31-L115R/K242A (E), pUL31-G250R/C241-243A (F), pUL31-L115R (G), or pUL31-G250R (H), infected with PrV- Δ UL31 (MOI, 1), fixed, and processed for electron microscopy at 14 h p.i. Asterisks mark empty vesicles in the PNS, nucleocapsids close to the INM are indicated by arrows, and nucleocapsids or virions in the cytoplasm or at the plasma membrane are highlighted by arrowheads. Bars, 300 nm (A) and 600 nm (B to H).

with the wild-type NEC. Nucleocapsids in close proximity to the INM could be observed in PrV- Δ UL31-infected cells expressing pUL31-L115R and pUL31-G250R, while membrane bending did not ensue (Fig. 9G and H).

DISCUSSION

Elucidation of the structures of several NECs by X-ray diffraction (17–20) as well as a multimodal imaging approach (21) shed light on this exceptional viral vesicle forma-

tion and scission machinery. Identification of a clear polarity in the NEC with a membrane-proximal and a membrane-distal face revealed that the major portion of the NEC components is involved in oligomerization and vesicle coat formation, leaving only the most membrane-distal part as a potential interaction interface with the nucleocapsid (21). In line with this, mutation of lysine 242 to alanine in the most membrane-distal helical region (H10) in PrV pUL31 (16) or a R281A/D282A exchange in HSV-1 pUL31 (14) (corresponding to amino acids R244 and D245, respectively, in PrV pUL31) resulted in accumulations of empty membrane vesicles in the PNS, indicating that capsid uptake into the nascent vesicles was impaired. However, in contrast to the findings for HSV-1, a direct physical interaction between H10 and the nucleocapsid cargo was not shown for PrV.

Although H10 and, in particular, K242 appeared to be surface exposed in the crystal structure of the PrV NEC heterodimer, modeling of this position into the hexagonal array showed that it might be more deeply buried in the interior and not available for a direct capsid interaction. To investigate this in more detail, we replaced the lysine K242 with either the smaller amino acid serine (S) or glutamine (Q), the negatively charged aspartate (D) or glutamate (E), the bulky but also basic arginine (R), or the large aromatic tyrosine (Y).

Modeling the different residues into the PrV NEC dimer (Fig. 1C) revealed that the side chains of the substituted amino acids occupy the available space differently. While the original lysine contains the longest extension pointing toward the neighboring pUL31 molecules (Fig. 1B and C), alanine is small and compact, leaving some empty space. The positions of serine and, especially, tyrosine with its aromatic ring and aspartic acid partly mimicked the position of lysine. In contrast, side chains of arginine, glutamine, and glutamic acid were kinked and directed inwards but not toward the neighboring pUL31 in the hexameric ring.

All pUL31 mutants translocated to the nucleus indistinguishably from the wild-type protein and interacted with coexpressed pUL34 to deform the nuclear membrane, resulting in the typical punctate speckled pattern observed for the wild-type proteins (7). Only the coexpression of pUL31-K242D slightly affected the localization of pUL34 and showed reduced colocalization. Nevertheless, a double-positive fluorescent punctate pattern was also evident. Modeling of aspartic acid into the NEC structure indicates that it fits into the position of the original lysine, but the negative charge seems to influence the binding affinity to the NEC partner or the NEC oligomer.

The function of the mutated pUL31 was tested by complementation assays and ultrastructural analyses using stably expressing cell lines. Surprisingly, none of the novel mutations resulted in prominent accumulations of empty vesicles, as observed for pUL31-K242A or pUL31-C241-243A (16). Surprisingly, maintaining the basic character by alteration of lysine to arginine led to significantly reduced titers. Thus, the presence of a basic amino acid at this position does not *per se* result in the proper function of the NEC, arguing against a simple charge interaction. Only intranuclear nucleocapsids were observed, and these were often in close proximity to the INM, suggesting that capsid transport to and docking at the INM occurs but that membrane bending is impaired. A similar phenotype could be found in virus mutants lacking the CVSC component pUL25 (24) or expressing pUL31 with mutations in the neighboring alpha-helical region, H11, which affect the nuclear export signal (pUL31-NES^{PM}) (16, 25). These data indicate that alpha-helical regions H10 and H11 may indeed cooperate in the structural rearrangements during nuclear egress, leading from a flat NEC patch to a curved shape. A similar phenotype was also found in cells expressing pUL31-K242Q.

In contrast, the replacement of K242 by the small and neutral serine (K242S) and by the large and aromatic tyrosine (K242Y) had only a limited effect on the production of infectious progeny, with the titers being approximately 5- to 10-fold lower than those of PrV-Ka. Electron microscopic images showed all stages of herpesvirus assembly and egress, although nucleocapsids and virions were only rarely detected in the cytoplasm or in the extracellular space, which is in line with the reduced titers and the relatively

low sensitivity of electron microscopy. In contrast to pUL31-K242A expression, no empty vesicles were observed in the PNS.

Cells expressing pUL31-K242D or pUL31-K242E, which reverted the net charge at position 242, were unable to complement the defect of PrV- Δ UL31, and the titers were comparable to those derived from nontransgenic RK13 cells. Only intranuclear nucleocapsids were observed, in line with the severe drop in viral progeny titers. Very rarely, single empty vesicles in the PNS were found, but these were in striking contrast to the abundant vesiculation in cells expressing pUL31-K242A (Fig. 5A) or pUL31-C241-243A (16).

Thus, the question remains why K242A resulted in these massive accumulations of membrane vesicles in the PNS. Alanine is the only amino acid tested with an apolar side chain, in contrast to the wild-type lysine and all other amino acids substituted. In addition, modeling shows that the side chain does not fill the space between the pUL31 molecules in the dimeric interface of the hexamers (Fig. 1B and C), with less restriction and/or higher flexibility probably resulting in deregulated vesicle budding and scission. A similar dysregulation of vesicle formation from the INM was reported for HSV-1 when a basic patch in pUL34 was mutated to alanine (R158A/R161A, CL13) (26). These two mutations are located in the interaction surface between pUL34 and pUL31 within the core NEC and close to an intramolecular salt bridge (18). It is feasible that both changes, the alanine substitution in PrV pUL31-K242A and the double alanine exchange in HSV-1 pUL34, resulted in a greater flexibility and an enhanced propensity for oligomerization, resulting in increased capsid-independent budding and vesicle scission.

The defect in HSV-1 pUL34 could be compensated for by inter- or intramolecular second-site mutations (26). Thus, we were interested in whether this might also be the case for PrV pUL31-K242A and pUL31-C241-243A. For this, recombinant viruses expressing pUL31-K242A or pUL31-C241-243A were generated and passaged in RK13 and Vero cells. Although severely impaired in viral replication, infectious progeny was formed in nontransgenic cells infected with these mutants, which served as a basis for reversion analysis. Within less than 10 passages, viral titers increased to wild-type-like values of 10^6 PFU/ml. Surprisingly, second-site mutations occurred at different amino acid positions in pUL31 as well as in pUL34, pointing to higher flexibility of the NEC than expected.

The relevance of mutations uncovered in pUL34 is difficult to test in our *trans*-complementation assays since the native pUL34 was still present. Therefore, in this study, we focused on the mutations found in pUL31. Cell lines expressing the second-site pUL31 mutants in the presence of the H10 substitutions all replicated PrV- Δ UL31 to significantly higher titers than the parental cell lines RK13-UL31-K242A and RK13-UL31-C241-243A or nontransgenic RK13 cells. Titers only 6- to 12-fold lower than those of PrV-Ka were achieved with pUL31-K242T, pUL31-M79I/K242A, pUL31-L115R/K242A, pUL31-A137T/K242A, pUL31-Y121H/C241-243A, and pUL31-C241-243A/G250R, pointing to at least a partial functional complementation of the nuclear egress defect and infectious virion maturation. Approximately 30-fold-lower titers were obtained on RK13-UL31-S40A/K242A and RK13-UL31-A126T/C241-243A cells than were obtained for PrV-Ka, still pointing to a partial functional rescue of the defect induced by the K242A/C241-243A mutations.

Modeling the second-site mutations into the NEC structure showed that the substitutions L115R, Y121H, A126T, A137T, and G250R were located in close proximity to the alpha-helical region H10 or a direct reversion of K242A (K242T) within the membrane-distal part of pUL31 (Fig. 10), indicating that these mutations compensate for the structural defects imposed by the amino acid changes in H10.

The second-site mutations resulting in amino acid substitutions L115R and G250R both introduce a positive charge, which was lost in pUL31-K242A and pUL31-C241-243A. L115 is located at the end of H5, which is supposed to form the trimeric interface in hexamers (17). Addition of this positive charge might rearrange and stabilize the hexamers forming the trimeric interaction interface. G250R is located in H11, which also carries the nuclear export signal sequence (25). The simultaneous substitutions L252A

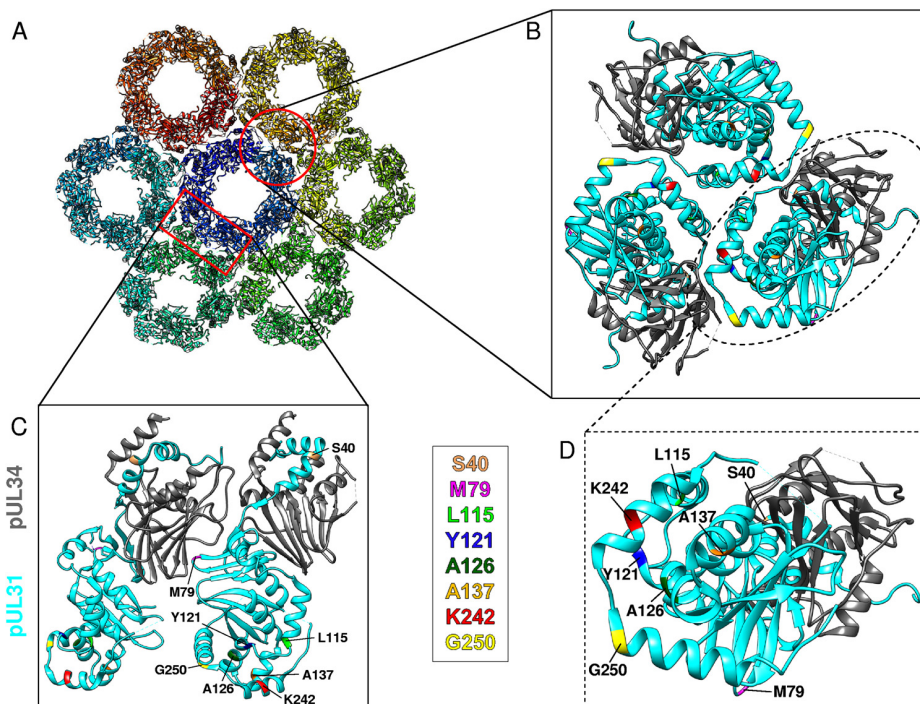


FIG 10 Location of the pUL31 mutations in the NEC dimer and in the hexagonal lattice. (A) Top view of the NEC hexameric lattice (PDB accession number 5FKI) (17, 21). The chains are rainbow colored. (B to D) Close-up views of NEC heterodimer interfaces of the hexameric lattice, with the mutations being marked in color. pUL31 is shown in cyan, while pUL34 is shown in gray. The interfaces indicated in panel A are represented by a red circle for panel B and a red rectangle for panel C. (B) Top view of the trimer interface between hexamers. (C) Side view of the dimer-dimer interface. (D) Zoom of the membrane-distal part of the NEC shown in panel B. The amino acids that were mutated are highlighted by different colors and labeled. Molecular graphics and analysis were performed with the UCSF Chimera package (34).

and L254A, which are part of the predicted NES (pUL31-NES^{PM}), resulted in a nonfunctional protein (25), further supporting the suggestion that H10 and H11 may collaborate for membrane deformation and budding during nuclear egress. L115R and G250R, however, resulted in a nonfunctional pUL31 in the absence of the K242A/C241-243A mutation. In ultrastructural analyses, a phenotype similar to that achieved with pUL31- Δ NES, i.e., nucleocapsids lined up at the INM but no detectable membrane deformation or budding events, was observed (25), indicating that H5, in addition to H10 and H11, facilitates membrane deformation and budding.

The second-site mutations S40A and M97I are located distantly from H10 and the membrane-distal part of the NEC (Fig. 10). S40 is located in the second of the two α helices forming the hinge region of the pUL31 N-terminal arm, which reaches around and inserts into a groove of the pUL34 core. This arm is one of the major interaction domains between the complex partners in the NEC dimer (17–20). In PrV pUL31, the neighboring D41 forms an intramolecular hydrogen bond with Y34, stabilizing the kink at an angle of ca. 80° (17). It is conceivable that the exchange of the polar serine in the wild-type protein for the nonpolar alanine (S40A) allows more flexibility of this arm and, thus, orientation between the complex partners. In addition, S40 is predicted to be a putative phosphorylation site (<http://www.cbs.dtu.dk/services/NetPhos>), which may play a regulatory role in assembly and/or disassembly of the NEC during nuclear egress and which is lost by the S40A substitution.

The region comprising amino acids 77 to 79 in PrV pUL31 forms a loop between two β sheets (17) (Fig. 10). This loop, together with the zinc finger (ZNF) motif coordinated by amino acids C73, C89, C92, and H188, is anticipated to form an important intrahexamer interface connecting to a loop comprising amino acids 88 to 93 in pUL34 of a

neighboring NEC dimer (17) (Fig. 10). Mutations in or close to the loop as well as mutations in the ZNF motif (L76A, S77A, G80A, C73S, C89S, C92S, and H188A) resulted in nonfunctional proteins (17), highlighting the importance of this region for higher-order complex formation and NEC function. The exchange of methionine at position 79 for the more hydrophobic isoleucine might impose a higher flexibility on the dimer-dimer interaction interface.

None of the revertants revealed a mutation back to K242. However, in one of the revertants, which efficiently replicated in cell culture, the alanine substitution in pUL31-K242A was changed to threonine (pUL31-K242T). Cell lines expressing pUL31-K242T partially complemented the defect of PrV- Δ UL31, and the titers derived from these cells were similar to those observed for RK13-UL31-K242S and RK13-UL31-K242Y cells (Fig. 4), adding another example of a functional amino acid exchange of the lysine at position 242. It is noteworthy that all amino acid substitutions at this position which complemented PrV- Δ UL31 could serve as a potential phosphorylation site. The phosphomimetic amino acids aspartic acid (D) and glutamic acid (E), however, were nonfunctional at this position (Fig. 4). Lysine, besides adding a positive charge, is also a major target for posttranslational modifications, such as ubiquitination, acetylation, sumoylation, and methylation, which play critical roles in regulating biological processes (27). Further studies are needed to uncover putative protein modifications in the NEC, especially at this particular site.

Several K242A second-site revertants had no additional mutations in pUL31 but in pUL34 (Table 2). All these mutations were located in predicted loop regions (G15W, T25M, A26V, T98A, A99V) (17). The loop region comprising amino acids 22 to 26 of PrV pUL34 is thought to form the dimeric interface in the hexagonal lattice (17). In addition, in HSV-1 the dominant negative mutation D35A/E37A in pUL34 (corresponding to amino acids D22/E24 in PrV pUL34) (28, 29) impairs curvature formation of the coat (5). The functional relevance of these mutations will be analyzed in the future.

In summary, our data indicate that K242 in H10 in PrV pUL31 may, in fact, not mediate a direct interaction with the nucleocapsid cargo but indicate that this part of the NEC is important for rearrangements leading to the correct curvature of the coated vesicle, allowing for uptake of the nucleocapsid into the nascent primary virion envelope.

MATERIALS AND METHODS

Cells and viruses. Rabbit kidney (RK13) cells, RK13-UL31 cells, and Vero cells were cultivated in Dulbeccó's modified Eagle's minimum essential medium supplemented with 10% or 5% (Vero) fetal calf serum. PrV laboratory strain Kaplan (PrV-Ka) (30) was propagated in RK13 cells, while PrV- Δ UL31 was grown in RK13-UL31 cells (23).

Site-specific mutagenesis of pUL31. pUL31 mutants were generated using a QuikChange II XL site-directed mutagenesis kit (Agilent Technologies) as described previously (16) and the primers listed in Table 1 with the respective UL31 genes cloned in pcDNA3 (Invitrogen) as the template. Correct mutagenesis was verified by sequencing.

Laser-scanning confocal microscopy. For localization and colocalization studies, RK13 cells were transfected either with the corresponding pUL31 expression plasmids singly or with the corresponding pUL31 expression plasmids cotransfected with pcDNA-UL34 (22) by calcium phosphate coprecipitation (31). At 2 days posttransfection, the cells were fixed with 4% paraformaldehyde, permeabilized with 0.1% Triton X-100 in phosphate-buffered saline (PBS), and incubated with a recently generated anti-pUL31 monoclonal antibody (1:50) and with the monospecific rabbit anti-pUL34 serum (1:500) (22). For detection, Alexa Fluor 488-conjugated goat anti-mouse IgG and Alexa 568-conjugated goat anti-rabbit IgG (Invitrogen) were used. Images were acquired with a confocal laser-scanning microscope (63 \times oil immersion objective, single slice; SP5; Leica, Germany) and processed using ImageJ software (32).

Generation of stably expressing RK13 cell lines. To generate stably expressing RK13 cell lines, calcium phosphate coprecipitation was used (31). At 2 days posttransfection, the cells were split and transferred into selection medium containing 500 μ g/ml G418 (Invitrogen). After 10 to 14 days, resistant cell colonies were picked by aspiration and screened by indirect immunofluorescence for pUL31 expression using the polyclonal rabbit anti-pUL31 serum (23). Cell clones homogeneously expressing wild-type or mutated pUL31 were used.

Immunoblot analysis. Cells were cultivated in 24-well plates for 2 days, scraped into medium, and pelleted by centrifugation at 2,000 \times g for 5 min. The pellets were resuspended after washing with phosphate-buffered saline (PBS) in sample buffer (0.13 M Tris-HCl, pH 6.8, 4% SDS, 20% glycerol, 0.01% bromophenol blue, 10% β -mercaptoethanol). Lysates were sonicated and boiled for 3 min before separation of proteins in an SDS-10% polyacrylamide gel. Proteins were transferred onto a nitrocellulose

membrane and incubated with the polyclonal rabbit anti-pUL31 serum (23) and a monoclonal anti- α -tubulin antibody (Sigma) as a loading control. Bound antibody was detected by peroxidase-coupled goat anti-rabbit and goat anti-mouse immunoglobulin antibodies and visualized by enhanced chemiluminescence (Bio-Rad Clarity Western ECL blotting substrate), recorded in an image analyzer (Bio-Rad).

Generation of virus recombinants expressing pUL31-K242A and pUL31-C241-243A. Virus recombinants PrV-UL31-K242A and PrV-UL31-C241-243A were generated by homologous recombination. For this, the corresponding mutations were introduced into cloned genomic 3.3-kb Sall fragment 1C, comprising the UL31 gene region (23). Mutations were introduced using the QuikChange II XL site-directed mutagenesis kit (Agilent Technologies) and the primers described previously (16). Recombination plasmids were cotransfected with PrV- Δ UL31 (green fluorescent protein-positive) genomic DNA (7), followed by purification of nonfluorescing plaques on RK13-UL31 cells. Correct mutagenesis and recombination were tested after PCR amplification by sequencing of the corresponding gene region.

Serial passaging of virus recombinants. For serial passaging, monolayers of RK13 and Vero cells were infected with either PrV-UL31-K242A or PrV-UL31-C241-243A in 24-well cell culture plates in dilutions of 10^{-1} to 10^{-6} . Infected cells were incubated for 3 to 5 days. The contents of the well with the highest virus dilution showing a 100% cytopathic effect were harvested and centrifuged at $15,000 \times g$ for 5 min. The supernatant was again titrated on 24-well culture plates. After 10 and 30 passages, the supernatants were titrated under plaque assay conditions and single virus plaques were picked. After a second round of plaque purification, virus stocks were prepared and the titer was determined on RK13 cells. Plaque isolates which reached titers of at least 10^6 PFU/ml were further investigated. For this, viral DNA was isolated, and the UL31 and UL34 genes were amplified by PCR (23) and sequenced. UL31 PCR products carrying additional mutations were cloned into pcDNA3, and stably expressing cells were generated as described above.

In vitro complementation studies. To test for functional complementation, stably expressing cell lines were infected on ice with PrV-Ka or PrV- Δ UL31 at a multiplicity of infection (MOI) of 5 for 1 h to allow for attachment of viruses to the cells. Subsequently, the inoculum was replaced by prewarmed medium to initiate infection and incubated at 37°C for 1 h. Thereafter, the remaining extracellular virus was inactivated by low-pH treatment (33), and cells were kept for an additional 24 h at 37°C. Cells and supernatant were harvested, frozen, and thawed. After the removal of cellular debris by centrifugation, progeny virus in the supernatant was titrated on RK13-UL31 cells. The mean values from at least three independent experiments were calculated. Statistical significance was determined by a two-way analysis of variance, followed by Sidak's multiple-comparison test. All statistical tests were performed using GraphPad Prism (version 8.1.0) software (GraphPad Software, La Jolla, CA, USA). Significant differences between PrV-Ka and PrV- Δ UL31 infection are indicated by asterisks in the appropriate figures.

Electron microscopy. Stably expressing cell lines infected with PrV- Δ UL31 or RK13 cells infected with PrV-UL31-K242A or PrV-UL31-C241-243A at an MOI of 1 were processed for electron microscopy at 14 h p.i. as described previously (22).

ACKNOWLEDGMENTS

This study was supported by the Deutsche Forschungsgemeinschaft (grant DFG ME 854/12-2). Molecular graphics and analyses were performed with the UCSF Chimera package, which was developed by the Resource for Biocomputing, Visualization, and Informatics at the University of California, San Francisco (supported by NIGMS grant P41-GM103311).

We thank Cindy Krüper, Karla Günther, and Petra Meyer for technical help and Mandy Jörn for photographic assistance. Molecular graphics and analyses were performed with the UCSF Chimera package.

REFERENCES

- Johnson DC, Baines JD. 2011. Herpesviruses remodel host membranes for virus egress. *Nat Rev Microbiol* 9:382–394. <https://doi.org/10.1038/nrmicro2559>.
- Mettenleiter TC, Klupp BG, Granzow H. 2009. Herpesvirus assembly: an update. *Virus Res* 143:222–234. <https://doi.org/10.1016/j.virusres.2009.03.018>.
- Mettenleiter TC, Muller F, Granzow H, Klupp BG. 2013. The way out: what we know and do not know about herpesvirus nuclear egress. *Cell Microbiol* 15:170–178. <https://doi.org/10.1111/cmi.12044>.
- Mettenleiter TC. 2002. Herpesvirus assembly and egress. *J Virol* 76:1537–1547. <https://doi.org/10.1128/jvi.76.4.1537-1547.2002>.
- Bigalke JM, Heuser T, Nicastro D, Heldwein EE. 2014. Membrane deformation and scission by the HSV-1 nuclear egress complex. *Nat Commun* 5:4131. <https://doi.org/10.1038/ncomms5131>.
- Lorenz M, Vollmer B, Unsay JD, Klupp BG, Garcia-Saez AJ, Mettenleiter TC, Antonin W. 2015. A single herpesvirus protein can mediate vesicle formation in the nuclear envelope. *J Biol Chem* 290:6962–6974. <https://doi.org/10.1074/jbc.M114.627521>.
- Klupp BG, Granzow H, Fuchs W, Keil GM, Finke S, Mettenleiter TC. 2007. Vesicle formation from the nuclear membrane is induced by coexpression of two conserved herpesvirus proteins. *Proc Natl Acad Sci U S A* 104:7241–7246. <https://doi.org/10.1073/pnas.0701757104>.
- Klupp BG, Granzow H, Mettenleiter TC. 2011. Nuclear envelope breakdown can substitute for primary envelopment-mediated nuclear egress of herpesviruses. *J Virol* 85:8285–8292. <https://doi.org/10.1128/JVI.00741-11>.
- Newcomb WW, Fontana J, Winkler DC, Cheng N, Heymann JB, Steven AC. 2017. The primary enveloped virion of herpes simplex virus 1: its role in nuclear egress. *mBio* 8:e00825-17. <https://doi.org/10.1128/mBio.00825-17>.
- Funk C, Ott M, Raschbichler V, Nagel CH, Binz A, Sodeik B, Bauerfeind R, Bailer SM. 2015. The herpes simplex virus protein pUL31 escorts nucleocapsids to sites of nuclear egress, a process coordinated by its N-terminal domain. *PLoS Pathog* 11:e1004957. <https://doi.org/10.1371/journal.ppat.1004957>.
- Trus BL, Newcomb WW, Cheng N, Cardone G, Marekov L, Homa FL,

- Brown JC, Steven AC. 2007. Allosteric signaling and a nuclear exit strategy: binding of UL25/UL17 heterodimers to DNA-filled HSV-1 capsids. *Mol Cell* 26:479–489. <https://doi.org/10.1016/j.molcel.2007.04.010>.
12. Yang K, Baines JD. 2011. Selection of HSV capsids for envelopment involves interaction between capsid surface components pUL31, pUL17, and pUL25. *Proc Natl Acad Sci U S A* 108:14276–14281. <https://doi.org/10.1073/pnas.1108564108>.
 13. Yang K, Wills E, Lim HY, Zhou ZH, Baines JD. 2014. Association of herpes simplex virus pUL31 with capsid vertices and components of the capsid vertex-specific complex. *J Virol* 88:3815–3825. <https://doi.org/10.1128/JVI.03175-13>.
 14. Takeshima K, Arai J, Maruzuru Y, Koyanagi N, Kato A, Kawaguchi Y. 2019. Identification of the capsid binding site in the herpes simplex virus 1 nuclear egress complex and its role in viral primary envelopment and replication. *J Virol* 93:e01290-19. <https://doi.org/10.1128/JVI.01290-19>.
 15. Leelawong M, Guo D, Smith GA. 2011. A physical link between the pseudorabies virus capsid and the nuclear egress complex. *J Virol* 85:11675–11684. <https://doi.org/10.1128/JVI.05614-11>.
 16. Ronfeldt S, Klupp BG, Franzke K, Mettenleiter TC. 2017. Lysine 242 within helix 10 of the pseudorabies virus nuclear egress complex pUL31 component is critical for primary envelopment of nucleocapsids. *J Virol* 91:e01182-17. <https://doi.org/10.1128/JVI.01182-17>.
 17. Zeev-Ben-Mordehai T, Weberruß M, Lorenz M, Cheleski J, Hellberg T, Whittle C, El Omari K, Vasishtan D, Dent KC, Harlos K, Franzke K, Hagen C, Klupp BG, Antonin W, Mettenleiter TC, Grünewald K. 2015. Crystal structure of the herpesvirus nuclear egress complex provides insights into inner nuclear membrane remodeling. *Cell Rep* 13:2645–2652. <https://doi.org/10.1016/j.celrep.2015.11.008>.
 18. Bigalke JM, Heldwein EE. 2015. Structural basis of membrane budding by the nuclear egress complex of herpesviruses. *EMBO J* 34:2921–2936. <https://doi.org/10.15252/embj.201592359>.
 19. Lye MF, Sharma M, El Omari K, Filman DJ, Schuermann JP, Hogle JM, Coen DM. 2015. Unexpected features and mechanism of heterodimer formation of a herpesvirus nuclear egress complex. *EMBO J* 34:2937–2952. <https://doi.org/10.15252/embj.201592651>.
 20. Walzer SA, Egerer-Sieber C, Sticht H, Sevvana M, Hohl K, Millbradt J, Muller YA, Marschall M. 2015. Crystal structure of the human cytomegalovirus pUL50-pUL53 core nuclear egress complex provides insight into a unique assembly scaffold for virus-host protein interactions. *J Biol Chem* 290:27452–27458. <https://doi.org/10.1074/jbc.C115.686527>.
 21. Hagen C, Dent KC, Zeev-Ben-Mordehai T, Grange M, Bosse JB, Whittle C, Klupp BG, Siebert CA, Vasishtan D, Bäuerlein FJB, Cheleski J, Werner S, Gutmann P, Rehbein S, Henzler K, Demmerle J, Adler B, Koszinowski U, Schermelleh L, Schneider C, Enquist LW, Plietzko JM, Mettenleiter TC, Grünewald K. 2015. Structural basis of vesicle formation at the inner nuclear membrane. *Cell* 163:1692–1701. <https://doi.org/10.1016/j.cell.2015.11.029>.
 22. Klupp BG, Granzow H, Mettenleiter TC. 2000. Primary envelopment of pseudorabies virus at the nuclear membrane requires the UL34 gene product. *J Virol* 74:10063–10073. <https://doi.org/10.1128/jvi.74.21.10063-10073.2000>.
 23. Fuchs W, Klupp BG, Granzow H, Osterrieder N, Mettenleiter TC. 2002. The interacting UL31 and UL34 gene products of pseudorabies virus are involved in egress from the host-cell nucleus and represent components of primary enveloped but not mature virions. *J Virol* 76:364–378. <https://doi.org/10.1128/jvi.76.1.364-378.2002>.
 24. Klupp BG, Granzow H, Keil GM, Mettenleiter TC. 2006. The capsid-associated UL25 protein of the alphaherpesvirus pseudorabies virus is nonessential for cleavage and encapsidation of genomic DNA but is required for nuclear egress of capsids. *J Virol* 80:6235–6246. <https://doi.org/10.1128/JVI.02662-05>.
 25. Paßvogel L, Klupp BG, Granzow H, Fuchs W, Mettenleiter TC. 2015. Functional characterization of nuclear trafficking signals in pseudorabies virus pUL31. *J Virol* 89:2002–2012. <https://doi.org/10.1128/JVI.03143-14>.
 26. Roller RJ, Haugo AC, Kopping NJ. 2011. Intragenic and extragenic suppression of a mutation in herpes simplex virus 1 UL34 that affects both nuclear envelope targeting and membrane budding. *J Virol* 85:11615–11625. <https://doi.org/10.1128/JVI.05730-11>.
 27. Xu HD, Zhou JQ, Lin SF, Deng WK, Zhang Y, Xue Y. 2017. PLMD: an updated data resource of protein lysine modifications. *J Genet Genomics* 44:243–250. <https://doi.org/10.1016/j.jgg.2017.03.007>.
 28. Bjerke SL, Cowan JM, Kerr JK, Reynolds AE, Baines JD, Roller RJ. 2003. Effects of charged cluster mutations on the function of herpes simplex virus type 1 U(L)34 protein. *J Virol* 77:7601–7610. <https://doi.org/10.1128/jvi.77.13.7601-7610.2003>.
 29. Roller RJ, Bjerke SL, Haugo AC, Hanson S. 2010. Analysis of a charge cluster mutation of herpes simplex virus type 1 UL34 and its extragenic suppressor suggests a novel interaction between pUL34 and pUL31 that is necessary for membrane curvature around capsids. *J Virol* 84:3921–3934. <https://doi.org/10.1128/JVI.01638-09>.
 30. Kaplan AS, Vatter AE. 1959. A comparison of herpes simplex and pseudorabies viruses. *Virology* 7:394–407. [https://doi.org/10.1016/0042-6822\(59\)90068-6](https://doi.org/10.1016/0042-6822(59)90068-6).
 31. Graham FL, van der Eb AJ. 1973. A new technique for the assay of infectivity of human adenovirus 5 DNA. *Virology* 52:456–467. [https://doi.org/10.1016/0042-6822\(73\)90341-3](https://doi.org/10.1016/0042-6822(73)90341-3).
 32. Schneider CA, Rasband WS, Eliceiri KW. 2012. NIH Image to ImageJ: 25 years of image analysis. *Nat Methods* 9:671–675. <https://doi.org/10.1038/nmeth.2089>.
 33. Mettenleiter TC. 1989. Glycoprotein gIII deletion mutants of pseudorabies virus are impaired in virus entry. *Virology* 171:623–625. [https://doi.org/10.1016/0042-6822\(89\)90635-1](https://doi.org/10.1016/0042-6822(89)90635-1).
 34. Pettersen EF, Goddard TD, Huang CC, Couch GS, Greenblatt DM, Meng EC, Ferrin TE. 2004. UCSF Chimera—a visualization system for exploratory research and analysis. *J Comput Chem* 25:1605–1612. <https://doi.org/10.1002/jcc.20084>.

Own Contribution to Publications 3

Paper I

Function of Torsin AAA+ ATPases in Pseudorabies Virus Nuclear Egress

Julia E. Hölper, Barbara G. Klupp, G.W. Gant Luxton, Kati Franzke and Thomas C. Mettenleiter

Cells 2020, 9, 738; DOI: 10.3390/cells9030738

Julia E. Hölper: Design of the study; Generation of stably expressing cell lines; Generation of the knock-out constructs; Generation of knock-out cell lines; Characterization of the generated mutant cell lines; Performance of fluorescence microscopic examinations; Evaluation of the results; Main participation in the preparation and correction of the manuscript and figures

Barbara G. Klupp: Design of the study; Contribution to the evaluation of the results; Main participation in the preparation and correction of the manuscript and figures

G. W. Gant Luxton: Provision of Torsin expression constructs; Contribution to the evaluation of the results; Participation in correction of the manuscript

Kati Franzke: Preparation of the electron microscopic images; Quantification of TEM results

Thomas C. Mettenleiter: Design of the study; Contribution to the evaluation of the results; Participation in the preparation and correction of the manuscript and figures; Corresponding author

Paper II

Generation and Characterization of Monoclonal Antibodies Specific for the Pseudorabies Virus Nuclear Egress Complex

Julia E. Hölper, Sven Reiche, Kati Franzke, Thomas C. Mettenleiter, Barbara G. Klupp
Virus Research, *submitted* June 2020

Julia E. Hölper: Design of the study; Initial testing and characterization of hybridoma supernatants; Performance of fluorescence microscopic examinations; Evaluation of the results; Main participation in the preparation and correction of the manuscript and figures

Sven Reiche: Immunization of mice; Generation and provision of hybridoma supernatants

Kati Franzke: Preparation of the electron microscopic images; immunoelectron microscopic analyses

Thomas C. Mettenleiter: Design of the study; Contribution to the evaluation of the results; Participation in the preparation and correction of the manuscript

Barbara G. Klupp: Design of the study; Initial testing and characterization of hybridoma supernatants; Contribution to the evaluation of the results; Main participation in the preparation and correction of the manuscript and figures; Corresponding author

Paper III

Mutational Functional Analysis of the Pseudorabies Virus Nuclear Egress Complex-Nucleocapsid Interaction

Sebastian Röfeldt, Kati Franzke, Julia E. Hölper, Barbara G. Klupp, Thomas C. Mettenleiter

Journal of Virology Feb 2020, JVI.01910-19; DOI: 10.1128/JVI.01910-19

Sebastian Röfeldt: Design of the study; Generation of pUL31 substitution mutants; Generation of stably expressing cell lines; Characterization of the generated mutants; Passage of viral mutants; Evaluation of the results; Performance of fluorescence microscopic examinations; Main participation in the preparation and correction of the manuscript and figures

Kati Franzke: Preparation of the electron microscopic images

Julia E. Hölper: Performance of fluorescence microscopic examinations; Participation in the preparation and correction of the manuscript and figures

Barbara G. Klupp: Design of the study; Generation of substitution mutants; Generation of stably expressing cell lines; Characterization of generated mutants; Passage of virus mutants; Contribution to the evaluation of the results; Main participation in the preparation and correction of the manuscript and figures

Thomas C. Mettenleiter: Design of the study; Contribution to the evaluation of the results; Participation in the preparation and correction of the manuscript; Corresponding author

In agreement (Paper I to III):

.....
Place, Date

.....
Prof. Dr. Dr. h.c. Thomas C. Mettenleiter Julia E. Hölper

Results and Discussion 4

Herpesviruses are large DNA viruses that use two sub-cellular compartments for their morphogenesis. After assembly, the newly formed nucleocapsids must leave the nucleus for their final maturation in the cytoplasm. To overcome the nuclear barrier, herpesviruses engage a vesicle-mediated transport process, named nuclear egress [Mettenleiter, 2002; Johnson and Baines, 2011; Mettenleiter *et al.*, 2013; Bigalke and Heldwein, 2015a]. Initiator of this process is the conserved herpesviral NEC consisting of pUL31 and pUL34 orthologues. The NEC mediates budding of the nucleocapsids at the INM resulting in primary enveloped virions located in the PNS. In the second step, the capsids are released into the cytoplasm by fusion of their primary envelope with the ONM.

The main goal of this thesis was to further elucidate the molecular details of the herpesviral nuclear egress. In *Paper I*, the role of cellular Torsins in fusion of the primary envelope with the ONM was investigated, while *Paper II* and *Paper III* focused on the characterization of the PrV NEC and how it interacts with the nucleocapsid.

4.1 Analyzing the Role of Cellular Proteins in Nuclear Egress

While the assembly and function of the viral NEC has been studied to some detail, little is known about the fusion process of the primary virion envelope with the ONM. Fusion of the primary envelope with the ONM and most likely, disassembly of the tight NEC lattice surrounding the capsid are required for efficient release. While herpesviruses rely on pUL31 and pUL34 for orchestrating budding at and scission from the INM, both are not directly involved in the subsequent fusion step (reviewed in Mettenleiter *et al.* [2009]; Johnson and Baines [2011]; Mettenleiter *et al.* [2013]).

The viral protein kinase pUS3 appears to execute a regulatory function in this fusion process in α -herpesviruses, which is manifested by an accumulation of primary virions in the PNS in the absence of the protein (Δ US3) or in presence of a non-functional kinase (US3 Δ kin) [Wagenaar *et al.*, 1995; Klupp *et al.*, 2001; Reynolds *et al.*, 2002; Schumacher *et al.*, 2005; Kato *et al.*, 2011; Sehl *et al.*, 2020]. The regulatory effect is most likely based on its ability to phosphorylate NEC components [Purves *et al.*, 1991, 1992; Ryckman

and Roller, 2004; Mou *et al.*, 2009], thereby potentially weakening their interaction. It is supposed that phosphorylation of pUL31 within the primary virion results in NEC disassembly or its detachment from the capsid [Mou *et al.*, 2009].

Since extensive research on PrV did not reveal a viral protein mediating this fusion event, we were interested whether and which cellular player(s) could be involved in the fusion of the primary envelope with the ONM. Viruses frequently depend for their replication on cellular pathways and proteins. Although vesicle-mediated transport processes between the plasma membrane and cytoplasmic organelles are well studied [Mironov and Beznoussenko, 2019], knowledge on vesicular transport mechanisms and fusion events at the NE is poor. Besides the herpesviral nuclear egress, budding at the NE has also been observed for baculoviruses [Yuan *et al.*, 2011] and for large RNP particles in *Drosophila* [Hatch and Hetzer, 2012; Speese *et al.*, 2012], pointing to a potential cellular mechanism. How much this herpesviral and the cellular egress mechanisms might have in common remains to be investigated.

Our laboratory started research on the LINC complex, because it was described to be involved in NE spacing at least in cell culture [Sosa *et al.*, 2013; Rothballer *et al.*, 2013; Cain and Starr, 2015]. During PrV infection, it was observed that the spacing of the membranes remained similar between the INM and ONM and between the primary envelope and both nuclear membranes. Overexpression of the SUN2_{LD} resulted in 10-fold decreased virus titers and a dilated PNS and ER lumen. The most prominent result was that primary enveloped virions appeared not only in the PNS, but also escaped into the ER lumen, which was not observed in infected WT cells [Klupp *et al.*, 2017].

To further validate these findings, cell lines were generated lacking either SUN1, SUN2 or both (unpublished). For this, we used CRISPR/Cas9-based mutagenesis, which is used widely to modify eukaryotic genomes [Cong *et al.*, 2013; Mali *et al.*, 2013]. Analysis of these KO cell lines allowed the confirmation of previous results from Klupp *et al.* [2017] regarding the role of the LINC components in herpesvirus nuclear egress. The results of infection experiments with RK13-SUN2_{KO} cells were comparable to those of the RK13-SUN2_{LD} cells. In particular, the 10-fold titer loss, the dilation of the NE/ER structures and the escape of primary virions into the ER were detected. However, no apparent defect in nuclear egress was identified in SUN1_{KO} cells, as it was reported for SUN1_{LD} expressing cells [Klupp *et al.*, 2017]. A SUN1/2_{DKO} cell line showed a similar phenotype to RK13-SUN2_{KO} demonstrating that the role in herpesvirus nuclear egress is specific for SUN2.

It is not well understood yet, how the LINC complex is assembled, disassembled and/or regulated. First results suggest that the AAA+ ATPase TorA might be involved [Nery *et al.*, 2008; Vander Heyden *et al.*, 2009; Saunders *et al.*, 2017; Dominguez Gonzalez *et al.*, 2018; Gill *et al.*, 2019; Chalfant *et al.*, 2019]. A similar phenotype as seen in SUN2_{LD} overexpression was also observed in HSV-1-infected, TorA-overexpressing cells

[Maric *et al.*, 2011]. The escape of primary enveloped virions in both SUN2_{LD}- or TorA-overexpressing cells into the ER indicated that an intact LINC/Torsin interaction is necessary to restrict primary virions in the PNS.

The Role of Torsins in Nuclear Egress - Paper I In the first paper (*Paper I*), the role of Torsin AAA+ ATPases in nuclear egress of PrV was examined.

AAA+ ATPases as e.g. NSF (N-ethylmaleimide sensitive factor) and Vps4 are known to be involved in membrane fusion processes such as organelle biogenesis or vesicle trafficking [White and Lauring, 2007; Zhao *et al.*, 2007, 2012]. Therefore it seemed plausible that Torsins might be involved in fusogenic processes at the NE as well. NSF participates in vesicular trafficking [Stenbeck, 1998] and is most likely required for the post-fusion recycling of SNAREs (soluble NSF attachment protein receptors) [Zhao *et al.*, 2012]. Interestingly, functional NSF was also described to play a role in budding of baculovirus progeny nucleocapsids from the nucleus. Expression of a dominant-negative NSF version resulted in accumulations of nucleocapsids in large PNS dilations [Guo *et al.*, 2017]. Vps4, however, drives neck constriction during multivesicular body formation in lysosomes [Adell *et al.*, 2014] and subsequently leads to scission of the neck in an ATP-dependent manner coupling to the ESCRT-III complex [Schoneberg *et al.*, 2018]. Vps4 has already been analyzed in the context of HSV-1 infection, where it was shown to be required for cytoplasmic envelopment but not for nuclear egress [Crump *et al.*, 2007].

Torsins have been described to be involved in NE maintenance and modulation [Naismith *et al.*, 2004; Goodchild and Dauer, 2005; Jungwirth *et al.*, 2010; Kim *et al.*, 2010] as well as vesicle transport through the NE [Rose and Schlieker, 2012; Jokhi *et al.*, 2013]. Additionally, defects in TorA cause blebbing of the NE in neuronal cells [Naismith *et al.*, 2004; Goodchild *et al.*, 2005; Kim *et al.*, 2010], which resembles vesicle budding induced by NEC expression [Klupp *et al.*, 2007], making them exciting candidates for our studies on their influence on herpesvirus nuclear egress.

We analyzed a possible involvement of Torsins in PrV replication by individually overexpressing Torsins. Among the five predicted mammalian Torsins A, B, 2, 3 and 4, we focused on the ubiquitously expressed TorA and B. Since Torsins are well conserved between humans, mice and rabbits we used already existing expression constructs encoding human TorA and B WT and the corresponding mutated forms, all tagged with EGFP at the N-terminus [Jungwirth *et al.*, 2010; Goodchild and Dauer, 2004; Kim *et al.*, 2010; Saunders *et al.*, 2017]. The mutated proteins exert a dominant-negative effect on the endogenous WT protein either by disturbing the interaction with the cofactor essential for ATP-hydrolysis (TorA Δ E302/303) [Ozelius *et al.*, 1997] or by generating a substrate trap where the ATPase can bind, but no longer hydrolyze ATP (TorB_{E178Q}) [Whiteheart *et al.*, 1994; Hewett *et al.*, 2000; Hanson and Whiteheart, 2005; Vander Heyden *et al.*, 2009; Rose *et al.*, 2014].

4 Results and Discussion

Infection of rabbit kidney (RK13) cells stably overexpressing TorA_{WT} and TorB_{E178Q}, resulted in a small drop in virus titers, while RK13-TorA_{ΔE302/303} and -TorB_{WT} yielded virus titers comparable to parental RK13 cells. None of the overexpressing cell lines showed a detectably increased number of primary virions in cytoplasmic structures or an alteration of the NE ultrastructure.

Since TorA and TorB serve partially redundant functions [Kim *et al.*, 2010; Rose *et al.*, 2014], we were interested to investigate whether the effects on PrV infection might be more pronounced when TorA and TorB were targeted simultaneously. Since equivalent overexpression of both proteins in cell lines is difficult to achieve and maintain, we aimed at analyzing the effects by generating single and double KO (DKO) cell lines using CRISPR/Cas9. Overexpression of a protein is an artificial model, which might have several side effects on the metabolism of the cell [Prelich, 2012]. Therefore, the specific targeting of a single protein by KO might disturb the cell to a lesser extent. The generated KO cells were used for infection experiments, where, in contrast to the overexpression experiments the single KO cell lines propagated PrV to titers comparable to unmodified RK13 cells. Further, we did not observe any impairment of nuclear egress or virion morphogenesis in ultrastructural analyses.

Interestingly, we did observe a 10-fold titer decrease after infection of TorA/B_{DKO} cells. The proposed redundancy for TorA and B may compensate the defect in the single KO by a partial functional overlap of both proteins. The detected effect on the titer in RK13-TorA/B_{DKO} was evident at early time points (4 h, 6 h, 8 h *p.i.*), pointing to a delay in capsid release from the nucleus that is compensated over time.

The most interesting finding was that in RK13-TorA/B_{DKO} cells primary enveloped virions accumulated in the PNS, whereas in infected parental RK13 cells single primary enveloped virions were found rarely. In contrast to the large accumulations found after infection with PrV-ΔUS3 or PrV-US3Δkin [Wagenaar *et al.*, 1995; Klupp *et al.*, 2001; Sehl *et al.*, 2020], the primary virions were mainly found lined-up in the PNS and not within herniations of the INM. Furthermore, the envelope of primary virions in RK13-TorA/B_{DKO} cells was often still connected to the INM by a small neck indicating that vesicle scission might be less efficient.

For HSV-1, overexpression of TorA_{WT} also resulted in a similar titer reduction compared to PrV infection and primary enveloped virions were reported to escape into the ER [Maric *et al.*, 2011]. Interestingly, and in contrast to Maric *et al.* [2011], we did not detect any primary enveloped virions within ER structures either after overexpression or deletion of single or both Torsins. Consistent with our results, HSV-1 replication was reduced in HeLa cells lacking both TorA and TorB [Turner *et al.*, 2015]. The fusion with the ONM seemed to be less efficient in the TorA/B_{DKO} cells, which is comparable to the results for TorA_{WT} overexpression in HSV-1 [Maric *et al.*, 2011], as well as SUN2_{LD} overexpression [Klupp *et al.*, 2017] or SUN2_{KO} in PrV infection. It would be interesting to

further analyze the Torsin_{KO} cells with specific attention to the structure or regulation of the LINC complex. So far, no impact on spacing between INM and ONM was apparent in the TorA/B_{DKO} cells indicating that the LINC complex may not be altered.

Detection of primary envelopes which are still connected to the INM supports the hypothesis of Jokhi *et al.* [2013] that Torsins have a role in vesicle scission. This hypothesis is based on the analysis of Torsins role in primary envelopment of large RNP complexes. A Torsin knock-down resulted in abnormal attachment of these large RNP particles to the INM [Jokhi *et al.*, 2013]. A similar phenotype was described for uninfected HeLa cells where multiple members of the Torsin family were deleted simultaneously and membrane vesicles were described that were still connected to the INM. Interestingly, the authors identified different Nups and ubiquitin as constituents of the neck and the lumen of the blebs [Laudermilch *et al.*, 2016], indicating that NPC biogenesis is impaired [Rampello *et al.*, 2020].

Alteration of the NE in form of luminal vesicles was shown to occur predominantly in neuronal cells defective for TorA [Naismith *et al.*, 2004; Goodchild *et al.*, 2005; Kim *et al.*, 2010], where TorA is the predominant Torsin [Jungwirth *et al.*, 2010]. Analysis of murine embryonic fibroblasts (MEFs) from TorA_{KO} mice showed a normal NE architecture. Interestingly, the expression of a short hairpin RNA against TorB in TorA_{KO}-MEFs induced blebbing at the NE, suggesting a clear functional overlap between both Torsins [Kim *et al.*, 2010; Rose *et al.*, 2014]. Despite this redundancy, the different Torsins are suspected to operate also in independent pathways and to have tissue-specific functions [Laudermilch *et al.*, 2016]. Considering these results, we anticipated to detect membrane blebbing at least in the TorA/B_{DKO} cells. Contrary to expectations, in none of the generated cell lines nuclear membrane blebbing was detected. The KO of more than two Torsins was described to increase the nuclear blebbing effect drastically [Laudermilch *et al.*, 2016]. It is tempting to speculate that not only TorA and B, but also Tor2, Tor3 and Tor4 might share functions, influencing NE integrity. This redundancy between the Torsins complicates the analysis of this protein family and therefore it is interesting to test also the less characterized Torsins singly as well as in different combinations.

Do the Torsin Cofactors LAP1 or LULL1 Play a Role in Nuclear Egress? Torsins need a cofactor for activation of their ATPase function [Zhao *et al.*, 2013; Sosa *et al.*, 2014; Brown *et al.*, 2014]. Whether one or both known cofactors LAP1 or LULL1 influence the vesicle-based nuclear transport of either herpesviral capsids or other cellular cargo as large RNPs is not yet known. For this, we also investigated whether the cofactors are involved in PrV infection (unpublished).

To test this, we either overexpressed the N-terminally GFP-tagged full-length (FL) protein or only the LD of the cofactors LAP1 and LULL1 or generated single KOs as well as a DKO. However, no effect on nuclear egress or on infectious virus production was observed in any of the cell lines.

Interestingly, for HSV-1 a KO of LULL1 resulted in reduced genome copy numbers accompanied by approx. 10-fold decreased viral titers [Turner *et al.*, 2015], pointing to an effect of the LULL1_{KO} prior to primary envelopment and nuclear egress. How the KO of the ER-localized LULL1 affects the genome copy number in the nuclear compartment remained unclear.

Furthermore, it is unclear how the DKO of TorA and TorB, but not that of LAP1 and LULL1 - either singly or in combination - can have an effect on the PrV replication, since both cofactors are needed for activation of the AAA+ ATPase function of Torsins [Zhao *et al.*, 2013; Sosa *et al.*, 2014; Brown *et al.*, 2014]. Therefore, it seems plausible that the DKO of TorA and B somehow perturbs the function of a yet unidentified cellular or viral factor that is directly or indirectly involved in the fusion of the primary enveloped virion with the ONM or additionally that there are yet unknown functions for Torsins and/or SUN2. Identifying factors which can physically interact with SUN2, TorA or TorB in PrV-infected cells might provide novel information on the de-envelopment process.

A Future Approach to Identify Cellular Key Players. In addition to the specific targeting of single genes, whole cellular genomes can be targeted to analyze multiple factors simultaneously in a high-throughput screening [Miles *et al.*, 2016]. To gain more information on putative cellular proteins involved in the herpesviral replication cycle, we used a genome-scale CRISPR-Cas9 knockout (GeCKO) screening. Here, pseudotyped lentiviral particles were used as vectors for a CRISPR/Cas9 gene knock-out library containing gRNAs targeting every porcine gene.

The GeCKO screening method provides an unbiased approach to identify viral strategies and potentially reveals novel genes and molecular pathways used by viruses (reviewed in Panda and Cherry [2012]). The technology offers an enormous potential to identify cellular key factors involved in early stages of infection and was used multiple times to identify receptor-related pathways of different viruses [Orchard *et al.*, 2016; Han *et al.*, 2018; Staring *et al.*, 2018; Vanarsdall *et al.*, 2018; Karakus *et al.*, 2019]. An optimization could result in a more efficient screening set-up, allowing a broader analysis of viral processes.

With specific regard to PrV, we try to adapt the system to not only target early stages of infection but also allow the analysis of later stages of the replication cycle. By optimization and usage of different virus mutants we want to create a bottleneck, which could provide a breakthrough in finding the fusion mediator during nuclear egress.

4.2 How the NEC Facilitates the Initial Budding Step

Herpesvirus nuclear egress was extensively studied in the last decades. Composed of the viral proteins pUL31 and pUL34, the NEC is the major determinant for the vesicle-mediated nuclear egress of herpesviral capsids. During infection, but also at artificial membranes in the absence of any other viral and cellular proteins, the NEC can induce membrane bending, budding and scission, thereby resulting in vesicular structures [Klupp *et al.*, 2007; Desai *et al.*, 2012; Bigalke *et al.*, 2014; Lorenz *et al.*, 2015]

4.2.1 Characterization of the Viral Nuclear Egress Complex - Paper II

In previous studies, the NEC was analyzed using monospecific sera against the individual components in localization and expression analyses. This has already resulted in a number of results. However, it is still not clear when and where the NEC is formed. To gain more insight into NEC formation and rearrangement leading to capsid budding during nuclear egress, we aimed at generating NEC-specific monoclonal antibodies (mAbs).

The second paper (*Paper II*) provides the first direct labeling of the PrV NEC in transfected and infected cells. For generation of the mAbs truncated versions of bacterially expressed pUL31 and pUL34 were utilized to immunize mice. The same expression constructs were recently used for elucidation of the PrV NEC crystal structure [Zeev-Ben-Mordehai *et al.*, 2015]. Supernatants of the hybridoma cells were screened by indirect immunofluorescence on PrV-Ka-, PrV- Δ UL31-, PrV- Δ UL34-infected cells or after transfection of the expression plasmids for pUL31, pUL34 or both. This approach resulted in identification of mAbs specific for either pUL31 or pUL34, but also in mAbs reacting only in the presence of both proteins, indicating a specificity for the complex.

pUL31- and pUL34-specific mAbs. The newly generated mAbs against the individual components and the hitherto used polyclonal sera were compared by immunofluorescence analysis of transfected as well as PrV-infected RK13 cells.

Using the mAbs, we detected pUL31 in transfected cells in a diffuse staining in the nucleus, whereas the membrane-anchored pUL34 was detected at the nuclear rim and to some extent additionally in cytoplasmic, most likely ER structures.

Co-expression of both proteins results in complex formation and vesicle budding from the INM with accumulation of vesicles in the PNS, which appeared in the immunofluorescence analyses as pUL31- and pUL34-positive speckles [Klupp *et al.*, 2007; Passvogel *et al.*, 2015].

4 Results and Discussion

Analysis of infected cells showed that pUL31 was partly recruited to the nuclear rim colocalizing with pUL34, which was localized in a smooth nuclear rim staining without additional cytoplasmic fluorescence. After infection with PrV- Δ UL34, pUL31 was as expected not detected at the nuclear rim, while the staining pattern for pUL34 in PrV- Δ UL31-infected cells did not change.

In PrV- Δ US3-infected cells immunostaining resulted in a punctate pattern using the pUL31 and/or pUL34 mAbs, most likely representing accumulations of primary enveloped particles in invaginations of the INM, as described before [Wagenaar *et al.*, 1995; Klupp *et al.*, 2001]. The enrichment of primary virions in the PNS after infection with this mutant is an invaluable tool to study primary envelopment and the composition of these particles, which in WT virus infection are only rarely observed and difficult to analyze.

In summary, the newly generated mAbs against pUL31 and pUL34 showed staining patterns in immunofluorescence analyses that were comparable to already the existing monospecific rabbit sera (pAbs).

The combined use of the newly generated mAbs in association with the already existing pAbs enabled the analysis of NEC component expression at different time points after infection in immunofluorescence analyses. Expression kinetics showed as expected increasing protein expression over time and first signals for pUL31 and pUL34 4 h after PrV-Ka infection of RK13 cells. Interestingly, recruitment of pUL31 to the nuclear rim was not detected until 6 h *p.i.* After infection with the PrV- Δ US3 mutant, detection of both proteins was slightly delayed but was comparable at 6 h *p.i.* where small punctae were observed. Compared to the huge speckles detected in cells at later time points of infection e.g. cells infected under plaque assay conditions, those punctae were smaller, indicating that the primary virions accumulate over time.

We tested the different pUL31- and pUL34-specific mAbs in immunoelectron microscopy on PrV-Ka- and PrV- Δ US3-infected cells. Unfortunately, the anti-pUL34 mAbs showed no specific reaction in the immunogold labeling. In contrast, after incubation with the pUL31 specific mAb, gold particles were found associated with the NE and only rarely labeled intranuclear capsids or other structures in the nucleus.

Until now, it is not clear how the mature capsids reach the inner nuclear membrane for budding. One of the hypotheses suggests that HSV-1 capsids are escorted by pUL31 to the sites of nuclear egress [Funk *et al.*, 2015]. In our studies, however, using either the potent pUL31-specific pAb or the newly generated mAbs binding of pUL31 to the nucleocapsids was only rarely detected.

PrV NEC-specific mAbs. Interestingly, our screening of the hybridoma supernatants resulted in four monoclonal antibodies showing reactivity with PrV-Ka-, PrV- Δ US3-infected or pUL31/ pUL34 co-expressing cells, but no signal after infection with

PrV- Δ UL34, PrV- Δ UL31 or singly transfected cells. This suggested that these antibodies are specific for the NEC, allowing the analysis of the localization and expression kinetics without visualizing the single proteins, offering a new perspective on NEC analysis.

The missing reactivity with single expressing cells either transfected or infected, might be explained by structural changes in either pUL31 or pUL34 during complex formation. Previous structural analyses suggested that binding of pUL31 results in conformational changes in pUL34 [Zeev-Ben-Mordehai *et al.*, 2015]. Further, it is likely that the N-terminal hook of pUL31 is differently folded in the absence of pUL34 [Bigalke and Heldwein, 2017]. Therefore, complex formation might alter the structure of either protein, presenting epitopes not accessible or present on the single proteins. Moreover, the NEC formation could create novel epitopes with contribution from either component. In fact, the extensive interaction interface between pUL31 and pUL34 in the NEC heterodimer or after assembly into higher oligomeric structures could create specific antibody binding sites.

Staining of co-expressed pUL31/pUL34 with the NEC-specific mAbs in transfected cells as well as PrV- Δ US3-infected cells resulted in a punctate pattern, comparable to the typical double-positive speckles observed using the pUL31- or pUL34-specific pAbs/ mAbs. A different staining pattern with the NEC mAbs was detected in PrV-Ka-infected cells. NEC-specific mAbs revealed a diffuse pattern with additional small punctae at the nuclear rim. These small dots are suggested to represent either nascent NEC platforms at the INM or primary enveloped virions in the PNS. All four NEC-specific mAbs showed comparable staining patterns in transfected, as well as in infected cells.

Co-staining of the NEC-specific mAbs with the pUL31- or pUL34-specific pAbs was used to evaluate if both proteins can be detected in the same structures as labeled by the anti-NEC mAbs. Transfection experiments, as well as PrV- Δ US3 infection of cells revealed a strong signal conformity of the punctae with the corresponding pUL31- or pUL34-specific pAb staining.

Infection with PrV-Ka gave an ambiguous result. Whereas a co-staining with pUL34 pAb revealed a colocalization of the punctate structures in addition to the pUL34-specific rim staining, co-staining with the pUL31 pAb revealed no clear colocalization with the NEC-specific mAbs. The failure to detect the dotted structures with the pUL31 monospecific serum might be explained by high levels of diffuse pUL31 in the nucleus relative to low protein levels in those budding events.

Despite using a confocal laser scanning microscope, it appeared that the punctae are distributed throughout the nucleus and not specifically associated with the nuclear membrane. A 3D reconstruction of a PrV-Ka- and a PrV- Δ US3-infected nucleus from serial z-stack images revealed an equal distribution of NEC complexes over the entire nuclear membrane. Further, we did not detect any obvious 'hot spots' which would point to

specific budding sites. In addition, we saw larger dots in PrV- Δ US3-infected cells compared to PrV-Ka-infected cells, indicating that these mAbs most likely label primary enveloped virions.

Unfortunately, these mAbs did not label specific structures in ultrathin sections. As judged by the weak labeling in indirect immunofluorescence analyses, the amount of antigen might be too small for a positive signal in immunoelectron microscopy.

As for the single components, the NEC-specific mAbs were used on PrV-Ka- or PrV- Δ US3-infected cells to analyze protein expression. First positive signals were detected at 6 h *p.i.*, which fits the assumption that these indeed detect the NEC and not the single components. Furthermore, this is consistent with published data for HSV-1 that capsid egress from the nucleus occurred around 6 h *p.i.* [Nagel *et al.*, 2008].

Future Perspectives. The newly generated mAbs provide a promising tool to address some of the remaining questions regarding NEC formation and regulation.

First, it is interesting to map the epitopes detected by these NEC-specific mAbs and differentiate whether these mAbs detect the nascent NEC platforms and/or the primary enveloped virions.

For this, it would be helpful to test different point-mutated or truncated pUL31 or pUL34 forms and check if the mAbs still detect the mutant and its corresponding WT partner in transfected cells. Of particular interest are mutants that are able to form speckles after coexpression, as visualized by previous colocalization studies, but do not complement a PrV- Δ UL31 or PrV- Δ UL34 virus.

Based on the assumption that we detect NEC platforms, one would expect that non-functional NECs cannot be detected with the newly generated NEC-specific mAbs. This might be explained by structural changes of the protein caused by the mutation that allow interaction with the partner but prevent or interfere with correct or functional oligomerization and subsequent budding.

Beside this, the panel of different PrV deletion mutants with defects in nuclear egress should be checked for the localization and/or distribution of the punctae in immunofluorescence analyses.

A PrV mutant deficient for the viral protein pUL25 for example allows docking of capsids to the INM, while budding does not ensue [Klupp *et al.*, 2006]. It would be exciting to investigate if and where the NEC-specific staining can be detected after infection with this mutant. Furthermore, infection with a genome cleavage-/ encapsidation-defective mutant like PrV- Δ UL28 [Mettenleiter *et al.*, 1993; Fuchs *et al.*, 2009] might lack the trigger for reorganization of the suspected planar NEC layer to the formation of a curved NEC patch and also miss the budding step, which might result in fewer or even no punctae.

Furthermore, it would be interesting to test whether cellular as well as viral proteins influence the formation of the NEC or the initiation of budding. The budding activity is likely to be influenced both positively and negatively by viral and cellular proteins [Bigalke and Heldwein, 2017]. The targeted overexpression of different cellular/viral proteins in combination with the NEC could reveal colocalizations which point to an involvement in the process, allowing focused future analyses.

For instance, a recent publication described a member of the cellular VAMP family, namely VAPB, to accumulate in the nuclear fraction after HSV-1 infection and furthermore to colocalize with pUL34 [Saiz-Ros *et al.*, 2019]. An analysis of the distribution of NEC-specific fluorescence would allow a more specific way of detecting interaction of cellular proteins with the NEC lattice, than analysis of the single components.

In conclusion, these mAbs form the basis for a variety of further analyses and are a useful tool addressing some of the unsolved questions.

4.2.2 Analyzing the NEC - Capsid Interaction - Paper III

The molecular basis for the incorporation of the nucleocapsid into the budding vesicles at the INM remains incompletely understood. The availability of the NEC structures from different herpesviruses [Bigalke and Heldwein, 2015b; Lye *et al.*, 2015; Walzer *et al.*, 2015; Zeev-Ben-Mordehai *et al.*, 2015] allowed the targeted mutagenesis for identification of functional and/or structural domains. A specific region in the membrane-distal part of the NEC was predicted to be responsible for a possible electrostatic interaction between the capsid and the NEC [Zeev-Ben-Mordehai *et al.*, 2015; Bigalke and Heldwein, 2015b]. For PrV, this region could be mapped to the alpha-helical region 10, where the lysine (K) at position 242 in pUL31 was found to be important for efficient capsid incorporation [Rönfeldt *et al.*, 2017].

The analysis of HSV-1 pUL31 revealed two aa, R281 and D282, possessing a similar role in nuclear egress mediating efficient NEC binding to the nucleocapsid [Takeshima *et al.*, 2019]. These residues, corresponding to the aa R244 and D245 in PrV, were also shown to convey binding to pUL25, thereby providing evidence that the budding of mature virions in HSV-1 infection is indeed dependent on pUL25 [Yang and Baines, 2011; Yang *et al.*, 2014; Takeshima *et al.*, 2019]. It has been demonstrated earlier that pUL25 is located on the outside of the mature capsid and is involved in efficient nuclear egress [Klupp *et al.*, 2006; Trus *et al.*, 2007]. Interestingly, the indicated residues from PrV and HSV-1 are located in corresponding alpha-helical regions, which once more show the importance of this region for efficient nuclear egress.

Replacing the pUL31-K242 by alanine (A) resulted in the accumulation of empty vesicles in large invaginations of the INM in the PNS, while mature nucleocapsids were present in the nucleus often even in close proximity. The same effect was detected

in a pUL31-C241-243A mutant [Rönfeldt *et al.*, 2017]. Most likely, the mutation at the membrane-distal site of pUL31 blocks the interaction between the NEC and the capsid. However, it remained unclear whether the missing incorporation into the budding vesicle was due to electrostatic interference or structural restrictions.

The third paper (*Paper III*) focused on characterizing the mode of interaction between the NEC and the nucleocapsid. As a basis, the NEC structure as well as the hexagonal lattice was analyzed in more detail. This revealed that the lysine residue at position 242 in pUL31 seemed freely accessible in the NEC heterodimer, while in the predicted hexagonal lattice, this aa appeared more deeply buried than expected for a direct interaction interface.

The Functional Analysis of the Essential K242 Position in pUL31. To analyze whether that the interaction of the nucleocapsid with the membrane-distal part of pUL31 is mediated by electrostatic interference, the aa at position K242 was analyzed for functional substitutes. K242 was replaced by aa with side chains of different charge, size and orientation including the basic but larger arginine (R), the negatively charged but smaller glutamic acid (E) or aspartic acid (D), the small neutral serine (S), the large aromatic tyrosine (Y), or the medium-sized glutamine (Q). The resulting mutants were analyzed in transient expression assays for speckle formation and, after establishment of stably expressing cell lines, for functional complementation of the PrV- Δ UL31 mutant.

After single transfection all generated mutants localized as the WT protein diffusely in the nucleus and complex formation with pUL34 after coexpression was unaffected except for pUL31-K242D.

Exchange to D resulted in higher levels of pUL34 at the nuclear rim and in cytoplasmic structures. Besides the exchange to D, the position was also exchanged to another negatively charged aa, pUL31-K242E. Interestingly, stable expression of pUL31-K242D or pUL31-K242E was not sufficient to complement PrV- Δ UL31. However, in contrast to pUL31-K242A expression, only a few vesicle-like structures were detected in the PNS of pUL31-K242E expressing cells, while for pUL31-K242D no budding events were evident in ultrastructural analyses. The introduction of a negative charge might lower the binding affinities of the NEC partners or the NEC oligomer, thereby probably destabilizing the complex.

Propagation of the pUL31 deletion mutant on pUL31-K242Q and -K242R expressing cells resulted in decreased progeny titers compared to WT infection and nucleocapsids were found in close proximity to the INM, while membrane bending or budding was detected only infrequently. The exchange to R shows that a basic aa at that position 242 does not imply that the NEC is fully functional, arguing against a charge interaction.

The replacement to K242S and K242Y had only a minor effect on viral progeny titers of PrV- Δ UL31 and all stages of herpesvirus replication were detected in ultrastructural analyses, indicating that S and Y are tolerated at this position.

Assuming that charge does not play a role, it is likely that either the structure or the size of the side chain are important for efficient incorporation of the nucleocapsid into budding vesicles. Although some mutations resulted in severely reduced titers, none led to an accumulation of empty vesicles, as seen in pUL31-K242A. We assume that the side chain of alanine might not fill the space between the pUL31 molecules of interacting heterodimers. The resulting steric effects might enable a greater flexibility of the hexagonal lattice. Thereby, an enhanced capsid-independent budding and vesicle scission at the INM might be triggered.

Second-site mutations correct the capsid incorporation defect of pUL31-K242A.

In a subsequent step the mutations K242A and C241-243A were introduced into the genome of PrV-Ka, thereby generating PrV-UL31-K242A and PrV-UL31-C241-243A viruses. Infection with these viruses resulted in decreased viral titers with accumulation of empty vesicles in the PNS while nucleocapsids were trapped in the nucleus, as reported after PrV- Δ UL31 infection of cells expressing these mutant proteins [Rönfeldt *et al.*, 2017]. Still, a small amount of infectious virus was observed in the supernatant, which was used for serial passaging of the virus mutants in different cell lines. The resulting revertants harbored a number of mutations in pUL31 and pUL34.

Studying viral revertants provides a valuable tool for identification of functional domains which compensate for defects imposed by mutations.

To test whether the second site-mutations in pUL31, identified in the different revertants, are sufficient to compensate the defect of K242A, stable cell lines were generated. The second site mutations did not influence the localization of the mutated pUL31 or their ability to form the NEC with WT pUL34.

The analysis of the stably expressing cell lines in complementation of PrV- Δ UL31 revealed an at least partial compensation of the K242A-dependent titer defect. Subsequent ultrastructural analysis of these mutants infected with PrV- Δ UL31 revealed that all resulted in partial reversion of the capsid incorporation defect induced by the K242A mutation, although some empty vesicles were still detected.

After modeling of the mutations into the NEC structure, the majority of the mutations were found to be in close proximity to the membrane distal part of pUL31. It is likely that these mutations compensate for structural effects triggered by the K242A mutation. One of the revertants carried a direct exchange of the K242 position to threonine (K242T). This constitutes another example of a functional exchange of the lysine, as seen for K242S or K242Y in the first part of the study.

Interestingly, two mutations were found to be located distant from this region. One is

located in the N-terminal arm of pUL31, which directly interacts with pUL34 [Zeev-Ben-Mordehai *et al.*, 2015; Bigalke and Heldwein, 2015b; Lye *et al.*, 2015; Walzer *et al.*, 2015]. This mutation is likely to change the flexibility of the arm. We suppose a similar effect for the second mutation, which is part of a loop and together with the zinc finger motif important for the intra-hexamer interface stabilized by hydrophobic interactions [Zeev-Ben-Mordehai *et al.*, 2015]. Mutations at those sites could increase the flexibility of intra- or inter-complex interactions, allowing to compensate for the structural changes induced by K242A mutation.

In summary, these data suggest that the K242 residue in H10 of pUL31 does not mediate a direct electrostatic interaction with the capsid. It is likely that this part of the NEC is important for correct curvature of the NEC coat thereby allowing the incorporation of the nucleocapsid.

Future Perspectives. So far, only revertants carrying mutations in pUL31 have been characterized in more detail, but some mutations were also found in pUL34. The characterization should shed light on the interaction and structural changes during oligomerization.

Lysine residues are often targeted by posttranslational modifications [Zee and Garcia, 2012], like acetylation, formylation, methylation, sumoylation and ubiquitination. These could affect protein stability and activity, thereby being critical for the regulation of various biological processes [Xu *et al.*, 2017]. An analysis of the putative modifications on K242 or on other aa within the NEC could reveal further information on the regulation of NEC formation and its interaction with the nucleocapsid.

Besides alanine, all aa exchanges tested so far were polar aa. It would be interesting to test if other apolar aa of different size have a similar effect on nuclear egress, resulting in uncontrolled vesicle budding. For example, the small glycine, the medium-sized leucine or the large tryptophan could be considered.

Summary

Herpesviruses are enveloped DNA viruses which are dependent on two fusion steps for efficient replication in the host cell. First, they have to fuse their envelope with the cellular plasma membrane or with the vesicle membrane after endocytic uptake to enter the host cell and second, they have to export the newly generated nucleocapsids from the site of assembly to the cytoplasm by fusion of the primary virion envelope with the outer nuclear membrane (ONM). The main goal of this project was to provide a better understanding of how herpesvirus capsids exit the nucleus. On the one hand this thesis aimed at finding cellular proteins involved in nuclear egress (Paper I), while on the other the focus was on further characterization of the viral nuclear egress complex (NEC, Paper II) and its interaction with the capsid (Paper III).

It is the hallmark of viruses, including herpesviruses, to hijack host cell proteins for their efficient replication. Some of those interactions are well characterized, while others might not yet have been discovered. In the last step of the nuclear egress, where the primary virion membrane fuses with the ONM, most likely a cellular machinery is involved. The presented work focused on Torsin, the only known AAA+ ATPase localizing in the endoplasmic reticulum and the perinuclear space (PNS). For this, the effect of overexpression of WT and mutant proteins, as well as CRISPR/Cas9 generated knock-out cell lines, on PrV replication was analyzed. Neither single overexpression nor single knockouts of TorA or TorB had any significant effects on virus titers. However, infection of TorA/B double knockout cells revealed reduced viral titers and an accumulation of primary virions in the PNS at early infection times, indicating a delay in nuclear egress.

The process of nuclear egress has been intensively investigated without revealing all its details. To address some of the missing aspects we generated monoclonal antibodies (mAbs) against the NEC and its components (pUL31 and pUL34) for a better visualization of the process in transfected as well as infected cells. These mAbs provide a useful tool for future analyses.

The publication of the NEC crystal structure formed the basis for intensive research on the molecular details of the NEC formation and its interaction with the nucleocapsid. Recently, our lab showed that lysine (K) at position 242 in the membrane-distal part of pUL31 is crucial for incorporation of the nucleocapsid into budding vesicles. Replacing K by alanine (A) resulted in accumulations of vesicles in the PNS, while mature capsids were not incorporated. To test whether this is due to electrostatic interference or structural restrictions we substituted K242 by different aa to determine the requirements for nucleocapsid uptake into the nascent primary particles. To analyze whether the defect of pUL31-K242A can be compensated by second-site mutations, PrV-UL31-K242A was passaged and mutations in revertants were analyzed. Different mutations have been identified compensating for the K242A defect. A considerable number of mutations indicates that the NEC is much more flexible than previously thought. Further, we gained information that the K at position 242 is not directly involved in capsid interaction, while it is more likely involved in rearrangements within the NEC coat.

Zusammenfassung

Herpesviren sind umhüllte DNA-Viren, die zur effizienten Replikation in der Wirtszelle auf zwei Fusionsmechanismen angewiesen sind. Erstens müssen sie ihre Hülle entweder mit der zellulären Plasmamembran oder der Vesikelmembran nach erfolgter Endozytose verschmelzen, um in die Wirtszelle einzudringen. Zweitens müssen die neu gebildeten Nukleokapside aus dem Zellkern durch Fusion der primären Virushülle mit der äußeren Kernmembran in das Zytoplasma exportiert werden. Das Hauptziel dieser Arbeit war es, den herpesviralen Kernaustritt, auch "*Nuclear Egress*" genannt, besser zu verstehen. Zum einen zielte die Arbeit auf eine Identifizierung von zellulären Proteinen, die beim *Nuclear Egress* eine Rolle spielen, ab (Publikation I). Zum anderen sollte der für den Kernaustritt wichtige *Nuclear Egress Complex* (NEC) genauer charakterisiert (Publikation II) und die Interaktion mit dem Kapsid entschlüsselt werden (Publikation III).

Herpesviren nutzen für ihre effiziente Replikation Proteine der Wirtszelle. Einige dieser Interaktionen wurden in der Vergangenheit bereits gut charakterisiert, während andere möglicherweise noch nicht entdeckt wurden. Im letzten Schritt des *Nuclear Egress* fusioniert die primäre Hülle der Kapside mit der äußeren Kernmembran. Dieser Schritt wird höchstwahrscheinlich durch eine zelluläre Maschinerie vermittelt. Die vorliegende Arbeit konzentrierte sich dabei auf die AAA+ ATPase Torsin, die als einzige im endoplasmatischen Retikulum und im Kernspalt vorhanden ist. Es wurden die Auswirkungen der Überexpression (von Wildtyp und Mutanten) sowie die Erzeugung von Knock-outs (mit Hilfe der CRISPR/Cas9 Technik) auf die PrV-Vermehrung analysiert. Weder die Expression noch die einzelnen Gen Knock-outs zeigten signifikante Auswirkungen auf die Virusvermehrung. Ein gleichzeitiger Knock-out von Torsin A und B führte zu reduzierten Virustitern zu frühen Zeitpunkten nach der Infektion und einer Anhäufung primärer Virionen im Kernspalt. Auffällig war, dass die primäre Virushülle häufig noch mit der inneren Kernmembran verbunden war. Dies könnte darauf hindeuten, dass Torsine bei der Abschnürung der primären Viruspartikel eine Rolle spielen.

Der *Nuclear Egress* wurde im Laufe der letzten Jahrzehnte intensiv untersucht. Um einige der noch unbekanntesten Aspekte zu beleuchten, wurden im Rahmen dieser Arbeit monoklonale Antikörper gegen den NEC sowie seine einzelnen Komponenten pUL31 und pUL34 generiert. Diese sollen zur besseren Visualisierung des NEC in transfizierten, aber auch infizierten Zellen dienen. Diese Antikörper sind ein nützliches Werkzeug für zukünftige Analysen.

Mit der Aufklärung der Kristallstruktur des NEC wurde der Grundstein für eine genauere Untersuchung und Aufklärung der molekularen Details sowie seiner Wechselwirkungen mit dem Nukleokapsid gelegt. Unser Labor konnte kürzlich zeigen, dass ein Lysin (K) an Position 242 in pUL31 für den Einbau des Nukleokapsids in die primären Vesikel von entscheidender Bedeutung ist. Tauscht man das Lysin gegen ein Alanin (A) aus, werden zwar Vesikel von der inneren Kernmembrane abgeschnürt, aber keine Kapside eingebaut. Im Rahmen dieser Arbeit wurde das Lysin an Position 242 nicht nur gegen Alanin ausgetauscht, sondern auch durch eine Reihe

anderer Aminosäuren mit unterschiedlicher Ladung oder Größe ersetzt, um zu untersuchen, ob der Effekt auf elektrostatische Interferenzen oder strukturelle Restriktionen zurückzuführen ist. Reversionsanalysen zeigten, dass der K242A-Defekt durch unterschiedliche Mutationen in pUL31 kompensiert werden konnte. Die große Zahl und Diversität dieser Mutationen weisen auf eine größere Flexibilität des NEC hin als bisher angenommen. Weiterhin ergaben sich Hinweise, dass das Lysin an Position 242 nicht direkt an der Kapsidinteraktion, sondern vermutlich eher an strukturellen Veränderungen in der NEC-Hülle beteiligt ist.

Bibliography A

- S. A. Adam. The nuclear pore complex. *Genome Biol*, 2(9):REVIEWS0007, 2001. doi: 10.1186/gb-2001-2-9-reviews0007.
- S. A. Adam. The nucleoskeleton. *Cold Spring Harb Perspect Biol*, 9(2), 2017. doi: 10.1101/cshperspect.a023556.
- M. A. Adell, G. F. Vogel, M. Pakdel, M. Muller, H. Lindner, M. W. Hess and D. Teis. Coordinated binding of vps4 to escrt-iii drives membrane neck constriction during mvb vesicle formation. *J Cell Biol*, 205(1):33–49, 2014. doi: 10.1083/jcb.201310114.
- V. Aho, M. Myllys, V. Ruokolainen, S. Hakanen, E. Mantyla, J. Virtanen, V. Hukkanen, T. Kuhn, J. Timonen, K. Mattila, C. A. Larabell and M. Vihinen-Ranta. Chromatin organization regulates viral egress dynamics. *Sci Rep*, 7(1):3692, 2017. doi: 10.1038/s41598-017-03630-y.
- F. Alber, S. Dokudovskaya, L. M. Veenhoff, W. Zhang, J. Kipper, D. Devos, A. Suprpto, O. Karni-Schmidt, R. Williams, B. T. Chait, A. Sali and M. P. Rout. The molecular architecture of the nuclear pore complex. *Nature*, 450(7170):695–701, 2007. doi: 10.1038/nature06405.
- J. Arii, M. Watanabe, F. Maeda, N. Tokai-Nishizumi, T. Chihara, M. Miura, Y. Maruzuru, N. Koyanagi, A. Kato and Y. Kawaguchi. Escrt-iii mediates budding across the inner nuclear membrane and regulates its integrity. *Nat Commun*, 9(1):3379, 2018. doi: 10.1038/s41467-018-05889-9.
- L. Astrachan and E. Volkin. Properties of ribonucleic acid turnover in t2-infected escherichia coli. *Biochim Biophys Acta*, 29(3):536–44, 1958. doi: 10.1016/0006-3002(58)90010-6.
- J. D. Baines, P. L. Ward, G. Campadelli-Fiume and B. Roizman. The ul20 gene of herpes simplex virus 1 encodes a function necessary for viral egress. *J Virol*, 65(12):6414–24, 1991.
- B. W. Banfield. Beyond the nec: Modulation of herpes simplex virus nuclear egress by viral and cellular components. *Current Clinical Microbiology Reports*, 6(1):1–9, 2019. doi: 10.1007/s40588-019-0112-7.

A Bibliography

- L. J. Barton, A. A. Soshnev and P. K. Geyer. Networking in the nucleus: a spotlight on leucine-rich repeat domain proteins. *Curr Opin Cell Biol*, 34:1–8, 2015. doi: 10.1016/j.ceb.2015.03.005.
- T. Ben-Porat, R. A. Veach and S. Ihara. Localization of the regions of homology between the genomes of herpes simplex virus, type 1, and pseudorabies virus. *Virology*, 127(1): 194–204, 1983. doi: 10.1016/0042-6822(83)90383-5.
- J. M. Bigalke and E. E. Heldwein. The great (nuclear) escape: New insights into the role of the nuclear egress complex of herpesviruses. *J Virol*, 89(18):9150–3, 2015a. doi: 10.1128/JVI.02530-14.
- J. M. Bigalke and E. E. Heldwein. Structural basis of membrane budding by the nuclear egress complex of herpesviruses. *EMBO J*, 34(23):2921–36, 2015b. doi: 10.15252/embj.201592359.
- J. M. Bigalke and E. E. Heldwein. Nuclear exodus: Herpesviruses lead the way. *Annu Rev Virol*, 3(1):387–409, 2016. doi: 10.1146/annurev-virology-110615-042215.
- J. M. Bigalke and E. E. Heldwein. *Chapter Three - Have NEC Coat, Will Travel: Structural Basis of Membrane Budding During Nuclear Egress in Herpesviruses*, volume 97, pages 107–141. Academic Press, 2017. ISBN 0065-3527. doi: <https://doi.org/10.1016/bs.aivir.2016.07.002>.
- J. M. Bigalke, T. Heuser, D. Nicastro and E. E. Heldwein. Membrane deformation and scission by the hsv-1 nuclear egress complex. *Nat Commun*, 5:4131, 2014. doi: 10.1038/ncomms5131.
- S. L. Bjerke and R. J. Roller. Roles for herpes simplex virus type 1 ul34 and us3 proteins in disrupting the nuclear lamina during herpes simplex virus type 1 egress. *Virology*, 347(2):261–76, 2006. doi: 10.1016/j.virol.2005.11.053.
- F. P. Booy, W. W. Newcomb, B. L. Trus, J. C. Brown, T. S. Baker and A. C. Steven. Liquid-crystalline, phage-like packing of encapsidated dna in herpes simplex virus. *Cell*, 64(5):1007–15, 1991. doi: 10.1016/0092-8674(91)90324-r.
- J. Borrego-Pinto, T. Jegou, D. S. Osorio, F. Aurade, M. Gorjanacz, B. Koch, I. W. Mattaj and E. R. Gomes. Samp1 is a component of tan lines and is required for nuclear movement. *J Cell Sci*, 125(Pt 5):1099–105, 2012. doi: 10.1242/jcs.087049.
- J. B. Bosse and L. W. Enquist. The diffusive way out: Herpesviruses remodel the host nucleus, enabling capsids to access the inner nuclear membrane. *Nucleus*, 7(1):13–9, 2016. doi: 10.1080/19491034.2016.1149665.
- J. B. Bosse, S. Viriding, S. Y. Thiberge, J. Scherer, H. Wodrich, Z. Ruzsics, U. H. Koszowski and L. W. Enquist. Nuclear herpesvirus capsid motility is not dependent on f-actin. *mBio*, 5(5):e01909–14, 2014. doi: 10.1128/mBio.01909-14.

- J. B. Bosse, I. B. Hogue, M. Feric, S. Y. Thiberge, B. Sodeik, C. P. Brangwynne and L. W. Enquist. Remodeling nuclear architecture allows efficient transport of herpesvirus capsids by diffusion. *Proc Natl Acad Sci U S A*, 112(42):E5725–33, 2015. doi: 10.1073/pnas.1513876112.
- S. Boulant, M. Stanifer and P. Y. Lozach. Dynamics of virus-receptor interactions in virus binding, signaling, and endocytosis. *Viruses*, 7(6):2794–815, 2015. doi: 10.3390/v7062747.
- A. Brachner and R. Foisner. Evolvement of lem proteins as chromatin tethers at the nuclear periphery. *Biochem Soc Trans*, 39(6):1735–41, 2011. doi: 10.1042/BST20110724.
- A. Brachner, S. Reipert, R. Foisner and J. Gotzmann. Lem2 is a novel man1-related inner nuclear membrane protein associated with a-type lamins. *J Cell Sci*, 118(Pt 24): 5797–810, 2005. doi: 10.1242/jcs.02701.
- A. Brachner, J. Braun, M. Ghodgaonkar, D. Castor, L. Zlopasa, V. Ehrlich, J. Jiricny, J. Gotzmann, S. Knasmuller and R. Foisner. The endonuclease ankle1 requires its lem and giy-yig motifs for dna cleavage in vivo. *J Cell Sci*, 125(Pt 4):1048–57, 2012. doi: 10.1242/jcs.098392.
- X. O. Breakefield, C. Kamm and P. I. Hanson. Torsina. *Neuron*, 31(1):9–12, 2001. doi: 10.1016/s0896-6273(01)00350-6.
- A. E. Briner, P. D. Donohoue, A. A. Gooma, K. Selle, E. M. Slorach, C. H. Nye, R. E. Haurwitz, C. L. Beisel, A. P. May and R. Barrangou. Guide rna functional modules direct cas9 activity and orthogonality. *Mol Cell*, 56(2):333–339, 2014. doi: 10.1016/j.molcel.2014.09.019.
- R. S. Brown, C. Zhao, A. R. Chase, J. Wang and C. Schlieker. The mechanism of torsin atpase activation. *Proc Natl Acad Sci U S A*, 111(45):E4822–31, 2014. doi: 10.1073/pnas.1415271111.
- M. Cai, Y. Huang, R. Ghirlando, K. L. Wilson, R. Craigie and G. M. Clore. Solution structure of the constant region of nuclear envelope protein lap2 reveals two lem-domain structures: one binds baf and the other binds dna. *EMBO J*, 20(16):4399–407, 2001. doi: 10.1093/emboj/20.16.4399.
- N. E. Cain and D. A. Starr. Sun proteins and nuclear envelope spacing. *Nucleus*, 6(1): 2–7, 2015. doi: 10.4161/19491034.2014.990857.
- D. Camozzi, S. Pignatelli, C. Valvo, G. Lattanzi, C. Capanni, P. Dal Monte and M. P. Landini. Remodelling of the nuclear lamina during human cytomegalovirus infection: role of the viral proteins pul50 and pul53. *J Gen Virol*, 89(Pt 3):731–740, 2008. doi: 10.1099/vir.0.83377-0.

A Bibliography

- G. L. Cano-Monreal, K. M. Wylie, F. Cao, J. E. Tavis and L. A. Morrison. Herpes simplex virus 2 ul13 protein kinase disrupts nuclear lamins. *Virology*, 392(1):137–47, 2009. doi: 10.1016/j.virol.2009.06.051.
- G. Cardone, J. B. Heymann, N. Cheng, B. L. Trus and A. C. Steven. Procapsid assembly, maturation, nuclear exit: dynamic steps in the production of infectious herpesvirions. *Adv Exp Med Biol*, 726:423–39, 2012. doi: 10.1007/978-1-4614-0980-9_19.
- M. Chalfant, K. W. Barber, S. Borah, D. Thaller and C. P. Lusk. Expression of torsina in a heterologous yeast system reveals interactions with luminal domains of linc and nuclear pore complex components. *Mol Biol Cell*, 30(5):530–541, 2019. doi: 10.1091/mbc.E18-09-0585.
- A. R. Chase, E. Laudermitch, J. Wang, H. Shigematsu, T. Yokoyama and C. Schlieker. Dynamic functional assembly of the torsin aaa+ atpase and its modulation by lap1. *Mol Biol Cell*, 28(21):2765–2772, 2017. doi: 10.1091/mbc.E17-05-0281.
- M. Cohen, K. L. Wilson and Y. Gruenbaum. *Integral Proteins of the Nuclear Pore Membrane*, book section Chapter 2, pages 28–34. Molecular Biology Intelligence Unit. Springer US, Boston, MA, 2005. ISBN 978-0-306-48241-0. doi: 10.1007/0-387-27747-1_2.
- L. Cong, F. A. Ran, D. Cox, S. Lin, R. Barretto, N. Habib, P. D. Hsu, X. Wu, W. Jiang, L. A. Marraffini and F. Zhang. Multiplex genome engineering using crispr/cas systems. *Science*, 339(6121):819–23, 2013. doi: 10.1126/science.1231143.
- F. H. Crick, L. Barnett, S. Brenner and R. J. Watts-Tobin. General nature of the genetic code for proteins. *Nature*, 192:1227–32, 1961. doi: 10.1038/1921227a0.
- M. Crisp, Q. Liu, K. Roux, J. B. Rattner, C. Shanahan, B. Burke, P. D. Stahl and D. Hodzic. Coupling of the nucleus and cytoplasm: role of the linc complex. *J Cell Biol*, 172(1): 41–53, 2006. doi: 10.1083/jcb.200509124.
- K. D. Croen. Latency of the human herpesviruses. *Annu Rev Med*, 42:61–7, 1991. doi: 10.1146/annurev.me.42.020191.000425.
- C. M. Crump, C. Yates and T. Minson. Herpes simplex virus type 1 cytoplasmic envelopment requires functional vps4. *J Virol*, 81(14):7380–7, 2007. doi: 10.1128/JVI.00222-07.
- M. A. D’Angelo, D. J. Anderson, E. Richard and M. W. Hetzer. Nuclear pores form de novo from both sides of the nuclear envelope. *Science*, 312(5772):440–3, 2006. doi: 10.1126/science.1124196.
- A. J. Davison. Herpesvirus systematics. *Vet Microbiol*, 143(1):52–69, 2010. doi: 10.1016/j.vetmic.2010.02.014.
- A. J. Davison and N. M. Wilkie. Location and orientation of homologous sequences in the genomes of five herpesviruses. *J Gen Virol*, 64 (Pt 9):1927–42, 1983. doi: 10.1099/0022-1317-64-9-1927.

- A. J. Davison, R. Eberle, B. Ehlers, G. S. Hayward, D. J. McGeoch, A. C. Minson, P. E. Pellett, B. Roizman, M. J. Studdert and E. Thiry. The order herpesvirales. *Arch Virol*, 154(1):171–7, 2009. doi: 10.1007/s00705-008-0278-4.
- T. Dechat, K. Pflieger, K. Sengupta, T. Shimi, D. K. Shumaker, L. Solimando and R. D. Goldman. Nuclear lamins: major factors in the structural organization and function of the nucleus and chromatin. *Genes Dev*, 22(7):832–53, 2008. doi: 10.1101/gad.1652708.
- T. Dechat, S. A. Adam and R. D. Goldman. Nuclear lamins and chromatin: when structure meets function. *Adv Enzyme Regul*, 49(1):157–66, 2009. doi: 10.1016/j.advenzreg.2008.12.003.
- T. Dechat, S. A. Adam, P. Taimen, T. Shimi and R. D. Goldman. Nuclear lamins. *Cold Spring Harb Perspect Biol*, 2(11):a000547, 2010. doi: 10.1101/cshperspect.a000547.
- F. E. Demircioglu, B. A. Sosa, J. Ingram, H. L. Ploegh and T. U. Schwartz. Structures of torsina and its disease-mutant complexed with an activator reveal the molecular basis for primary dystonia. *Elife*, 5:e17983, 2016. doi: 10.7554/eLife.17983.
- C. M. Denais, R. M. Gilbert, P. Isermann, A. L. McGregor, M. te Lindert, B. Weigelin, P. M. Davidson, P. Friedl, K. Wolf and J. Lammerding. Nuclear envelope rupture and repair during cancer cell migration. *Science*, 352(6283):353–8, 2016. doi: 10.1126/science.aad7297.
- P. J. Desai, E. N. Pryce, B. W. Henson, E. M. Luitweiler and J. Cothran. Reconstitution of the kaposi’s sarcoma-associated herpesvirus nuclear egress complex and formation of nuclear membrane vesicles by coexpression of orf67 and orf69 gene products. *J Virol*, 86(1):594–8, 2012. doi: 10.1128/JVI.05988-11.
- B. Dominguez Gonzalez, K. Billion, S. Rous, B. Pavie, C. Lange and R. Goodchild. Excess linc complexes impair brain morphogenesis in a mouse model of recessive tor1a disease. *Hum Mol Genet*, 27(12):2154–2170, 2018. doi: 10.1093/hmg/ddy125.
- J. A. Doudna and E. J. Sontheimer. Methods in enzymology. the use of crispr/cas9, zfn, and talens in generating site-specific genome alterations. preface. *Methods Enzymol*, 546:xix–xx, 2014. doi: 10.1016/B978-0-12-801185-0.09983-9.
- E. Dultz and J. Ellenberg. Live imaging of single nuclear pores reveals unique assembly kinetics and mechanism in interphase. *J Cell Biol*, 191(1):15–22, 2010. doi: 10.1083/jcb.201007076.
- A. M. Dupuy-Coin, P. Moens and M. Bouteille. Three-dimensional analysis of given cell structures: nucleolus, nucleoskeleton and nuclear inclusions. *Methods Achiev Exp Pathol*, 12:1–25, 1986.

A Bibliography

- R. J. Eisenberg, D. Atanasiu, T. M. Cairns, J. R. Gallagher, C. Krummenacher and G. H. Cohen. Herpes virus fusion and entry: a story with many characters. *Viruses*, 4(5): 800–32, 2012. doi: 10.3390/v4050800.
- J. P. Erzberger and J. M. Berger. Evolutionary relationships and structural mechanisms of aaa+ proteins. *Annu Rev Biophys Biomol Struct*, 35:93–114, 2006. doi: 10.1146/annurev.biophys.35.040405.101933.
- A. Farina, R. Feederle, S. Raffa, R. Gonnella, R. Santarelli, L. Frati, A. Angeloni, M. R. Torrisi, A. Faggioni and H. J. Delecluse. Bfrf1 of epstein-barr virus is essential for efficient primary viral envelopment and egress. *J Virol*, 79(6):3703–12, 2005. doi: 10.1128/JVI.79.6.3703-3712.2005.
- A. Farnsworth, T. W. Wisner, M. Webb, R. Roller, G. Cohen, R. Eisenberg and D. C. Johnson. Herpes simplex virus glycoproteins gb and gh function in fusion between the virion envelope and the outer nuclear membrane. *Proc Natl Acad Sci U S A*, 104(24):10187–92, 2007. doi: 10.1073/pnas.0703790104.
- G. Felsenfeld and M. Groudine. Controlling the double helix. *Nature*, 421(6921):448–53, 2003. doi: 10.1038/nature01411.
- B. Fichtman, C. Ramos, B. Rasala, A. Harel and D. J. Forbes. Inner/outer nuclear membrane fusion in nuclear pore assembly: biochemical demonstration and molecular analysis. *Mol Biol Cell*, 21(23):4197–211, 2010. doi: 10.1091/mbc.E10-04-0309.
- T. Forest, S. Barnard and J. D. Baines. Active intranuclear movement of herpesvirus capsids. *Nat Cell Biol*, 7(4):429–31, 2005. doi: 10.1038/ncb1243.
- E. Fossum, C. C. Friedel, S. V. Rajagopala, B. Titz, A. Baiker, T. Schmidt, T. Kraus, T. Stellberger, C. Rutenberg, S. Suthram, S. Bandyopadhyay, D. Rose, A. von Brunn, M. Uhlmann, C. Zeretzke, Y. A. Dong, H. Boulet, M. Koegl, S. M. Bailer, U. Koszinski, T. Ideker, P. Uetz, R. Zimmer and J. Haas. Evolutionarily conserved herpesviral protein interaction networks. *PLoS Pathog*, 5(9):e1000570, 2009. doi: 10.1371/journal.ppat.1000570.
- E. B. Frankel and A. Audhya. Escrt-dependent cargo sorting at multivesicular endosomes. *Semin Cell Dev Biol*, 74:4–10, 2018. doi: 10.1016/j.semcdb.2017.08.020.
- C. M. Freuling, T. F. Muller and T. C. Mettenleiter. Vaccines against pseudorabies virus (prv). *Vet Microbiol*, 206:3–9, 2017. doi: 10.1016/j.vetmic.2016.11.019.
- M. Fricker, M. Hollinshead, N. White and D. Vaux. Interphase nuclei of many mammalian cell types contain deep, dynamic, tubular membrane-bound invaginations of the nuclear envelope. *J Cell Biol*, 136(3):531–44, 1997. doi: 10.1083/jcb.136.3.531.

- W. Fuchs, B. G. Klupp, H. Granzow, N. Osterrieder and T. C. Mettenleiter. The interacting ul31 and ul34 gene products of pseudorabies virus are involved in egress from the host-cell nucleus and represent components of primary enveloped but not mature virions. *J Virol*, 76(1):364–78, 2002.
- W. Fuchs, B. G. Klupp, H. Granzow, T. Leege and T. C. Mettenleiter. Characterization of pseudorabies virus (prv) cleavage-encapsidation proteins and functional complementation of prv pul32 by the homologous protein of herpes simplex virus type 1. *J Virol*, 83(8):3930–43, 2009. doi: 10.1128/JVI.02636-08.
- C. Funk, M. Ott, V. Raschbichler, C. H. Nagel, A. Binz, B. Sodeik, R. Bauerfeind and S. M. Bailer. The herpes simplex virus protein pul31 escorts nucleocapsids to sites of nuclear egress, a process coordinated by its n-terminal domain. *PLoS Pathog*, 11(6): e1004957, 2015. doi: 10.1371/journal.ppat.1004957.
- K. Furukawa, N. Pante, U. Aebi and L. Gerace. Cloning of a cDNA for lamina-associated polypeptide 2 (lap2) and identification of regions that specify targeting to the nuclear envelope. *EMBO J*, 14(8):1626–36, 1995.
- J. E. Garneau, M. E. Dupuis, M. Villion, D. A. Romero, R. Barrangou, P. Boyaval, C. Fremaux, P. Horvath, A. H. Magadan and S. Moineau. The CRISPR/Cas bacterial immune system cleaves bacteriophage and plasmid DNA. *Nature*, 468(7320):67–71, 2010. doi: 10.1038/nature09523.
- A. T. Gatta and J. G. Carlton. The ESCRT-machinery: closing holes and expanding roles. *Curr Opin Cell Biol*, 59:121–132, 2019. doi: 10.1016/j.ceb.2019.04.005.
- N. K. Gill, C. Ly, P. H. Kim, C. A. Saunders, L. G. Fong, S. G. Young, G. W. G. Luxton and A. C. Rowat. Dyt1 dystonia patient-derived fibroblasts have increased deformability and susceptibility to damage by mechanical forces. *Front Cell Dev Biol*, 7(103):103, 2019. doi: 10.3389/fcell.2019.00103.
- S. E. Glynn, A. Martin, A. R. Nager, T. A. Baker and R. T. Sauer. Structures of asymmetric clpX hexamers reveal nucleotide-dependent motions in a AAA+ protein-unfolding machine. *Cell*, 139(4):744–56, 2009. doi: 10.1016/j.cell.2009.09.034.
- S. E. Glynn, A. R. Nager, T. A. Baker and R. T. Sauer. Dynamic and static components power unfolding in topologically closed rings of a AAA+ proteolytic machine. *Nat Struct Mol Biol*, 19(6):616–22, 2012. doi: 10.1038/nsmb.2288.
- E. Gob, J. Schmitt, R. Benavente and M. Alsheimer. Mammalian sperm head formation involves different polarization of two novel LINC complexes. *PLoS One*, 5(8):e12072, 2010. doi: 10.1371/journal.pone.0012072.
- R. Gonnella, A. Farina, R. Santarelli, S. Raffa, R. Feederle, R. Bei, M. Granato, A. Modesti, L. Frati, H. J. Delecluse, M. R. Torrisi, A. Angeloni and A. Faggioni. Characterization and intracellular localization of the Epstein-Barr virus protein BFLF2: interactions with

A Bibliography

- bfrf1 and with the nuclear lamina. *J Virol*, 79(6):3713–27, 2005. doi: 10.1128/JVI.79.6.3713-3727.2005.
- P. Gonzalez-Alegre. Advances in molecular and cell biology of dystonia: Focus on torsina. *Neurobiol Dis*, 127:233–241, 2019. doi: 10.1016/j.nbd.2019.03.007.
- R. E. Goodchild and W. T. Dauer. Mislocalization to the nuclear envelope: an effect of the dystonia-causing torsina mutation. *Proc Natl Acad Sci U S A*, 101(3):847–52, 2004. doi: 10.1073/pnas.0304375101.
- R. E. Goodchild and W. T. Dauer. The aaa+ protein torsina interacts with a conserved domain present in lap1 and a novel er protein. *J Cell Biol*, 168(6):855–62, 2005. doi: 10.1083/jcb.200411026.
- R. E. Goodchild, C. E. Kim and W. T. Dauer. Loss of the dystonia-associated protein torsina selectively disrupts the neuronal nuclear envelope. *Neuron*, 48(6):923–32, 2005. doi: 10.1016/j.neuron.2005.11.010.
- H. Granzow, F. Weiland, A. Jons, B. G. Klupp, A. Karger and T. C. Mettenleiter. Ultrastructural analysis of the replication cycle of pseudorabies virus in cell culture: a reassessment. *J Virol*, 71(3):2072–82, 1997.
- H. Granzow, B. G. Klupp and T. C. Mettenleiter. The pseudorabies virus us3 protein is a component of primary and of mature virions. *J Virol*, 78(3):1314–23, 2004. doi: 10.1128/jvi.78.3.1314-1323.2004.
- H. Granzow, B. G. Klupp and T. C. Mettenleiter. Entry of pseudorabies virus: an immunogold-labeling study. *J Virol*, 79(5):3200–5, 2005. doi: 10.1128/JVI.79.5.3200-3205.2005.
- B. Grinde. Herpesviruses: latency and reactivation - viral strategies and host response. *J Oral Microbiol*, 5, 2013. doi: 10.3402/jom.v5i0.22766.
- I. Grissa, G. Vergnaud and C. Pourcel. The crisprdb database and tools to display crisprs and to generate dictionaries of spacers and repeats. *BMC Bioinformatics*, 8:172, 2007. doi: 10.1186/1471-2105-8-172.
- M. Gu, D. LaJoie, O. S. Chen, A. von Appen, M. S. Ladinsky, M. J. Redd, L. Nikolova, P. J. Bjorkman, W. I. Sundquist, K. S. Ullman and A. Frost. Lem2 recruits chmp7 for escrt-mediated nuclear envelope closure in fission yeast and human cells. *Proc Natl Acad Sci U S A*, 114(11):E2166–E2175, 2017. doi: 10.1073/pnas.1613916114.
- Y. Guo, Q. Yue, J. Gao, Z. Wang, Y. R. Chen, G. W. Blissard, T. X. Liu and Z. Li. Roles of cellular nsf protein in entry and nuclear egress of budded virions of autographa californica multiple nucleopolyhedrovirus. *J Virol*, 91(20), 2017. doi: 10.1128/JVI.01111-17.

- S. Guttinger, E. Laurell and U. Kutay. Orchestrating nuclear envelope disassembly and reassembly during mitosis. *Nat Rev Mol Cell Biol*, 10(3):178–91, 2009. doi: 10.1038/nrm2641.
- C. Hagen, K. C. Dent, T. Zeev-Ben-Mordehai, M. Grange, J. B. Bosse, C. Whittle, B. G. Klupp, C. A. Siebert, D. Vasishtan, F. J. Bauerlein, J. Cheleski, S. Werner, P. Guttmann, S. Rehbein, K. Henzler, J. Demmerle, B. Adler, U. Koszinowski, L. Schermelleh, G. Schneider, L. W. Enquist, J. M. Plitzko, T. C. Mettenleiter and K. Grunewald. Structural basis of vesicle formation at the inner nuclear membrane. *Cell*, 163(7):1692–701, 2015. doi: 10.1016/j.cell.2015.11.029.
- J. Han, J. T. Perez, C. Chen, Y. Li, A. Benitez, M. Kandasamy, Y. Lee, J. Andrade, B. tenOever and B. Manicassamy. Genome-wide crispr/cas9 screen identifies host factors essential for influenza virus replication. *Cell Rep*, 23(2):596–607, 2018. doi: 10.1016/j.celrep.2018.03.045.
- P. I. Hanson and S. W. Whiteheart. Aaa+ proteins: have engine, will work. *Nat Rev Mol Cell Biol*, 6(7):519–29, 2005. doi: 10.1038/nrm1684.
- R. P. Hanson. The history of pseudorabies in the united states. *J Am Vet Med Assoc*, 124(925):259–61, 1954.
- F. Haque, D. J. Lloyd, D. T. Smallwood, C. L. Dent, C. M. Shanahan, A. M. Fry, R. C. Trembath and S. Shackleton. Sun1 interacts with nuclear lamin a and cytoplasmic nesprins to provide a physical connection between the nuclear lamina and the cytoskeleton. *Mol Cell Biol*, 26(10):3738–51, 2006. doi: 10.1128/MCB.26.10.3738-3751.2006.
- C. A. Harris, P. J. Andryuk, S. W. Cline, S. Mathew, J. J. Siekierka and G. Goldstein. Structure and mapping of the human thymopoietin (tmpo) gene and relationship of human tmpo beta to rat lamin-associated polypeptide 2. *Genomics*, 28(2):198–205, 1995. doi: 10.1006/geno.1995.1131.
- E. M. Hatch and M. W. Hetzer. Rnp export by nuclear envelope budding. *Cell*, 149(4):733–5, 2012. doi: 10.1016/j.cell.2012.04.018.
- E. M. Hatch and M. W. Hetzer. Nuclear envelope rupture is induced by actin-based nucleus confinement. *J Cell Biol*, 215(1):27–36, 2016. doi: 10.1083/jcb.201603053.
- A. C. Haugo, M. L. Szpara, L. Parsons, L. W. Enquist and R. J. Roller. Herpes simplex virus 1 pul34 plays a critical role in cell-to-cell spread of virus in addition to its role in virus replication. *J Virol*, 85(14):7203–15, 2011. doi: 10.1128/JVI.00262-11.
- E. E. Heldwein and C. Krummenacher. Entry of herpesviruses into mammalian cells. *Cell Mol Life Sci*, 65(11):1653–68, 2008. doi: 10.1007/s00018-008-7570-z.

A Bibliography

- T. Hellberg, L. Passvogel, K. S. Schulz, B. G. Klupp and T. C. Mettenleiter. Nuclear egress of herpesviruses: The prototypic vesicular nucleocytoplasmic transport. *Adv Virus Res*, 94:81–140, 2016. doi: 10.1016/bs.aivir.2015.10.002.
- J. D. Heming, J. F. Conway and F. L. Homa. Herpesvirus capsid assembly and dna packaging. *Adv Anat Embryol Cell Biol*, 223:119–142, 2017. doi: 10.1007/978-3-319-53168-7_6.
- M. J. Hendzel. The f-act's of nuclear actin. *Curr Opin Cell Biol*, 28:84–9, 2014. doi: 10.1016/j.ceb.2014.04.003.
- J. Hewett, C. Gonzalez-Agosti, D. Slater, P. Ziefer, S. Li, D. Bergeron, D. J. Jacoby, L. J. Ozelius, V. Ramesh and X. O. Breakefield. Mutant torsina, responsible for early-onset torsion dystonia, forms membrane inclusions in cultured neural cells. *Hum Mol Genet*, 9(9):1403–13, 2000. doi: 10.1093/hmg/9.9.1403.
- F. Hille, H. Richter, S. P. Wong, M. Bratovic, S. Ressel and E. Charpentier. The biology of crispr-cas: Backward and forward. *Cell*, 172(6):1239–1259, 2018. doi: 10.1016/j.cell.2017.11.032.
- Y. Hirohata, J. Aarii, Z. Liu, K. Shindo, M. Oyama, H. Kozuka-Hata, H. Sagara, A. Kato and Y. Kawaguchi. Herpes simplex virus 1 recruits cd98 heavy chain and beta1 integrin to the nuclear membrane for viral de-envelopment. *J Virol*, 89(15):7799–812, 2015. doi: 10.1128/JVI.00741-15.
- C. Y. Ho, D. E. Jaalouk, M. K. Vartiainen and J. Lammerding. Lamin a/c and emerin regulate mkl1-srf activity by modulating actin dynamics. *Nature*, 497(7450):507–11, 2013. doi: 10.1038/nature12105.
- H. Hofemeister and P. O'Hare. Nuclear pore composition and gating in herpes simplex virus-infected cells. *J Virol*, 82(17):8392–9, 2008. doi: 10.1128/JVI.00951-08.
- J. M. Holaska, A. K. Kowalski and K. L. Wilson. Emerin caps the pointed end of actin filaments: evidence for an actin cortical network at the nuclear inner membrane. *PLoS Biol*, 2(9):E231, 2004. doi: 10.1371/journal.pbio.0020231.
- L. Holmer and H. J. Worman. Inner nuclear membrane proteins: functions and targeting. *Cell Mol Life Sci*, 58(12-13):1741–7, 2001. doi: 10.1007/PL00000813.
- R. W. Honess and B. Roizman. Regulation of herpesvirus macromolecular synthesis. i. cascade regulation of the synthesis of three groups of viral proteins. *J Virol*, 14(1):8–19, 1974.
- R. W. Honess and B. Roizman. Regulation of herpesvirus macromolecular synthesis: sequential transition of polypeptide synthesis requires functional viral polypeptides. *Proc Natl Acad Sci U S A*, 72(4):1276–80, 1975. doi: 10.1073/pnas.72.4.1276.

- H. F. Horn, D. I. Kim, G. D. Wright, E. S. Wong, C. L. Stewart, B. Burke and K. J. Roux. A mammalian kash domain protein coupling meiotic chromosomes to the cytoskeleton. *J Cell Biol*, 202(7):1023–39, 2013. doi: 10.1083/jcb.201304004.
- P. D. Hsu, D. A. Scott, J. A. Weinstein, F. A. Ran, S. Konermann, V. Agarwala, Y. Li, E. J. Fine, X. Wu, O. Shalem, T. J. Cradick, L. A. Marraffini, G. Bao and F. Zhang. Dna targeting specificity of rna-guided cas9 nucleases. *Nat Biotechnol*, 31(9):827–32, 2013. doi: 10.1038/nbt.2647.
- F. Huguet, S. Flynn and P. Vagnarelli. The role of phosphatases in nuclear envelope disassembly and reassembly and their relevance to pathologies. *Cells*, 8(7):687, 2019. doi: 10.3390/cells8070687.
- J. H. Hurley. Escrts are everywhere. *EMBO J*, 34(19):2398–407, 2015. doi: 10.15252/embj.201592484.
- A. Hübner, B. Petersen, G. M. Keil, H. Niemann, T. C. Mettenleiter and W. Fuchs. Efficient inhibition of african swine fever virus replication by crispr/cas9 targeting of the viral p30 gene (cp204l). *Sci Rep*, 8(1):1449, 2018. doi: 10.1038/s41598-018-19626-1.
- L. M. Iyer, D. D. Leipe, E. V. Koonin and L. Aravind. Evolutionary history and higher order classification of aaa+ atpases. *J Struct Biol*, 146(1-2):11–31, 2004. doi: 10.1016/j.jsb.2003.10.010.
- Z. Jahed and M. R. Mofrad. The nucleus feels the force, lincd in or not! *Curr Opin Cell Biol*, 58:114–119, 2019. doi: 10.1016/j.ceb.2019.02.012.
- R. Jansen, J. D. Embden, W. Gastra and L. M. Schouls. Identification of genes that are associated with dna repeats in prokaryotes. *Mol Microbiol*, 43(6):1565–75, 2002. doi: 10.1046/j.1365-2958.2002.02839.x.
- M. Jinek, K. Chylinski, I. Fonfara, M. Hauer, J. A. Doudna and E. Charpentier. A programmable dual-rna-guided dna endonuclease in adaptive bacterial immunity. *Science*, 337(6096):816–21, 2012. doi: 10.1126/science.1225829.
- D. C. Johnson and J. D. Baines. Herpesviruses remodel host membranes for virus egress. *Nat Rev Microbiol*, 9(5):382–94, 2011. doi: 10.1038/nrmicro2559.
- D. C. Johnson and M. T. Huber. Directed egress of animal viruses promotes cell-to-cell spread. *J Virol*, 76(1):1–8, 2002. doi: 10.1128/jvi.76.1.1-8.2002.
- N. Johnson, M. Krebs, R. Boudreau, G. Giorgi, M. LeGros and C. Larabell. Actin-filled nuclear invaginations indicate degree of cell de-differentiation. *Differentiation*, 71(7):414–24, 2003. doi: 10.1046/j.1432-0436.2003.7107003.x.
- V. Jokhi, J. Ashley, J. Nunnari, A. Noma, N. Ito, N. Wakabayashi-Ito, M. J. Moore and V. Budnik. Torsin mediates primary envelopment of large ribonucleoprotein granules at the nuclear envelope. *Cell Rep*, 3(4):988–95, 2013. doi: 10.1016/j.celrep.2013.03.015.

A Bibliography

- M. Jungwirth, M. L. Dear, P. Brown, K. Holbrook and R. Goodchild. Relative tissue expression of homologous torsinb correlates with the neuronal specific importance of dyt1 dystonia-associated torsina. *Hum Mol Genet*, 19(5):888–900, 2010. doi: 10.1093/hmg/ddp557.
- M. T. Jungwirth, D. Kumar, D. Y. Jeong and R. E. Goodchild. The nuclear envelope localization of dyt1 dystonia torsina-deltae requires the sun1 linc complex component. *BMC Cell Biol*, 12:24, 2011. doi: 10.1186/1471-2121-12-24.
- D. Kalderon, B. L. Roberts, W. D. Richardson and A. E. Smith. A short amino acid sequence able to specify nuclear location. *Cell*, 39(3 Pt 2):499–509, 1984. doi: 10.1016/0092-8674(84)90457-4.
- U. Karakus, T. Thamamongood, K. Ciminski, W. Ran, S. C. Gunther, M. O. Pohl, D. Eletto, C. Jeney, D. Hoffmann, S. Reiche, J. Schinkothe, R. Ulrich, J. Wiener, M. G. B. Hayes, M. W. Chang, A. Hunziker, E. Yanguez, T. Aydililo, F. Krammer, J. Oderbolz, M. Meier, A. Oxenius, A. Halenius, G. Zimmer, C. Benner, B. G. Hale, A. Garcia-Sastre, M. Beer, M. Schwemmle and S. Stertz. Mhc class ii proteins mediate cross-species entry of bat influenza viruses. *Nature*, 567(7746):109–112, 2019. doi: 10.1038/s41586-019-0955-3.
- A. Kato, Z. Liu, A. Minowa, T. Imai, M. Tanaka, K. Sugimoto, Y. Nishiyama, J. Arii and Y. Kawaguchi. Herpes simplex virus 1 protein kinase us3 and major tegument protein ul47 reciprocally regulate their subcellular localization in infected cells. *J Virol*, 85(18): 9599–613, 2011. doi: 10.1128/JVI.00845-11.
- S. S. Katta, C. J. Smoyer and S. L. Jaspersen. Destination: inner nuclear membrane. *Trends Cell Biol*, 24(4):221–9, 2014. doi: 10.1016/j.tcb.2013.10.006.
- H. Kharkwal, C. G. Smith and D. W. Wilson. Blocking escrt-mediated envelopment inhibits microtubule-dependent trafficking of alphaherpesviruses in vitro. *J Virol*, 88(24):14467–78, 2014. doi: 10.1128/JVI.02777-14.
- M. Kielian. Mechanisms of virus membrane fusion proteins. *Annu Rev Virol*, 1(1):171–89, 2014. doi: 10.1146/annurev-virology-031413-085521.
- C. E. Kim, A. Perez, G. Perkins, M. H. Ellisman and W. T. Dauer. A molecular mechanism underlying the neural-specific defect in torsina mutant mice. *Proc Natl Acad Sci U S A*, 107(21):9861–6, 2010. doi: 10.1073/pnas.0912877107.
- D. I. Kim, K. C. Birendra and K. J. Roux. Making the linc: Sun and kash protein interactions. *Biol Chem*, 396(4):295–310, 2015. doi: 10.1515/hsz-2014-0267.
- Y. H. Kim, M. E. Han and S. O. Oh. The molecular mechanism for nuclear transport and its application. *Anat Cell Biol*, 50(2):77–85, 2017. doi: 10.5115/acb.2017.50.2.77.

- B. Klupp, J. Altenschmidt, H. Granzow, W. Fuchs and T. C. Mettenleiter. Glycoproteins required for entry are not necessary for egress of pseudorabies virus. *J Virol*, 82(13): 6299–309, 2008. doi: 10.1128/JVI.00386-08.
- B. G. Klupp, H. Granzow and T. C. Mettenleiter. Effect of the pseudorabies virus us3 protein on nuclear membrane localization of the ul34 protein and virus egress from the nucleus. *J Gen Virol*, 82(Pt 10):2363–2371, 2001. doi: 10.1099/0022-1317-82-10-2363.
- B. G. Klupp, C. J. Hengartner, T. C. Mettenleiter and L. W. Enquist. Complete, annotated sequence of the pseudorabies virus genome. *J Virol*, 78(1):424–40, 2004. doi: 10.1128/jvi.78.1.424-440.2004.
- B. G. Klupp, H. Granzow, G. M. Keil and T. C. Mettenleiter. The capsid-associated ul25 protein of the alphaherpesvirus pseudorabies virus is nonessential for cleavage and encapsidation of genomic dna but is required for nuclear egress of capsids. *J Virol*, 80(13):6235–46, 2006. doi: 10.1128/JVI.02662-05.
- B. G. Klupp, H. Granzow, W. Fuchs, G. M. Keil, S. Finke and T. C. Mettenleiter. Vesicle formation from the nuclear membrane is induced by coexpression of two conserved herpesvirus proteins. *Proc Natl Acad Sci U S A*, 104(17):7241–6, 2007. doi: 10.1073/pnas.0701757104.
- B. G. Klupp, H. Granzow and T. C. Mettenleiter. Nuclear envelope breakdown can substitute for primary envelopment-mediated nuclear egress of herpesviruses. *J Virol*, 85(16):8285–92, 2011. doi: 10.1128/JVI.00741-11.
- B. G. Klupp, T. Hellberg, H. Granzow, K. Franzke, B. Dominguez Gonzalez, R. E. Goodchild and T. C. Mettenleiter. Integrity of the linker of nucleoskeleton and cytoskeleton is required for efficient herpesvirus nuclear egress. *J Virol*, 91(19), 2017. doi: 10.1128/JVI.00330-17.
- A. Kohler and E. Hurt. Exporting rna from the nucleus to the cytoplasm. *Nat Rev Mol Cell Biol*, 8(10):761–73, 2007. doi: 10.1038/nrm2255.
- E. Kokai, H. Beck, J. Weissbach, F. Arnold, D. Sinske, U. Sebert, G. Gaiselmann, V. Schmidt, P. Walther, J. Munch, G. Posern and B. Knoll. Analysis of nuclear actin by overexpression of wild-type and actin mutant proteins. *Histochem Cell Biol*, 141(2): 123–35, 2014. doi: 10.1007/s00418-013-1151-4.
- K. Kustedjo, M. H. Bracey and B. F. Cravatt. Torsin a and its torsion dystonia-associated mutant forms are luminal glycoproteins that exhibit distinct subcellular localizations. *J Biol Chem*, 275(36):27933–9, 2000. doi: 10.1074/jbc.M910025199.
- A. D. Kwong and N. Frenkel. The herpes simplex virus virion host shutoff function. *J Virol*, 63(11):4834–9, 1989.

A Bibliography

- E. Laudermitch, P. L. Tsai, M. Graham, E. Turner, C. Zhao and C. Schlieker. Dissecting torsin/cofactor function at the nuclear envelope: a genetic study. *Mol Biol Cell*, 27(25): 3964–3971, 2016. doi: 10.1091/mbc.E16-07-0511.
- N. Leach, S. L. Bjerke, D. K. Christensen, J. M. Bouchard, F. Mou, R. Park, J. Baines, T. Haraguchi and R. J. Roller. Emerin is hyperphosphorylated and redistributed in herpes simplex virus type 1-infected cells in a manner dependent on both ul34 and us3. *J Virol*, 81(19):10792–803, 2007. doi: 10.1128/JVI.00196-07.
- N. R. Leach and R. J. Roller. Significance of host cell kinases in herpes simplex virus type 1 egress and lamin-associated protein disassembly from the nuclear lamina. *Virology*, 406(1):127–37, 2010. doi: 10.1016/j.virol.2010.07.002.
- M. Leelawong, D. Guo and G. A. Smith. A physical link between the pseudorabies virus capsid and the nuclear egress complex. *J Virol*, 85(22):11675–84, 2011. doi: 10.1128/JVI.05614-11.
- M. R. Lieber. The mechanism of human nonhomologous dna end joining. *J Biol Chem*, 283(1):1–5, 2008. doi: 10.1074/jbc.R700039200.
- F. Lin, D. L. Blake, I. Callebaut, I. S. Skerjanc, L. Holmer, M. W. McBurney, M. Paulin-Levasseur and H. J. Worman. Man1, an inner nuclear membrane protein that shares the lem domain with lamina-associated polypeptide 2 and emerin. *J Biol Chem*, 275(7):4840–7, 2000. doi: 10.1074/jbc.275.7.4840.
- R. E. Lindeman and F. Pelegri. Localized products of futile cycle/lrmp promote centrosome-nucleus attachment in the zebrafish zygote. *Curr Biol*, 22(10):843–51, 2012. doi: 10.1016/j.cub.2012.03.058.
- Z. Liu, A. Kato, M. Oyama, H. Kozuka-Hata, J. Arii and Y. Kawaguchi. Role of host cell p32 in herpes simplex virus 1 de-envelopment during viral nuclear egress. *J Virol*, 89(17):8982–98, 2015. doi: 10.1128/JVI.01220-15.
- M. Lorenz, B. Vollmer, J. D. Unsay, B. G. Klupp, A. J. Garcia-Saez, T. C. Mettenleiter and W. Antonin. A single herpesvirus protein can mediate vesicle formation in the nuclear envelope. *J Biol Chem*, 290(11):6962–74, 2015. doi: 10.1074/jbc.M114.627521.
- K. Lui and Y. Huang. Rangtpase: A key regulator of nucleocytoplasmic trafficking. *Mol Cell Pharmacol*, 1(3):148–156, 2009. doi: 10.4255/mcpharmacol.09.19.
- G. W. Luxton and D. A. Starr. Kashing up with the nucleus: novel functional roles of kash proteins at the cytoplasmic surface of the nucleus. *Curr Opin Cell Biol*, 28:69–75, 2014. doi: 10.1016/j.ceb.2014.03.002.
- G. W. Luxton, J. I. Lee, S. Haverlock-Moyns, J. M. Schober and G. A. Smith. The pseudorabies virus vp1/2 tegument protein is required for intracellular capsid transport. *J Virol*, 80(1):201–9, 2006. doi: 10.1128/JVI.80.1.201-209.2006.

- G. W. Luxton, E. R. Gomes, E. S. Folker, E. Vintinner and G. G. Gundersen. Linear arrays of nuclear envelope proteins harness retrograde actin flow for nuclear movement. *Science*, 329(5994):956–9, 2010. doi: 10.1126/science.1189072.
- G. W. Luxton, E. R. Gomes, E. S. Folker, H. J. Worman and G. G. Gundersen. Tan lines: a novel nuclear envelope structure involved in nuclear positioning. *Nucleus*, 2(3):173–81, 2011. doi: 10.1073/pnas.100082410810.4161/nucl.2.3.16243.
- M. F. Lye, M. Sharma, K. El Omari, D. J. Filman, J. P. Schuermann, J. M. Hogle and D. M. Coen. Unexpected features and mechanism of heterodimer formation of a herpesvirus nuclear egress complex. *EMBO J*, 34(23):2937–52, 2015. doi: 10.15252/embj.201592651.
- M. T. Mackmull, B. Klaus, I. Heinze, M. Chokkalingam, A. Beyer, R. B. Russell, A. Ori and M. Beck. Landscape of nuclear transport receptor cargo specificity. *Mol Syst Biol*, 13(12):962, 2017. doi: 10.15252/msb.20177608.
- C. Maison, A. Pырpasopoulou, P. A. Theodoropoulos and S. D. Georgatos. The inner nuclear membrane protein lap1 forms a native complex with b-type lamins and partitions with spindle-associated mitotic vesicles. *EMBO J*, 16(16):4839–50, 1997. doi: 10.1093/emboj/16.16.4839.
- K. S. Makarova, D. H. Haft, R. Barrangou, S. J. Brouns, E. Charpentier, P. Horvath, S. Moineau, F. J. Mojica, Y. I. Wolf, A. F. Yakunin, J. van der Oost and E. V. Koonin. Evolution and classification of the crispr-cas systems. *Nat Rev Microbiol*, 9(6):467–77, 2011. doi: 10.1038/nrmicro2577.
- A. Malhas, C. Goulbourne and D. J. Vaux. The nucleoplasmic reticulum: form and function. *Trends Cell Biol*, 21(6):362–73, 2011. doi: 10.1016/j.tcb.2011.03.008.
- A. N. Malhas and D. J. Vaux. *Nuclear Envelope Invaginations and Cancer*, pages 523–535. Springer New York, New York, NY, 2014. ISBN 978-1-4899-8032-8. doi: 10.1007/978-1-4899-8032-8_24.
- P. Mali, J. Aach, P. B. Stranges, K. M. Esvelt, M. Moosburner, S. Kosuri, L. Yang and G. M. Church. Cas9 transcriptional activators for target specificity screening and paired nickases for cooperative genome engineering. *Nat Biotechnol*, 31(9):833–8, 2013. doi: 10.1038/nbt.2675.
- M. Mansharamani and K. L. Wilson. Direct binding of nuclear membrane protein man1 to emerin in vitro and two modes of binding to barrier-to-autointegration factor. *J Biol Chem*, 280(14):13863–70, 2005. doi: 10.1074/jbc.M413020200.
- A. Margalit, A. Brachner, J. Gotzmann, R. Foisner and Y. Gruenbaum. Barrier-to-autointegration factor—a baffling little protein. *Trends Cell Biol*, 17(4):202–8, 2007. doi: 10.1016/j.tcb.2007.02.004.

A Bibliography

- M. Maric, J. Shao, R. J. Ryan, C. S. Wong, P. Gonzalez-Alegre and R. J. Roller. A functional role for torsina in herpes simplex virus 1 nuclear egress. *J Virol*, 85(19):9667–79, 2011. doi: 10.1128/JVI.05314-11.
- A. Martin, T. A. Baker and R. T. Sauer. Pore loops of the aaa+ clpx machine grip substrates to drive translocation and unfolding. *Nat Struct Mol Biol*, 15(11):1147–51, 2008. doi: 10.1038/nsmb.1503.
- L. Martin, C. Crimauddo and L. Gerace. cDNA cloning and characterization of lamina-associated polypeptide 1c (lap1c), an integral protein of the inner nuclear membrane. *J Biol Chem*, 270(15):8822–8, 1995. doi: 10.1074/jbc.270.15.8822.
- J. McCullough, A. Frost and W. I. Sundquist. Structures, functions, and dynamics of esct-iii/vps4 membrane remodeling and fission complexes. *Annu Rev Cell Dev Biol*, 34(1):85–109, 2018. doi: 10.1146/annurev-cellbio-100616-060600.
- D. J. McGeoch, F. J. Rixon and A. J. Davison. Topics in herpesvirus genomics and evolution. *Virus Res*, 117(1):90–104, 2006. doi: 10.1016/j.virusres.2006.01.002.
- P. Meinke and E. C. Schirmer. Linc'ing form and function at the nuclear envelope. *FEBS Lett*, 589(19 Pt A):2514–21, 2015. doi: 10.1016/j.febslet.2015.06.011.
- T. C. Mettenleiter. Aujeszky's disease (pseudorabies) virus: the virus and molecular pathogenesis—state of the art, june 1999. *Vet Res*, 31(1):99–115, 2000. doi: 10.1051/vetres:2000110.
- T. C. Mettenleiter. Brief overview on cellular virus receptors. *Virus Research*, 82(1-2):3–8, 2001. doi: 10.1016/s0168-1702(01)00380-x.
- T. C. Mettenleiter. Herpesvirus assembly and egress. *J Virol*, 76(4):1537–47, 2002. doi: 10.1128/jvi.76.4.1537-1547.2002.
- T. C. Mettenleiter. Intriguing interplay between viral proteins during herpesvirus assembly or: the herpesvirus assembly puzzle. *Vet Microbiol*, 113(3-4):163–9, 2006. doi: 10.1016/j.vetmic.2005.11.040.
- T. C. Mettenleiter. *Pseudorabies Virus.*, volume 3rd, pages 341–351. Oxford: Academic Press., 2008.
- T. C. Mettenleiter, A. Saalmuller and F. Weiland. Pseudorabies virus protein homologous to herpes simplex virus type 1 icp18.5 is necessary for capsid maturation. *J Virol*, 67(3):1236–45, 1993.
- T. C. Mettenleiter, B. G. Klupp and H. Granzow. Herpesvirus assembly: an update. *Virus Res*, 143(2):222–34, 2009. doi: 10.1016/j.virusres.2009.03.018.

- T. C. Mettenleiter, F. Muller, H. Granzow and B. G. Klupp. The way out: what we know and do not know about herpesvirus nuclear egress. *Cell Microbiol*, 15(2):170–8, 2013. doi: 10.1111/cmi.12044.
- G. A. Meyer and K. D. Radsak. Identification of a novel signal sequence that targets transmembrane proteins to the nuclear envelope inner membrane. *J Biol Chem*, 275(6): 3857–66, 2000. doi: 10.1074/jbc.275.6.3857.
- J. Milbradt, S. Auerochs and M. Marschall. Cytomegaloviral proteins pul50 and pul53 are associated with the nuclear lamina and interact with cellular protein kinase c. *J Gen Virol*, 88(Pt 10):2642–50, 2007. doi: 10.1099/vir.0.82924-0.
- L. A. Miles, R. J. Garippa and J. T. Poirier. Design, execution, and analysis of pooled in vitro crispr/cas9 screens. *FEBS J*, 283(17):3170–80, 2016. doi: 10.1111/febs.13770.
- A. A. Mironov and G. V. Beznoussenko. Models of intracellular transport: Pros and cons. *Front Cell Dev Biol*, 7:146, 2019. doi: 10.3389/fcell.2019.00146.
- R. D. Moir, M. Yoon, S. Khuon and R. D. Goldman. Nuclear lamins a and b1: different pathways of assembly during nuclear envelope formation in living cells. *J Cell Biol*, 151(6):1155–68, 2000. doi: 10.1083/jcb.151.6.1155.
- K. L. Mossman, R. Sherburne, C. Lavery, J. Duncan and J. R. Smiley. Evidence that herpes simplex virus vp16 is required for viral egress downstream of the initial envelopment event. *J Virol*, 74(14):6287–99, 2000. doi: 10.1128/jvi.74.14.6287-6299.2000.
- F. Mou, T. Forest and J. D. Baines. Us3 of herpes simplex virus type 1 encodes a promiscuous protein kinase that phosphorylates and alters localization of lamin a/c in infected cells. *J Virol*, 81(12):6459–70, 2007. doi: 10.1128/JVI.00380-07.
- F. Mou, E. G. Wills, R. Park and J. D. Baines. Effects of lamin a/c, lamin b1, and viral us3 kinase activity on viral infectivity, virion egress, and the targeting of herpes simplex virus u(l)34-encoded protein to the inner nuclear membrane. *J Virol*, 82(16):8094–104, 2008. doi: 10.1128/JVI.00874-08.
- F. Mou, E. Wills and J. D. Baines. Phosphorylation of the u(l)31 protein of herpes simplex virus 1 by the u(s)3-encoded kinase regulates localization of the nuclear envelopment complex and egress of nucleocapsids. *J Virol*, 83(10):5181–91, 2009. doi: 10.1128/JVI.00090-09.
- M. Myllys, V. Ruokolainen, V. Aho, E. A. Smith, S. Hakanen, P. Peri, A. Salvetti, J. Timonen, V. Hukkanen, C. A. Larabell and M. Vihinen-Ranta. Herpes simplex virus 1 induces egress channels through marginalized host chromatin. *Sci Rep*, 6:28844, 2016. doi: 10.1038/srep28844.

A Bibliography

- C. H. Nagel, K. Dohner, M. Fathollahy, T. Strive, E. M. Borst, M. Messerle and B. Sodeik. Nuclear egress and envelopment of herpes simplex virus capsids analyzed with dual-color fluorescence hsv1(17+). *J Virol*, 82(6):3109–24, 2008. doi: 10.1128/JVI.02124-07.
- M. Nagy, H. C. Wu, Z. Liu, S. Kedzierska-Mieszkowska and M. Zolkiewski. Walker-a threonine couples nucleotide occupancy with the chaperone activity of the aaa+ atpase clpb. *Protein Sci*, 18(2):287–93, 2009. doi: 10.1002/pro.36.
- T. V. Naismith, J. E. Heuser, X. O. Breakefield and P. I. Hanson. Torsina in the nuclear envelope. *Proc Natl Acad Sci U S A*, 101(20):7612–7, 2004. doi: 10.1073/pnas.0308760101.
- F. C. Nery, J. Zeng, B. P. Niland, J. Hewett, J. Farley, D. Irimia, Y. Li, G. Wiche, A. Sonnenberg and X. O. Breakefield. Torsina binds the kash domain of nesprins and participates in linkage between nuclear envelope and cytoskeleton. *J Cell Sci*, 121(Pt 20):3476–86, 2008. doi: 10.1242/jcs.029454.
- W. W. Newcomb, R. M. Juhas, D. R. Thomsen, F. L. Homa, A. D. Burch, S. K. Weller and J. C. Brown. The ul6 gene product forms the portal for entry of dna into the herpes simplex virus capsid. *J Virol*, 75(22):10923–32, 2001. doi: 10.1128/JVI.75.22.10923-10932.2001.
- W. W. Newcomb, J. Fontana, D. C. Winkler, N. Cheng, J. B. Heymann and A. C. Steven. The primary enveloped virion of herpes simplex virus 1: Its role in nuclear egress. *mBio*, 8(3):e00825–17, 2017. doi: 10.1128/mBio.00825-17.
- N. Nozawa, Y. Kawaguchi, M. Tanaka, A. Kato, A. Kato, H. Kimura and Y. Nishiyama. Herpes simplex virus type 1 ul51 protein is involved in maturation and egress of virus particles. *J Virol*, 79(11):6947–56, 2005. doi: 10.1128/JVI.79.11.6947-6956.2005.
- A. L. Olins, G. Rhodes, D. B. Welch, M. Zwerger and D. E. Olins. Lamin b receptor: multi-tasking at the nuclear envelope. *Nucleus*, 1(1):53–70, 2010. doi: 10.4161/nucl.1.1.10515.
- Y. Olmos and J. G. Carlton. The escrt machinery: new roles at new holes. *Curr Opin Cell Biol*, 38:1–11, 2016. doi: 10.1016/j.ceb.2015.12.001.
- Y. Olmos, L. Hodgson, J. Mantell, P. Verkade and J. G. Carlton. Escrt-iii controls nuclear envelope reformation. *Nature*, 522(7555):236–9, 2015. doi: 10.1038/nature14503.
- R. C. Orchard, C. B. Wilen, J. G. Doench, M. T. Baldrige, B. T. McCune, Y. C. Lee, S. Lee, S. M. Pruett-Miller, C. A. Nelson, D. H. Fremont and H. W. Virgin. Discovery of a proteinaceous cellular receptor for a norovirus. *Science*, 353(6302):933–6, 2016. doi: 10.1126/science.aaf1220.
- S. Otsuka and J. Ellenberg. Mechanisms of nuclear pore complex assembly - two different ways of building one molecular machine. *FEBS Lett*, 592(4):475–488, 2018. doi: 10.1002/1873-3468.12905.

- M. Ott, G. Tascher, S. Hassdenteufel, R. Zimmermann, J. Haas and S. M. Bailer. Functional characterization of the essential tail anchor of the herpes simplex virus type 1 nuclear egress protein pul34. *J Gen Virol*, 92(Pt 12):2734–2745, 2011. doi: 10.1099/vir.0.032730-0.
- L. J. Ozelius, J. W. Hewett, C. E. Page, S. B. Bressman, P. L. Kramer, C. Shalish, D. de Leon, M. F. Brin, D. Raymond, D. P. Corey, S. Fahn, N. J. Risch, A. J. Buckler, J. F. Gusella and X. O. Breakefield. The early-onset torsion dystonia gene (*dyt1*) encodes an atp-binding protein. *Nat Genet*, 17(1):40–8, 1997. doi: 10.1038/ng0997-40.
- D. Panda and S. Cherry. Cell-based genomic screening: elucidating virus-host interactions. *Curr Opin Virol*, 2(6):784–92, 2012. doi: 10.1016/j.coviro.2012.10.007.
- N. Pante and M. Kann. Nuclear pore complex is able to transport macromolecules with diameters of about 39 nm. *Mol Biol Cell*, 13(2):425–34, 2002. doi: 10.1091/mbc.01-06-0308.
- R. Park and J. D. Baines. Herpes simplex virus type 1 infection induces activation and recruitment of protein kinase c to the nuclear membrane and increased phosphorylation of lamin b. *J Virol*, 80(1):494–504, 2006. doi: 10.1128/JVI.80.1.494-504.2006.
- L. Passvogel, P. Trube, F. Schuster, B. G. Klupp and T. C. Mettenleiter. Mapping of sequences in pseudorabies virus pul34 that are required for formation and function of the nuclear egress complex. *J Virol*, 87(8):4475–85, 2013. doi: 10.1128/JVI.00021-13.
- L. Passvogel, B. G. Klupp, H. Granzow, W. Fuchs and T. C. Mettenleiter. Functional characterization of nuclear trafficking signals in pseudorabies virus pul31. *J Virol*, 89(4):2002–12, 2015. doi: 10.1128/JVI.03143-14.
- P. E. Pellet and B. Roizman. *Herpesviridae*, volume 6th, pages 1802–1822. Lippincott Williams & Wilkins, Philadelphia, 2013.
- M. Pensaert and J. Kluge. Pseudorabies virus (ajeszky's disease). *Virus infections of porcines*, 2:39–65, 1989.
- A. Pickar-Oliver and C. A. Gersbach. The next generation of crispr-cas technologies and applications. *Nat Rev Mol Cell Biol*, 20(8):490–507, 2019. doi: 10.1038/s41580-019-0131-5.
- L. E. Pomeranz, A. E. Reynolds and C. J. Hengartner. Molecular biology of pseudorabies virus: impact on neurovirology and veterinary medicine. *Microbiol Mol Biol Rev*, 69(3): 462–500, 2005. doi: 10.1128/MMBR.69.3.462-500.2005.
- G. Prelich. Gene overexpression: uses, mechanisms, and interpretation. *Genetics*, 190(3): 841–54, 2012. doi: 10.1534/genetics.111.136911.

A Bibliography

- M. Prokocimer, M. Davidovich, M. Nissim-Rafinia, N. Wiesel-Motiuk, D. Z. Bar, R. Barkan, E. Meshorer and Y. Gruenbaum. Nuclear lamins: key regulators of nuclear structure and activities. *J Cell Mol Med*, 13(6):1059–85, 2009. doi: 10.1111/j.1582-4934.2008.00676.x.
- F. C. Purves, R. M. Longnecker, D. P. Leader and B. Roizman. Herpes simplex virus 1 protein kinase is encoded by open reading frame us3 which is not essential for virus growth in cell culture. *Journal of Virology*, 61(9):2896, 1987.
- F. C. Purves, D. Spector and B. Roizman. The herpes simplex virus 1 protein kinase encoded by the us3 gene mediates posttranslational modification of the phosphoprotein encoded by the ul34 gene. *J Virol*, 65(11):5757–64, 1991.
- F. C. Purves, D. Spector and B. Roizman. Ul34, the target of the herpes simplex virus u(s)3 protein kinase, is a membrane protein which in its unphosphorylated state associates with novel phosphoproteins. *J Virol*, 66(7):4295–303, 1992.
- M. Raab, M. Gentili, H. de Belly, H. R. Thiam, P. Vargas, A. J. Jimenez, F. Lautenschlaeger, R. Voituriez, A. M. Lennon-Dumenil, N. Manel and M. Piel. Escrt iii repairs nuclear envelope ruptures during cell migration to limit dna damage and cell death. *Science*, 352(6283):359–62, 2016. doi: 10.1126/science.aad7611.
- D. Rajgor and C. M. Shanahan. Nesprins: from the nuclear envelope and beyond. *Expert Rev Mol Med*, 15:e5, 2013. doi: 10.1017/erm.2013.6.
- A. J. Rampello, S. M. Prophet and C. Schlieker. The role of torsin aaa+ proteins in preserving nuclear envelope integrity and safeguarding against disease. *Biomolecules*, 10(3), 2020. doi: 10.3390/biom10030468.
- D. Rath, L. Amlinger, A. Rath and M. Lundgren. The crispr-cas immune system: biology, mechanisms and applications. *Biochimie*, 117:119–28, 2015. doi: 10.1016/j.biochi.2015.03.025.
- D. Razafsky and D. Hodzic. Bringing kash under the sun: the many faces of nucleocytoplasmic connections. *J Cell Biol*, 186(4):461–72, 2009. doi: 10.1083/jcb.200906068.
- S. Reber, J. Mechttersheimer, S. Nasif, J. A. Benitez, M. Colombo, M. Domanski, D. Jutzi, E. Hedlund and M. D. Ruepp. Crispr-trap: a clean approach for the generation of gene knockouts and gene replacements in human cells. *Mol Biol Cell*, 29(2):75–83, 2018. doi: 10.1091/mbc.E17-05-0288.
- A. E. Reynolds, B. J. Ryckman, J. D. Baines, Y. Zhou, L. Liang and R. J. Roller. U(l)31 and u(l)34 proteins of herpes simplex virus type 1 form a complex that accumulates at the nuclear rim and is required for envelopment of nucleocapsids. *J Virol*, 75(18):8803–17, 2001. doi: 10.1128/jvi.75.18.8803-8817.2001.

- A. E. Reynolds, E. G. Wills, R. J. Roller, B. J. Ryckman and J. D. Baines. Ultrastructural localization of the herpes simplex virus type 1 ul31, ul34, and us3 proteins suggests specific roles in primary envelopment and egress of nucleocapsids. *J Virol*, 76(17): 8939–52, 2002. doi: 10.1128/jvi.76.17.8939-8952.2002.
- A. E. Reynolds, L. Liang and J. D. Baines. Conformational changes in the nuclear lamina induced by herpes simplex virus type 1 require genes u(1)31 and u(1)34. *J Virol*, 78(11): 5564–75, 2004. doi: 10.1128/JVI.78.11.5564-5575.2004.
- R. J. Roller, Y. Zhou, R. Schnetzer, J. Ferguson and D. DeSalvo. Herpes simplex virus type 1 u(1)34 gene product is required for viral envelopment. *J Virol*, 74(1):117–29, 2000. doi: 10.1128/jvi.74.1.117-129.2000.
- R. J. Roller, A. C. Haugo, K. Yang and J. D. Baines. The herpes simplex virus 1 ul51 gene product has cell type-specific functions in cell-to-cell spread. *J Virol*, 88(8):4058–68, 2014. doi: 10.1128/JVI.03707-13.
- A. Rose and C. Schlieker. Alternative nuclear transport for cellular protein quality control. *Trends Cell Biol*, 22(10):509–14, 2012. doi: 10.1016/j.tcb.2012.07.003.
- A. E. Rose, C. Zhao, E. M. Turner, A. M. Steyer and C. Schlieker. Arresting a torsin atpase reshapes the endoplasmic reticulum. *J Biol Chem*, 289(1):552–64, 2014. doi: 10.1074/jbc.M113.515791.
- A. E. Rose, R. S. Brown and C. Schlieker. Torsins: not your typical aaa+ atpases. *Crit Rev Biochem Mol Biol*, 50(6):532–49, 2015. doi: 10.3109/10409238.2015.1091804.
- A. Rothballer and U. Kutay. The diverse functional links of the nuclear envelope to the cytoskeleton and chromatin. *Chromosoma*, 122(5):415–29, 2013. doi: 10.1007/s00412-013-0417-x.
- A. Rothballer, T. U. Schwartz and U. Kutay. Lincing complex functions at the nuclear envelope: what the molecular architecture of the linc complex can reveal about its function. *Nucleus*, 4(1):29–36, 2013. doi: 10.4161/nucl.23387.
- M. P. Rout and J. D. Aitchison. The nuclear pore complex as a transport machine. *J Biol Chem*, 276(20):16593–6, 2001. doi: 10.1074/jbc.R100015200.
- B. J. Ryckman and R. J. Roller. Herpes simplex virus type 1 primary envelopment: Ul34 protein modification and the us3-ul34 catalytic relationship. *J Virol*, 78(1):399–412, 2004. doi: 10.1128/jvi.78.1.399-412.2004.
- S. Rönfeldt, B. G. Klupp, K. Franzke and T. C. Mettenleiter. Lysine 242 within helix 10 of the pseudorabies virus nuclear egress complex pul31 component is critical for primary envelopment of nucleocapsids. *J Virol*, 91(22):e01182–17, 2017. doi: 10.1128/JVI.01182-17.

A Bibliography

- N. Saiz-Ros, R. Czapiewski, I. Epifano, A. Stevenson, S. K. Swanson, C. R. Dixon, D. B. Zamora, M. McElwee, S. Vijayakrishnan, C. A. Richardson, L. Dong, D. A. Kelly, L. Pytowski, M. W. Goldberg, L. Florens, S. V. Graham and E. C. Schirmer. Host vesicle fusion protein vapb contributes to the nuclear egress stage of herpes simplex virus type-1 (hsv-1) replication. *Cells*, 8(2), 2019. doi: 10.3390/cells8020120.
- R. Santarelli, A. Farina, M. Granato, R. Gonnella, S. Raffa, L. Leone, R. Bei, A. Modesti, L. Frati, M. R. Torrisi and A. Faggioni. Identification and characterization of the product encoded by orf69 of kaposi's sarcoma-associated herpesvirus. *J Virol*, 82(9): 4562–72, 2008. doi: 10.1128/JVI.02400-07.
- M. Saraste, P. R. Sibbald and A. Wittinghofer. The p-loop—a common motif in atp- and gtp-binding proteins. *Trends Biochem Sci*, 15(11):430–4, 1990. doi: 10.1016/0968-0004(90)90281-f.
- C. A. Saunders. Regulation of directional cell migration from within the nuclear envelope. *Dissertation*, Faculty of University of Minnesota, 2017.
- C. A. Saunders and G. W. Luxton. Lincing defective nuclear-cytoskeletal coupling and dyt1 dystonia. *Cell Mol Bioeng*, 9(2):207–216, 2016. doi: 10.1007/s12195-016-0432-0.
- C. A. Saunders, N. J. Harris, P. T. Willey, B. M. Woolums, Y. Wang, A. J. McQuown, A. Schoenhofen, H. J. Worman, W. T. Dauer, G. G. Gundersen and G. W. Luxton. Torsina controls tan line assembly and the retrograde flow of dorsal perinuclear actin cables during rearward nuclear movement. *J Cell Biol*, 216(3):657–674, 2017. doi: 10.1083/jcb.201507113.
- E. C. Schirmer and R. Foisner. Proteins that associate with lamins: many faces, many functions. *Exp Cell Res*, 313(10):2167–79, 2007. doi: 10.1016/j.yexcr.2007.03.012.
- E. C. Schirmer, L. Florens, T. Guan, r. Yates, J. R. and L. Gerace. Nuclear membrane proteins with potential disease links found by subtractive proteomics. *Science*, 301(5638):1380–2, 2003. doi: 10.1126/science.1088176.
- M. Schnee, Z. Ruzsics, A. Bubeck and U. H. Koszinowski. Common and specific properties of herpesvirus ul34/ul31 protein family members revealed by protein complementation assay. *J Virol*, 80(23):11658–66, 2006. doi: 10.1128/JVI.01662-06.
- J. Schoneberg, I. H. Lee, J. H. Iwasa and J. H. Hurley. Reverse-topology membrane scission by the escrt proteins. *Nat Rev Mol Cell Biol*, 18(1):5–17, 2017. doi: 10.1038/nrm.2016.121.
- J. Schoneberg, M. R. Pavlin, S. Yan, M. Righini, I. H. Lee, L. A. Carlson, A. H. Bahrami, D. H. Goldman, X. Ren, G. Hummer, C. Bustamante and J. H. Hurley. Atp-dependent force generation and membrane scission by escrt-iii and vps4. *Science*, 362(6421):1423–1428, 2018. doi: 10.1126/science.aat1839.

- D. Schumacher, B. K. Tischer, S. Trapp and N. Osterrieder. The protein encoded by the us3 orthologue of marek's disease virus is required for efficient de-envelopment of perinuclear virions and involved in actin stress fiber breakdown. *J Virol*, 79(7): 3987–97, 2005. doi: 10.1128/JVI.79.7.3987-3997.2005.
- F. Schuster, B. G. Klupp, H. Granzow and T. C. Mettenleiter. Structural determinants for nuclear envelope localization and function of pseudorabies virus pul34. *J Virol*, 86(4): 2079–88, 2012. doi: 10.1128/JVI.05484-11.
- J. Sehl, S. Portner, B. G. Klupp, H. Granzow, K. Franzke, J. P. Teifke and T. C. Mettenleiter. Roles of the different isoforms of the pseudorabies virus protein kinase pus3 in nuclear egress. *J Virol*, pages JVI.02029–19, 2020. doi: 10.1128/JVI.02029-19.
- J. Y. Shin, I. Mendez-Lopez, Y. Wang, A. P. Hays, K. Tanji, J. H. Lefkowitz, P. C. Schulze, H. J. Worman and W. T. Dauer. Lamina-associated polypeptide-1 interacts with the muscular dystrophy protein emerin and is essential for skeletal muscle maintenance. *Dev Cell*, 26(6):591–603, 2013. doi: 10.1016/j.devcel.2013.08.012.
- D. K. Shumaker, E. R. Kuczmarski and R. D. Goldman. The nucleoskeleton: lamins and actin are major players in essential nuclear functions. *Curr Opin Cell Biol*, 15(3):358–66, 2003. doi: 10.1016/s0955-0674(03)00050-4.
- D. N. Simon, M. S. Zastrow and K. L. Wilson. Direct actin binding to a- and b-type lamin tails and actin filament bundling by the lamin a tail. *Nucleus*, 1(3):264–72, 2010. doi: 10.4161/nucl.1.3.11799.
- M. Simpson-Holley, J. Baines, R. Roller and D. M. Knipe. Herpes simplex virus 1 u(l)31 and u(l)34 gene products promote the late maturation of viral replication compartments to the nuclear periphery. *J Virol*, 78(11):5591–600, 2004. doi: 10.1128/JVI.78.11.5591-5600.2004.
- J. N. Skepper, A. Whiteley, H. Browne and A. Minson. Herpes simplex virus nucleocapsids mature to progeny virions by an envelopment → deenvelopment → reenvelopment pathway. *J Virol*, 75(12):5697–702, 2001. doi: 10.1128/JVI.75.12.5697-5702.2001.
- B. Sodeik, M. W. Ebersold and A. Helenius. Microtubule-mediated transport of incoming herpes simplex virus 1 capsids to the nucleus. *J Cell Biol*, 136(5):1007–21, 1997. doi: 10.1083/jcb.136.5.1007.
- V. Sood and J. H. Brickner. Nuclear pore interactions with the genome. *Curr Opin Genet Dev*, 25:43–9, 2014. doi: 10.1016/j.gde.2013.11.018.
- B. A. Sosa, A. Rothballer, U. Kutay and T. U. Schwartz. Linc complexes form by binding of three kash peptides to domain interfaces of trimeric sun proteins. *Cell*, 149(5): 1035–47, 2012. doi: 10.1016/j.cell.2012.03.046.

A Bibliography

- B. A. Sosa, U. Kutay and T. U. Schwartz. Structural insights into linc complexes. *Curr Opin Struct Biol*, 23(2):285–91, 2013. doi: 10.1016/j.sbi.2013.03.005.
- B. A. Sosa, F. E. Demircioglu, J. Z. Chen, J. Ingram, H. L. Ploegh and T. U. Schwartz. How lamina-associated polypeptide 1 (lap1) activates torsin. *Elife*, 3:e03239, 2014. doi: 10.7554/eLife.03239.
- S. D. Speese, J. Ashley, V. Jokhi, J. Nunnari, R. Barria, Y. Li, B. Ataman, A. Koon, Y. T. Chang, Q. Li, M. J. Moore and V. Budnik. Nuclear envelope budding enables large ribonucleoprotein particle export during synaptic wnt signaling. *Cell*, 149(4):832–46, 2012. doi: 10.1016/j.cell.2012.03.032.
- L. M. Stannard, S. Himmelhoch and S. Wynchank. Intra-nuclear localization of two envelope proteins, gb and gd, of herpes simplex virus. *Arch Virol*, 141(3-4):505–24, 1996. doi: 10.1007/BF01718314.
- J. Staring, L. G. van den Hengel, M. Raaben, V. A. Blomen, J. E. Carette and T. R. Brummelkamp. Kremen1 is a host entry receptor for a major group of enteroviruses. *Cell Host Microbe*, 23(5):636–643 e5, 2018. doi: 10.1016/j.chom.2018.03.019.
- D. A. Starr. Kash and sun proteins. *Curr Biol*, 21(11):R414–5, 2011. doi: 10.1016/j.cub.2011.04.022.
- D. A. Starr and H. N. Fridolfsson. Interactions between nuclei and the cytoskeleton are mediated by sun-kash nuclear-envelope bridges. *Annu Rev Cell Dev Biol*, 26(1):421–44, 2010. doi: 10.1146/annurev-cellbio-100109-104037.
- G. Stenbeck. Soluble nsf-attachment proteins. *Int J Biochem Cell Biol*, 30(5):573–7, 1998. doi: 10.1016/s1357-2725(97)00064-2.
- B. M. Stinson, A. R. Nager, S. E. Glynn, K. R. Schmitz, T. A. Baker and R. T. Sauer. Nucleotide binding and conformational switching in the hexameric ring of a aaa+ machine. *Cell*, 153(3):628–39, 2013. doi: 10.1016/j.cell.2013.03.029.
- A. Stralfors and K. Ekwall. *Heterochromatin and Euchromatin-Organization, Boundaries, and Gene Regulation*. R.A. Meyers (Ed.), 2011. ISBN 3527600906 9783527600908. doi: 10.1002/3527600906.mcb.200400018.pub2.
- B. L. Strang and N. D. Stow. Circularization of the herpes simplex virus type 1 genome upon lytic infection. *J Virol*, 79(19):12487–94, 2005. doi: 10.1128/JVI.79.19.12487-12494.2005.
- N. Stuurman, S. Heins and U. Aebi. Nuclear lamins: their structure, assembly, and interactions. *J Struct Biol*, 122(1-2):42–66, 1998. doi: 10.1006/jsbi.1998.3987.
- M. S. Szollosi and D. Szollosi. ‘blebbing’ of the nuclear envelope of mouse zygotes, early embryos and hybrid cells. *Journal of Cell Science*, 91(2):257, 1988.

- K. Takeshima, J. Arai, Y. Maruzuru, N. Koyanagi, A. Kato and Y. Kawaguchi. Identification of the capsid binding site in the herpes simplex virus 1 nuclear egress complex and its role in viral primary envelopment and replication. *J Virol*, 93(21):JVI.01290–19, 2019. doi: 10.1128/JVI.01290-19.
- R. Tandon, E. S. Mocarski and J. F. Conway. The a, b, cs of herpesvirus capsids. *Viruses*, 7(3):899–914, 2015. doi: 10.3390/v7030899.
- E. C. Tapley and D. A. Starr. Connecting the nucleus to the cytoskeleton by sun-kash bridges across the nuclear envelope. *Curr Opin Cell Biol*, 25(1):57–62, 2013. doi: 10.1016/j.ceb.2012.10.014.
- D. J. Thaller, M. Allegretti, S. Borah, P. Ronchi, M. Beck and C. P. Lusk. An escrt-lem protein surveillance system is poised to directly monitor the nuclear envelope and nuclear transport system. *Elife*, 8:36, 2019. doi: 10.7554/eLife.45284.
- K. Toropova, J. B. Huffman, F. L. Homa and J. F. Conway. The herpes simplex virus 1 ul17 protein is the second constituent of the capsid vertex-specific component required for dna packaging and retention. *J Virol*, 85(15):7513–22, 2011. doi: 10.1128/JVI.00837-11.
- B. L. Trus, W. W. Newcomb, N. Cheng, G. Cardone, L. Marekov, F. L. Homa, J. C. Brown and A. C. Steven. Allosteric signaling and a nuclear exit strategy: binding of ul25/ul17 heterodimers to dna-filled hsv-1 capsids. *Mol Cell*, 26(4):479–89, 2007. doi: 10.1016/j.molcel.2007.04.010.
- E. M. Turner, R. S. Brown, E. Lauder Milch, P. L. Tsai and C. Schlieker. The torsin activator lull1 is required for efficient growth of herpes simplex virus 1. *J Virol*, 89(16):8444–52, 2015. doi: 10.1128/JVI.01143-15.
- A. L. Vanarsdall, S. R. Pritchard, T. W. Wisner, J. Liu, T. S. Jardetzky and D. C. Johnson. Cd147 promotes entry of pentamer-expressing human cytomegalovirus into epithelial and endothelial cells. *mBio*, 9(3):e00781–18, 2018. doi: 10.1128/mBio.00781-18.
- A. B. Vander Heyden, T. V. Naismith, E. L. Snapp, D. Hodzic and P. I. Hanson. Lull1 retargets torsina to the nuclear envelope revealing an activity that is impaired by the dyt1 dystonia mutation. *Mol Biol Cell*, 20(11):2661–72, 2009. doi: 10.1091/mbc.E09-01-0094.
- A. B. Vander Heyden, T. V. Naismith, E. L. Snapp and P. I. Hanson. Static retention of the luminal monotopic membrane protein torsina in the endoplasmic reticulum. *EMBO J*, 30(16):3217–31, 2011. doi: 10.1038/emboj.2011.233.
- M. J. VanGompel, K. C. Nguyen, D. H. Hall, W. T. Dauer and L. S. Rose. A novel function for the caenorhabditis elegans torsin ooc-5 in nucleoporin localization and nuclear import. *Mol Biol Cell*, 26(9):1752–63, 2015. doi: 10.1091/mbc.E14-07-1239.

A Bibliography

- L. N. Ventimiglia, M. A. Cuesta-Geijo, N. Martinelli, A. Caballe, P. Macheboeuf, N. Miguet, I. M. Parnham, Y. Olmos, J. G. Carlton, W. Weissenhorn and J. Martin-Serrano. Cc2d1b coordinates escrt-iii activity during the mitotic reformation of the nuclear envelope. *Dev Cell*, 47(5):547–563 e6, 2018. doi: 10.1016/j.devcel.2018.11.012.
- M. Vietri, K. O. Schink, C. Campsteijn, C. S. Wegner, S. W. Schultz, L. Christ, S. B. Thoresen, A. Brech, C. Raiborg and H. Stenmark. Spastin and escrt-iii coordinate mitotic spindle disassembly and nuclear envelope sealing. *Nature*, 522(7555):231–5, 2015. doi: 10.1038/nature14408.
- M. Vietri, H. Stenmark and C. Campsteijn. Closing a gap in the nuclear envelope. *Curr Opin Cell Biol*, 40:90–97, 2016. doi: 10.1016/j.ceb.2016.03.001.
- A. von Appen and M. Beck. Structure determination of the nuclear pore complex with three-dimensional cryo electron microscopy. *J Mol Biol*, 428(10 Pt A):2001–10, 2016. doi: 10.1016/j.jmb.2016.01.004.
- F. Wagenaar, J. M. Pol, B. Peeters, A. L. Gielkens, N. de Wind and T. G. Kimman. The us3-encoded protein kinase from pseudorabies virus affects egress of virions from the nucleus. *J Gen Virol*, 76 (Pt 7):1851–9, 1995. doi: 10.1099/0022-1317-76-7-1851.
- N. Wagner and G. Krohne. Lem-domain proteins: New insights into lamin-interacting proteins. *International Review of Cytology*, 261:1–46, 2007. doi: 10.1016/s0074-7696(07)61001-8.
- S. A. Walzer, C. Egerer-Sieber, H. Sticht, M. Sevvana, K. Hohl, J. Milbradt, Y. A. Muller and M. Marschall. Crystal structure of the human cytomegalovirus pul50-pul53 core nuclear egress complex provides insight into a unique assembly scaffold for virus-host protein interactions. *J Biol Chem*, 290(46):27452–8, 2015. doi: 10.1074/jbc.C115.686527.
- B. Wang, M. Wang, W. Zhang, T. Xiao, C. H. Chen, A. Wu, F. Wu, N. Traugh, X. Wang, Z. Li, S. Mei, Y. Cui, S. Shi, J. J. Lipp, M. Hinterndorfer, J. Zuber, M. Brown, W. Li and X. S. Liu. Integrative analysis of pooled crispr genetic screens using mageckflute. *Nat Protoc*, 14(3):756–780, 2019. doi: 10.1038/s41596-018-0113-7.
- D. Wang, X. Tao, M. Fei, J. Chen, W. Guo, P. Li and J. Wang. Human encephalitis caused by pseudorabies virus infection: a case report. *J Neurovirol*, 26(3):442–448, 2020. doi: 10.1007/s13365-019-00822-2.
- B. M. Webster, P. Colombi, J. Jager and C. P. Lusk. Surveillance of nuclear pore complex assembly by escrt-iii/vps4. *Cell*, 159(2):388–401, 2014. doi: 10.1016/j.cell.2014.09.012.
- B. M. Webster, D. J. Thaller, J. Jager, S. E. Ochmann, S. Borah and C. P. Lusk. Chm7 and heh1 collaborate to link nuclear pore complex quality control with nuclear envelope sealing. *EMBO J*, 35(22):2447–2467, 2016. doi: 10.15252/embj.201694574.

- R. G. Webster and A. Granoff. *Encyclopedia of virology*. Academic Press, San Diego, 1994. ISBN 0122269616 (v. 1) 0122269624 (v. 2) 0122269632 (v. 3) 0122269608 (set).
- M. Weidner-Glunde, E. Kruminis-Kaszkiel and M. Savanagouder. Herpesviral latency-common themes. *Pathogens*, 9(2):125, 2020. doi: 10.3390/pathogens9020125.
- J. P. Weir. Genomic organization and evolution of the human herpesviruses. *Virus Genes*, 16(1):85–93, 1998. doi: 10.1023/a:1007905910939.
- P. Wendler, S. Ciniawsky, M. Kock and S. Kube. Structure and function of the aaa+ nucleotide binding pocket. *Biochim Biophys Acta*, 1823(1):2–14, 2012. doi: 10.1016/j.bbamcr.2011.06.014.
- S. R. Wentz and M. P. Rout. The nuclear pore complex and nuclear transport. *Cold Spring Harb Perspect Biol*, 2(10):a000562, 2010. doi: 10.1101/cshperspect.a000562.
- S. R. White and B. Lanning. Aaa+ atpases: achieving diversity of function with conserved machinery. *Traffic*, 8(12):1657–67, 2007. doi: 10.1111/j.1600-0854.2007.00642.x.
- S. W. Whiteheart, K. Rossmagel, S. A. Buhrow, M. Brunner, R. Jaenicke and J. E. Rothman. N-ethylmaleimide-sensitive fusion protein: a trimeric atpase whose hydrolysis of atp is required for membrane fusion. *J Cell Biol*, 126(4):945–54, 1994. doi: 10.1083/jcb.126.4.945.
- K. L. Wilson and R. Foisner. Lamin-binding proteins. *Cold Spring Harb Perspect Biol*, 2(4):a000554, 2010. doi: 10.1101/cshperspect.a000554.
- H. J. Worman and J. C. Courvalin. The inner nuclear membrane. *J Membr Biol*, 177(1):1–11, 2000. doi: 10.1007/s002320001096.
- H. J. Worman, J. Yuan, G. Blobel and S. D. Georgatos. A lamin b receptor in the nuclear envelope. *Proc Natl Acad Sci U S A*, 85(22):8531–4, 1988. doi: 10.1073/pnas.85.22.8531.
- C. C. Wright, T. W. Wisner, B. P. Hannah, R. J. Eisenberg, G. H. Cohen and D. C. Johnson. Fusion between perinuclear virions and the outer nuclear membrane requires the fusogenic activity of herpes simplex virus gb. *J Virol*, 83(22):11847–56, 2009. doi: 10.1128/JVI.01397-09.
- H. Xu, J. Zhou, S. Lin, W. Deng, Y. Zhang and Y. Xue. Plmd: An updated data resource of protein lysine modifications. *J Genet Genomics*, 44(5):243–250, 2017. doi: 10.1016/j.jgg.2017.03.007.
- K. Yang and J. D. Baines. Selection of hsv capsids for envelopment involves interaction between capsid surface components pul31, pul17, and pul25. *Proc Natl Acad Sci U S A*, 108(34):14276–81, 2011. doi: 10.1073/pnas.1108564108.

A Bibliography

- K. Yang, E. Wills, H. Y. Lim, Z. H. Zhou and J. D. Baines. Association of herpes simplex virus pul31 with capsid vertices and components of the capsid vertex-specific complex. *J Virol*, 88(7):3815–25, 2014. doi: 10.1128/JVI.03175-13.
- M. Yuan, Z. Huang, D. Wei, Z. Hu, K. Yang and Y. Pang. Identification of autographa californica nucleopolyhedrovirus ac93 as a core gene and its requirement for intranuclear microvesicle formation and nuclear egress of nucleocapsids. *J Virol*, 85(22):11664–74, 2011. doi: 10.1128/JVI.05275-11.
- B. M. Zee and B. A. Garcia. Discovery of lysine post-translational modifications through mass spectrometric detection. *Essays Biochem*, 52:147–63, 2012. doi: 10.1042/bse0520147.
- T. Zeev-Ben-Mordehai, M. Weberuss, M. Lorenz, J. Cheleski, T. Hellberg, C. Whittle, K. El Omari, D. Vasishtan, K. C. Dent, K. Harlos, K. Franzke, C. Hagen, B. G. Klupp, W. Antonin, T. C. Mettenleiter and K. Grunewald. Crystal structure of the herpesvirus nuclear egress complex provides insights into inner nuclear membrane remodeling. *Cell Rep*, 13(12):2645–52, 2015. doi: 10.1016/j.celrep.2015.11.008.
- X. H. Zhang, L. Y. Tee, X. G. Wang, Q. S. Huang and S. H. Yang. Off-target effects in crispr/cas9-mediated genome engineering. *Mol Ther Nucleic Acids*, 4:e264, 2015. doi: 10.1038/mtna.2015.37.
- C. Zhao, J. T. Slevin and S. W. Whiteheart. Cellular functions of nsf: not just snaps and snares. *FEBS Lett*, 581(11):2140–9, 2007. doi: 10.1016/j.febslet.2007.03.032.
- C. Zhao, E. C. Smith and S. W. Whiteheart. Requirements for the catalytic cycle of the n-ethylmaleimide-sensitive factor (nsf). *Biochim Biophys Acta*, 1823(1):159–71, 2012. doi: 10.1016/j.bbamcr.2011.06.003.
- C. Zhao, R. S. Brown, A. R. Chase, M. R. Eisele and C. Schlieker. Regulation of torsin atpases by lap1 and lull1. *Proc Natl Acad Sci U S A*, 110(17):E1545–54, 2013. doi: 10.1073/pnas.1300676110.
- W. L. Zhao, Y. H. Wu, H. F. Li, S. Y. Li, S. Y. Fan, H. L. Wu, Y. J. Li, Y. L. Lu, J. Han, W. C. Zhang, Y. Zhao, G. L. Li, X. D. Qiao, H. T. Ren, Y. C. Zhu, B. Peng, L. Y. Cui and H. Z. Guan. [clinical experience and next-generation sequencing analysis of encephalitis caused by pseudorabies virus]. *Zhonghua Yi Xue Za Zhi*, 98(15):1152–1157, 2018. doi: 10.3760/cma.j.issn.0376-2491.2018.15.006.
- R. Zheng, R. Ghirlando, M. S. Lee, K. Mizuuchi, M. Krause and R. Craigie. Barrier-to-autointegration factor (baf) bridges dna in a discrete, higher-order nucleoprotein complex. *Proc Natl Acad Sci U S A*, 97(16):8997–9002, 2000. doi: 10.1073/pnas.150240197.
- X. Zhou, K. Graumann, D. E. Evans and I. Meier. Novel plant sun-kash bridges are involved in rangap anchoring and nuclear shape determination. *J Cell Biol*, 196(2):203–11, 2012. doi: 10.1083/jcb.201108098.

- Z. H. Zhou, D. H. Chen, J. Jakana, F. J. Rixon and W. Chiu. Visualization of tegument-capsid interactions and dna in intact herpes simplex virus type 1 virions. *J Virol*, 73(4):3210–8, 1999.
- L. Zhu, J. O. Wrabl, A. P. Hayashi, L. S. Rose and P. J. Thomas. The torsin-family aaa+ protein ooc-5 contains a critical disulfide adjacent to sensor-ii that couples redox state to nucleotide binding. *Mol Biol Cell*, 19(8):3599–612, 2008. doi: 10.1091/mbc.E08-01-0015.
- L. Zhu, L. Millen, J. L. Mendoza and P. J. Thomas. A unique redox-sensing sensor ii motif in torsina plays a critical role in nucleotide and partner binding. *J Biol Chem*, 285(48):37271–80, 2010. doi: 10.1074/jbc.M110.123471.
- L. Zsak, F. Zuckermann, N. Sugg and T. Ben-Porat. Glycoprotein gi of pseudorabies virus promotes cell fusion and virus spread via direct cell-to-cell transmission. *J Virol*, 66(4):2316–25, 1992.
- N. Zuleger, M. I. Robson and E. C. Schirmer. The nuclear envelope as a chromatin organizer. *Nucleus*, 2(5):339–49, 2011. doi: 10.4161/nucl.2.5.17846.

Curriculum Vitae **B**

C.1 Publications that are part of this thesis

Hölper, J.E., Klupp, B.G., Luxton, G.W.G., Franzke, K., & Mettenleiter, T.C. (2020).
Function of Torsin AAA+ ATPases in Pseudorabies Virus Nuclear Egress.
Cells, 9(3). doi:10.3390/cells9030738

Hölper, J.E., Reiche, S., Franzke, K., Mettenleiter, T.C. & Klupp, B.G.
Generation and Characterization of Monoclonal Antibodies Specific for the Pseudorabies Virus Nuclear Egress Complex.
submitted June 2020, Virus Research

Rönfeldt, S., Franzke, K., Hölper, J.E., Klupp, B.G., & Mettenleiter, T.C. (2020).
Mutational Functional Analysis of the Pseudorabies Virus Nuclear Egress Complex-Nucleocapsid Interaction.
Journal of Virology, JVI.01910-01919. doi:10.1128/JVI.01910-19

C.2 Publications that are not part of this thesis

Sehl, J., Hölper, J.E., Klupp, B.G., Baumbach, C., Teifke, J.P., & Mettenleiter, T.C. (2020).
An Improved Animal Model for Herpesvirus Encephalitis in Humans.
PLOS Pathogens, 16(3), e1008445. doi:10.1371/journal.ppat.1008445

Holzerland, J., Fénéant, L., Banadyga, L., Hölper, J.E., Knittler, M.R., & Groseth, A.
BH3-only sensors Bad, Noxa and Puma are Key Regulators of Tacaribe virus-induced Apoptosis.
submitted June 2020, PLOS Pathogens

Scientific presentations

D

- 8. FLI Junior Scientist Symposium** 25-27 September 2019, Jena, Germany. Poster presentation. *'Using CRISPR/Cas9 mutagenesis to uncover cellular key players during herpesvirus nuclear egress.'* Hölper, J.E. , Franzke, K., Luxton, G.W.G., Klupp, B.G., Mettenleiter, T.C.
- 8. FLI Junior Scientist Symposium** 25-27 September 2019, Jena, Germany. Talk by J. Sehl. *'An animal model for herpes simplex virus induced encephalitis.'* Sehl, J., Hölper, J.E. , Teifke, J.P., Klupp, B.G., Mettenleiter, T.C.
- 13th Annual Meeting EPIZONE** 26-28 August 2019, Berlin, Germany. Poster presentation by J. Carlson. *'Inhibition of African swine fever virus replication by CRISPR/Cas9-mediated knock-out of viral and cellular genes in wild boar lung (WSL) cells.'* Carlson, J., Hölper, J.E. , Grey, F., Thamamongood, T., Baillie, K. Hübner, A., Kabuuka, T., Höper, D., Petersen, B., Schwemmle, M., Mettenleiter, T.C., Fuchs, W.
- 29th Annual Meeting of the Society for Virology** 20-23 March 2019, Düsseldorf, Germany. Poster presentation. *'Development and characterization of monoclonal antibodies specifically detecting the herpesvirus nuclear egress complex.'* Hölper, J.E. , Klupp, B.G., Reiche, S., Ben-Mordehai, T., Grünewald, K., Mettenleiter, T.C.
- 29th Annual Meeting of the Society for Virology** 20-23 March 2019, Düsseldorf, Germany. Talk by J. Sehl. *'Simultaneous absence of two viral proteins in the Alphaherpesvirus Pseudorabies virus results in a drastically reduced mortality in mice despite widespread neuroinvasion.'* Sehl, J., Teifke, J. P., Klupp, B.G., Hölper, J.E. , Mettenleiter, T.C.

62. Jahrestagung der Fachgruppe Pathologie der DVG 01-03 March 2019, Fulda, Germany. Talk by J. Sehl. *'Funktionelle Charakterisierung von 2 Pseudorabiesvirus-Proteinen während der neuronalen Invasion in der Maus.'* Sehl, J., Hölper, J.E., Klupp, B.G., Teifke, J.P., Mettenleiter, T.C.

Mini-Herpesvirus Workshop 05 October 2018, Hamburg, Germany. Abstract. *'Herpes Viruses hijacking cellular pathways – how to find cellular proteins important for virus propagation?'* Hölper, J.E., Franzke, K., Luxton, G.W.G., Thamamongood, T., Schwemmler, M., Klupp, B.G. Mettenleiter, T.C.

7. FLI Junior Scientist Symposium 24-26 September 2018, Greifswald - Insel Riems, Germany. Poster presentation. *'Viruses hijacking cellular pathways – how to find cellular proteins important for the herpesvirus replication cycle?'* Hölper, J.E., Franzke, K., Luxton, G.W.G., Thamamongood, T., Schwemmler, M., Klupp, B.G. Mettenleiter, T.C.

28th Annual Meeting of the Society for Virology 14-17 March 2018, Würzburg, Germany. Poster presentation. *'LINCing cellular proteins to nuclear egress of herpesviruses.'* Hölper, J.E., Klupp B.G., Franzke, K., Mettenleiter, T.C.

6. FLI Junior Scientist Symposium 20-22 September 2017, FLI Braunschweig, Germany. Poster presentation. *'Cellular proteins involved in nuclear egress of herpesvirus capsids.'* Hölper, J.E., Klupp, B.G., Mettenleiter, T.C.

The pleiotropic nuclear envelope 22-25 August 2017, University of Edinburgh, UK. Poster presentation. *'Nuclear egress of herpesvirus - powered by cellular nuclear envelope proteins?'* Hölper, J.E., Klupp, B.G., Mettenleiter, T.C.

Eigenständigkeitserklärung E

Hiermit erkläre ich, dass diese Arbeit bisher von mir weder an der Mathematisch-Naturwissenschaftlichen Fakultät der Universität Greifswald noch einer anderen wissenschaftlichen Einrichtung zum Zwecke der Promotion eingereicht wurde. Ferner erkläre ich, dass ich diese Arbeit selbstständig verfasst und keine anderen, als die darin angegebenen Hilfsmittel und Hilfen benutzt und keine Textabschnitte eines Dritten ohne Kennzeichnung übernommen habe.

.....
Ort, Datum

.....
Unterschrift

Acknowledgments

All this work would not have been possible without the direct or indirect help, inspiration and support of many different people.

First and foremost, I am incredibly grateful to my supervisor, Prof. Dr. Dr. h.c. Thomas C. Mettenleiter, for the exciting project, the helpful advice, the opportunities offered and his sympathetic ear during my doctoral thesis. It was an honor to learn from such a remarkable scientist and mentor.

My special thanks goes to Dr. Barbara G. Klupp for the intensive support in the laboratory, her richness of ideas, the many constructive suggestions and discussions throughout all the years. I am grateful for the opportunity to work as a member of her laboratory.

I would like to thank the members of Lab Klupp/Met, especially Karla Günther, Cindy Krüper, Kathrin Müller, Sebastian Rönfeldt, Julia Sehl, Annemarie Seyfarth, Dr. Melina Vallbracht and the master student Anna Dorsch, for the wonderful cooperation and the constant help during the last years. Even the dumbest questions were always answered in a helpful way. I could not have wished for better colleagues!

Many thanks to all present and former members of the IMVZ for the great working atmosphere, the support through all these years, the helpfulness and the nice evenings together. Some of them deserve special mention:

A big thank you goes to Viola Damrau, *'unserer guten Seele'*, for all the help with basically everything. Thanks also to the Labor Fuchs for being our dearest laboratory neighbors! And especially to Dr. Walter Fuchs for discussion of any questions one can imagine and Dr. Alexandra Hübner for giving me an easy start into the CRISPR method. Thanks to Katrin Giesow and Barbara Bettin for your collection of knowledge, chemicals and equipment, that you shared with me at any time. I would also like to thank the Lab Finke, especially PD Dr. Stefan Finke and Luca Zaack, for their extraordinary help in the field of microscopy and for always having good advises. Special thanks to Dr. Melina Vallbracht, Lisa Wendt and Stephanie Peitsch - your advice, the good mood, the humor and the many wonderful hours within and outside the institute will remain in good memory. Finally, I will definitely miss our *'Mittagsrunde'* with alternating cast. You ensured a short break from science and minimized stress by laughing.

I would also like to emphasize my scientific cooperation partners: First, special thanks are due to my cooperation partner Dr. G. W. Gant Luxton, who has made a substantial contribution to this doctoral thesis by providing expression plasmids and engaging in helpful discussions. Secondly, I thank Dr. Sven Reiche and Sven Sander for the generation, provision and help regarding the monoclonal antibodies. Third, I like to acknowledge Dr. Kati Franzke, Mandy Jörn and Petra Meyer for the preparation of the TEM samples, the recording of excellent images and the help with subsequent visualization. Finally, thanks to a collaboration that is not part of the present work, but which was nevertheless an exciting part of my time at FLI. I would like to thank Prof. Dr. Martin Schwemmle, Thiprampai (Van) Thamamongood, Dr. Finn Grey, Dr. Kenneth Baillie, Dr. Dirk Höper, Dr. Jolene Carlson and Dr. Katrin Pannhorst for their collaboration and help with the genome-wide CRISPR project.

With and from you I learned a lot!

I would like to thank the Friedrich-Loeffler-Institut Collection of Cell Lines for their assistance and all institute helpers of *Institutsservice*, *Technik* and *Transport*, who have made the daily work easier.

This dissertation would not have been possible without the financial support of the Deutsche Forschungsgemeinschaft (DFG).

A special thank is reserved for my family and friends for their endless support. Most of all, I want to thank Jan for his encouragement and patience over all these years - thank you for believing in me.

DANKESCHÖN!